Sudesh Kumar Yadav *Editor*

Nanoscale Materials in Targeted Drug Delivery, Theragnosis and Tissue Regeneration

Springer

Nanoscale Materials in Targeted Drug Delivery, Theragnosis and Tissue Regeneration

Sudesh Kumar Yadav
Editor

Nanoscale Materials in Targeted Drug Delivery, Theragnosis and Tissue Regeneration

Springer

Editor
Sudesh Kumar Yadav
Department of Biotechnology
Council of Scientific and Industrial
Research-Institute of Himalayan
Bioresource Technology
Palampur, Himachal Pradesh
India

and

Department of Biotechnology
Center of Innovative and Applied
Bioprocessing (CIAB)
Mohali, Punjab
India

ISBN 978-981-10-0817-7 ISBN 978-981-10-0818-4 (eBook)
DOI 10.1007/978-981-10-0818-4

Library of Congress Control Number: 2016936976

© Springer Science+Business Media Singapore 2016
This work is subject to copyright. All rights are reserved by the Publisher, whether the whole or part of the material is concerned, specifically the rights of translation, reprinting, reuse of illustrations, recitation, broadcasting, reproduction on microfilms or in any other physical way, and transmission or information storage and retrieval, electronic adaptation, computer software, or by similar or dissimilar methodology now known or hereafter developed.
The use of general descriptive names, registered names, trademarks, service marks, etc. in this publication does not imply, even in the absence of a specific statement, that such names are exempt from the relevant protective laws and regulations and therefore free for general use.
The publisher, the authors and the editors are safe to assume that the advice and information in this book are believed to be true and accurate at the date of publication. Neither the publisher nor the authors or the editors give a warranty, express or implied, with respect to the material contained herein or for any errors or omissions that may have been made.

Printed on acid-free paper

This Springer imprint is published by Springer Nature
The registered company is Springer Science+Business Media Singapore Pte Ltd.

Preface

Advancements in nanotechnology promise to revolutionize drug manufacturing, drug delivery, and medical diagnostics. Nanoscale materials hold great potential for medical applications due to their differential behavior at the cellular and molecular level. In this context, the term nanomedicine has been coined to refer to the application of nanoscale materials, which can be used as drug delivery vehicles to develop highly selective and effective drugs. Nanomedicine market is expected to grow at a compounded annual growth rate (CAGR) of 12.3 % during the period 2013–2019 to reach US$177.60 billion.

The existing generation of drugs is largely based on small molecules with a mass of 1000 Da or less. These small molecules possess certain limitations, viz., poor bioavailability, lesser in vivo stability, first pass metabolism, non-targeted delivery to site of action, therapeutic ineffectiveness, side effects, etc. Nanomedicines have an upper hand compared to the standard drugs in view of several aspects, e.g., these reduce renal excretion, volume of distribution, improve the ability of drugs to accumulate at pathological sites and improve their therapeutic value. In addition, nanomedicine also assist therapeutic agents to overcome biological barriers. Nanotechnology-based drug delivery systems have been used to overcome this problem by combining specificity, targeted delivery and therapeutic action. Recent trend in nanomedicine research which came into play has developed a lot of formulations containing both drugs and imaging agents. Nanotechnology combined with molecular imaging probes has generated theragnostic nanoparticles which allow simultaneous detection and monitoring of diseases.

Tissue engineering has also become an advanced research interest during the last decade, offering the potential for regenerating almost every tissue and organ of human body. The production of artificial skin, tissue-engineered trachea and blood vessels, cartilages, urinary bladder, urethra substitutes, and cellular therapies are among the most exciting medical applications. Fabricating scaffolds that imitate the design of tissue at nanoscale is one of the key challenges in the tissue engineering field. Fortunately, nanofibers have really improved the scope for biomedical scaffolds, as nanofibers easily mimic the architecture of natural human tissues to support cell adhesion, proliferation, migration, and differentiation.

Despite the fast progress in nanomedicine, we are aware of the lack of good books in the area of biomedical applications of nanoscale materials. Though there are excellent reviews, books, and book chapters dealing with

one or several topics in the area of nanomedicine, a book containing a comprehensive coverage and up-to-date progress of drug delivery, theragnosis, and tissue engineering is not available.

This book aims to discuss the use of nanoscale materials for biomedical applications with special emphasis on drug delivery, theragnosis, and tissue regeneration. The book mainly focuses on nanomedicine which comprises of biodegradable nanoparticles, metallic nanoparticles, liposomal formulations, and nanocellulose along with the cellular response of therapeutic and theragnostic nanoparticles.

The book mainly consists of seven chapters. Chapter 1 gives a brief introduction about nanotechnology and elaborates the topic to discuss different techniques used in nanoparticle synthesis and characterization. Additionally it also provides information on various nanoscale carriers used as drug delivery vehicle. Chapter 2 gives detailed information about the synthesis methods of different biodegradable nanoparticles, their use as targeted drug delivery agent, corresponding drug release mechanisms, and biological barriers encountered by such biodegradable nanoparticles with their in vivo fate and toxicity reports. Chapter 3 emphasizes on various aspects of metallic nanoparticles, including their synthesis (physical, chemical, and biological) and characterization, properties, behavioral dependency based on particle size, shape, and surface chemistry and finally the wide applications of metal nanoparticles in biomedical field with reports of toxicity studies. Chapter 4 takes into account various preparation methodologies of liposomes and phytosomes, their physico-chemical characterisation, surface modifications, delivery of different molecules, behavior in biological systems, and applications in medical field. Chapter 5 includes the introduction of nanocellulose, a specific biomaterial of current interest due to its exciting properties. A discussion is made on the structure and morphology, types and dimensions, sources, physico-chemical properties, preparation approaches, surface modifications, applications of nanocellulose in formation of nanocomposites, drug delivery and tissue engineering and regeneration. Chapter 6 discusses the definition of theragnosis keeping specific focus on different imaging modalities related to nanoparticles as molecular imaging probes, disease diagnosis, and therapy. This chapter will also cover the various factors affecting nanotechnology-based disease diagnosis and therapy and future directions of theragnosis. Chapter 7 reports cellular response of nanoscale materials. Different types of nanomaterials are administered into the body by various routes. This chapter will focus on characteristics of different types of nanoscale materials affecting cellular response.

In this book, we have tried to cover recent developments in the area of drug delivery, theragnosis, and tissue regeneration. To make this book understandable, contents of book are methodically and rationally developed from the elementary level. To make each chapter more informative we have compressed available literature into an understandable description within a reasonable size. Important references have been included in each chapter for the benefit of readers who wish to pursue any of these topics further in a greater depth. We aim to satisfy the need of textbook for research students and a reference book for professionals in this field.

Contents

About the Editor

Sudesh Kumar Yadav worked as scientist from 2004 to principal scientist till 2016 at CSIR-Institute of Himalayan Bioresource Technology, Palampur. In 2016, he joined as Scientist-F at Center of Innovative and Applied Bioprocessing (CIAB), Department of Biotechnology, Mohali 160071, Punjab, India.

Abbreviations

2D-PAGE	Two-dimensional polyacrylamide gel electrophoresis
3-APTES	3-aminopropyltriethoxysilane
A549	Human lung adenocarcinoma
ACDC-Co/NCC	Aminated β-cyclodextrin-modified-carboxylated cobalt/nanocellulose composite
AFM	Atomic force microscope
AgNPs	Silver nanoparticles
ALMWP	Activatable low molecular weight protamine
araC	Cytosine β-D-arabinofuranoside
ASGPR	Asialoglycoprotein receptors
AuNPs	Gold nanoparticles
B16 cells	Mus musculus skin melanoma cells
BACE1	β-secretase
BBB	Blood brain barrier
BCG	Bacillus Calmette–Guerin
BEAS-2B	Human bronchial epithelium cell line
BHK21	Baby hamster kidney
BNCs	Bacterial nanocellulose
BNPs	Biodegradable nanoparticles
BSA	Bovine serum albumin
Caco-2	Colon cancer cell line
CMC	Critical micellar concentration
CNCs	Cellulose nanocrystals
CNFs	Cellulose nanofibers
CNTs	Carbon nanotubes
COS-7	*Cercopithecus aethiops* fibroblast-like kidney cells
CPT-11	Irinotecan hydrochloride
CS	Chitosan
CT	Computed tomography
CTAB	Cetyl trimethylammonium bromide
CTL	Cytotoxic T lymphocyte
CuNPs/CuO	Copper nanoparticles
CVD	Chemical vapor deposition
DCS	Differential centrifugal sedimentation
DLS	Dynamic light scattering
DMEM	Dulbecco's modified eagle's medium
DNA	Deoxyribonucleic acid

DOTA	^{64}Cu-1,4,7,10-tetraazacyclododecane-1,4,7,10-tetraacetic acid
DOTAP	1,2-diacyl-trimethylammonium propane
DOX	Doxorubicin
Doxo-PLA	Doxorubicin polylactide
DPPH	2,2-diphenyl-1-picrylhydrazyl
DSC	Differential scanning calorimetry
EA	Ellagic acid
ECL	Electrochemiluminescence
ECM	Extracellular matrix
EFGR	Epidermal growth factor receptor
EPR	Enhanced permeability and retention
FA	Folic acid
FCS	Fluorescence correlation spectroscopy
FDA	Food and Drug Administration
Fe_2O_3/Fe_3O_4	Iron oxide
FITC	Fluorescein-5′-isothiocyanate
Fmp	Fibronectin-mimetic peptide
FRET	Fluorescence resonance energy transfer
FTIR	Fourier transform infrared spectroscopy
G5 PAMAM	Polyamidoamine fifth generation dendrimers
GA	Glycyrrhetinic acid
Gal-CS	Galactosylated chitosan
Gal-m-C	Galactose residues
GAS	Gas anti-solvent technique
GS-Au	Glutathione-capped gold
GSH	Glutathione
HA-AuNP/TCZ	Hyaluronate-AuNPs/tocilizumab
HBEC	Human bronchial epithelial cells
HepG2	Human hepatocellular carcinoma
HER2	Human epidermal growth factor
HFT	Heparin folic acid paclitaxel
HL-60	Human promyelocytic leukemia cells
hMSCs	Human mesenchymal stem cells
HPLC	High-performance liquid chromatography
HSA	Human serum albumin
HT-1080	Human fibrosarcoma cell line
HU	Hounsfield units
HUVEC	Primary umbilical vein endothelial cell line
IgG	Immunoglobulin G
IO	Iron oxide
IPTS	3-isocyanatepropyltriethoxysilane
ITC	Isothermal titration calorimetry
KB	Human carcinoma of nasopharynx
LC-MS	Liquid chromatography-mass spectrometry
LUV	Large unilamellar vesicles
MALDI	Matrix-assisted laser desorption ionization
MCCs	Microcrystalline cellulose
MCF-7	Human breast adenocarcinoma cell line

MDA-MB-231	Human breast adenocarcinoma cell line
MDR	Multidrug resistance
MEF	Metal-enhanced fluorescence
MEF	Mouse embryonic fibroblast
MES	Mouse embryonic stem cells
MFCs	Microfibrillated cellulose
MIC	Minimum inhibitory concentration
MLV	Multilamellar liposomes
MMP	Matrix metalloprotease
Mn/MnO	Manganese/manganese oxide
MNPs	Magnetic nanoparticles
MPA	Mercaptopropionic acid
MPS	Mononuclear phagocytic system
MRI	Magnetic resonance imaging
MSA	2-mercaptosuccinic acid
MUV	Medium unilamellar vesicles
MWCNTs	Multiwalled carbon nanotubes
NADH	Nicotinamide adenine dinucleotide dehydrogenase
NC	Nanoconjugate
NCCs	Nanocrystalline cellulose
Nd:YAG	Neodymium-doped yttrium aluminum garnet; $Nd:Y_3Al_5O_{12}$
nf-BC/SA	Sodium alginate hydrogel
NIR	Near-infrared region
NIRF	Near-infrared fluorescence
NMR	Nuclear magnetic resonance
NMs	Nanomaterials
NPs	Nanoparticles
NRs	Nanorods
NSCLC	Non-small cell lung cancer
NSMs	Nanoscale materials
NTA	Nitrilotriacetate
o/w	Oil-in-water microemulsion
ODN	Oligonucleotide
PACL	Poly-alkyl-cyanoacrylates
PAMAM	Polyamidoamine
PAT	Photo acoustic tomography
PBLA	Poly(β-benzyl-L-aspartate)
PC	Phosphatidylcholine
PCL	Poly-ε-caprolactone
PCM	Pericellular matrix
pDNA	Plasmid DNA
PDT	Photodyanamic therapy
PEG	Polyethylene glycol
PEG-PDLLA	Poly(ethylene glycol)-block-poly(D,L-lactide)
PEI	Polyethyleneimine
PEO	Polyethylene oxide
PET	Positron emission tomography
PLA	Polylactic acid

PLA-TPGS	Poly(lactide)-tocopheryl polyethylene glycol succinate
PLGA	Poly(lactic-co-glycolic acid)
PLGA-PEG	Poly(lactic-co-glycolic) acid-polyethylene glycol
PMMA	Polymethylmetacrylate
PODO	Podophyllotoxin
PSMA	Prostate-specific membrane antigen
PTMC	Poly(trimethylenecarbonate)
PTX	Paclitaxel
PUFA	Polyunsaturated fatty acids
PVA	Polyvinyl alcohol
PVP	Poly(*N*-vinylpyrrolidone)
PVP	Polyvinylpyrollidone
QDs	Quantum dots
RA	Rheumatoid arthritis
RAW 264.7	Macrophage from blood
RBCs	Red blood corpuscles
RES	Reticulo-endothelial system
RGD	Arginine-glycine-aspartic acid
RGDS	Arg–Gly–Asp–Ser
Rhsa	Recombinant human serum albumin
RNA	Ribonucleic acid
ROS	Reactive oxygen species
RPMI	Roswell Park Memorial Institute
RT	Repetition time
RT	Retention time
SCFs	Supercritical fluids
SDS	Sodium dodecyl sulfate
SEDS	Solution enhanced dispersion by supercritical fluids
SEM	Scanning electron microscope
SERS	Surface enhanced Raman spectroscopy
siRNA	Small interfering ribonucleic acid
SLNs	Sentinel lymph nodes
SOD	Superoxide dismutase
SPECT	Single photon emission computed tomography
SPION	Superparamagnetic iron oxide nanoparticles
SPR	Surface plasmon resonance
STZ	Streptozotocin
SUV	Small unilamellar vesicles
SWCNTs	Single-walled carbon nanotubes
Tat-QDs	Tat peptide-conjugated quantum dots
TB	Tuberculosis
TBAB	Tetrabutylammonium bromide
T_c	Gel-liquid crystal transition temperature
TEM	Transmission electron microscope
TEMPO	2,2,6,6-tetramethylpiperidine-1-oxyl
TfRs	Transferrin receptors
TGA	Thermo-gravimetric analysis
TGA	Thioglycolic acid
TiO_2	Titanium dioxide

TMC	*N*-trimethyl chitosan chloride
$TMSi_3As$	Tris(trimethylsilyl)arsine
TOP	Trioctylphosphine
TOPO	Trioctylphosphine oxide
TPAB	Tetrapropylammonium bromide
TPP	Triphenylphosphonium
TPP	Tripolyphosphate solution
TT1	Human ATI cell line
TTIP	Titanium tetraisopropoxide
US	Ultrasound
UV	Ultraviolet
UV-vis	Ultraviolet-visible
VEGF	Vascular endothelial growth factor
w/o	Water-in-oil microemulsion
XPS	X-ray photoelectron spectroscopy
XRD	X-ray diffraction
XRF	X-ray fluorescence
ZnO	Zinc oxide

Nanoscale Materials in Targeted Drug Delivery

1

Avnesh Kumari, Rubbel Singla, Anika Guliani, Shanka Walia, Amitabha Acharya and Sudesh Kumar Yadav

Abstract

Nanoscale materials (NSMs) are gaining attention due to their small size and unique physiochemical properties. Different approaches are used for the synthesis of NSMs. NSMs cannot be visualized by ordinary instruments. Instruments with high resolution are required for their characterisation. NSMs offer enhanced activity and specificity to encapsulate drugs. NSM are used as vehicles for site specific delivery of drugs inside the body. In this chapter, approaches for the synthesis of NSMs, and characterisation techniques for NSMs like SEM, TEM, AFM, DLS, XRD, and FTIR have been explained briefly. In addition, this chapter also covers zero dimensional one dimensional, two dimensional and three dimensional NSMs briefly. Detailed information about approaches of targeted delivery like passive and active have been covered in this chapter. NSMs like polymeric nanoparticles, metallic nanoparticles, liposomes, quantum dots, polymeric micelles, carbon nanotubes, dendrimers, and magnetic nanoparticles used in targeted drug delivery have also been explained in this chapter.

Keywords

NSMS · Active targeting · Passive targeting · Top-down · Bottom up

A. Kumari · R. Singla · A. Guliani · S. Walia · A. Acharya · S.K. Yadav
Department of Biotechnology, Council of Scientific and Industrial Research-Institute of Himalayan Bioresource Technology, Palampur 176061, Himachal Pradesh, India

A. Kumari · R. Singla · A. Guliani · S. Walia · A. Acharya · S.K. Yadav
Academy of Scientific and Innovative Research, New Delhi, India

S.K. Yadav (✉)
Department of Biotechnology, Center of Innovative and Applied Bioprocessing (CIAB), Mohali 160071, Punjab, India
e-mail: skyt@rediffmail.com; sudesh@ciab.res.in

© Springer Science+Business Media Singapore 2016

S.K. Yadav (ed.), *Nanoscale Materials in Targeted Drug Delivery, Theragnosis and Tissue Regeneration*, DOI 10.1007/978-981-10-0818-4_1

Contents

1.1 Introduction

Nantechnology deals with properties and responses of materials at atomic, molecular, and macromolecular scales. The properties of matter at nanoscale differ significantly from their bulk counterparts (Logothetidis 2006). Nanotechnological tools are used to fabricate novel nanoscale materials (NSMs) which can be used for tuning the responses of living and non living matter (Logothetidis 2006). NSMs are particles having a size range of 10–1000 nm (Mohanpuria et al. 2008; Kumar and Yadav 2009; Kumari et al. 2010; Acharya 2013; Walia and Acharya 2015). Nanomedicine is the field of nanotechnology which deals with the use of NSMs for diagnosis, imaging, and treatment of various chronic diseases and ailments (Samad et al. 2007; Madaan et al. 2014; Nigam et al. 2014). Due to the small size and high surface area to volume ratio, they possess unique properties which can be exploited for different biomedical applications especially in the area of nanomedicine. Size of NSMs is smaller than human cells but larger than biomolecules such as enzymes and receptors. NSMs can easily enter cells and move out of the blood vessels or some of them are able to pass the blood brain barrier (BBB) (Wohlfart et al. 2012).

Basically, two approaches are used for the synthesis of NSMs which includes'top down' and 'bottom up' approach (Iqbal et al. 2012). In the'top down' approach, bulk materials are broken down to smaller materials whereas in 'bottom up' approach, NSMs are build into larger structures from small building blocks or units. Both of these approaches are used by the scientists for the synthesis of NSMs (Iqbal et al. 2012). NSMs are classified into three types depending upon their dimensionality, i.e., zero dimensional, one dimensional and two dimensional (Cao 2004). Zero-dimensional NSMs are synthesized by thermodynamic and kinetic approach. Thermodynamic approach comprises generation of supersaturation, nucleation, and subsequent growth. Reduction in free energy of the reaction mixture is the driving force for the nucleation and growth of NSMs. The newly formed nucleus is stable only when its radius exceeds a critical size. A nucleus smaller than critical size will dissolve into the solution to reduce the overall free energy, whereas a nucleus larger than critical size is stable and continues to grow bigger (Cao 2004). Kinetic approach involves limited amount of source materials or the available space to stop the synthesis of NSMs (Cao 2004). Many spatial confinements have been established for the synthesis of NSMs.

Targeting of drugs require increased accumulation of drug at the disease site as compared to other tissues and organs selectively and quantitatively. Targeting of drugs help in reducing the dose, increasing patient compliance and cost of therapy (Kumari et al. 2011). NSMs have been extensively exploited for targeted delivery of drugs. NSMs can be actively or passively targeted so as to release the drug at diseased site. Passive targeting relies on the loose architecture of tissues and makes use of the endothelial gaps for permeation and retention inside the tissues (Kunjachan et al. 2014). This effect known as enhanced permeation and retention (EPR) has been heavily exploited for treatment of different types of cancers with the help of NSMs. In contrast, active targeting makes use of the

interactions between receptors, and antigens overexpressed on the surface of target tissues. NSMs are grafted with ligands or molecules which have tendency for binding with these antigens and receptors. Active targeting increases the efficacy and specificity of NSMs (Kunjachan et al. 2014).

NSMs have great potential for the treatment of various diseases. NSMs that have been explored for the drug delivery include polymeric NPs, metallic, liposomes, quantum dots, carbon nanotubes, dendrimers, polymeric micelles, and magnetic nanoparticles (MNPs). NSMs provide advantages over the traditional drug delivery systems in terms of high stability, high specificity, high drug loading, ability for controlled release, possibility of different routes of administration for drugs and the ability to encapsulate both hydrophilic and hydrophobic drugs (Kumari et al. 2010; Kumari et al. 2012; Yadav et al. 2013, Kumar et al. 2014). The drugs may be encapsulated inside NSMs or linked to the surface of NSMs. Once they are at the target site, the drug payload may be released from the NSMs by diffusion, swelling, erosion or degradation (Mohanraj and Chen 2006). These NSMs protect the drug, reduce the drug toxicity, provide controlled release and help in releasing the drugs at target site. In addition to this, surface of the NSMs can be coated with ligands for targeted delivery to diseased site (Ashley et al. 2011). In this chapter, we have briefly described various approaches used for the synthesis of NSMs, various state of art techniques used for their characterisation, active and passive strategies used for targeted drug delivery and various nanoscale carriers used for targeted drug delivery.

1.2 Approaches for Synthesis of Nanoscale Materials

Synthesis of nanomaterials is one of the most dynamic fields in nanotechnology. An essential challenge in synthesis of NSMs is controlling the size of NSMs at a high yield for industrial applications. The precise control of atomic and molecular building blocks at nanoscale level is of utmost importance so that these can be assembled, used, and tailored for fabricating devices of multifunctionality in diverse applications.

Synthesis methods for NSM can be classified according to the strategy followed (Iqbal et al. 2012). Two strategies that are broadly followed for the synthesis of NSMs are 'top down' and 'bottom up' approaches. 'Bottom up' approach refers to the buildup of a material from the bottom: atom by atom, molecule by molecule or cluster by cluster. In contrast, 'top down' approach refers to successive cutting of bulk material to get NSM (Iqbal et al. 2012). Preparing NSMs by attrition or milling is an example of top down method, where as the colloidal dispersion is a good example of bottom up approach in the synthesis of NSM. Both of these approaches play an important role in nanotechnology and are associated with both merits and demerits. Bottom up approach gives rise to macroscopic disorder in synthesized NSMs. 'Top down' approach results in the imperfection and crystallographic damage to the synthesized NSMs (Cao 2004). Lithography is an example of top down approach which can cause significant crystallographic damage to the processed patterns and additional defects may be introduced during etching (Das et al. 1993). Such imperfections will have strong impact on physical properties and surface chemistry of NSMs, since the surface area to volume ratio of NSMs is very large. At present, most commonly used top down approach is photolithography to manufacture computer chips and produce structures smaller than 100 nm (Cao 2004). Though the concept of photolithography is simple, its implementation is very complex and expensive. On the contrary, bottom up approach promises better NSM with less defects, more homogeneous chemical composition and long and short range ordering. This is because bottom up approach is determined mainly by reduction in Gibbs free energy (Cao 2004). Self-assembly is an example of bottom-up approach which has excited many researchers across the world. Dendrimers are one of the classic examples of self assembled NSMs synthesized using bottom up self assembly strategy.

Production of glass and ceramic materials using sol gel technique is also an example of bottom up approach. Despite the difficulties and demerits of these approaches, both the strategies are followed by nanotechnologist across the world for synthesizing NSMs (Cao 2004).

1.3 Characterisation of Nanoscale Materials

Morphological characterization of NSMs requires sophisticated instruments with high resolution and accuracy. Characterization of NSMs by more than one technique is essential for the authenticity and validity of NSMs size, shape, and morphology. Many of the techniques that have been used for characterization of NSMs are transmission electron microscope (TEM), scanning electron microscope (SEM), atomic force microscope (AFM), dynamic light scattering (DLS), X-ray based methods and spectroscopic techniques.

SEM and TEM are electron microscopic techniques that have been used for the characterisation of wide range of NSMs. Both these instruments require high vacuum for imaging of samples. SEM consists of three main components electron gun, series of lenses within vacuum chamber and detector. When a specimen is hit with a beam of the electrons, it emits X-rays and three kinds of electrons: primary backscattered electrons, secondary electrons, and Auger electrons. SEM uses primary backscatter electrons and secondary electrons. Secondary electrons carry information about the surface topography of the sample, backscattered electrons give information about the atomic number of the sample and X-rays give information about the elemental composition of the sample. In most of the cases SEM requires conducting samples and hence non-conducting samples are often coated with a material known as a sputter coater. Sputter coaters provide the specimen with a thin layer of conductive material, gold or graphite. In addition, sample preparation traditionally includes the removal of all water molecules, otherwise molecules will vaporize in a vacuum, create obstacles for the electron beams and obscure the clarity of the image (Molpeceres et al. 2000). For SEM analysis, sample is coated on aluminium stub on double adhesive carbon tape and coated with gold or carbon using sputter coating unit. The sample is then scanned with focused beam of electrons. Scattered electrons carry information about the surface topography of sample (Molpeceres et al. 2000). TEM uses electrons as source instead of light. Because the wavelength of electrons is much smaller than that of light, the optimal resolution attained for TEM images is better than that from a light microscope. Thus, TEM can reveal the minute details of internal structure of samples. For TEM analysis, sample is coated on carbon coated grids. Surface topography of sample is obtained with electron beam that is transmitted through ultra thin sample (Polakovic et al. 1999). However, both these techniques can lead to image artifacts due to high vacuum and other harsh treatments during sample preparation.

To avoid image artifacts due to electron beam, another technique which is mostly preferred these days is scanning probe microscopy or AFM. AFM is based on physical scanning of sample surface using tip of atomic scale. The surface topography of sample is based on the force between tip and sample surface. AFM can also be used for imaging non conducting samples in their native state without any chemical treatment (DeAssis et al. 2008). AFM also provides 3-D image of sample surface. Light scattering techniques such as dynamic light scattering (DLS), are commonly used for size determination of NPs. DLS is based on scattering of light at different intensities by Brownian motion of particles in suspension. Analysis of intensity fluctuations gives velocity of Brownian motion and hence particle size using Stokes-Einstein equation. DLS gives information about hydrodynamic diameter of NPs (López-Serrano et al. 2014). X-ray based methods such as X-ray absorption (XAS), X-ray fluorescence (XRF), X-ray photoelectron spectroscopy (XPS), and X-ray diffraction (XRD) provide information about the surface structure, crystallographic structure and elemental composition.

Fourier transform infrared (FTIR) spectroscopy is used to obtain information about the

encapsulation or conjugation of chemical compounds on nanomaterials (Kumari et al. 2011). Energy from light source is transferred to the molecule and molecule gets excited to higher energy state. FTIR is concerned only with molecular vibrations and rotations of different functional groups and bonds with different vibrational frequency.

1.4 Types of Nanoscale Materials

NSMs are mainly classified into four types namely zero dimensional, one dimensional and two dimensional and three dimensional (Fig. 1.1). Zero-dimensional NSMs are NPs which include single crystals, polycrystalline, and amorphous NSMs with all possible morphologies. One dimensional NSMs have been called by different names like nanowhiskers, nanofibers, nanowires, or nanorods. Two-dimensional NSMs include thin films and three dimensional include fullerenes, dendrimers, etc. Different techniques have been used for the synthesis of zero dimensional, one dimensional and two dimensional NSM. Here in this chapter, we will briefly discuss the synthesis of zero dimensional NSM using thermodynamic (Cao 2004).

Thermodynamic approaches are used for the synthesis of NPs and these are homogenous and heterogeneous nucleation (Cao 2004). Homogenous nucleation involves creation of supersaturation of growth species which is created by reduction in temperature of an equilibrium mixture of saturated solution. This happens when the concentration of a solute in a solvent exceeds its equilibrium solubility or temperature decreases below the phase transformation point and a new phase appears. A supersaturated solution will have high Gibbs free energy and overall energy of the system would be reduced by segregating solute from the solution. The driving force for nucleation and growth is the reduction in Gibbs free energy. The change in Gibbs free energy (ΔG_v) is dependent on the concentration of the solute and is given by the equation

$$\Delta G_v = -\frac{kT}{\Omega}\ln\left(\frac{C}{C_o}\right) = -\frac{kT}{\Omega}\ln\ (1+\sigma) \tag{1.1}$$

where C is the concentration of the solute, C_o is the equilibrium concentration or solubility, k is the Boltzmann constant, T is the temperature, Ω is the atomic volume, and σ is the supersaturation defined by $(C - C_o)/C_o$.

Assuming a spherical nucleus with a radius of r, the change of Gibbs free energy or volume energy, $\Delta\mu_v$ can be given by the equation

$$\Delta\mu_v = \frac{4}{3}\pi r^3 \Delta G_v \tag{1.2}$$

Increase in surface energy of the system, $\Delta\mu_s$ is given by the equation

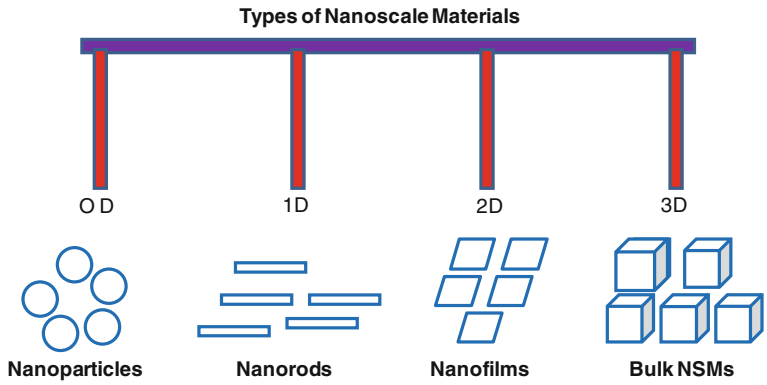

Fig. 1.1 Types of nanoscale materials according to dimensionality

$$\Delta\mu_s = 4\pi r^2\gamma \tag{1.3}$$

where γ is the surface energy per unit area. The total change of chemical potential for the formation of the nucleus, ΔG, is given by

$$\Delta G = \Delta\mu_v + \Delta\mu_s = \frac{4}{3}\pi r^3\Delta G_v + 4\pi r^2\gamma \tag{1.4}$$

Newly formed nucleus is stable when its radius exceeds a critical size, r^*. A nucleus smaller than r^* will dissolve into solution to reduce the overall free energy, and nucleus with larger r^* is stable and will continue to grow larger. At the critical size $r = r^*$ and, $d\Delta G/dr = 0$, the critical size, r^*, and critical energy ΔG^*, are defined by the equation

$$r^* = -2\frac{\gamma}{\Delta G_v} \tag{1.5}$$

$$\Delta G^* = \frac{16\pi\gamma}{(3\Delta G_v)^2} \tag{1.6}$$

ΔG^* is the minimum energy barrier that a nucleation process must overcome and r^* is the minimum size of a stable spherical nucleus. In the synthesis of NPs by homogenous nucleation, the critical size represents the limit on how small the NPs can be synthesized. The nucleation occurs only when the super saturation reaches a certain value above the solubility and is defined by the energy barrier in Eq. (1.6). For the synthesis of NPs with uniform size distribution, it is good if all the nuclei are formed at same time. Once nuclei are formed, growth occurs simultaneously. Formation of uniform sized NPs is possible if growth process is appropriately controlled. Synthesis of metallic NPs, semiconductor NPs and metal oxide NPs occurs by homogenous nucleation (Cao 2004).

NPs can also be formed through heterogeneous nucleation which involves formation of a new phase on surface of another material (Cao 2004). Heterogeneous nucleation also involves decrease in the Gibbs free energy and an increase in surface or interface energy. The total change of the chemical energy, ΔG, associated with the formation of nucleus is given by the equation.

$$\Delta G = a_3 r^3\Delta\mu + a_1 r^2\gamma_{vf} + a_2 r^2\gamma_{fs} - a_2 r^2\gamma_{sv} \tag{1.7}$$

where r is the mean diameter of the nucleus, $\Delta\mu_v$ is the change of Gibbs free energy per unit volume, γ_{vf}, γ_{fs}, and γ_{sv} are the surface or interface energy of vapor nucleus, nucleus substrate, and substrate-vapor interface, respectively. Respective geometric constants are given by:

$$a_1 = 2\pi(1 - \cos\theta) \tag{1.8}$$

$$a_2 = \pi\sin^2\theta \tag{1.9}$$

$$a_3 = 3\pi(2 - 3\cos\theta + \cos^2\theta) \tag{1.10}$$

where θ is the contact angle, which is dependent only on the surface properties of the surfaces or interfaces involved, and is defined by Young's equation

$$\gamma_{sv} = \gamma_{fs} + \gamma_{vf}\cos\theta \tag{1.11}$$

Similar to homogenous nucleation, the formation of new phase results in a reduction of the Gibbs free energy, but an increase in the total surface energy. The nucleus is stable only when its size is larger than the critical size, r^*

$$r* = \frac{-2(a\gamma_{vf} + a\gamma_{fs} - a\gamma_{sv})}{3a_3\Delta G_v} \tag{1.12}$$

and the critical energy barrier, ΔG^*, is given by

$$\Delta G* = \frac{4\left(a_1\gamma_{vf} + a_2\gamma_{fs} - a_2\gamma_{sv}\right)^3}{27a_3^2\Delta G_v} \tag{1.13}$$

Substituting all the geometric constants, we get

$$r* = \frac{2\pi\gamma}{\Delta G}\left\{\frac{\sin^2\theta\cdot\cos\theta + 2\cos\theta - 2}{2 - 3\cos\theta + \cos\theta}\right\} \quad (1.14)$$

$$\Delta G* = \left\{\frac{16\pi\gamma_{vf}}{3(\Delta G)^2}\right\}\left\{\frac{2 - 3\cos\theta + \cos^3\theta}{4}\right\} \quad (1.15)$$

First term in Eq. (1.15) is the critical energy barrier and second term is the wetting factor.

1.5 Targeted Drug Delivery

Targeted drug delivery refers to drug accumulation within a target tissue (Torchilin 2000). Targeted drug delivery to specific sites in the body requires NSM. Targeted drug delivery has been divided into two processes passive and active (Fig. 1.2). Passive targeting involves accumulation of NSMs in loose vasculature of tumors and is also known as EPR effect. EPR makes use of the anatomical and physiological abnormalities of tumor tissue, particularly the tumor vasculature (Matsumura and Maeda 1986; Maeda et al. 2001; Iyer et al. 2006). Angiogenesis is produced to meet the rising requirement for nutrition and oxygen as the tumor grows to attain the size of 2–3 mm. Neovasculature characterizes irregular, dilated, defective blood vessels, poorly arranged endothelial cells; abnormal perivascular cells; and smooth muscle layers in vascular walls. In addition, the tumor vessels have wide lumens and impaired lymphatic drainage. These traits work jointly to cause extensive permeation of NSMs into tumor tissues. The EPR effect is affected mainly by the size and plasma residence time of NSMs. The NSMs of size ≥8 nm showed greater tumor distribution owing to the EPR effect. NSMs can be localized in tumors by passive targeting (Maeda et al. 2001). Polyethylene glycol (PEG) NSMs showed tumor distribution which increased with increase in molecular weight ($10 < 20 < 30 \ll 40 \ll 60$ kDa). The 10 kDa PEG NSMs was not detected in tumors at 24 h, whereas 40–60 kDa NSM were detected in tumors for up to 96 h. The 30, 40, and 60 kDa PEG NSMs showed 2.1, 5.3, and 4.1 times higher passive distribution in tumors at 24 h, respectively, as compared to the 20 kDa PEG NSM. The 60 kDa NSMs exhibited 1.5 times higher tumor distribution than 40 kDa nanocarrier at 96 h (Singh et al. 2012). Glutathione-capped gold NPs (GS-AuNPs) with size of ~2.5 nm exhibited a much longer tumor retention time and faster normal tissue clearance, indicating that the well-known enhanced permeability and retention effect still exists in such small NPs (Liu et al. 2013).

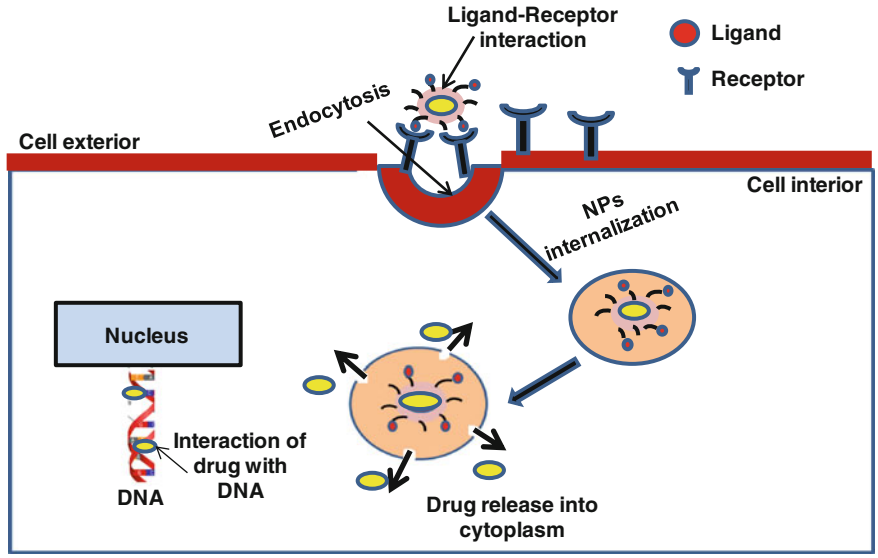

Fig. 1.2 Targeted delivery of nanoscale materials loaded with drug to cancer cells

The size of NSM also affects the kinetics and extent of tumor accumulation. Positively charged non- PEGylated liposomes containing the lipid 1,2-diacyl-trimethylammonium propane (DOTAP) displayed higher accumulation in tumor vs surrounding tissue compared to their negative or neutral counterpart (Campbell et al. 2002; Krasnici et al. 2003; Schmitt-Sody et al. 2003). Positively charged Sterically stabilized colloids have also shown enhanced tumor accumulation (Meng et al. 2011; Ho et al. 2010) while others appear less effective (He et al. 2010; Xiao et al. 2011). Shape of NSMs also affects accumulation in tumors via EPR effect. Recently, it has been reported that nanorods have extravasated to the interstitium 4 times faster and diffused deeper into the tumor, than nanospheres of 35 nm size (Chauhan et al. 2011). Doxorubicin-loaded polycaprolactone-PEG NSMs were passively targeted to the tumor tissue in treated mice bearing subcutaneous C-26 tumors and released doxorubicin in tumor tissue rather than normal tissue (Gou et al. 2009). Polyethylene oxide-modified poly(β-aminoester) NSMs also accumulated in tumor by means of a passive targeting mechanism (Shenoy et al. 2005). Polymeric micelles of PEG-phosphatidyl-ethanolamine conjugates showed 8-fold higher accumulation in the infarction zone by EPR effect (Lukyanov et al. 2004).

Active targeting relies on tagging of ligands on the surface of NSM and is used to describe interactions between NSM and the target cells, usually through specific ligand-receptor interactions (Beduneau et al. 2007; Deckert 2009; Hong et al. 2009; Zensi et al. 2009; Canal et al. 2010). NSMs with specific ligands bound to the surface have good potential for targeted drug delivery (Dinauer et al. 2005) and strategies have been used to direct NPs to cell surface carbohydrates, receptors and antigens (Sinha et al. 2006). Ligands whose antigen or receptors are overexpressed on cancer cells can be used for targeted drug delivery. Antibodies, oligopeptides, carbohydrates, glycolipids, and folic acid are the most widely used ligands for targeting different organs and tissues. Ligands like transferrin (Yang et al. 2005), folic acid (Dixit et al. 2006), and wheat-germ agglutinin (Mo and Lim 2005) have been conjugated to various NSMs for increasing their specificity and targeting ability (Table 1.1).

Folate receptor has been found to be over expressed on the surface of ovarian, endometrial, colorectal, breast, lung, renal cell carcinoma, brain metastases derived from epithelial cancer, and neuroendocrine carcinoma cells. Folic acid (Table 1.1) has been used as the ligand for targeting folate expressing cancer cells. Folic acid conjugated silica NPs have shown targeted delivery to high folate receptor expressing HeLa cells than normal cells (Rosenholm et al. 2009). In another study, folic acid conjugated to poly (lactic-co-glycolic) acid (PLGA)-PEG NPs have shown selective uptake and cytotoxicity to folate receptor rich cells (El-Gogary et al. 2014). Folic acid conjugated dendrimers have shown selected and targeted doxorubicin delivery to folate expressing KB cells (Wang et al. 2011). Folate-decorated liposomes have shown targeted delivery to folate receptor positive macrophages (Turk et al. 2004). Folate-targeted liposomes have shown 10 times greater cytotoxicity than non targeted liposomes (Goren et al. 2000). Folate-conjugated polymeric micelles have shown greater cellular uptake and targeted delivery in folate expressing KB cells (Yoo and Park 2004). Folate functionalised thermosensitive gels also have effectively targeted folate expressing KB cells (Nayak et al. 2004). Folic acid targeted micelles have shown enhanced intracellular delivery and cytotoxicity in folate receptor rich cancer cells (Lu et al. 2014). Folate conjugated micelles showed more cellular uptake in MCF-7 cells through interaction with overexpressed folate receptors on the surface of cancer cells (Park et al. 2005). Folate conjugated poly (L-histidine)-poly (L-lactic acid) micelles have been found to be more effective in killing cancer cells (Lee et al. 2003). Poly(dimethylaminoethyl methacrylate)-poly(butylmethacrylate) polymeric micelles transfected COS-7 and OVCAR-3 cells efficiently with minor toxicity (Funhoff et al. 2005). Folate-targeted chitosan NPs intracellular delivery was more target specific than non targeted ones (Senthilkumar et al. 2015). In another

Table 1.1 Various types of ligands used in active targeting of NSMs

Ligand	NSM	Target	Reference
Folic acid	Chitosan NPs	FA receptor	Senthilkumar et al. 2015
Folic acid	PLGA-PEG NPs	FA receptor	El-Gogary et al. (2014)
Folic acid	Dendrimers	FA receptor	Wang et al. (2011)
Folic acid	Silica NPs	FA receptor	Rosenholm et al. (2009)
Folic acid	Polymeric NPs	FA receptor	Werner et al. (2011)
Folic acid	Liposomes	FA receptor	Turk et al. (2004)
Folic acid	Liposomes	FA receptor	Goren et al. (2000)
Folic acid	Polymeric micelles	FA receptor	Yoo and Park (2004)
Folic acid	Thermosensitive gels	FA receptor	Nayak et al. (2004)
Folic acid	Micelles	FA receptor	Lu et al. (2014)
Folic acid	Polymeric micelles	FA receptor	Funhoff et al. (2005)
Folic acid	Polymeric micelles	FA receptor	Lee et al. (2003)
Transferrin	Gold NPs	Trans receptor	Li et al. (2009)
Transferrin	MNPs	Trans receptor	Yan et al. (2013)
Transferrin	PLGA NPs	Trans receptor	Frasco et al. (2015)
Transferrin	PLGA NPs	Trans receptor	Zheng et al. (2010)
Transferrin	Gold NPs	Trans receptor	Choi et al. (2010)
Transferrin	Polyphosphoester micelles	Trans receptor	Zhang et al. (2012)
EGF	Iron oxide	EGFR	Creixell et al. (2010)
Lactobionic acid	Dendrimers	ASGPR	Guo et al. (2012)
Antibody-EGF	PLGA NPs	EGFR	Acharya et al. (2009)
Heptameric Z^{EGFR} domain	Ni-NPs	EGFR	Benhabbour et al. (2012)
Aptamers	Gold NPs	EGFR	Melancon et al. (2014)
A10 aptamer	Polymeric NPs	PSMA	Farokhzad et al. (2006); Cheng et al.2007
A9 CGA aptamer	Gold NPs	PSMA	Kim et al. (2010)
F3 peptide	Iron oxide NPs	Nucleolin	Park et al. (2008)
scFv	Liposome	HER2	Kirpotin et al. (2006)
TPP	Polymeric NPs	Mitochondria	Marrache and Dhar (2012)
iRGD	Iron oxide NPs	αvβ3	Sugahara et al. (2009)
c(RGDfk)	Polymeric NPs	$\alpha_v\beta_3$ integrin	Graf et al. (2012)
RGD	Liposome	αvβ3	Guo et al. (2014)
F(ab′)2	Liposome	GAH	Hamaguchi et al. (2004)
F(ab′)	Liposome	HER2	Park et al. (2002)
KLWVLPKGGGC	Polymeric NPs	Collagen IV	Kamaly et al. (2013)
ACUPA	Polymeric NPs	PSMA	Hrkach et al. (2012)
CGNKRTRGC (LyP-1)	Protein NPs	gC1qR (p32)	Karmali et al. (2009)

study, folate-conjugated chitosan NPs showed greater cytotoxicity and uptake in folate receptor expressing cells (Song et al. 2013).

Transferrin receptors (TfRs) are expressed in all nucleated cells in the body, such as red blood cells, erythroid cells, hepatocytes, intestinal cells, monocytes (macrophages), and the BBB (Zhong et al. 2001). Transferrin (Tf), an iron-binding plasma glycoprotein of approximately 80 kDa, is crucial for the cellular transport of iron mediated by cell surface transferrin receptors (TfRs) (Qian et al. 2002a, b). Tf has been widely used to target cells overexpressing TfRs. Tf modified polyphosphoester micelles demonstrated stronger anti-glioma activity in mice bearing intracranial U87 MG glioma (Zhang et al. 2012). Tf coated gold NPs showed greater uptake in non parenchymal cells than that of lesser uptake in hepatocytes. Tf targeted NPs have shown greater intracellular delivery of therapeutic agents than non targeted NPs (Choi et al. 2010). Tf-conjugated PLGA NPs showed enhanced aromatase inhibition activity than non targeted PLGA NPs (Zheng et al. 2010). Tf has enhanced the targeted delivery of bortezomib-loaded PLGA NPs to pancreatic cancer (Frasco et al. 2015). Tf-conjugated NPs of poly(lactide)-tocopheryl polyethylene glycol succinate (PLA-TPGS) have effectively crossed the BBB (Gan and Feng 2010). Tf-coated PEGylated albumin NPs enhanced the brain localisation of antiviral drug azidothymidine (Mishra et al. 2006). Tf-coated fluorescein-loaded MNPs crossed the BBB effectively (Yan et al. 2013). It has been reported that BBB permeability was enhanced by vectorising NSMs with Tf (Roney et al. 2005). Tf-coated gold NPs showed four times greater cellular uptake by cancerous cells than normal cells (Li et al. 2009). Tf-conjugated paclitaxel loaded NPs showed greater antiproliferative activity of the drug due to their more cellular uptake and reduced exocytosis (Sahoo and Labhasetwar 2005).

Hepatocellular carcinoma or liver cancer cells overexpress asialoglycoprotein receptors (ASGPR). Lactobionic acid (LA)-modified G5 PAMAM dendrimers with terminal acetyl group have shown targeted delivery to liver cancer cells overexpressing ASGPR (Guo et al. 2012). In a recent study, LA modified dendrimers has been used for targeted delivery to HepG2 cells. Dendrimers modified with LA have shown specific targeted delivery to ASGPR overexpressing liver cancer cells (Fu et al. 2014).

Epidermal growth factor receptor (EGFR) signaling pathways have also been exploited for targeted delivery to different types of cancers. Heptameric Z^{EGFR} domain conjugated Ni-NPs has been targeted to the highly EGFR overexpressing epidermoid carcinoma cells. Targeted Ni-NPs showed up to 90 % internalization in cells (Benhabbour et al. 2012). Gold nanospheres conjugated to EGFR-targeting aptamers showed selective binding to EGFR and more tumor uptake (Melancon et al. 2014). Antibody-EGFR conjugated PLGA NPs loaded with rapamycin showed the better antiproliferative activity than unconjugated NPs and blank rapamycin due to higher cellular internalization in malignant breast cancer cells. Western blotting revealed the involvement of a cytoplasmic protein in activating the programmed cell death pathway (Acharya et al. 2009). Epidermal growth factor (EGF)-containing polyamidoamine dendrimers can localize within cells that express the EGFR in a receptor-dependent manner, whereas uptake into cells lacking the receptor was low (Yuan et al. 2010). EGF-conjugated iron oxide MNPs were reported to accumulate very fast in both small vesicles and large circular endocytic structures through clathrin-dependent and clathrin-independent receptors mediated endocytosis pathways (Creixell et al. 2010). Integrins are overexpressed in tumor cells compared to normal endothelial cells. Arginylglycylaspartic acid (RGD) modified liposomes have been used for targeted delivery to αvβ3 integrin positive melanoma B16 cells. RGD modified liposomes have demonstrated strongest interaction with melanoma B16 cells and shown enhanced cellular uptake via clathrin-dependent pathway (Guo et al. 2014). Cyclic pentapeptide c(RGDfk) conjugated polymeric NPs with cisplatin encapsulated in the core has been used for targeted delivery to $\alpha_v\beta_3$ integrin expressing MCF-7 cells. Their in vitro cytotoxicity was enhanced 6-fold

in MCF-7 breast cancer cells (Graf et al. 2012). Triphenylphosphonium (TPP) and its derivatives are used for mitochondria targeting (Smith et al. 2003; Marrache and Dhar 2012). TPP is a cationic, and hydrophobic molecule that can penetrate easily through the cell membrane. An investigation has indicated that the positively charged TPP could accumulate several hundred folds within mitochondria (Smith et al. 2003). TPP modified NPs showed efficient internalization and escape from the endosomal compartment when their size was around 100 nm and their zeta potential was higher than +22 mV (Smith et al. 2003).

1.6 Various Nanoscale Materials in Drug Delivery

1.6.1 Polymeric Nanoparticles

Polymeric NPs (Fig. 1.3) are colloidal particles in which drug of interest can be embedded or encapsulated within their matrix or adsorbed or conjugated onto the surface of NPs. Polymeric NPs protect the drug form premature degradation, increase efficacy of drugs, increase half life in blood and provide controlled and sustained release to encapsulated drugs. These NPs have been exploited as a vehicle for delivery of a number of biomolecules, drugs, genes, and vaccines. These NPs are discussed in detail in Chap. 2 of this book.

1.6.2 Metallic Nanoparticles

The term metal NPs (Fig. 1.3) is used to describe nanosized metals with dimensions (length, width or thickness) within the size range of 1–100 nm. These materials are of prime interest due to their large surface-area-to-volume ratio as compared to the bulk equivalents, large surface energies, easy transition between molecular and metallic states providing specific electronic structures, plasmon excitation, quantum confinement, etc. These materials can be synthesized and modified with various chemical functional groups which allow them to be conjugated with different biomolecules and thus opening a wide range of potential applications in biotechnology and other industries. This part has been covered in detail in Chap. 3 of this book.

1.6.3 Liposomes

Liposomes are spherical vesicles with a phospholipid bilayer which have been extensively used in drug and gene delivery. Liposomes (Fig. 1.3) protect therapeutic agents from premature degradation, deliver it at target site and are versatile enough to allow tagging of small molecules for targeted delivery (Felnerova et al. 2004). Liposomes are synthesized by using cationic lipids, anionic lipids, or neutral lipids depending upon the mode of use and drug to be encapsulated. Liposomes solely composed of charged lipids may not be suitable for drug delivery because they do not form charged vesicles that are capable of entrapping drug molecules (Shi et al. 2002). We have elaborated detailed information about liposome in Chap. 4 of this book.

1.6.4 Quantum Dots

The development of novel semiconductor quantum dots (QDs), is considered a valuable supplement to the conventional fluorescent proteins and organic dyes. These materials are usually refer to the II–VI, III–V, and IV–VI binary and their alloyed semiconductor materials having confined size in the nanoscale range of $\sim 1-20$ nm. Advantages of using QDs include their high end optical performance with good photostability, high quantum yield (QY), narrow, symmetrical, and size-tunable emission spectra coupled with wide absorption spectra, etc., which have attracted tremendous attention amongst all branches of science. This part has been partially covered in Chap. 3 of this book.

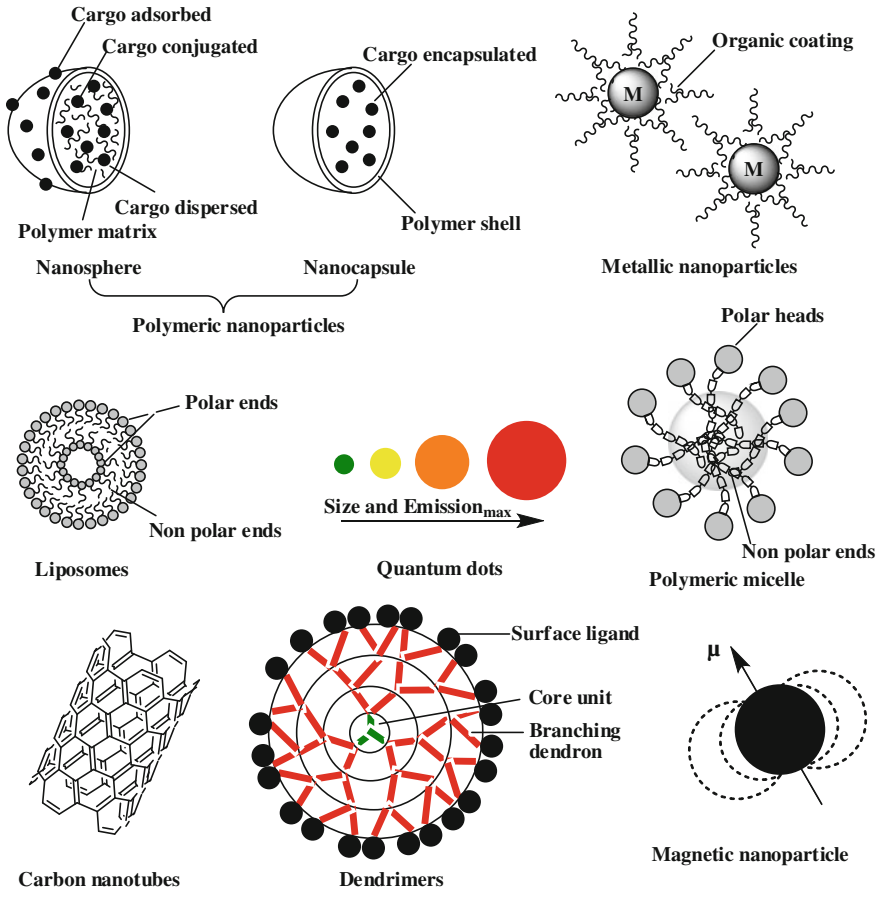

Fig. 1.3 Various nanoscale materials used for targeted drug delivery

1.6.5 Polymeric Micelles

Polymeric micelles are NSMs which have small size and high structural stability (Yamamoto et al. 2007). Polymeric micelles are of three types, viz., amphiphilic micelles, polyion complex micelles and micelles formed through metal ion complexation (Gaucher et al. 2005). Polymers that have been used as hydrophobic segment in polymeric micelles are poly(propylene glycol) (PPO, Pluronics®) (Marin et al. 2002), poly(aspartic acid) with chemically conjugated doxorubicin (PAsp(DOX)) (Yokoyama et al.1998), poly (β-benzyl-L-aspartate) (PBLA) (Kwon et al.1995), and poly(ester)s such as poly(lactic acid) (PLA) (Liggins and Burt 2002), poly (ε-caprolactone) (PCL) (Allen et al. 2000), and poly (trimethylenecarbonate) (PTMC) (Zhang et al. 2006). Stability, drug loading and drug release profile are affected by core forming material. Micelles are formed at critical micellar concentration commonly known as CMC (Rijcken et al. 2007).

Conventional micelles are rapidly eliminated from the blood circulation. To increase persistence time in blood, surface of micelles is modified with hydrophilic polymers. Among all, PEG is the most commonly used hydrophilic polymer for increasing half life inside the blood (Gaucher et al. 2005). PEG forms a brush like corona projecting out from the surface of polymeric micelles and prevents opsonin adsorption and clearance by mononuclear phagocytic system (Kwon 2003). Stealth properties and half life of PEG-b-PDLLA micelles have been

enhanced by attaching anionic peptidyl ligand on the surface of micelles (Yamamoto et al. 2001). Micelles have also been used for targeted drug delivery by attaching ligands, receptors or antibodies to the hydrophilic segment. Ligand-tagged micelles showed greater cellular uptake and improved efficacy than unmodified counterparts (Gaucher et al. 2005). Physical entrapment or chemical conjugation has been used for loading drugs into micelles (Gaucher et al. 2005). Oil-in-water emulsion, dialysis and solid dispersion methods have been used for loading drugs into the core of micelles. Many factors such as the length of the core forming polymer segment, affinity between the drug and the core, and the amount of the loaded drug affect the release profile of drug from polymeric micelles (Huh et al. 2005). Diffusion and partition coefficient of the drug from the micellar core and diffusion affect the release of physically adsorbed drug from polymeric micelles.

1.6.6 Carbon Nanotubes

The carbon nanotubes (CNTs) are NSMs that have wide applicability in the nanotechnology, electronic devices (Frank et al. 1998; Kong et al. 1999), gas storage media (Liu et al. 1999) and nanotweezers (Kim and Lieber 1999). The high aspect ratio, high conductivity and intrinsic strength of carbon–carbon sp^2 bond (Ijima 1991) are unique properties that give them highest strength and conductivity (Wong et al. 1997; Ajayan et al. 2000). CNTs are of two types viz single walled nanotubes (SWCNTs) and multi walled nanotubes (MWCNTs). SWCNTs consist of a single graphite sheet wrapped into a cylindrical tube and MWCNTs comprise an array of nanotubes one concentrically placed inside another like rings of a tree trunk (Qian et al. 2002a, b). CNTs have been synthesized by arc discharge (Zeng et al. 1998), laser ablation (Ma et al. 2000), carbon monoxide disproportionation (Herreyre and Gadelle 1995), chemical vapor deposition (CVD) (Benito et al. 1998), and hydrothermal method (Gogotsia and Libera 2000). The CNTs synthesized by the above methods are mixture of varied dimensions and chirality of CNTs and often contaminated with metallic and amorphous impurities. SWCNTs can undergo reactions not at the ends and defect sites, but along the side walls also and unique mechanical and electronic properties can be changed by the controlled chemical functionalisation (Banerjee et al. 2005). The interfacial interaction of MWCNTs with the matrix has been improved by attaching epoxy functional group to the nanotubes (Gojny et al. 2003). MWCNTs have been silanized using a coupling agent, 3-aminopropyltriethoxysilane (3-APTES) (Kathi and Rhee 2008) to improve the chemical compatibility of MWCNTs with specific polymers for application in nanotube-based polymer matrix composites. Gold NPs has been attached on CN to enhance the potential applications for the generation of electrical, optical, and sensor devices (Jiang and Gao 2003). Drug loading to CNTs has been done by incorporation at the time of synthesis or by adsorption method where the drug is loaded after the synthesis of nanoparticle (Singh and Lillard 2009). Drugs can be loaded by covalent conjugation or by non covalent supramolecular chemistry via π-π stacking (Liu et al. 2009). The drug release from CNTs can be modulated by varying pH and temperature of reaction conditions. Cellular uptake mechanism of CNTs is determined by functional nature of the functional groups attached on the surface of CNTs and may vary depending on the size of the CNTs, including endocytosis or passive diffusion. PVA/halloysite nanotubes (HNTs) favored fibroblasts attachment and growth (Zhou et al. 2010). Doxorubicin-PEG-Folic acid (DOX/PEG-FA/SWCNTs) attached to cell membrane of HeLa cells by folic acid (FA) and entered the lysosomes or endosomes by clathrin-mediated endocytosis. DOX is released in the acidic environment of lysosomes and migrated into nucleus to inhibit transcription by binding to DNA and induced cell death (Niu et al. 2013).

1.6.7 Dendrimers

The dendrimer is a macromolecule which is highly branched, monodispersive, symmetric, and spherical three-dimensional polymeric molecules having a well-defined molecular mass

(Newkome et al. 1985; Tomalia et al. 1985). Surface of dendrimers provide a high degree of versatility and can be modified using various functionalities. Bioactive agents can also be encapsulated or conjugated on the surface of dendrimers (Tomalia and Frechet 2002). Three components of dendrimers are core, branches, and surface moieties (Buhleier et al. 1978; Newkome et al. 1985; Tomalia et al. 1985). Dendrimers have been widely used in the field of chemistry and biology, especially in applications like drug delivery, gene therapy, and chemotherapy. Dendrimers have been synthesized by repeated reaction sequence through the selection of a suitable initiator which can be transformed into a core, the core then react with a number of molecules of high molecular weight, to form branched dendrimers (Tomalia and Frechet 2002). The synthesis methods used for dendrimer preparation allow control over parameters such as size, shape, surface/interior chemistry, flexibility, and topology.

Dendrimers properties like biological stability, efficacy, purity and long shelf life allow their use as drug delivery vehicles. Physical entrapment or chemical conjugation methods are used for loading of drugs on dendrimers. The drug molecule is released inside the cells by in vivo break down of covalent bond between the drug and dendrimer in the presence of suitable environment or enzymes. The another mechanism for releasing the drug depends on variation in pH and temperature inside the cells (Mishra 2011).

Charge density and flexibility of dendrimers determine the cellular uptake of drugs (Morgan et al. 2006). The G-4 polypropylenimine dendrimers showed 14-fold increase in the cellular uptake of a 31 nucleotide triplex-forming oligonucleotide (ODN) in MDA-MB-231 breast cancer cells (Santhakumaran et al. 2004). Dendrimers improved availability and antiproliferative activity of ODN within cells. The SWCNT surface modified dendrimers showed intracellular delivery by endocytosis but the uncoated SWCNT were unable to traverse the cell membranes (Pan et al. 2007). The 10-hydroxy camptothecin load dendrimers enhanced the cellular uptake and also increased the half-life of the drug in cancer cell lines (Morgan et al. 2006).

1.6.8 Magnetic Nanoparticles

The magnetic nanoparticles (MNPs) are of great interest to the scientists from the last few decades due to their great magnetic properties for the use in various novel applications from high density data storage to biomedical applications. The surface of MNPs allows their attachment to the functional molecules which provide the magnetic behavior to the target (Ahn et al. 2004). It helps to manipulate and transport the molecules to the desired target organ by controlling the magnetic field produced. The three functional parts of a MNP carrier are magnetic core, a surface coat and a functional outer coating (Vatta et al. 2006). The magnetic core consists of a supermagnetic molecule whose composition depends upon the application. The detail description about MNPs will be covered in Chap. 3 of this book.

1.7 Conclusions

In summary, NSMs are important candidates for pharmaceutical industry and for the delivery of therapeutic agents. They have advantages over conventional carriers. NSMs tend to improve the efficacy and bioavailability of many therapeutic agents which are otherwise difficult to deliver. NSMs increase the half-life and persistence of many therapeutic agents; ultimately increase their therapeutic index. Surface modified NSMs with ligands increase the targeting ability and specificity of many therapeutic cargos. Surface modification of NSMs offers way for increasing cellular uptake and binding. Passive and active targeting will enhance the effectiveness and specificity of NSMs. NSMs like polymeric NPs, metallic NPs, liposomes, QDs, polymeric micelles, CNTs, dendrimers, and MNPs hold great potential for targeted delivery of drugs. The smart designing of NSMs may lead to many therapeutic agents into clinical trials.

Acknowledgments We are grateful to the Director, CSIR-IHBT for providing valuable suggestions and motivations. Financial assistance from Council of Scientific and Industrial Research, Government of India is genuinely acknowledged.

References

Acharya A (2013) Luminescent magnetic quantum dots for in vitro/in vivo imaging and applications in therapeutics. J Nanosci Nanotechnol 13(6):3753–3768

Acharya S, Dilnawaz F, Sahoo SK (2009) Targeted epidermal growth factor receptor nanoparticle bioconjugates for breast cancer therapy. Biomaterials 30:5737–5750

Ahn CH, Choi JW, Cho HJ (2004) Nanomagnetics for biomedical applications. In: Nalwa HS (ed) Encyclopedia of nanoscience and nanotechnology, vol 6. American Scientific Publishers, Stevenson Ranch, pp 815–821

Ajayan PM, Schadler LS, Giannaris C et al (2000) Single-walled carbon nanotube-polymer composites: strength and weakness. Adv Mater 12:750–753

Allen C, Han J, Yu Y et al (2000) Polycaprolactone-bpoly (ethylene oxide) copolymer micelles as a delivery vehicle for dihydrotestosterone. J Control Release 63:275–286

Ashley CE, Carnes EC, Phillips GK et al (2011) The targeted delivery of multicomponent cargos to cancer cells by nanoporous particle-supported lipid bilayers. Nature Mater 10:389–397

Banerjee S, Benny TH, Wong SS (2005) Covalent surface chemistry of single walled nanotubes. Adv Mater 17:17–29

Beckera C, Hodeniusb M, Blendingera G et al (2007) Uptake of magnetic nanoparticles into cells for cell tracking. J Magn Magn Mater 311:234–237

Beduneau A, Saulnier P, Hindre F et al (2007) Design of targeted lipid nanocapsules by conjugation of whole antibodies and antibody Fab' fragments. Biomaterials 28:4978–4990

Benhabbour SR, Luft JC, Kim D et al (2012) In vitro and in vivo assessment of targeting lipid-based nanoparticles to the epidermal growth factor-receptor (EGFR) using a novel Heptameric Z^{EGFR} domain. J Control Release 158:63–71

Benito AM, Maniette Y, Munoz E et al (1998) Carbon nanotubes production by catalytic pyrolysis of benzene. Carbon 36:681–683

Buhleier E, Wehner W, Vogtle F (1978) Cascade and nonskid-chain-like synthesis of molecular cavity topologies. Synthesis 2:155–158

Campbell RB, Fukumura D, Brown EB et al (2002) Cationic charge determines the distribution of liposomes between the vascular and extravascular compartments of tumors. Cancer Res 62:6831–6836

Canal F, Vicent MJ, Pasut G et al (2010) Relevance of folic acid/polymer ratio in targeted PEG-epirubicin conjugates. J Control Release 146:388–399

Cao G (ed) (2004) Nanostructures and nanomaterials, synthesis, properties and applications. Imperial College Press, London

Chauhan VP, Popović Z, Chen O et al (2011) Fluorescent nanorods and nanospheres for real-time in vivo probing of nanoparticle shape-dependent tumor penetration. Angew Chem Int Ed Eng 50:11417–11420

Cheng J, Teply BA, Sherifi I et al (2007) Formulation of functionalized PLGA-PEG nanoparticles for in vivo targeted drug delivery. Biomaterials 28:869–876

Choi CHJ, Alabi CA, Webster P et al (2010) Mechanism of active targeting in solid tumors with transferrin-containing gold nanoparticles. Proc Natl Acad Sci 107:1235–1240

Creixell M, Herrera AP, Ayala V et al (2010) Preparation of epidermal growth factor (EGF) conjugated iron oxide nanoparticles and their internalization into colon cancer cells. J Magn Magn Mater 322:2244–2250

Das B, Subramaniam S, Melloch MR (1993) Effects of electron-beam-induced damage on leakage currents in back-gated GaAs/AlGaAs devices. Semicond Sci Technol 8:1347

DeAssis DN, Mosqueira VC, Vilela JM et al (2008) Release profiles and morphological characterization by atomic force microscopy and photon correlation spectroscopy of 99 m Technetium– fluconazole nanocapsules. Int J Pharm 349:152–160

Deckert PM (2009) Current constructs and targets in clinical development for antibodybased cancer therapy. Curr Drug Targets 10:158–175

Dinauer N, Balthasar S, Weber C et al (2005) Selective targeting of antibody-conjugated nanoparticles to leukemic cells and primary T-lymphocytes. Biomaterials 26:5898–5906

Dixit V, Van den Bossche J, Sherman DM et al (2006) Synthesis and grafting of thioctic acid-PEG-folate conjugates onto Au nanoparticles for selective targeting of folate receptor-positive tumor cells. Bioconjugate Chem 17:603–609

El-Gogary RI, Rubio N, Wang JT et al (2014) Polyethylene glycol conjugated polymeric nanocapsules for targeted delivery of quercetin to folate-expressing cancer cells in vitro and in vivo. ACS Nano 8:1384–1401

Farokhzad OC, Cheng J, Teply BA et al (2006) Targeted nanoparticle-aptamer bioconjugates for cancer chemotherapy in vivo. Proc Natl Acad Sci 103:6315–6320

Felnerova D, Viret JF, Gluck R et al (2004) Liposomes and virosomes as delivery systems for antigens, nucleic acids and drugs. Curr Opin Biotechnol 15:518–529

Frank S, Poncharal P, Wang ZL et al (1998) Carbon nanotube quantum resistors. Science 280:1744–1746

Frasco MF, Almeida GM, Santos-Silva F et al (2015) Transferrin surface-modified PLGA nanoparticles-mediated delivery of a proteasome inhibitor to human

pancreatic cancer cells. J Biomed Mater Res Part A103A:1476–1484

Fu F, Wu Y, Zhu J et al (2014) Multifunctional lactobionic acid-modified dendrimers for targeted drug delivery to liver cancer cells: investigating the role played by PEG Spacer. ACS Appl Mater Interfaces 6:16416–16425

Funhoff AM, Monge S, Teeuwen R et al (2005) PEG shielded polymeric double-layered micelles for gene delivery. J Control Release 102:711–724

Gan CW, Feng SS (2010) Transferrin-conjugated nanoparticles of poly(lactide)-D-α-tocopheryl polyethylene glycol succinate diblock copolymer for targeted drug delivery across the blood-brain barrier. Biomaterials 31:7748–7757

Gaucher G, Dufresne MH, Sant VP et al (2005) Block copolymer micelles: preparation, characterization and application in drug delivery. J Control Release 109:169–188

Gogotsia Y, Libera JA (2000) Hydrothermal synthesis of multiwall carbon nanotubes. J Mater Res 15:2591–2594

Gojny FH, Nastalczyk J, Roslaniec Z et al (2003) Surface modified multi-walled carbon nanotubes in CNT/epoxy-composites. Chem Phys Lett 370:820–824

Goren D, Horowitz AT, Tzemach D et al (2000) Nuclear delivery of doxorubicin via folate targeted liposomes with bypass of multidrug resistance efflux pump. Clin Cancer Res 6:1949–1957

Gou M, Zheng X, Men K et al (2009) Poly (epsilon-caprolactone)/poly(ethylene glycol)/poly (epsilon-caprolactone) nanoparticles: Preparation, characterization, and application in doxorubicin delivery. J Phys Chem B 113:12928–12933

Graf N, Bielenberg DR, Kolishetti N et al (2012) αVβ3 integrin-targeted PLGA-PEG nanoparticles for enhanced anti-tumor efficacy of a Pt(IV) prodrug. ACS Nano 6:4530–4539

Guo R, Yao Y, Cheng G et al (2012) Synthesis of glycoconjugated poly(amindoamine) dendrimers for targeting human liver cancer cells. RSC Adv 2:99–102

Guo Z, He B, Jin H et al (2014) Targeting efficiency of RGD-modified nanocarriers with different ligand intervals in response to integrin αvβ3 clustering. Biomaterials 35:6106–6117

Hamaguchi T, Matsumura Y, Nakanishi Y et al (2004) Antitumor effect of MCC-465, pegylated liposomal doxorubicin tagged with newly developed monoclonal antibody GAH, in colorectal cancer xenografts. Cancer Sci 95:608–613

He C, Hu Y, Yin L et al (2010) Effects of particle size and surface charge on cellular uptake and biodistribution of polymeric nanoparticles. Biomaterials 31:3657–3666

Herreyre S, Gadelle P (1995) Effect of hydrogen on the morphology of carbon deposited from the catalytic disproportionation of CO. Carbon 33:234–237

Ho EA, Ramsay E, Ginj M et al (2010) Characterization of cationic liposome formulations designed to exhibit extended plasma residence times and tumor vasculature targeting properties. J Pharm Sci 99:2839–2853

Hong M, Zhu S, Jiang Y et al (2009) Efficient tumor targeting of hydroxycamptothecin loaded PEGylated niosomes modified with transferring. J Control Release 133:96–102

Hrkach J, Von Hoff D, Ali MM et al (2012) Preclinical development and clinical translation of a PSMA-targeted docetaxel nanoparticle with a differentiated pharmacological profile. Sci Transl Med 4:128–139

Huh KM, Lee SC, Cho YW et al (2005) Hydrotropic polymer micelle system for delivery of paclitaxel. J Control Release 101:59–68

Ijima S (1991) Helical microtubes of graphitic carbon. Nature 354:56–58

Iqbal P, Preece JA, Paula M (2012) The "top-down" and "bottom-up" approaches. In: Steed JW (ed) Supramolecular chemistry: from molecules to nanomaterials. Wiley, Gale PA

Iyer AK, Khaled G, Fang J et al (2006) Exploiting the enhanced permeability and retention effect for tumor targeting. Drug Discov Today 11:812–818

Jiang L, Gao L (2003) Modified carbon nanotubes: An effective way to selective attachment of gold nanoparticles. Carbon 41:2923–2929

Kamaly N, Fredman G, Subramanian M et al (2013) Development and in vivo efficacy of targeted polymeric inflammation-resolving nanoparticles. Proc Natl Acad Sci 110:6506–6511

Karmali PP, Kotamraju VR, Kastantin M et al (2009) Targeting of albumin-embedded paclitaxel nanoparticles to tumors. Nanomedicine 5:73–82

Kathi J, Rhee KY (2008) Surface modification of multi-walled carbon nanotubes using 3-amino propyltriethoxysilane. J Mater Sci 43:33–37

Kim P, Lieber CM (1999) Nanotube nanotweezers. Science 286:2148–2150

Kim D, Jeong YY, Jon S (2010) A drug-loaded aptamer–gold nanoparticle bioconjugate for combined ct imaging and therapy of prostate cancer. ACS Nano 4:3689–3696

Kirpotin DB, Drummond DC, Shao Y et al (2006) Antibody targeting of long-circulating lipidic nanoparticles does not increase tumor localization but does increase internalization in animal models. Cancer Res 66:6732–6740

Kong J, Zhou C, Morpurgo A et al (1999) Synthesis, integration, and electrical properties of individual single-walled carbon nanotubes. Appl Phys A Mater 69:305–308

Krasnici S, Werner A, Eichhorn ME et al (2003) Effect of the surface charge of liposomes on their uptake by angiogenic tumor vessels. Int J Cancer 105:561–567

Kumar V, Yadav SK (2009) Plant-mediated synthesis of silver and gold nanoparticles and their applications. J Chem Tech Biotech 84:151–157

Kumar V, Kumari A, Kumar D et al (2014) Biosurfactant stabilized anticancer biomolecule-loaded poly (D, L-lactide) nanoparticles. Colloid Surf B 117:505–511

Kumari A, Yadav SK, Yadav SC (2010) Biodegradable polymeric nanoparticles based drug delivery systems. Colloids Surf B 75:1–18

Kumari A, Yadav SK, Pakade YB et al (2011) Nanoencapsulation and characterization of Albizia chinensis isolated antioxidant quercitrin on PLA nanoparticles. Colloid Surf B 82:224–232

Kumari A, Kumar V, Yadav SK (2012) Plant extract synthesized PLA nanoparticles for controlled and sustained release of quercetin: a green approach. PLoS ONE 7(7):e41230

Kunjachan S, Pola R, Gremse F et al (2014) Passive versus active tumor targeting using rgd- and ngr-modified polymeric nanomedicines. Nano Lett 14:972–981

Kwon GS (2003) Polymeric micelles for delivery of poorly watersoluble compounds. Crit Rev Ther Drug Carrier Syst 20:357–403

Kwon GS, Naito M, Yokoyama M et al (1995) Physical entrapment of adriamycin in AB block-copolymer micelles. Pharm Res 12:192–195

Lee ES, Na K, Bae YH (2003) Polymeric micelle for tumor pH and folate-mediated targeting. J Control Release 9:103–113

Li J, Wang L, Liu X et al (2009) *In vitro* cancer cell imaging and therapy using transferrin-conjugated gold nanoparticles. Cancer Lett 274:319–326

Liggins RT, Burt HM (2002) Polyether-polyester diblock copolymers for the preparation of paclitaxel loaded polymeric micelle formulations. Adv Drug Delivery Rev 54:191–202

Liu C, Fan YY, Liu M et al (1999) Hydrogen storage in single-walled carbon nanotubes at room temperature. Science 286:1127–1129

Liu Z, Tabakman S, Welsher K et al (2009) Carbon nanotubes in biology and medicine: In vitro and in vivo detection, imaging and drug delivery. Nano Res 2:85–120

Liu J, Yu M, Zhou C et al (2013) Passive tumor targeting of renal-clearable luminescent gold nanoparticles: long tumor retention and fast normal tissue clearance. J Am Chem Soc 135:4978–4981

Logothetidis S (2006) Nanotechnology in medicine: the medicine of tomorrow and nanomedicine. Hippokratia 10:7–21

López-Serrano A, Olivas RM, Landaluze JS et al (2014) Nanoparticles: A global vision. Characterization, separation, and quantification methods. Potential environmental and health impact. Anal Methods 6:38–56

Lu J, Zhao W, Huang Y et al (2014) Targeted delivery of doxorubicin by folic acid decorated dual functional nanocarrier. Mol Pharm 11:4164–4178

Lukyanov AN, Hartner WC, Torchilin VP (2004) Increased accumulation of PEG–PE micelles in the area of experimental myocardial infarction in rabbits. J Control Release 94:187–193

Ma RZ, Wei BQ, Xu CL et al (2000) The morphology changes of carbon nanotubes under laser irradiation. Carbon 38:636–638

Madaan K, Kumar S, Poonia N et al (2014) Dendrimers in drug delivery and targeting: Drug-dendrimer interactions and toxicity issues. J Pharm Bioallied Sci 6:139–150

Maeda H (2001) The enhanced permeability and retention (EPR) effect in tumor vasculature: the key role of tumor-selective macromolecular drug targeting. Adv Enzyme Regul 41:189–207

Maeda H, Sawa T, Konno T (2001) Mechanism of tumor-targeted delivery of macromolecular drugs, including the EPR effect in solid tumor and clinical overview of the prototype polymeric drug SMANCS. J Control Release 74:47–61

Marin A, Sun H, Husseini GA et al (2002) Drug delivery in pluronic micelles: effect of high-frequency ultrasound on drug release from micelles and intracellular uptake. J Control Release 84:39–47

Marrache S, Dhar S (2012) Engineering of blended nanoparticle platform for delivery of mitochondria-acting therapeutics. Proc Natl Acad Sci 109:16288–16293

Matsumura Y, Maeda H (1986) A new concept for macromolecular therapeutics in cancer chemotherapy: mechanism of tumoritropic accumulation of proteins and the antitumor agent smancs. Cancer Res 46:6387–6392

Melancon MP, Zhou M, Zhang R et al (2014) Selective uptake and imaging of aptamer- and antibody-conjugated hollow nanospheres targeted to epidermal growth factor receptors overexpressed in head and neck cancer. ACS Nano 8:4530–4538

Meng H, Xue M, Xia T et al (2011) Use of size and a copolymer design feature to improve the biodistribution and the enhanced permeability and retention effect of doxorubicin-loaded mesoporous silica nanoparticles in a murine xenograft tumor model. ACS Nano 5:4131–4144

Morgan MT, Nakanishi Y, Kroll DJ et al (2006) Dendrimer-encapsulated camptothecins: increased solubility, cellular uptake, and cellular retention affords enhanced anticancer activity in vitro. Cancer Res 66:11913–11921

Mishra I (2011) Dendrimer: a novel drug delivery system. J Drug Deliv Ther 1:70–74

Mishra V, Mahor S, Rawat A et al (2006) Targeted brain delivery of AZT via transferrin anchored pegylated albumin nanoparticles. J Drug Target 14:45–53

Mo Y, Lim LY (2005) Preparation and in vitro anticancer activity of wheat germ agglutinin (WGA)-conjugated PLGA nanoparticles loaded with paclitaxel and isopropyl myristate. J Control Release 107:30–42

Mohanpuria P, Rana NK, Yadav SK (2008) Biosynthesis of nanoparticles: technological concepts and future applications. J Nanopart Res 10:507–517

Mohanraj VJ, Chen Y (2006) Nanoparticles: A review. Trop J Pharm Res 5:561–573

Molpeceres J, Aberturas MR, Guzman M et al (2000) Biodegradable nanoparticles as a delivery system for cyclosporine: preparation and characterization. J Microencapsul 17:599–614

Nayak S, Lee H, Chmielewski J et al (2004) Folate-mediated cell targeting and cytotoxicity using thermoresponsive microgels. J Am Chem Soc 126:10258–10259

Newkome GR, Yao ZQ, Baker GR, Gupta VK (1985) Cascade molecules: A new approach to micelles. J Org Chem 50:2003–2006

Nigam P, Waghmode S, Louis M et al (2014) Graphene quantum dots conjugated albumin nanoparticles for targeted drug delivery and imaging of pancreatic cancer. J Mater Chem B 2:3190–3195

Niu L, Meng L, Lu Q (2013) Folate-conjugated PEG on single walled carbon nanotubes for targeting delivery of doxorubicin to cancer cells. Macromol Biosci 13:735–744

Pan BF, Cui DX, Xu P et al (2007) Cellular uptake enhancement of polyamidoamine dendrimer modified single walled carbon nanotubes. JBPE 1:13–16

Park JW, Hong K, Kirpotin DB et al (2002) Anti-HER2 immunoliposomes: Enhanced efficacy attributable to targeted delivery. Clin Cancer Res 8:1172–1181

Park EK, Kim SY, Lee SB et al (2005) Folate-conjugated methoxy poly(ethylene glycol)/poly(ε-caprolactone) amphiphilic block copolymeric micelles for tumor-targeted drug delivery. J Control Rel 109:158–168

Park H, Maltzahn GV, Zhang L et al (2008) Magnetic iron oxide nanoworms for tumor targeting and imaging. Adv Mater 20:1630–1635

Polakovic M, Görner T, Gref R et al (1999) Lidocaine loaded biodegradable nanospheres: II. Modelling of drug release. J Control Rel 60:169–177

Qian D, Wagner GJ, Liu WK (2002a) Mechanics of carbon nanotubes. Appl Mech Rev 55:495–533

Qian ZM, Li H, Sun H et al (2002b) Targeted drug delivery via the transferrin receptor-mediated endocytosis pathway. Pharmacol Rev 54:561–587

Rijcken CJF, Soga O, Hennink WE et al (2007) Triggered destabilisation of polymeric micelles and vesicles by changing polymers polarity: An attractive tool for drug delivery. J Control Release 120:131–148

Roney C, Kulkarni P, Arora V et al (2005) Targeted nanoparticles for drug delivery through the blood–brain barrier for Alzheimer's disease. J Control Release 108:193–214

Rosenholm JM, Meinander A, Peuhu E et al (2009) Targeting of porous hybrid silica nanoparticles to cancer cells. ACS Nano 3:197–206

Sahoo SK, Labhasetwar V (2005) Enhanced antiproliferative activity of transferrin-conjugated paclitaxel-loaded nanoparticles is mediated via sustained intracellular drug retention. Mol Pharm 2:373–383

Samad A, Sultana Y, Aqil M (2007) Liposomal drug delivery systems: An update review. Curr Drug Deliv 4:297–305

Santhakumaran LM, Thomas T, Thomas TJ (2004) Enhanced cellular uptake of a triplex-forming oligonucleotide by nanoparticle formation in the presence of polypropylenimine dendrimers. Nucleic Acid Res 32:2102–2112

Schmitt-Sody M, Strieth S, Krasnici S et al (2003) Neovascular targeting therapy: Paclitaxel encapsulated in cationic liposomes improves antitumoral efficacy. Clin Cancer Res 9:2335–2341

Senthilkumar R, Karamanb DS, Paula P et al (2015) Targeted delivery of a new anticancer compound anisomelic acid using chitosan-coated porous silica nanorods for an enhanced apoptotic effect in vitro. Biomater Sci 3:103–111

Shenoy D, Little S, Langer R et al (2005) Poly(ethylene oxide)-modified poly(beta-amino ester) nanoparticles as a pH-sensitive system for tumor-targeted delivery of hydrophobic drugs: part 2. In vivo distribution and tumor localization studies. Pharm Res 22:2107–2114

Shi G, Guo W, Stephenson SM et al (2002) Efficient intracellular drug and gene delivery using folate receptor-targeted pH-sensitive liposomes composed of cationic anionic lipid combinations. J Control Release 80:309–319

Singh R, Lillard JW (2009) Nanoparticle-based targeted drug delivery. Exp Mol Pathol 86:215–223

Singh Y, Gao D, Gu Z et al (2012) Noninvasive detection of passively targeted poly(ethylene glycol) nanocarriers in tumors. Mol Pharm 9:144–155

Sinha R, Kim GJ, Nie S et al (2006) Nanotechnology in cancer therapeutics: bioconjugated nanoparticles for drug delivery. Mol Cancer Ther 5:1909–1917

Smith RAJ, Porteous CM, Gane AM et al (2003) Delivery of bioactive molecules to mitochondria in vivo. Proc Natl Acad Sci 100:5407–5412

Song H, Su C, Cui W et al (2013) Folic acid-chitosan conjugated nanoparticles for improving tumor-targeted drug delivery. BioMed Res Int 2013. doi:10.1155/2013/723158

Sugahara KN, Teesalu T, Karmali PP et al (2009) Tissue-penetrating delivery of compounds and nanoparticles into tumors. Cancer Cell 16:510–520

Tomalia DA, Frechet JMJ (2002) Discovery of dendrimers and dendritic polymers: A brief historical perspective. J Polym Sci, Part A: Polym Chem 40:2719–2728

Tomalia DA, Baker H, Dewald J et al (1985) A new class of polymers: starburst-dendritic macromolecules. Polym J 17:117–132

Torchilin VP (2000) Drug targeting. Eur J Pharm Sci 11: S81–S91

Turk MJ, Waters DJ, Low PS (2004) Folate conjugated liposomes preferentially target macrophages associated with ovarian carcinoma. Cancer Lett 213:165–172

Vatta LL, Sanderson RD, Koch KR (2006) Magnetic nanoparticles: Properties and potential applications. Pure Appl Chem 78:1793–1801

Walia S, Acharya A (2015) Silica micro/nanospheres for theranostics: from bimodal MRI and fluorescent imaging probes to cancer therapy. Beilstein J Nanotechnol 6:546–558

Wang Y, Cao X, Guo R et al (2011) Targeted delivery of doxorubicin into cancer cells using a folic acid dendrimer conjugate. Polym Chem 2:1754–1760

Werner ME, Karve S, Sukumar R et al (2011) Folate-targeted nanoparticle delivery of chemo- and radiotherapeutics for the treatment of ovarian cancer peritoneal metastasis. Biomaterials 32:8548–8554

Wohlfart S, Gelperina S, Kreuter J (2012) Transport of drugs across the blood-brain barrier by nanoparticles. J Control Release 161:264–273

Wong EW, Sheehan PE, Lieber CM (1997) Nanobeam mechanics: elasticity, strength, and toughness of nanorods and nanotubes. Science 277:1971–1975

Xiao K, Li Y, Luo J et al (2011) The effect of surface charge on in vivo biodistribution of PEG-oligocholic acid based micellar nanoparticles. Biomaterials 32:3435–3446

Yadav R, Kumar D, Kumari A et al (2014) Encapsulation of podophyllotoxin and etoposide in biodegradable poly-D, L-lactide nanoparticles improved their anti-cancer activity. J Microencapsul 31:211–219

Yamamoto Y, Nagasaki Y, Kato Y et al (2001) Long-circulating poly(ethylene glycol)–poly(D, L-lactide) block copolymer micelles with modulated surface charge. J Control Release 77:27–38

Yamamoto T, Yokoyama M, Opanasopit P et al (2007) What are determining factors for stable drug incorporation into polymeric micelle carriers? Consideration on physical and chemical characters of the micelle inner core. J Control Release 123:11–18

Yan F, Wang Y, He S et al (2013) Transferrin-conjugated, fluorescein-loaded magnetic nanoparticles for targeted delivery across the blood-brain barrier. J Mater Sci Mater Med 24:2371–2379

Yang PH, Sun X, Chiu JF et al (2005) Transferrin-mediated gold nanoparticle cellular uptake. Bioconjugate Chem 16:494–496

Yokoyama M, Fukushima S, Uehara R et al (1998) Characterization of physical entrapment and chemical conjugation of adriamycin in polymeric micelles and their design for in vivo delivery to a solid tumour. J Control Release 50:79–92

Yoo HS, Park TG (2004) Folate receptor targeted biodegradable polymeric doxorubicin micelles. J Control Release 96:273–283

Yuan Q, Lee E, Yeudall WA et al (2010) Dendrimer-triglycine-EGF nanoparticles for tumor imaging and targeted nucleic acid and drug delivery. Oral Oncol 46:698–704

Zeng H, Zhu L, Hao GM et al (1998) Synthesis of various forms of carbon nanotubes by AC arc discharge. Carbon 36:259–261

Zensi A, Begley D, Pontikis C et al (2009) Albumin nanoparticles targeted with ApoE enter the CNS by transcytosis and are delivered to neurons. J Control Release 137:78–86

Zhang Z, Grijpma DW, Feijen J (2006) Thermo-sensitive transition of monomethoxy poly(ethylene glycol)-block-poly(trimethylene carbonate) films to micellar-like nanoparticles. J Control Release 112:57–63

Zhang PC, Hu LJ, Yin Q et al (2012) Transferrin-conjugated polyphosphoester hybrid micelle loading paclitaxel for brain-targeting delivery: synthesis, preparation and in vivo evaluation. J Control Release 159:429–434

Zheng Y, Yu B, Weecharangsan W et al (2010) Transferrin-conjugated lipid-coated PLGA nanoparticles for targeted delivery of aromatase inhibitor 7α-APTADD to breast cancer cells. Int J Pharm 390:234–241

Zhong W, Lafuse WP, Zwilling BS (2001) Infection with Mycobacterium avium differentially regulates the expression of iron transport protein mRNA in murine peritoneal macrophages. Infect Immun 69:6618–6624

Zhou WY, Guo B, Liu M et al (2010) Poly(vinyl alcohol)/halloysite nanotubes bionanocomposite films: Properties and in vitro osteoblasts and fibroblasts response. J Biomed Mater Res A 93:1574–1587

Biodegradable Nanoparticles and Their In Vivo Fate

2

Avnesh Kumari, Rubbel Singla, Anika Guliani and Sudesh Kumar Yadav

Abstract

Biodegradable nanoparticles (BNPs) are seeking augmented attention for their ability to serve as a carrier for site-specific delivery of drugs, biomolecules, proteins and peptides in the body. They offer enhanced biocompatibility, better drug encapsulation and sustained release profile of a great number of drugs and biomolecules to be used in a variety of applications in nanomedicine. The use of BNPs for controlled drug delivery has shown significant therapeutic potential. Concurrently, targeted delivery technologies are becoming an increasingly important area of scientific investigation. The fate of BNPs is decided by virtue of their physiochemical properties in biological medium. Another important area which is gaining attention of researchers is the behaviour of BNPs in biological milieu. In the present chapter, efforts are made to give the readers a comprehensive outlook of the topic covering the following major points: (1) brief introduction to BNPs; (2) synthesis methodologies of BNPs; (3) characterisation of BNPs; (4) BNPs for drug delivery; (5) drug release mechanisms from BNPs; (6) targeted drug delivery using BNPs; (7) biological barriers encountered by BNPs; and (8) in vivo fate of BNPs.

Keywords

Biodegradable nanoparticles · Drug delivery · Nanomedicine · Characterisation · In vivo fate

A. Kumari · R. Singla · A. Guliani · S.K. Yadav
Department of Biotechnology, Council of Scientific and Industrial Research-Institute of Himalayan Bioresource Technology, Palampur 176061, Himachal Pradesh, India

A. Kumari · R. Singla · A. Guliani · S.K. Yadav
Academy of Scientific and Innovative Research, New Delhi, India

S.K. Yadav (✉)
Department of Biotechnology, Center of Innovative and Applied Bioprocessing (CIAB), Mohali 160071, Punjab, India
e-mail: skyt@rediffmail.com; sudesh@ciab.res.in

© Springer Science+Business Media Singapore 2016

S.K. Yadav (ed.), *Nanoscale Materials in Targeted Drug Delivery, Theragnosis and Tissue Regeneration*, DOI 10.1007/978-981-10-0818-4_2

Contents

2.1 Introduction

The field of nanotechnology is unique since it represents an enormous number of disciplines ranging from material science, physical science, biological science and medical science. The application of nanotechnology to drug delivery is expected to change the outlook of pharmaceutical and biotechnology industries in the near future (Langer 1998; Langer 1990; Whitesides 2003). Nanotechnology-based products may play vital role in adding a novel set of therapeutics to the pipeline of many existing drugs in pharmaceutical companies (Table 2.1).

Nanotechnological tools can be used to improve solubility of poorly water soluble drugs with improved targeting ability, endocytosis of drugs across tight epithelial and endothelial junctions, delivery of drugs to intracellular sites of action, and co-delivery of two or more drugs (Farokhzad and Langer 2009). Additionally, drug manufacturing companies may face obstacles in creating drugs equivalent to nanodrugs due to the manufacturing complexity of nanotechnology-based products (Farokhzad and Langer 2009). There are many nanotechnology-based drugs that have been approved for clinical use till date (Wagner et al. 2006). The majority of these nano products have improved the therapeutic efficacy and reduced the doses of clinically approved drugs. There have been considerably fewer clinical examples where nanotechnology has given new therapeutics that did not exist earlier; we find this as a promising area for nanotechnology in the future. Indeed, we expect the appearance of nanotechnology-based tools to facilitate growth and commercialisation of entirely new classes of bioactive molecules (Farokhzad and Langer 2009).

One of the important areas of nanotechnology is nanomedicine, which refers to highly precise therapeutic involvement at the molecular scale for diagnosis, prevention and treatment of diseases. Delivery of drugs using NPs is one of the important areas of nanomedicine where researchers are currently focussing. Nanomedicine involves the use of different types of NPs for improving the stability, specificity, efficacy and therapeutic activity of many useful drugs. Among NPs, BNPs have been used for improving therapeutic activity of drugs used for treatment of a variety of dreadful diseases like cancer (Mu and Feng 2003), diabetes (Damge 2007), malaria (Date et al. 2007), prion disease (Calvo et al. 2001) and tuberculosis (Ahmad et al. 2006). BNPs protect the drug from premature degradation, improve their bioavailability, increase persistence time in blood and also help in improving the cellular uptake and intracellular penetration of drugs (Alexis et al. 2008). BNPs have also been extensively used for improving efficacy and

Table 2.1 Drugs with different therapeutic activity loaded on various biodegradable nanoparticles

Name of nanoparticles	Name of drug	Therapeutic activity	Reference
PLGA	Taxol	Anticancer	Fonseca et al. (2002)
Gelatin	Taxol	Anticancer	Lu et al. (2004)
PLGA	5-fluorouracil	Anticancer	Laquintana et al. (2014)
PLGA	9-Nitrocamptothecin	Anticancer	Derakhshandeh et al. (2007)
PLGA	Cisplatin	Anticancer	Avgoustakis et al. (2002)
Chitosan	Chlorpromazine hydrochloride	Psychotic	Chalikwar et al. (2013)
PLGA	Haloperidol	Psychotic	Budhian et al. (2005)
PLA	Savoxepine	Psychotic	Leroux et al. (1996)
PLGA	Azithromycin	Antimicrobial	Azhdarzadeh et al. (2012)
PCL-PGA	Amphotericin B	Antifungal	Tang et al. (2015b)
Polycaprolactone	Amphotericin B	Antifungal	Espuelas et al. (2002)
PLA	Quercitrin	Anticancer	Kumari et al. (2011a, b)
PLA	Quercetin	Anticancer	Kumari et al. (2011a, b)
PLA	Podophyllotoxin	Anticancer	Yadav et al. (2014)
PLA	Picroliv	Hepatoprotective	Guliani et al. (2015)
Chitosan	Silymarin	Hepatoprotective	Gupta et al. (2014b)

therapeutic index of many small molecules, proteins, peptides and nucleic acids(Coester et al. 2000) (Kumari et al. 2011a, b). These NPs have drastically improved the performance of these molecules under in vivo and in vitro conditions. BNPs improve the performance of loaded drugs through controlled and sustained release. They can also be smartly designed for targeted delivery to specific organs and tissues.

BNPs are formed from natural or synthetic polymers by various well-established methods in literature (Kumari et al. 2010a, b). Natural polymers that have been extensively used for the preparation of BNPs are gelatin, albumin and chitosan. Synthetic polymers like polylactic-co-glycolic acid (PLGA), polylactic acid (PLA), and polyalkylcyanoacrylates have also been widely used for the synthesis of BNPs (Kumari et al. 2010a, b). Characterisation of synthesized blank and drug-loaded NPs is important to know their exact size, shape and surface charge. Many sophisticated techniques like scanning electron microscope (SEM), atomic force microscope (AFM) and transmission electron microscope (TEM) are used for the estimation of size and shape of BNPs (Kumari et al. 2010a, b). Surface charge of NPs is determined by zeta potential measurements (Kumar et al. 2014). Encapsulation of loaded drugs on BNPs and in vitro release of drug-loaded NPs is quantified by techniques like high performance liquid chromatography (HPLC) (Kumari et al. 2012; Kumari et al. 2012).

Conventional NPs are recognised by the body as foreign particles and are eliminated from the body by mononuclear phagocytic system (MPS). Surfaces of conventional NPs are modified with hydrophilic polymers to increase persistence time in blood. Hydrophilic polymers like polyethylene glycol (PEG) form a cloud of chains at the NPs surface which will repel plasma proteins and avoid clearance by MPS (Brigger et al. 2002). Finally, the performance of BNPs in vivo is influenced by their size, shape, surface charge and composition. Surface charge of NPs is important for determining cellular uptake and internalisation. Positively charged NPs are internalised by the cells as compared to neutral and negatively charged NPs (Shenoy and Amiji 2005). Size and shape of NPs is also vital players in determining the distribution of BNPs in different organs. NPs less than 200 nm

undergo uptake by reticuloendothelial system (RES) and are eliminated from the body (Kumari et al. 2010a, b). NPs with a hydrophilic surface and size less than 100 nm have the greatest ability to evade the MPS system (Brannon-Peppas and Blanchette 2004). Kidney and liver cells can filter NPs based on their size. Interestingly, 100–200 nm size NPs showed maximum accumulation in liver followed by kidney and brain (Semete et al. 2010a, b, c).

After administration into body, BNPs encounter many biological barriers which finally affect their in vivo fate. The main biological barriers faced by BNPs in vivo are MPS clearance, blood rheology and fluid dynamics of blood flow, pressure within tumors and BNP extravasation, cellular membrane permeability and subsequent endosomal accumulation, and removal of drugs from drug efflux pumps (Blanco et al. 2015). BNPs shape, size and surface charge play vital role in crossing biological barriers which in turn affect their interaction and uptake under in vivo conditions. NPs designing with appropriate size, shape, surface charge, targeting ligands and protein corona characterisation are of great help in efficiently crossing the biological barriers (Blanco et al. 2015).

BNPs may enter our body via many routes, for example, by inhalation, ingestion, or penetration through skin. However, irrespective of the administration route, biological millieu will surround BNPs once they have entered into biological environment. Proteins in human plasma form a coating on the surface of BNPs (protein corona) after which BNPs lose their identity. The composition of the protein corona depends on the physiochemical properties of BNPs, which determine protein binding specificities and affinities. Proteins with strong binding will form hard corona while proteins with weak binding will form soft corona around NPs. Protein corona of BNPs will determine its biological fate, as it is this corona of proteins that cells see and interact with (Tenzer et al. 2013). Characterisation of protein corona is essential for predicting the biological fate of BNPs. Positive impacts of BNPs have been widely revealed and documented, potential fear to human health are just beginning to come out. Studies on the toxic effect of BNPs on human health have gained momentum recently. Different studies have reported different doses, different responses and different levels of toxicity of same BNPs to measure the corresponding threats on human health (Thomas et al. 2006). There is no agreement and consensus on the toxicity data of BNPs used for drug delivery. Factors like agglomeration, sedimentation and diffusion of BNPs at physiologically relevant concentrations should be taken into account while carrying out quantitative studies on the cellular uptake of BNPs into biological systems. More extensive studies are needed to assess the toxicity of BNPs to throw light on long term adverse effects of their use on human health.

In this chapter we have covered brief introduction about BNPs, synthesis, characterisation and use of BNPs for drug and gene delivery. We have also included in this surface modification of BNPs for increasing their efficacy in vivo as well as the description of biological barriers encountered by BNPs. A brief knowledge about the toxicity of BNPs is also provided.

2.2 Synthesis of Biodegradable Nanoparticles

2.2.1 Synthesis of PLGA and PLA Nanoparticles

BNPs have been prepared by various methods according to the nature of drugs and route of administration. PLGA and PLA NPs have mostly been prepared by solvent evaporation, emulsification-diffusion, interfacial deposition and nanoprecipitation method. In solvent evaporation method, polymers (PLA and PLGA) are dissolved in organic solvents (CH_2Cl_2, acetone, $CHCl_3$ and ethyl acetate) and sonicated. The resulting solution is then poured into aqueous phase containing surfactants like polyvinyl alcohol (PVA) and polyvinylpyrollidone (PVP) and

again sonicated to form emulsion (Kumari et al. 2010a, b). This mixture is then diluted with aqueous phase to desired volume. NPs are separated by centrifugation at high speeds ≥ 16500 rpm. Solvent evaporation involves the formation of oil-in-water (O/W) emulsion, the oily phase of which is an organic solvent that diffuses properly in the aqueous phase. Organic solvent should undergo adequate diffusion in the aqueous phase for perfect spheres to be obtained. The PLA NPs are formed either from one emulsion droplet or NP arises from several emulsion droplets (Kumari et al. 2010a, b).

In emulsification-diffusion method, polymer dissolved in organic solvent was added to aqueous phase containing stabiliser followed by high pressure homogenisation. Emulsification-diffusion method involves the formation of a conventional oil-in-water emulsion within a partially water soluble solvent. Homogenisation results in the dispersion of the solvent as globules on equilibrium with the continuous phase. The addition of water causes diffusion of the solvent to the external phase and formation of super saturation region (Kumari et al. 2010a, b). Therefore, polymer aggregation was provoked in the form of solid colloidal particles and NPs were formed. In interfacial deposition polymers along with drug are dissolved in solvent mixture such as benzyl benzoate, acetone, and phospholipids. This mixture is then slowly added to stirred aqueous medium, resulting in the deposition of polymer in the form of NPs (Kumari et al. 2010a, b). Nanoprecipitation method involves dissolution of drug and polymer in acetone. This solution is then added to stirred aqueous phase containing surfactants. Acetone is removed by evaporation under reduced pressure and NPs are obtained by centrifugation (Jawahar et al. 2009).

2.2.2 Synthesis of Chitosan Nanoparticles

Chitosan NPs are mostly formed by ionotropic gelation, microemulsion, emulsification solvent diffusion and polyelectrolyte complex method. In ionotropic gelation method chitosan dissolved in 1 % acetic acid solution is added to equal volume of tripolyphosphate solution (TPP). Formation of NPs takes place by TPP initiated ionotropic gelation method. Chitosan has free amino groups at the surface which get protonated in acidic medium. NPs formation takes place due to interaction between the negative groups of TPP and the positively charged amino groups of chitosan. The ratio between chitosan and TPP is critical and controls the size distribution of the NPs (Janes et al. 2001).

Microemulsion method has also been used for the preparation of chitosan NPs. In this method chitosan dissolved in acetic acid and glutaraldehyde was added to surfactant dissolved in n-hexane under continuous stirring at room temperature. The system was stirred overnight to complete cross-linking process (Singh and Mishra 2013). Emulsification solvent diffusion method was used for the synthesis of chitosan NPs. In this method oil in water emulsion was obtained by adding organic phase into chitosan solution containing surfactant followed by high pressure homogenisation. This method gives high entrapment efficiency with hydrophobic drugs (Singh and Mishra 2013). Chitosan NPs have also been prepared by polyelectrolyte complex method. Polyelectrolyte complex method involves charge neutralisation of positively charged chitosan and negatively charged deoxyribonucleic acid (DNA). The NPs are spontaneously formed after addition of DNA solution into chitosan dissolved in acetic acid solution, under stirring at room temperature (Singh and Mishra 2013).

2.2.3 Synthesis of Protein Nanoparticles

Protein NPs have mostly been prepared by desolvation/coacervation (Shutava et al. 2009), emulsion method (Zambaux et al. 1999), ionotropic gelation and nanoprecipiation method. Desolvation/coacervation is a method in which a homogeneous solution of protein undergoes

liquid-liquid phase separation, giving rise to a protein rich dense phase at the bottom and a transparent solution above. The addition of natural salt or alcohol normally triggers coacervation and the control of turbidity/crosslinking was resulted in desired NPs. Protein was dissolved in deionised water by gentle heating at 50 °C, then acetone was rapidly added to the solution and slightly shaken. The milky solution was started to form upon acetone introduction into the mixture at pH 3.0. Immediately after addition of acetone, glutaraldehyde was admixed to the stirring mixture to form NPs (Shutava et al. 2009). Both hydrophobic and hydrophilic drugs can be entrapped in gelatin NPs using this process.

Emulsion method (Li et al. 1998) is based on the addition of aqueous phase (gelatine in phosphate buffer saline) to organic phase (polymer in organic solvent) followed by homogenisation. The reaction is stopped by addition of glutarladehyde and followed by centrifugation for collecting NPs (Zambaux et al. 1999). Bovine serum albumin (BSA) NPs have mostly been prepared by desolvation or coacervation process. BSA dissolved in water was added to acetone continuously or intermittently. The reaction was stopped by addition of glutaraldehyde (Sailaja and Amareshwar 2012). Soy protein NPs have also been prepared using the above method but in this ethanol was used as desolvating agent (Teng et al. 2012). Recently one study has reported synthesis of protein NPs by UV illumination in physiological conditions (Xie et al. 2013). UV illumination of α-lactalbumin triggered the rupture of disulfide bonds leading to assembly of protein NPs. The free thiol groups on the surface of these NPs can be used for the conjugation of targeting ligands. In addition, the protection of these abundant thiols can effectively decrease the aggregation of NPs and increase their in vivo stability (Xie et al. 2013). Zein NPs have been prepared by pH controlled nanoprecipitation method (Satheesh and Omathanu 2010). While casein NPs have been prepared by ionotropic gelation method using TPP as cross-linker (Elzoghby et al. 2013).

2.3 Biodegradable Nanoparticles for Drug Delivery

BNPs are preferred as drug delivery systems because of their size, controlled/sustained release behaviour, and compatibility with cells and tissues (Panyam and Labhasetwar 2003). In addition to this, BNPs are stable in blood, non-thrombogenic, non-immunogenic, non-inflammatory, do not activate neutrophils, and avoid RES (des Rieux et al. 2006). BNPs are formed by using natural or synthetic polymers. Synthetic polymers that have been extensively used for the preparation of BNPs are PLGA, PLA, poly-ε-caprolactone (PCL), and poly-alkyl-cyanoacrylates (PACL) (Kumari et al. Kumari et al. 2010a, b). Apart from this, natural polymers like gelatin, albumin, chitosan have also been explored for the synthesis of biodegradable NPs. In the successive headings, BNPs of synthetic and natural polymers used for delivery of anticancer, psychotic, antimicrobial, plant isolated, protein, peptides, and drugs is discussed.

2.3.1 Biodegradable Nanoparticles for Delivery of Anticancer Drugs

Anticancer drugs suffer from some drawbacks like poor aqueous solubility, toxicity to normal tissues, and pH-dependent hydrolysis. These limitations have been overcome by encapsulating such anticancer drugs on BNPs (Fig. 2.1). The encapsulation on BNPs have improved their bioavailability, reduced toxicity to normal tissues and enhanced their stability in biological milieu (Cheng et al. 2012).

Alginic acid, a linear anionic polysaccharide consists of α-L-guluronic acid and β-D-mannuronic acid. Alginic acid has been declared safe by the US Food and Drug administration (Cheng et al. 2012). Doxorubicin loaded alginic acid NPs has been prepared by nonsolvent aided counterion complexation method. The mean size of doxorubicin loaded alginic acid NPs was about 100 nm. The encapsulation efficiency of doxorubicin on alginic acid NPs was also very high (95.5 %).

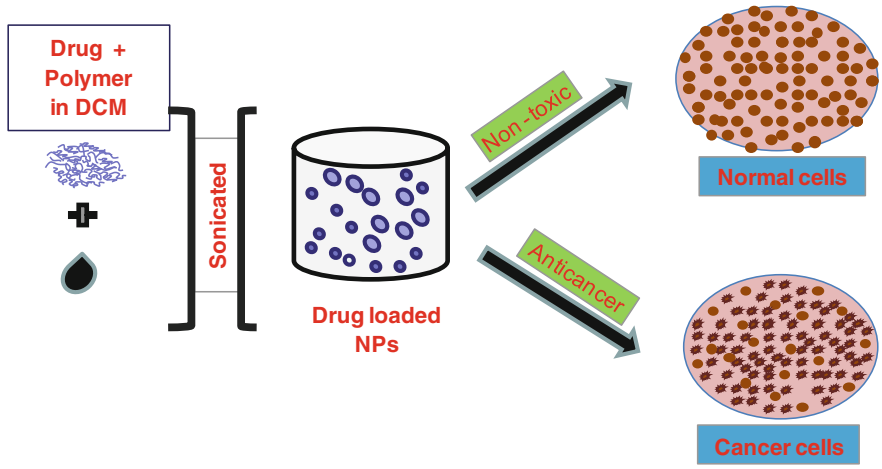

Fig. 2.1 In vitro anticancer activity of drug loaded nanoparticles. Drug loaded NPs are non-toxic to normal and show anticancer activity against anticancer cell lines

Doxorubicin loaded alginic acid NPs showed better antitumour effect than free doxorubicin (Cheng et al. 2012). In vivo distribution studies on model of murine hepatocellular carcinoma (H22) showed well accumulation and distribution of alginic acid NPs at tumor site by enhanced permeation and retention (EPR) effect. In vivo studies it is showed that doxorubicin loaded alginic acid NPs have superior efficacy which helps in reducing tumor growth and increasing the lifetime of H22 tumor bearing mice than free doxorubicin (Cheng et al. 2012). Treatment of tumor with polysaccharide-doxorubicin NPs drastically reduced the tumor volume, tumor cell counts, and increased lifespan in both the ascites and solid tumor models. Polysaccharide-doxorubicin NPs were observed to accumulate in tumour sites via EPR effect and released doxorubicin at tumor targeted sites (Joseph et al. 2014).

Taxol was loaded on gelatin NPs by desolvation method. Taxol loaded in gelatin NPs showed better activity against human bladder transitional cancer cells (Lu et al. 2004). Incorporation of taxol into PLGA NPs has enhanced its antitumor efficacy. Taxol encapsulated in PLGA mixed with vitamin E-polyethylene glycol succinate (TPGS) NPs also showed better activity than traditional formulation of taxol (Fonseca et al. 2002). 5-fluorouracil, pyrimidine analogue used for the treatment of several malignancies such as colorectal and breast cancers, have been loaded on translocator protein-PLGA NPs. Anticancer efficacy of 5-fluorouracil against C6-glioma cells was significantly enhanced due to synergistic effect of translocator protein and 5-fluorouracil (Laquintana et al. 2014).

9-Nitrocamptothecin has been encapsulated on PLGA NPs by nanoprecipitation method. Encapsulation efficiency was 30 % and biological activity of 9-nitrocamptothecin was maintained after nanoencapsulation on PLGA NPs. In vitro drug release profile showed a sustained release up to 160 h (Derakhshandeh et al. 2007). Another anticancer drug cisplatin (Rosenberg 1985) was encapsulated on PLGA-mPEG NPs by double emulsion method and revealed prolonged persistence in blood upon intravenous administration (Avgoustakis et al. 2002). Camptothecin loaded PLGA NPs has been more effective in minimizing tumour growth than free drug in immune competent C57 albino mice. NPs treated mice showed median survival of 36.5 days as compared to mice receiving saline (Householder et al. 2015).

Quercitrin isolated from *Albizia chinensis* has been encapsulated on PLA NPs by solvent evaporation method. The size of quercitrin loaded PLA NPs was 250 ± 68 nm. The encapsulation efficiency of nanoencapsulated quercitrin was 40 %. The in vitro release studies of quercitrin reveals initial burst release followed by

slow and sustained release (Kumari et al. 2011a, b). Another plant isolated molecule encapsulated on PLA NPs was podophyllotoxin (PODO) isolated from *Podophyllum hexandrum*. The size of synthesised PODO-loaded PLA NPs was 100 ± 17 nm and the encapsulation efficiency was 17 %. PODO loaded PLA NPs showed slow and sustained release (Yadav et al. 2014). Ellagic acid (EA) is a polyphenolic phytonutrient found in wide varieties of berries and nuts. EA was loaded on chitosan-glycerol phosphate NPs and the system showed sustained release of ellagic acid from NPs (Sharma et al. 2007). 1-isopropenyl-5a,5b,8,8,11a-pentamethyl-1,2,3,4,5,5a,6,7,7a,8,11,11a,11b,12,13,13a,13b-octadeca hydro cyclopenta[a]chrysene-3a-carboxylic acid, presumably a derivative of betulinic acid was isolated from *Phytolacca decandra.* This molecule was encapsulated on PLGA NPs. The mean diameter of NPs was found to be 110 ± 0.5 nm, with a PDI of 0.254 and a zeta potential of −17.6 ± 0.24 mV (Das et al. 2014).

2.3.2 Biodegradable Nanoparticles for Delivery of Psychotic Drugs

Chlorpromazine possesses antiadrenergic, anti-serotonergic, anticholinergic and antihistaminergic properties and is used to treat schizophrenia. Chlorpromazine hydrochloride was loaded on chitosan grafted PLGA NPs. Chlorpromazine hydrochloride loaded PLGA NPs exhibited in vitro, a biphasic drug release profile with an initial burst release and then prolonged sustained release over 48 h under in vitro conditions. Accelerated stability study suggested that the formulation was robust and can stand extreme conditions of temperature and relative humidity (Chalikwar et al. 2013). Haloperidol is used for the treatment of schizophrenia and acute psychotic states. Haloperidol was loaded on PLGA NPs and showed slow and sustained release (Budhian et al. 2005). Another psychotic drug savoxepine was loaded on PLA NPs by salting out method. Nanospheres of savoxepine have been prepared and encapsulation efficiency and loading was 95 and 16.7 %, respectively. In vitro release studies showed that PLA NPs allows extended delivery of the drug over more than one week. NPs loaded with savoxepine were able to provide more half life in plasma after intramuscular and intravenous injection (Leroux et al. 1996).

2.3.3 Biodegradable Nanoparticles for Delivery of Antimicrobial Drugs

Many antimicrobial drugs have also been loaded on biodegradable NPs to increase their efficacy. Azithromycin acts by binding to the 50S ribosomal subunit of susceptible micro organism and interferes with microbial protein synthesis. Azithromycin was loaded on PLGA NPs to enhance its antibacterial activity. Azithromycin loaded PLGA NPs showed better activity than pure azithromycin against *E. coli*. The concentration of PLGA loaded azithromycin was reduced 8 times to achieve same antibacterial activity against *E. Coli* as compared to the pure (Azhdarzadeh et al. 2012).

Amphotericin B is a lipophilic polyene antifungal agent, which is separated from a strain of *Streptomyces nodosus*. It is an amphoteric compound composed of a hydrophilic polyhydroxyl chain along one side and a lipophilic polyene hydrocarbon chain on the other. Amphotericin B is sparingly soluble in water, and has a poor oral absorption. Amphotericin B was loaded on TPGS-b-(PCL-ran-PGA) NP which enhanced the bioavailability and antifungal activity of amphotericin B (Tang et al. 2015a, b). Amphotericin B was also loaded on PCL NPs. Nanoformulation of amphotericin B was found to be 3-fold more efficient than free amphotericin B in reducing parasite burden from Leishmania infected mice (Espuelas et al. 2002).

2.3.4 Biodegradable Nanoparticles for Delivery of Hepatoprotective Drugs

Picroliv isolated from rhizome of *Picrorhiza kurroa* has been encapsulated on PLA NPs. The size of picroliv loaded PLA NPs was 182 ± 20 nm. Zeta potential of picroliv loaded PLA NPs was −23.5 mV, which has indicated their good stability. In vitro picroliv release from picroliv loaded PLA NPs showed slow and sustained release (Guliani et al. 2015). Another hepatoprotective drug, silymarin was encapsulated on chitosan NPs. Silymarin loaded chitosan NPs showed zero order drug release from chitosan NPs. Chitosan NPs have been observed for enhanced hepatoprotective activity of silymarin by passive targeting (Gupta et al. 2014a). Eudragit NPs loaded with silymarin has been stabilized by PVA. Silymarin showed sustained release from all the formulations and prevented hepatic damage induced by paracetamol (Das et al. 2011).

2.3.5 Biodegradable Nanoparticles for Proteins, Peptides and Nucleic Acids Delivery

Proteins and peptides drugs are used for treatment of variety of ailments. However, their use as such is limited due to their poor bioavailability in vivo and high cost of production for these drugs. Encapsulation of proteins and peptides on suitable NPs may enhance the potential of therapeutic proteins to create nanoprotein/nanopeptide for therapeutics, and disease diagnosis (Astier et al. 2005). A variety of NPs have been used for the delivery of protein and peptide based drugs. BNPs are one of the useful tools for protein therapeutics and its targeted delivery.

BNPs used for the delivery of protein drugs include synthetic polymers like PLA, PLGA, PCL, poly(methyl methacrylates), and poly(alkyl cyanoacrylates) or natural polymers (albumin, gelatin, alginate, collagen or chitosan). N-trimethyl chitosan chloride (TMC) NPs has been used for the augmentation of permeability and inclusion of diverse protein drugs in neutral and basic-pH condition. Insulin loaded chitosan NPs have significantly increased intestinal absorption of insulin following oral administration (Sarmento et al. 2007). Chitosan NPs increased the systemic absorption and bioavailability of cyclosporine A (El-Shabouri 2002). BSA has been successfully encapsulated on gelatin NPs. The average diameter of the BSA containing gelatin NPs was approximately 840 nm (Li et al. 1998). Half life of BSA was extended to 4.5 h as compared to 13.6 min of pure BSA after encapsulation on PEG-PLGA NPs (Li et al. 2001). Tetanus toxoid encapsulated on PLA-PEG NPs showed more persistence in blood and greater penetration in lymph nodes (Vila et al. 2002). Calcitonin has been loaded on polyacrylamide nanospheres, polyisobutylcyanoacrylate nanocapsules and chitosan NPs (Lowe and Temple 1994). Dalargin loaded on double coated Tween 80 and PEG 20000 poly(butylcyanoacrylate) NPs showed significant dalargin-induced analgesia than single coated tween and PEG (Das and Lin 2005).

Octreotide-loaded polyalkylcyanoacrylate NPs have been reported for increased plasma concentration of octreotide, and prolonged therapeutic efficacy of a somatostatin analogue in estrogen-treated rats (Damge et al. 2007a). Genistein was encapsulated in islet homing peptide coated PLGA NPs. These NPs showed 3 times better binding to islet endothelial cells and a 200 times better anti-inflammatory effect on islet endothelial cell (Ghosh et al. 2012).

2.4 Drug Release Mechanisms from Biodegradable Nanoparticles

Drug release mechanism is very important to know whether a drug is adsorbed or encapsulated in NPs matrix (Fig. 2.2). Drug release from NPs template occurs through diffusion of drug bound to the surface of NPs, diffusion from the NPs template, NP matrix erosion, or a combined erosion—diffusion process (Ringe et al. 2004).

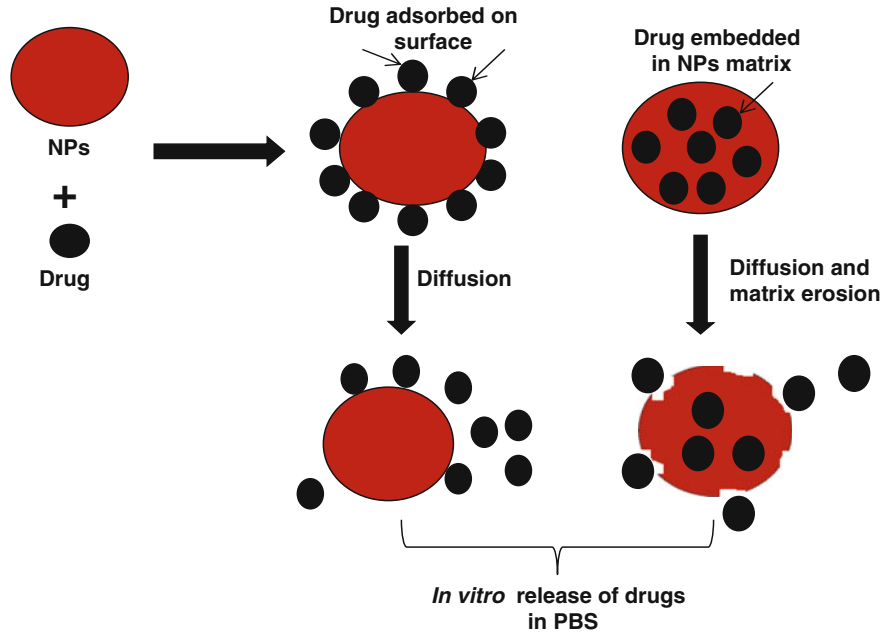

Fig. 2.2 In vitro release of drug from nanoparticles. Drug is adsorbed or embedded in the NPs matrix. Release of drug occurs by diffusion or matrix erosion of nanoparticles

Many mathematical models are used to replicate the release of drugs from NPs matrix. Mathematical models play an important role in the prediction of mechanism of drug release and also provide more general guidelines for development of drug delivery systems. Many models have been used for the prediction of drug release viz., zero order kinetic model, first order kinetic model, Higuchi model, Korsemeyer-Peppas model (the power law), Hixson-Crowell model, Weibull model, Baker- Lonsdale model, Hopfenberg model, Gompertz model, and Sequential layer model (Shaikh et al. 2015). The release models which best describe drug release from biodegradable NPs matrix are, in general, zero order model, first order model, Higuchi model and Korsemeyer-Peppas model (Singhvi and Singh 2011).

Zero-order model (Singhvi and Singh 2011) kinetic describes a system in which the release of the drug is not dependent on the drug concentration.

$$Q_t = Q_o - K_0 t$$

where Q_0, Q_t and K_0 represents initial amount of drug, cumulative amount of drug release at time "t" and zero-order rate constant, respectively.

Another model which has been used for the study of drug release is first order kinetic model (Singhvi and Singh 2011) which is based on the following equation,

$$A = A_0 e^{-kt}$$

where A is concentration at any time t, A_0 is initial amount of drug and k is first order rate constant.

Higuchi tried to relate the drug release rate to the physical constants based on simple laws of diffusion (Higuchi 1967). Higuchi model describes the release of a drug from an insoluble

matrix as the square root of a time-dependent process, given by the following equation:

$$Q_t = [2DS\varepsilon(A - 0.55\varepsilon)]^{0.5} * t^{0.5}$$

where, Q_t refers to the amount of drug released at time t, D refers to the diffusion coefficient, S is the solubility of drug in the dissolution medium, ε is the porosity, A is the drug content per cubic centimetre of NPs.

Another model which has been used for studying drug release is Korsmeyer-Peppas model (Korsmeyer et al. 1983). This model describes the drug release from polymeric systems and is based on the following equation:

$$\frac{M_t}{M_\infty} = Kt^n$$

where M_t/M_∞ is fraction of drug released at time t, K is the rate constant and n is the release exponent.

Physicochemical properties of the drug as well as polymer and the drug to polymer ratio rule the release of drug from the NPs and thus, adjust the release kinetics accordingly. Drug release mechanism can also be manipulated by the choice of matrices and size of BNPs. Larger sized BNPs show smaller initial burst release as compared to small sized NPs (Kumar et al. 2014). Initial burst release is related to the amount of the drug bound on the surface of NPs (Kumari et al. 2010a, b; Kumar et al. 2014) (Fig. 2.2). Drug release also depends on the nature of drug and interaction of drug with NPs matrix (Yadav et al. 2014).

2.5 Targeted Drug Delivery Using Biodegradable Nanoparticles

Targeted nanoformulations have started to draw noteworthy concentration in the last couple of years. Targeted drug delivery utilises both passive and active targeting strategies to deliver drug molecules more efficiently to pathological sites and preventing toxicity to healthy tissues (Allen and Cullis 2004; Peer et al. 2007; Davis et al. 2008; Farokhzad and Langer 2009). Passive drug targeting is dependent on the tumour vasculature. Endothelial gaps and inappropriately aligned vascular endothelium results in leaky blood vessels, which enable the internalisation of ~ 100 nm size NPs into the tumor tissues. Internalised NPs are retained in the tumor tissues due to dysfunctional lymphatic drainage. Together, these two qualities give rise to the EPR effect, which is widely used phenomenon by nanomedicines for accumulation in tumors (Matsumura and Maeda 1986; Maeda 2012). It is vital to know that EPR is an extremely changeable phenomenon, whose in vivo fate is determined by vascular volume, perfusion, permeability, penetration, and retention time. These parameters vary considerably between different types of tumors, and between different tumors within the same patient (Greish 2010; Lammers et al. 2012; Smith et al. 2012; Taurin et al. 2012; Prabhakar et al. 2013a, b). In reality, certain vessels are more permeable than others within a single tumour resulting in very diverse EPR. Actually, rapid growing and greatly vascularized tumors are likely to be more leaky than steadily growing and badly vascularized tumors, thereby making them more prone to EPR mediated passive drug targeting (Kunjachan et al. 2014).

In contrast, active targeting relies on integration of moieties capable of recognising/binding specifically to the target tissues. Commonly used targeting ligands are peptides, sugar molecules, aptamers antibodies, and epidermal growth factors (Kunjachan et al. 2014). These moieties specifically bind to receptors that are highly expressed either by the cancer cells such as epidermal growth factor receptor and prostate specific membrane antigen (PSMA) or by tumor endothelial cells such as vascular endothelial growth factor receptor or integrins (Pasqualini et al. 1997; Lammers et al. 2012). Although use of targeting moieties to enhance internalisation of NPs by diseased cells has recently augmented (Ross et al. 2004; Shiokawa et al. 2005), little is known concerning the effect of high affinity targeting molecules on the rate and extent of NPs uptake by tumor cell.

Herceptin antibody targeted mucic acid containing PEG polymer NPs loaded with camptothecin have demonstrated prolonged circulation in vivo. Targeted NPs showed their higher accumulation in the spleen that can be attributed to the herceptin antibody that remained associated with NPs (Han and Davis 2013). In another study, PLGA NPs modified with islet-homing peptide have exhibited 3-fold better binding to islet endothelial cells and a 200-fold better anti-inflammatory effect of an immunosuppressant drug (Ghosh et al. 2012). Cisplatin encapsulated PLGA-PEG NPs coated with cyclic pentapeptide (RGDfK) displayed enhanced cytotoxicity as compared to pure cisplatin (Graf et al. 2012). Docetaxel loaded cyclic asparagine-glycine-arginine peptide coated PEG-PLGA NPs showed higher cellular uptake into HUVEC and HT-1080 cells via receptor mediated endocytosis. The in vivo study has documented that targeted NPs exhibit elevated therapeutic activity by targeting the specific sites on tumours (Gupta et al. 2014a, b).

Activatable low molecular weight protamine (ALMWP) has been modified on PEG-PLGA NPs and has been used for delivery of paclitaxel to HT-1080 cells. PEG-PLGA NPs have exhibited an improved MMP reliant build up in HT-1080 cells. In vivo study showed that ALMWP-NP appreciably augmented the accumulation of paclitaxel at tumor site but not in the non target tissues. In addition, ALMWP-NP has shown deep penetration into the tumor parenchyma and paclitaxel loaded by ALMWP-NP has exhibited improved antitumor efficacy (Xia et al. 2013). In another study, folic acid conjugated PLA-PEG coated inorganic NPs loaded with paclitaxel showed better cellular uptake and drastically enhanced the drug effectiveness compared with the free drug (Chen and He 2015). Chitosan (CS) derivative grafted with multiple galactose residues (Gal-m-CS) and galactosylated CS (Gal-CS) was used for preparing NPs and developed NPs have been used for targeting hepatoma cells. Prepared Gal-m-CS NPs showed maximum interaction with HepG2 cells via the ligand-receptor interaction (Mi et al. 2007).

NPs prepared from ternary conjugate of heparin folic acid paclitaxel (HFT) and loaded with additional paclitaxel (HFT-T) showed higher cytotoxicity compared to the free form of paclitaxel in KB-3-1 cell line. HFT-T administration has enhanced the specific delivery of paclitaxel into tumor tissues and remarkably improved antitumor efficacy of paclitaxel (Wang et al. 2009). Doxorubicin loaded glycyrrhetinic acid (GA) modified recombinant human serum albumin (rHSA) NPs (DOX/GA-rHSA NPs) show increased cytotoxic activity in liver tumor cells compared to the non targeted NPs (DOX/rHSA NPs). The targeted NPs have exhibited higher cellular uptake in a GA positive hepatoma carcinoma cells (HepG2 cells) (Qi et al. 2015). An A10 aptamer-functionalized, sub-100 nm doxorubicin polylactide (Doxo-PLA) nanoconjugate (NC) was used for targeting malignant endothelial cells expressing prostate specific membrane antigen (PSMA). These A10 NCs were selectively internalized by PSMA expressing cancer cell lines. A10 Doxo-PLA NCs have exerted greater cytotoxic effects compared to nonfunctionalized Doxo-PLA NCs and free Doxorubicin. Interestingly, A10 NCs have selectively targeted PSMA-expressing tumor-associated endothelial cells at a cellular level and noticeably enhanced the uptake of NCs by endothelial cells within the tumor microenvironment (Tang et al. 2015a).

2.6 Biological Barriers Encountered by Biodegradable NPs

BNPs encounter many biological barriers after administration to site of action. The in vivo fate of BNPs is affected by these biological barriers. We highlight the fact if many of these barriers are not properly addressed at the time of synthesis of BNPs, the field of BNPs based drug delivery will continue to fail to realize its clinical potential (Blanco et al. 2015). The biological barriers encountered by BNPs under in vivo are elimination by MPS, blood rheology and fluid dynamics of blood flow, pressure within tumors and NP extravasation, cell membrane permeability and

subsequent endosomal accumulation, and removal of drugs from drug efflux pumps (Blanco et al. 2015).

The MPS, consists of phagocytic cells, removes NPs immediately after administration (Patel and Moghimi 1998). The course of elimination starts with adsorption of plasma proteins, onto the surface of NPs circulating in blood (Tenzer et al. 2013). This results in the formation of protein coating on the surface of NPs. The formation of protein coating around NPs is reliant on some parameters, including NP size, surface charge, lipophilicity and surface chemistry (Nel et al. 2009). NPs act as active entities instantly after systemic administration, and require assessment of the mechanism of protein coating formation and its effect on NPs stability, bioavailability, toxicity and fate (Docter et al. 2014; Röcker et al. 2009).

NPs solution dynamics in blood vessels is very much reliant on the size and shape. BNPs, typically possess a spherical geometry, and are synthesized specially for intravenous delivery. Recently, the intravascular walk of NPs following administration has been divided into flow, confinement, sticking to vascular walls and uptake. Opsonization and elimination by the MPS determine flow time of NPs in blood vessels. Surface properties of NPs are identified as crucial player in protein adsorption, which in turn affects pharmacokinetics and biodistribution of NPs. Positively charged NPs are quickly eliminated from blood flow than anionic NPs (Arvizo et al. 2011). In contrast, neutral NPs show appreciably prolonged persistence in blood. In vivo fates are also affected by NPs size. Bigger NPs >200 nm were collected in the liver and spleen. The side flow of NPs to endothelial walls is a very important concern of NPs synthesis. The union of NPs with the vessel walls favors their cell binding and receptor-ligand interactions in active targeting strategies and enables eructation through the loose vasculature of tumors (Blanco et al. 2015). NPs have the tendency to be favourably collected at the sites of injury, infection and inflammation. This passive targeting is mainly due to the existence of loose vasculature of endothelial cells. This effect known as EPR is exploited by NPs for accumulation in tumour cells (Matsumura and Maeda 1986; Maeda et al. 2013). NPs undergo cellular uptake, after which therapeutic load can be released to exert curative effects on cytoplasmic and nuclear targets. NPs require active uptake mechanisms to reach the cytoplasm and nucleus. Surface charge of NPs has proven to be a key factor for cellular uptake, with charge-based uptake vastly reliant on cell type (Blanco et al. 2015).

Drug resistance is a major hurdle in the treatment of several diseases, including infection, inflammation and cancer. Multidrug resistance (MDR) involves the removal of drugs from cells that results in a lowering of intracellular accumulation of drug and therapeutic efficacy. The MDR results in increased local toxicity, treatment doses, and consequent breakdown of select chemotherapeutic regimens (Blanco et al. 2015).

2.7 In Vivo Fate of Biodegradable Nanoparticles

BNPs are preferred for drug delivery because degradation products are metabolised in the body, and are non toxic (Kiss et al. 2010). Interactions with biological milieu are of utmost importance in designing and applications of BNPs based drug delivery systems. Surface hydrophobicity of BNPs and lack of specific functional groups on the surface of BNPs limit their applications in biological medium (Kiss et al. 2010).

BNPs with hydrophobic surfaces are rapidly cleared from the body by MPS. To avoid this and to increase the persistence of BNPs in the biological milieu many methods have been used. One such method is the use of hydrophilic polymers like PVA, PVP, PEG, poloxamers, polysorbate 80 (Gulyaev et al. 1999), ploysorbate 20, polysaccharides like dextran and different type of copolymers to efficiently coat BNPs and make their surface hydrophilic (Kumari et al. 2010a, b). These coatings provide a dynamic

cloud of hydrophilic and neutral chains at the surface, which repel plasma proteins. Hydrophilic polymers can be introduced on the surface of BNPs in two ways, either by adsorption or by making copolymers of biodegradable polymers with hydrophilic polymers like PEG (Kumari et al. 2010a, b).

Chemical coupling of PEG on PLGA surface has increased the water wettability and reduced protein adsorption on PEG coupled PLGA surfaces (Kiss et al. 2010). Surface modification of BSA NPs with PEG has also enhanced the sustained release characteristics of BSA NPs (Su et al. 2014). PEG coating on PLA NPs have enhanced the retention time in blood and reduced the interaction with digestive enzymes (Tobio et al. 2000). In a recent study, PEG-sheddable, mannose-modified PLGA NPs have been shown to efficiently target tumour associated macrophages after acid-sensitive PEG shedding in the acidic tumor microenvironment. Decreased accumulation in MPS organs due to successful PEG shielding at normal physiological pH was reported (Zhu et al. 2013).

Physicochemical properties of NPs which affect in vivo fate of BNPs are particle size, surface charge, NPs stability and residence time in blood. Depending upon the size and composition, BNPs are distributed and accumulated in the kidney, liver, and spleen and very less concentration is seen in other organs and tissues (Lorenzer et al. 2015). NPs are administered into body through oral, pulmonary, intravenous, nasal and dermal routes. NPs injected through oral route undergo degradation in the gastrointestinal (GI) tract and are eliminated or absorbed inside the body. Study has reported that NPs of size 50–200 nm are absorbed by payer's patches in the wall of intestine (Des Rieux et al. 2006). After entering into GI tract, NPs are distributed to other organs and tissues through the blood and lymphatic system. Similar to oral exposure, NPs administered via pulmonary route undergo absorption and clearance. NPs deposited in the tracheobronchial region are cleared by the mucociliary movement. These particles could enter the alveoli epithelium by endocytosis and enter the blood or lymphatic system underlying the alveolar epithelium (Oberdorster et al. 2005). NPs administered through subcutaneous (Moghimi 2003), intramuscular (Kreuter et al. 1979), intradermal (Lee et al. 2009), and intraperitoneal (Maincent et al. 1992) are absorbed and distributed into the blood circulation. Numerous studies have reported that NPs undergo distribution to different organs and tissues after administration by various routes (Hagens et al. 2007). Concentration of NPs in different organs depends on the composition and physiochemical properties of NPs. The organs where NPs are found in lesser concentrations include heart, brain and muscles (Lee et al. 2010). NPs distribution into abnormal organs tumor has been under investigation for targeted drug delivery. NPs were passively accumulated into tumor tissues through EPR effect. EPR effect has been reported for NPs in the size range 20–1000 nm on various tumour models (Greish 2010; Acharya and Sahoo 2011; Fang et al. 2011; Prabhakar et al. 2013a, b). In some cases EPR effect was observed to enhance preferential accumulation in tumour sites (Lorenzer et al. 2015). However, the optimal NPs size for achieving EPR effect will depend on tumour type, tumour location and size of tumour. BNPs undergo metabolism through the degradation of the matrix polymers. One of the advantages of BNPs is that their biodegradation rate can be controlled by modifying the polymer composition and molecular weight (Anderson and Shive 1997). BNPs are directly excreted from the body depending on their size and shape. Liver and kidney are the major excretory organs responsible for NPs excretion from the body.

2.8 Toxicity of Biodegradable Nanoparticles

BNPs possess unique physical and surface properties, and have wide applications, such as target-specific vehicles for in vivo sensing, diagnosis, and therapy. BNPs are small enough to penetrate and target certain tissues (Braydich et al. 2005). Several studies have shown that NPs can enter the brain and cause tissue injury

(Medina et al. 2007; Sharma et al. 2007). Toxicity is a critical aspect regarding the safe use of BNPs in drug delivery. Several studies have reported no cytotoxic effects against a wide variety of cell types following treatment with NPs (Basarkar et al. 2007; Patil and Panyam 2009; Tahara et al. 2010). Recently one study evaluated PLGA NPs for in vivo toxicity study in Balb/c mice. It was found that no anatomical pathological changes or tissue damage occurred. It can be concluded that the toxicity observed with various engineered BNPs will not be observed with NPs made of synthetic polymers such as PLGA when applied in the field of nanomedicines (Semete et al. 2010a, b, c). Many surfactants and stabilisers are used for modifying the surfaces of NPs to increase their persistence inside the blood. Certain modifiers have been shown to exhibit toxicity in cells. Polyethylene imine coating on the surface of PLGA NPs has exhibited toxicity within the cell lines. On the other hand, NPs stabilised with BSA have exhibited almost no cytotoxicity. BSA stabilised NPs seem to have a positive effect on cellular viability, which reaches value over 100 % for several cell lines. PVA modified PLGA NPs were non toxic up to a concentration of 370 μg/ml (Westedt et al. 2007). PEG-PLGA NPs engineered for oral applications have been observed for cytokine production (Semete et al. 2010a, b, c). While, biodegradable chitosan NPs have shown toxicity in zebrafish model. Use of emulsifiers and stabilisers is one issue which needs to be studied critically in formulation of nanomedicines. These studies have raised concern about the safety of BNPs used in drug delivery. More thorough studies are required on BNPs toxicity issues before they are declared safe for nanomedicine applications.

2.9 Conclusions

BNPs are potentially viable drug delivery systems capable of delivering multitude of therapeutic agents and biomolecules. They are very well functionalized for releasing the drugs inside human body, increasing the bioavailability and biocompatibility of drugs. To optimize BNPs as a delivery system, greater understanding of different mechanisms of biological interactions and NPs engineering is still required. However, BNPs appear to be promising drug delivery system because of their versatile formulation, controlled release properties, sub cellular size and biocompatibility with various cells and tissues in the body. Moreover, the use of BNPs can enhance the specificity for site of targeted cell. In the near- and medium-term, we can expect the emergence of many nanotechnology based BNPs for drug delivery applications. Technologies around controlled-release BNPs will likely to continue have the greatest clinical impact for the near future. This is an exciting time for nanotechnology research, and the pace of scientific discovery in this area is gaining momentum. It is broadly accepted that medicine and the field of targeted drug delivery will be an important recipient of nanotechnology for years to come.

Acknowledgments We are grateful to the Director, CSIR-IHBT for providing valuable suggestions and motivation. Financial assistance from Council of Scientific and Industrial Research, Government of India is genuinely acknowledged.

References

Acharya S, Sahoo SK (2011) PLGA nanoparticles containing various anticancer agents and tumour delivery by EPR effect. Adv Drug Deliv Rev 63:170–183

Ahmad Z, Pandey R, Sharma S et al (2006) Alginate nanoparticles as antituberculosis drug carriers: formulation development, pharmacokinetics and therapeutic potential. Indian J Chest Dis Allied Sci 48:171–176

Alexis F, Pridgen E, Molnar LK et al (2008) Factors affecting the clearance and biodistribution of polymeric nanoparticles. Mol Pharm 5(4):505–515

Allen TM, Cullis PR (2004) Drug delivery systems: entering the mainstream. Science 303:1818–1822

Anderson JM, Shive MS (1997) Biodegradation and biocompatibility of PLA and PLGA microspheres. Adv Drug Delivery Rev 28:5–24

Arvizo RR, Miranda OR, Moyano DF et al (2011) Modulating pharmacokinetics, tumor uptake and biodistribution by engineered nanoparticles. PLoS ONE 6:e24374

Astier Y, Bayley H, Howorka S (2005) Protein components for nanodevices. Curr Opin Chem Biol 9:576–584

Avgoustakis K, Beletsi A, Panagi Z et al (2002) PLGA-mPEG nanoparticles of cisplatin: in vitro nanoparticle degradation, in vitro drug release and in vivo drug residence in blood properties. J Control Rel 79:123–135

Azhdarzadeh M, Lotfipour F, Zakeri-Milani P et al (2012) Anti-bacterial performance of azithromycin nanoparticles as colloidal drug delivery system against different gram-negative and gram-positive bacteria. Adv Pharm Bull 2(1):17–24

Basarkar A, Devineni D, Palaniappan R et al (2007) Preparation, characterization, cytotoxicity and transfection efficiency of poly(DL-lactide-co-glycolide) and poly(DL-lactic acid) cationic nanoparticles for controlled delivery of plasmid DNA. Int J Pharm 343:247–254

Blanco E, Shen H, Ferrari M (2015) Principles of nanoparticle design for overcoming biological barriers to drug delivery. Nat Biotechnol 33:941–951

Brannon-Peppas L, Blanchette JO (2004) Nanoparticle and targeted systems for cancer therapy. Adv Drug Deliv Rev 56:1649–1659

Braydich-Stolle L, Hussain S, Schlager JJ et al (2005) In vitro cytotoxicity of nanoparticles in mammalian germline stem cells. Toxicol Sci 88:412–419

Brigger I, Dubernet C, Couvreur P (2002) Nanoparticles in cancer therapy and diagnosis. Adv Drug Deliv Rev 54:631–651

Budhian A, Siegel SJ, Winey KI (2005) Production of haloperidol-loaded PLGA nanoparticles for extended controlled drug release of haloperidol. J Microencapsul 22:773–785

Calvo P, Gouritin B, Brigger I et al (2001) PEGylated polycyanoacrylate nanoparticles as vector for drug delivery in prion diseases. J Neurosci Methods 111:151–155

Chalikwar SS, Mene BS, Pardeshi CV et al (2013) Self-Assembled, chitosan grafted PLGA nanoparticles for intranasal delivery: design, development and ex vivo characterization. Polym-Plast Technol Eng 52:368–380

Chen H, He S (2015) PLA–PEG coated multifunctional imaging probe for targeted drug delivery. Mol Pharm 12:1885–1892

Cheng Y, Yu S, Zhen Xu et al (2012) Alginic acid nanoparticles prepared through counterion complexation method as a drug delivery system. ACS Appl Mater Interfaces 4:5325–5332

Coester C, Kreuter J, von Briesen H et al (2000) Preparation of avidin-labelled gelatin nanoparticles as carriers for biotinylated peptide nucleic acid (PNA). Int J Pharm 196:147–149

Damge C, Maincent P, Ubrich N (2007) Oral delivery of insulin associated to polymeric nanoparticles in diabetic rats. J Control Rel 117:163–170

Das D, Lin S (2005) Double-coated poly (butylcynanoacrylate) nanoparticulate delivery systems for brain targeting of dalargin via oral administration. J Pharm Sci 94:1343–1353

Das J, Das S, Paul A et al (2014) Strong anticancer potential of nanotriterpenoid from phytolacca decandra against A549 adenocarcinoma via a Ca2D-dependent mitochondrial apoptotic pathway. J Acupunct Meridian Stud 7:140e150

Das S, Roy P, Auddy RG et al (2011) Silymarin nanoparticle prevents paracetamol-induced hepatotoxicity. Int J Nanomedicine 6:1291–1301

Date AA, Joshi MD, Patravale VB (2007) Parasitic diseases: liposomes and polymeric nanoparticles versus lipid nanoparticles. Adv Drug Deliv Rev 59:505–521

Davis ME, Chen Z, Shin DM (2008) Nanoparticle therapeutics: an emerging treatment modality for cancer. Nat Rev Drug Discovery 7:771–782

Derakhshandeh K, Erfan M, Dadashzadeh S (2007) Encapsulation of 9-nitrocamptothecin, a novel anticancer drug, in biodegradable nanoparticles: factorial design, characterization and release kinetics. Eur J Pharm Biopharm 66(1):34–41

des Rieux A, Fievez V, Garinot M et al (2006) Nanoparticles as potential oral delivery systems of proteins and vaccines: a mechanistic approach. J Control Rel 116:1–27

Docter D, Distler U, Storck W et al (2014) Quantitative profiling of the protein coronas that form around nanoparticles. Nat Protoc 9:2030–2044

El-Shabouri MH (2002) Positively charged nanoparticles for improving the oral bioavailability of cyclosporin-A. Int J Pharm 249:101–108

Elzoghby AO, Helmy MW, Samy WM et al (2013) Novel ionically crosslinked casein nanoparticles for flutamide delivery: formulation, characterization, and in vivo pharmacokinetics. Int J Nanomed 8:1721–1732

Espuelas MS, Legrand P, Loiseau PM et al (2002) In vitro antileishmanial activity of amphotericin B loaded n poly(epsilon-caprolactone) nanospheres. J Drug Target 10(8):593–599

Fang J, Nakamura H, Maeda H (2011) The EPR effect: unique features of tumour blood vessels for drug delivery, factors involved, and limitations and augmentation of the effect. Adv Drug Deliv Rev 63:136–151

Farokhzad OC, Robert Langer R (2009) Impact of nanotechnology on drug delivery. ACS Nano 3:16–20

Fonseca C, Simoes S, Gaspar R (2002) Paclitaxel-loaded PLGA nanoparticles: preparation, physicochemical characterization and in vitro anti-tumoral activity. J Control Rel 83(2):273–286

Ghosh K, Kanapathipillai M, Korin N et al (2012) Polymeric nanomaterials for islet targeting and immunotherapeutic delivery. Nano Lett 12:203–208

Graf N, Bielenberg DR, Kolishetti N et al (2012) RVβ3 Integrin-targeted PLGA-PEG nanoparticles for enhanced anti-tumor efficacy of a Pt(IV) prodrug. ACS Nano 6:4530–4539

Greish K (2010) Enhanced permeability and retention (EPR) effect for anticancer nanomedicine drug targeting. In: Grobmyer SR, Moudgil BM (eds) Cancer Nanotechnology, Methods in molecular biology. Humana Press, New York, pp 25–37

Guliani A, Kumari A, Yadav SK (2015) Development of nanoformulation of picroliv isolated from *Picrorrhiza kurroa*. IET Nanobiotechnol. doi:10.1049/iet-nbt.2015.0032

Gulyaev AE, Gelperina SE, Skidan IN et al (1999) Significant transport of doxorubicin into the brain with polysorbate 80-coated nanoparticles. Pharm Res 16:1564–1569

Gupta M, Chashoo G, Sharma PR et al (2014a) Dual targeted polymeric nanoparticles based on tumour endothelium and tumor cells for enhanced antitumor drug delivery. Mol Pharm 11:697–715

Gupta S, Singh SK, Girotra P (2014b) Targeting silymarin for improved hepatoprotective activity through chitosan nanoparticles. Int J Pharm Invest 4:156–163

Hagens WI, Oomen AG, de Jong WH et al (2007) What do we (need to) know about the kinetic properties of nanoparticles in the body. Regul Toxicol Pharmacol 49:217–229

Han H, Davis ME (2013) Single antibody targeted nanoparticle delivery of camptothecin. Mol Pharm 10:2558–2567

Higuchi WI (1967) Diffusional models useful in biopharmaceutics drug release rate processes. J Pharm Sci 56:315–324

Householder KT, DiPerna DM, Chung EP et al (2015) Intravenous delivery of camptothecin-loaded PLGA nanoparticles for the treatment of intracranial glioma. Int J Pharm 479:374–380

Janes KA, Fresneau MP, Marazuela A et al (2001) Chitosan nanoparticles as delivery systems for doxorubicin. J Control Rel 73:255–267

Jawahar N, Venkatesh DN, Sureshkumar R et al (2009) Development and characterization of PLGA-nanoparticles containing carvedilol. J Pharm Sci Res 1:123–128

Joseph MM, Aravind SR, George SK et al (2014) Co-encapsulation of doxorubicin with galactoxyloglucan nanoparticles for intracellular tumor-targeted delivery in murine ascites and solid tumors. Transl Oncol 7:525–536

Kiss E, Anszky EK, Bertoti I (2010) Modification of poly (lactic/glycolic acid) surface by chemical attachment of poly(ethylene glycol). Langmuir 26:1440–1444

Korsmeyer RW, Gurny R, Doelker E et al (1983) Mechanisms of solute release from porous hydrophilic polymers. Int J Pharm 15:25–35

Kreuter J, Tauber U, Illi V (1979) Distribution and elimination of poly(Methyl-2-14C-methacrylate) nanoparticle radioactivity after injection in rats and mice. J Pharm Sci 68:1443–1447

Kumar V, Kumari A, Kumar D et al (2014) Biosurfactant stabilized anticancer biomolecule-loaded poly (d, l-lactide) nanoparticles. Colloid Surf B 117:505–511Kumari A, Kumar V, Yadav SK (2012) Plant Extract Synthesized PLA Nanoparticles for Controlled and Sustained Release of Quercetin: A Green Approach. PLoS ONE 7(7): e41230.

Kumari A, Kumar V, Yadav SK (2012) Plant Extract Synthesized PLA Nanoparticles for Controlled and Sustained Release of Quercetin: A Green Approach. PLoS ONE 7(7): e41230

Kumari A, Yadav SK, Pakade YB et al (2011a) Nanoencapsulation and characterization of Albizia chinensis isolated antioxidant quercitrin on PLA nanoparticles. Colloid Surf B 82:224–232

Kumari A, Yadav SK, Yadav SC (2010a) Biodegradable polymeric nanoparticles based drug delivery systems. Colloid Surf B 75:1–18

Kumari A, Kumar V, Yadav SK (2011b) Nanocarriers: a tool to overcome biological barriers in siRNA delivery. Expert Opin Biol Ther 11:1327–1339

Kumari A, Yadav SK, Pakade YB et al (2010b) Development of biodegradable nanoparticles for delivery of quercetin. Colloid Surf B 80:184–192

Kunjachan S, Pola R, Gremse F et al (2014) Passive versus active tumor targeting using RGD- and NGR-modified polymeric nanomedicines. Nano Lett 14:972–981

Lammers T, Kiessling F, Hennink WE et al (2012) Drug targeting to tumors: Principles, pitfalls and (pre-) clinical progress. J Control Rel 161:175–187

Langer R (1990) New Methods Drug Deliv Sci 249:1527–1533

Langer R (1998) Drug delivery and targeting. Nature 392:5–10

Laquintana V, Denora N, Lopalco A et al (2014) Translocator protein ligand-PLGA conjugated nanoparticles for 5-fluorouracil delivery to glioma cancer cells. Mol Pharm 11:859–871

Lee HA, Leavens TL, Mason SE et al (2009) Comparison of quantum dot biodistribution with a blood-flow-limited physiologically based pharmacokinetic model. Nano Lett 9:794–799

Lee MJ, Omid Veiseh O, Bhattarai N et al (2010) Rapid Pharmacokinetic and Biodistribution Studies Using Cholorotoxin-Conjugated Iron Oxide Nanoparticles: A Novel Non-Radioactive Method. Plos ONE 5(4): 10

Leroux JC, Allémann E, Jaeghere FD et al (1996) Biodegradable nanoparticles from sustained release formulations to improved site specific drug delivery. J Control Rel 39:339–350

Li JK, Wang N, Wu XS (1998) Gelatin nanoencapsulation of protein/peptide drugs using an emulsifier-free emulsion method. J Microencapsul 15:163–172

Li M, Al-Jamal KT, Kostarelos K et al (2010) Physiologically based pharmacokinetic modeling of nanoparticles. ACS Nano 4:6303–6317

Li Y, Pei Y, Zhang X et al (2001) PEGylated PLGA nanoparticles as protein carriers: synthesis, preparation and biodistribution in rats. J Control Rel 71:203–211

Lorenzer C, Dirin M, Winkler AM et al (2015) Going beyond the liver: progress and challenges of targeted delivery of siRNA therapeutics. J Control Rel 203:1–15

Lowe PJ, Temple CS (1994) Calcitonin and insulin in isobutylcyanoacrylate nanocapsules: protection

against proteases and effect on intestinal absorption in rats. J Pharm Pharmacol 46:547–552
Lu Z, Yeh TK, Tsai M et al (2004) Paclitaxel-loaded gelatin nanoparticles for intravesical bladder cancer therapy. Clin Cancer Res 10:7677–7684
Maeda H (2012) Macromolecular therapeutics in cancer treatment: the EPR effect and beyond. J Control Rel 164:138–144
Maeda H, Nakamura H, Fang J (2013) The EPR effect for macromolecular drug delivery to solid tumors: improvement of tumor uptake, lowering of systemic toxicity, and distinct tumor imaging in vivo. Adv Drug Deliv Rev 65:71–79
Maincent P, Thouvenot P, Amicabile C et al (1992) Lymphatic targeting of polymeric nanoparticles after intraperitoneal administration in rats. Pharm Res 9:1534–1539
Matsumura Y, Maeda H (1986) A new concept for macromolecular therapeutics in cancer chemotherapy: mechanism of tumoritropic accumulation of proteins and the antitumor agent smancs. Cancer Res 46:6387–6392
Medina C, Santos-Martinez MJ, Radomski A et al (2007) Nanoparticles: pharmacological and toxicological significance. Br J Pharmacol 150:552–558
Mi FL, Wu YY, Chiu YL et al (2007) Synthesis of a novel glycoconjugated chitosan and preparation of its derived nanoparticles for targeting HepG2 cells. Biomacromolecules 8:892–898
Moghimi SM (2003) Modulation of lymphatic distribution of subcutaneously injected poloxamer 407-coated nanospheres: the effect of the ethylene oxide chain configuration. FEBS Lett 540:241–244
Mu L, Feng SS (2003) A novel controlled release formulation for the anticancer drug paclitaxel (Taxol): PLGA nanoparticles containing vitamin E TPGS. J Control Rel 86:33–48
Nel AE, Mädler L, Velegol D et al (2009) Understanding biophysicochemical interactions at the nano-bio interface. Nat Mater 8:543–557
Oberdorster G, Oberdorster E, Oberdorster J (2005) Nanotoxicology: An emerging discipline evolving from studies of ultrafine particles. Environ Health Perspect 113:823–839
Panyam J, Labhasetwar V (2003) Biodegradable nanoparticles for drug and gene delivery to cells and tissue. Adv Drug Deliv Rev 55:329–347
Pasqualini R, Koivunen E, Ruoslahti E (1997) αv Integrins as receptors for tumor targeting by circulating ligands. Nat Biotechnol 15:542–546
Patel HM, Moghimi SM (1998) Serum-mediated recognition of liposomes by phagocytic cells of the reticuloendothelial system the concept of tissue specificity. Adv Drug Deliv Rev 32:45–60
Patil Y, Panyam J (2009) Polymeric nanoparticles for siRNA delivery and gene silencing. Int J Pharm 367:195–203
Peer D, Karp JM, Hong S et al (2007) Nanocarriers as an emerging platform for cancer therapy. Nat Nanotechnol 2:751–760
Prabhakar U, Maeda H, Jain RK et al (2013a) Challenges and key considerations of the enhanced permeability and retention (EPR) effect for nanomedicine drug delivery in oncology. Cancer Res 73:2412–2417
Prabhakar U, Maeda H, Jain RK et al (2013b) Challenges and key considerations of the enhanced permeability and retention effect for nanomedicine drug delivery in oncology. Cancer Res 73:2412–2417
Qi WW, Yu HY, Guo H et al (2015) Doxorubicin-loaded glycyrrhetinic acid modified recombinant human serum albumin nanoparticles for targeting liver tumour chemotherapy. Mol Pharm 12:675–683
Ringe K, Walz C, Sabel B (2004) Nanoparticle drug delivery to the brain. In: Nalwa HS (ed) Encyclopedia of nanoscience and nanotechnology, vol 7. American Scientific Publishers, New York
Röcker C, Potzl M, Zhang F et al (2009) A quantitative fluorescence study of protein monolayer formation on colloidal nanoparticles. Nat Nanotechnol 4:577–580
Rosenberg B (1985) Fundamental studies with cisplatin. Cancer 55:2303–2306
Ross JS, Schenkein DP, Pietrusko R et al (2004) Targeted therapies for cancer. Am J Clin Pathol 122:598–609
Sailaja AK, Amareshwar P (2012) Preparation of BSA nanoparticles by desolvation technique using acetone as desolvating agent. Int J Pharm Sci Nanotechnology 5:1643–1647
Sarmento B, Ribeiro A, Veiga F et al (2007) Alginate/chitosan nanoparticles are effective for oral insulin delivery. Pharm Res 24:2198–21206
Satheesh P, Omathanu P (2010) Preparation of zein nanoparticles by pH controlled nanoprecipitation. J Biomed Nanotech 6:312–317
Semete B, Booysen L, Lemmer Y et al (2010a) In vivo evaluation of the biodistribution and safety of PLGA nanoparticles as drug delivery systems. Nanomed 6:662–671
Semete B, Booysen LI, Kalombo L et al (2010b) In vivo uptake and acute immune response to orally administered chitosan and PEG coated PLGA nanoparticles. Toxicol Appl Pharmacol 249:158–165
Semete B, Booysen L, Lemmer Y et al (2010c) In vivo evaluation of the biodistribution and safety of PLGA nanoparticles as drug delivery systems. Nanomed Nanotechnol 6:662–671
Shaikh HK, Kshirsagar RV, Patil SG (2015) Mathematical models for drug release characterization: a review. WJPPS 4:324–338
Sharma G, Italia JL, Sonaje K et al (2007) Biodegradable in situ gelling system for subcutaneous administration of ellagic acid and ellagic acid loaded nanoparticles: evaluation of their antioxidant potential against cyclosporine induced nephrotoxicity in rats. J Control Rel 118:27–37

Sharma HS (2007) Nanoneuroscience: emerging concepts on nanoneurotoxicity and nanoneuroprotection. Nanomed 2:753–758

Shenoy DB, Amiji MM (2005) Poly(ethylene oxide)-modified poly(epsiloncaprolactone) nanoparticles for targeted delivery of tamoxifen in breast cancer. Int J Pharm 293:261–270

Shiokawa T, Hattori Y, Kawano K et al (2005) Effect of polyethylene glycol linker chain length of folate-linked microemulsions loading aclacinomycin on targeting ability and antitumor effect in vitro and in vivo. Clin Cancer Res 11:2018–2025

Shutava TG, Balkundi SS, Vangala P et al (2009) Layer-by-layer-coated gelatin nanoparticles as a vehicle for delivery of natural polyphenols. ACS Nano 3:1877–1885

Singh K, Mishra A (2013) Water soluble chitosan nanoparticle for the effective delivery of lipophilic drugs: a review. Int J Appl Pharm 5:1–6

Singhvi G, Singh M (2011) In-vitro drug release characterization models. Int J Pharm Stud Res 2(1):77–84

Smith BR, Kempen P, Bouley D et al (2012) Real-time intravital imaging of RGD-quantum dot binding to luminal endothelium in mouse tumor neovasculature. Nano Lett 12:3369–3377

Su Z, Xing L, Chen Y et al (2014) Lactoferrin-modified poly(ethylene glycol)-grafted BSA nanoparticles as a dual-targeting carrier for treating brain gliomas. Mol Pharm 11:1823–1834

Tahara K, Yamamoto H, Kawashima Y (2010) Cellular uptake mechanisms and intracellular distributions of polysorbate 80-modified poly (D, L-lactide-co-glycolide) nanospheres for gene delivery. Eur J Pharm Biopharm 75:218–224

Tang L, Tong R, Coyle VJ et al (2015a) Targeting tumor vasculature with aptamer functionalized doxorubicin polylactide nanoconjugates for enhanced cancer therapy. ACS Nano 9:5072–5081

Tang X, Jiao R, Xie C et al (2015b) Improved antifungal activity of amphotericin B-loaded TPGS-b-(PCL-ran-PGA) nanoparticles. Int J Clin Exp Med 8:5150–5162

Taurin S, Nehoff H, Greish K (2012) Anticancer nanomedicine and tumor vascular permeability; where is the missing link. J Control Rel 164:265–275

Thomas T, Thomas K, Sadrieh N et al (2006) Research strategies for safely evaluation of nanomaterials, Part VII: evaluating consumer to nanoscale materials. Toxicol Sci 91: 14–19

Teng Z, Luo Y, Wang Q (2012) Nanoparticles synthesized from soy protein: preparation, characterization and application for nutraceutical encapsulation. J Agric Food Chem 60:2712–2720

Tenzer S, Docter D, Kuharev J et al (2013) Rapid formation of plasma protein corona critically affects nanoparticle pathophysiology. Nat Nanotechnol 8:772–781

Tobío M, Sánchez A, Vila A et al (2000) The role of PEG on the stability in digestive fluids and in vivo fate of PEG-PLA nanoparticles following oral administration. Colloid Surf B 18:315–323

Vila A, Sanchez A, Tobio M et al (2002) Design of biodegradable particles for protein delivery. J Control Rel 78:15–24

Wagner V, Dullaart A, Bock AK et al (2006) The emerging nanomedicine landscape. Nat Biotechnol 24:1211–1217

Wang X, Li J, Wang Y et al (2009) HFT-T, a targeting nanoparticle, enhances specific delivery of paclitaxel to folate receptor-positive tumors. ACS Nano 3:3165–3174

Westedt U, Kalinowski M, Wittmar M et al (2007) Poly (vinyl alcohol)-graft-poly(lactide-co-glycolide) nanoparticles for local delivery of paclitaxel for restenosis treatment. J Control Release 119:41–51

Whitesides GM (2003) The right size in nanobiotechnology. Nat Biotechnol 21:1161–1165

Xia H, Gu G, Hu Q et al (2013) Activatable cell penetrating peptide conjugated nanoparticles with enhanced permeability for site specific targeting delivery of anticancer drug. Bioconjug Chem 24:419–430

Xie J, Li Y, Cao Y et al (2013) Photo synthesis of protein-based drug-delivery nanoparticles for active tumor targeting. Biomater Sci 1:1216–1222

Yadav R, Kumar D, Kumari A et al (2014) Encapsulation of podophyllotoxin and etoposide in biodegradable poly-d, l-lactide nanoparticles improved their anticancer activity. J Microencapsul 31:211–219

Zambaux MF, Bonneaux F, Gref R et al (1999) Preparation and characterization of protein C-loaded PLA nanoparticles. J Control Rel 60:179–188

Zhu S, Niu M, O'Mary H et al (2013) Targeting of tumor associated macrophages made possible by PEG sheddable mannose modified nanoparticles. Mol Pharm 10:3525–3530

Metallic Nanoparticles, Toxicity Issues and Applications in Medicine

3

Rubbel Singla, Anika Guliani, Avnesh Kumari and Sudesh Kumar Yadav

Abstract

The metallic nanoparticles (NPs) and their synthetic biology are an active area fascinating both the academics as well as scientific research applications in the field of nanotechnology. These nanostructures are a versatile class of materials such as metal NPs, metal oxide NPs, magnetic NPs and quantum dots for biomedical sciences and engineering due to their huge potential. A handful number of methods are adopted for the synthesis of one or the other kind of metal NPs which includes physical and chemical approaches. Each of the chemical and physical synthesis procedures deals with some limitations such as cost ineffectiveness, use of hazardous chemicals, formation of toxic end products and involvement of high-energy processes. To overcome these drawbacks, an alternative approach of environmentally benign and inexpensive biological synthesis mediated by plants or microbes has been essentially adopted. The variations in size, shape and surface chemistry of NPs affect the properties of metal NPs to a greater extent which in turn have an influence on their biological behaviour. Few metal NPs offer unique optical properties while others possess paramagnetic behaviour and quantum size effect which make them suitable in bio-imaging diagnostic techniques. Some metallic NPs play a role in tissue engineering and other therapeutic applications due to their ease of surface modifications, large surface area to volume ratio, unique electrical and anti-microbial activities. Instead of

R. Singla · A. Guliani · A. Kumari · S.K. Yadav
Department of Biotechnology, Council of Scientific and Industrial Research-Institute of Himalayan Bioresource Technology, Palampur 176061, Himachal Pradesh, India

R. Singla · A. Guliani · S.K. Yadav
Academy of Scientific and Innovative Research, New Delhi, India

S.K. Yadav (✉)
Department of Biotechnology, Center of Innovative and Applied Bioprocessing (CIAB), Mohali 160071, Punjab, India
e-mail: skyt@rediffmail.com; sudesh@ciab.res.in

© Springer Science+Business Media Singapore 2016
S.K. Yadav (ed.), *Nanoscale Materials in Targeted Drug Delivery, Theragnosis and Tissue Regeneration*, DOI 10.1007/978-981-10-0818-4_3

multi-disciplinary applications of metallic NPs, there is a great concern regarding the toxicity issues associated with the use of these NPs which need to be sorted out by looking out certain ways for favourable architecture involving the synthesis methods and parameters for designing the non-toxic NPs for improving the quality of life.

Keywords
Metallic nanoparticles · Disease diagnostics · Drug delivery · Cancer therapy · Theranostics · Gene therapy

Contents

3.1 Introduction

Nanotechnology is a vast area at an interface of many disciplines like biology, physics, chemistry and engineering (Rosarin and Mirunalini 2011). It deals with miniaturize-sized particles with at least one dimension ranging from 1 to 100 nm (Zamborini et al. 2012). Few important questions which come into mind before dealing with nanomaterials are "why these tiny materials are so interesting?" and "what is the basic speciality in these nanomaterials when compared to their macroscopic counterparts?" Before going into detailed study of nanoparticles (NPs), it is necessary to give answers to these unavoidable questions. The development of metallic NPs has become the centre of attraction in the modern era of nanomaterials due to their unique intrinsic properties such as excellent optical, electrical, catalytic and magnetic behaviour, chemical and mechanical stability, ease of surface modification, large surface area for reactions, etc. (Rosarin and Mirunalini 2011; Kumari et al. 2014b). These properties are quiet different from the bulk counterparts from which these NPs are synthesized. The synthesis of metallic NPs mainly takes into account two different approaches named as "top-down" and "bottom-up". The top-down process is the breaking down of a system or a molecule to generate NPs whereas the bottom-up approach means to assemble or piece together the single atoms or molecules to build up nanostructures (Thakkar et al. 2010). Using these two approaches, a variety of physical and chemical methods have been devised for the synthesis of metallic NPs. Methods mainly include (1) thermal decomposition, (2) sonochemical, (3) microemulsion, (4) chemical reduction, (5) polyol method, (6) microwave, (7) laser ablation and many more (Tripathi et al. 2009; Kumari et al. 2014b). Stable and monodisperse NPs are synthesized using physical and chemical methods. But these methods

involve the use of hazardous chemical substrates, intense energy consumption, costly reaction setup and generation of harmful end products (Khodashenas and Ghorbani 2015). Therefore, these methods should be used depending on the ultimate use of end products. In view of this, an alternative eco-friendly and inexpensive approach for the formation of NPs has been developed employing the plants/plant parts or microbial cultures (Iravani et al. 2014).

For the synthesis of metal NPs, it is a critical step to determine the size, shape and morphology of NPs through characterization by using high-throughput instruments. Various factors such as temperature, incubation time, concentration of metal substrates used, ratio of metal precursor to reducing agent/stabilizing agent, types of surfactants used, concentration of plant extract, amount of microbial culture, age of culture and pH of media play a deciding role for alternating dimensions and shape of particles (Hyeon 2003; Dang et al. 2011; Korbekandi et al. 2013; Makarov et al. 2014). The particle properties are highly dependent on their characteristics (shape, surface functionality and size) which ultimately define the role of NPs in the biological environments. The metallic NPs are categorized into different types such as metal NPs (silver, gold, copper, platinum), metal oxide NPs (copper/cuprous, zinc, titanium), magnetic NPs (iron, nickel, cobalt, manganese) and semiconductor NPs or quantum dots. These kinds of NPs have smaller size and have a wavelength lesser than that of light. Due to these properties, NPs can easily traverse the cells or tissues inside the body to reach a target location. These potential features of metal NPs make them applicable in wide spectrum of biomedical areas including imaging for disease diagnosis, targeted drug delivery, cancer treatment, gene therapy, bactericidal activity, wound healing/tissue repair and tissue engineering (Mody et al. 2010). Imaging modalities such as magnetic resonance imaging (MRI), computed tomography (CT), positron-emission tomography (PET) and ultrasound imaging techniques have been developed to image the status of diseased organs (Thomas et al. 2013). These imaging techniques require a contrast agent with unique physico-chemical properties where metal NPs can serve as versatile agents.

Regardless of abundant extraordinary physico-chemical properties that metallic NPs possess, there are also reports concerning the toxicity of these NPs. While utilizing the metal NPs for applications involving living systems, it is a prior need to identify the risks associated with these. Thereby, it is required to design the surface of metal NPs in such a way so as to minimize the toxicity and to maximize their potentialities. This chapter provides the detailed description on physico-chemical properties of metallic NPs, various synthesis methods (physical, chemical and biological), various factors affecting the properties of NPs and their biological behaviour, applications of NPs in imaging, therapy, drug delivery and tissue engineering. Also, the toxicity issues associated with the use of these NPs are mentioned.

3.2 Physico-Chemical Properties of Metal and Metal Oxide NPs

The metal and metal oxide NPs impart unique and significant properties as compared to their bulk counterparts which play wide roles in a variety of applications on global scenario. Silver NPs (AgNPs) are prepared from different silver salts like silver chloride (AgCl), silver iodide (AgI) and silver nitrate ($AgNO_3$) having size range of 1–100 nm. AgNPs possess unique physical, chemical, optical, anti-microbial and electronic properties. The properties of AgNPs depend upon their size and morphology (Wei et al. 2015). The colour of AgNPs solution varies from light yellow to reddish brown and even black which provides a mere clue about the size and agglomeration tendency of AgNPs. The size and morphology of NPs also vary with the initial concentration of metal salt used for the synthesis of NPs. The stability or the tendencies of particle aggregations are keys to determine their properties up to a greater extent.

Gold NPs (AuNPs) are the particles ranging in dimensions of 3–150 nm and are also known as

colloidal gold. They possess many distinctive properties which make them 'star' among the other NPs. AuNPs have a tendency to change the colour of colloidal solutions depending upon their sizes. The important properties of AuNPs are high surface to volume ratio, optical, electrochemical and catalytic properties, low toxicity, easy to prepare, easily dispersed in liquids and ease of surface modifications. Nowadays, the research on copper NPs (CuNPs/CuO NPs) has become a focal point due to their unique properties, low cost of preparation and utility in wide array of applications. CuNPs possess good thermal and electrical conductivity, as well as optical properties. Zinc oxide NPs (ZnO NPs) is an important type of semiconductor material which possess good electrical, optical and piezo-electrical properties. Titanium dioxide (TiO_2) NPs of size less than 100 nm serve as advanced semiconductor materials of great interest due to their strong oxidation power, resistance to corrosion, abundance, optical activity and chemical stability as well as non-toxic nature.

Magnetic NPs (MNPs) are of great potential in the present era as they possess magnetic behaviour with utility in diverse fields. The researchers pay more attention to the synthesis methods to form uniform-sized MNPs because the properties of MNPs are size dependent. Three major functional parts of a MNPs carrier include magnetic core, a surface coat and a functional outer coating. The inner magnetic core consists of a supramagnetic molecule such as Fe, Ni, Co, Mn, etc. depending upon their applications. The surface coat is used to provide steric repulsions, to increase the stability and to restrain agglomeration of the particles. The functionalized outer coating may attach any ligand or the biologically active entity (Kumari et al. 2014b). These NPs exhibit superparamagnetism and play a role as fluorescence emitters.

Semiconductor nanocrystals are the type of inorganic NPs discovered in early 1980s ranging in size between 1 and 10 nm. These represent a state of matter in the transition regime in between the molecules and the bulk solid. A layer of organic ligand at the surface of semiconductor NPs stabilizes them in the colloidal form. The ligand consists of two parts: a polar head group that possesses the affinity for the attachment to the surface of semiconductor nanocrystals and a second part, tail which helps in the solubilization of semiconductor nanocrystals in the organic media. The properties of semiconductor nanocrystals arise due to the spatial arrangements of atoms in the crystalline lattice. The optical and electronic properties of semiconductor nanocrystals can be varied with the reduction in the size of nanocrystals and the phenomena can be described by the term 'size quantization effect'. The quantum dots (QDs) are the small-sized semiconductor nanocrystals to be fit in the quantum confinement region.

3.3 Synthesis of Metal and Metal Oxide NPs

Metallic NPs are of great demand as these have fascinated the scientific world over the past few decades with their astonishing applications in biomedical and engineering sciences. Metal and metal oxide NPs include AgNPs, AuNPs, copper (CuNPs or CuO NPs), ZnO NPs, TiO_2 NPs, iron oxide (Fe_2O_3/Fe_3O_4 NPs), manganese (Mn/MnO NPs) and semiconductor NPs or quantum dots/fluorescent NPs, etc. These nanomaterials are mainly synthesized by the use of chemical and physical methods (Senapati 2005). The chemical synthesis involves the use of chemicals that act to reduce the metal salts leading to the formation of NPs. The conventional methods of synthesis of NPs (physical and chemical methods) have few drawbacks such as the requirement of toxic hazardous chemicals, energy intensive and costly processes that make it difficult to be widely implemented. To overcome these limitations, the researchers have looked forward for an easy and feasible alternative approach for the synthesis of nanocompounds. The employment of alternative biogenic route for the NPs synthesis by using biological entities of unicellular living organisms such as bacteria, fungi, actinomycetes and also the plant and plant parts has seeked apparent attention of the scientists

throughout. The biological synthesis of metal NPs has been exploited using a wide variety of plants (leaf and seed extracts) and microorganisms such as bacteria, actinomycetes, yeast and fungi, etc. (Bhattacharya and Rajinder 2005). Various microbes ranging from unicellular to multicellular organisms are known to produce NPs either intracellularly or extracellularly (Mann 1996). The formation of NPs being intracellular or extracellular can easily be manipulated by controlling various process parameters like substrate concentration, pH, temperature and many more (Gericke and Pinches 2006). The metal NPs hold a variety of uses in the pharmaceutical sector, catalysis and sensors.

Several methods used for the formation of metallic NPs include electrochemical, sonochemical, thermal decomposition, laser ablation, chemical reduction, polyol and microemulsion method. These methods are described below in detail with suitable examples of each type of NPs. The synthesis of semiconductor nanocrystals can be categorized into two basic types, synthesis in aqueous media and synthesis in organic media. In current trends, a new approach using biological agents for the synthesis of NPs is also described herein.

3.3.1 Electrochemical Synthesis

This method involves the passing and conduction of electric current through an electrolytic solution resulting in chemical changes. In an electrochemical method, two electrodes of metal made as anode and cathode are dipped in the electrolytic solution containing metal salt and a stabilizer and electric voltage is applied over the electrodes (Ibrahim et al. 2013). In this process, a constant electric current flows into the electrolytic cell leading to the dissociation of metal salt solution due to its ionization. Oxidation occurs and metal sheet is dissolved at the anode while the reduction of intermediate salt takes place at cathode. Metal is removed from the anode terminal and gets deposited onto cathode plate. At the end of electrolysis process, metal atoms in the form of NPs are carefully collected from cathode terminal (Theivasanthi and Alagar 2011).

The highly pure AgNPs of different sizes can be obtained by just an alteration in the current density. The surfactants like poly (N-vinylpyrrolidone) (PVP) can be used for synthesis of AgNPs in the aqueous phase. By adding anionic surfactants to the electrolyte at an optimum level, the particle size distribution can be improved. PVP as a stabilizer favours the formation of monodisperse AgNPs and decreases the deposition of silver on cathode (Yin et al. 2003). In another report, electrochemical method has been used for the synthesis of AgNPs and AuNPs where rotating platinum (Pt) electrode was made cathode and Pt sheet as anode. Rotating Pt electrode helps in transfer of metal NPs from the cathode to the bulk of electrolytic solution. For AgNPs synthesis, base electrolyte was composed of $AgNO_3$, KNO_3 and PVP whereas for AuNPs preparation, it consisted of $HAuCl_4$, KNO_3 and PVP. KNO_3 acted as electrolyte and PVP as stabilizer. Sodium dodecyl benzene sulfonate as anionic surfactant and polyethylene glycol (PEG) as non-ionic surfactant was added to electrolyte to obtain particles of smaller dimensions with narrow size distributions (Ma et al. 2004).

Synthesis of CuNPs by electrolysis method has been conducted by an electrolytic setup where Cu wire was used as cathode and Pt as anode. The surface area of anode was 50 times greater than cathode, and both the electrodes were kept 30 mm apart. K_2CO_3 solution and citrate buffer served as two different electrolytes. The effect of applied voltage (105 and 130 V) and electrolysis time (60 and 5 min) has been examined on shape of synthesized NPs. CuO nanoflowers with many sharp nanorods have been obtained using K_2CO_3 and the size of CuO NPs was decreased with decreasing the concentration of the solution. Whereas spherical-shaped Cu particles with/without pores were synthesized using citrate buffer as electrolyte (Saito et al. 2011). A copper sheet has also been used as anode and a platinum sheet as cathode in an electrolysis reaction. Here, tetrabutylammonium

bromide (TBAB) in acetonitrile/tetrahydrofuran (4:1) served as electrolyte. After application of steady flow of current, the anode slowly dissolved, leading to the formation of CuO clusters which were further stabilized by TBAB. Electrolysis was carried out under inert atmosphere of N_2 bubbles for 2 h. The parameters such as current density, solvent polarity, distance between electrodes and concentration of stabilizers were used to control the size of CuO NPs (1–10 nm). The clusters' size was found to decrease with increase in current density (Jadhav et al. 2011).

ZnO NPs of spherical (50–100 nm) and cylindrical shapes (150–200 nm) have been synthesized by electrochemical method where Zn electrodes were used as anode and cathode along with aqueous oxalic acid as electrolyte. The parameters like pH, concentration of electrolyte, conductivity and electric voltage were optimized to obtain maximum productivity of ZnO NPs (Anand and Srivastava 2015). For the synthesis of TiO_2 NPs by this method, Ti metal sheet was made both as cathode and anode whereas tetrapropylammonium bromide (TPAB) in acetonitrile/tetrahydrofuran (4:1) acted as supporting electrolyte. The main parameters of current density, solvent polarity and stabilizer concentration were used to control the size of TiO_2 NPs which led to the formation of tetragonal NPs of dimensions 25–30 nm (Anandgaonker et al. 2015).

Electrochemical method possesses certain advantages over chemical methods as it leads to the formation of size and shape-controlled highly pure metal NPs. The significant features of electrochemical methods are its ease of operation, high productivity of NPs and absence of any undesired side products.

3.3.2 Sonochemical Method

This method has been used for the synthesis of metal NPs by the reduction of metal salt solution in the aqueous phase. A sonochemical reaction results from the acoustic cavitation produced by ultrasonic waves and implosion of bubbles. A pulse of high energy is given to produce heavy nuclei which in turn lead to sudden release of ultrasonic energy. The water molecules generate free radical species through the production of ultrasound in the aqueous phase. Generated H^+ ions cause the reduction of metal ions according to the following equations:

$$H_2O \rightarrow H^+ + OH^- \tag{3.1}$$

$$M^+ + H^\cdot \rightarrow M^0 + H^+ \tag{3.2}$$

Metal salt solution reduced to metallic NPs by the high temperature and pressure applied during this process (Gong and Hart 1998). The transient temperature and fast cooling rates are necessary for the formation of particles in the sonochemical process. This method aims at controlling the particle size and morphology of NPs within a much narrow size distribution. The productivity and properties of synthesized material depend upon the ultrasonic power and frequency, dissolved gas, type of solvent and temperature of the solution (Okitsu et al. 2005).

AgNPs of variable shapes including spherical, rod-like and dendritic NPs have been synthesized by the reduction of $AgNO_3$ solution in the aqueous phase in the presence of nitrilotriacetate (NTA). A Ti horn acted as cathode as well as ultrasound emitter. The concentration of Ag and NTA has an important role in deciding the shapes of NPs (Zhu et al. 2000). AuNPs have been formed within the pores of mesoporous silica by soaking and ultrasound has induced the reduction of $AuCl_4^-$ ions in the pores of silica (Chen et al. 2001). For the preparation of CuNPs by sonochemical method, Cu(II) hydrazine carboxylate [Cu-$(N_2H_3COO)_2 \cdot 2H_2O$] complex has been used in aqueous medium. A mixture of metallic copper (Cu) and copper oxide (Cu_2O) has been formed while $H^\cdot$ and $OH^\cdot$ radicals produced acted as reducing agents to reduce copper ions into Cu. The formation of Cu_2O was attributed to partial oxidation of Cu by the generation of oxidant H_2O_2 itself in the process. H_2O_2 generated can be scavenged in the atmosphere of argon and hydrogen, thereby

producing pure CuNPs (50–70 nm) and further eliminating Cu_2O formation (Dhas et al. 1998).

Clustered ZnO NPs of an average size 70 nm have been synthesized using this method by the reaction between zinc nitrate and hexamethylenetetramine using ultrasonic homogenizer for the generation of ultrasonic pulse (Pholnak et al. 2013). In another study, mesoporous TiO_2 has been obtained by ultrasound irradiation where octadecylamine was used as a structure-directing agent and Ti $(OPr^i)_4$ as a precursor. The authors have studied the effect of two different methodologies on particle morphology where in the first method, octadecylamine was mixed in ethanol and in the second method, octadecylamine was dispersed in a mixture of ethanol and distilled water. Spherical- or globular-shaped particles were obtained as aggregates of small particles when first method was applied whereas irregular inter-grown aggregates of small particles were formed from the application of second method (Wang et al. 2001). The synthesis of magnetic manganese dioxide (MnO_2) NPs has been investigated by the sonochemical reduction of MnO_4 in water under Ar atmosphere at 20 °C (Abulizi et al. 2014). The advantages of this method are that it is simple, much efficient and produces NPs of very small size (Salkar et al. 1999).

3.3.3 Thermal Decomposition

Thermal decomposition is a method widely suitable to synthesize monodisperse NPs in a powdered form. The synthesis by this method generally requires high temperature in the range of 120–250 °C, long reaction time, toxic chemicals or catalysts and inert atmosphere (Li et al. 2005). In a study reported by Lee and Kang (2004), Ag nanocrystallites have been prepared by the decomposition of Ag^{+1}-oleate complex by the reaction of $AgNO_3$ with sodium oleate in aqueous media at a temperature of 290 °C which has resulted in the formation of Ag atom and oleate molecule. The nanocrystallites formed by this reaction were packed in a highly ordered state with size range of 9.5 ± 0.7 nm. In another report, AgNPs of sizes 5.1–6.3 nm have been prepared from the decomposition of Ag complex termed as silver(I) [bis(alkylthio)methylene]-malonates which were formed by the reaction of $AgNO_3$ with potassium [bis(alkylthio) methylene]malonates. The Ag complex so formed was further decomposed in the presence of 1,2-dichlorobenzene without the addition of any external surfactant at a temperature of 110 °C to form AgNPs. The size of formed AgNPs could be altered by varying the chain length of alkyl precursors (Lee et al. 2012). AuNPs of spherical or partially coalesced shape with 63 nm diameter has been synthesized using the same method. For this, Au acetate powder was heated at a rate of 25 °C min^{-1} and its fragmentation was observed at 103 ± 20 °C which led to the formation of AuNPs (Bakrania et al. 2009).

Metallic CuNPs have been synthesized by this method using copper oxalate-oleylamine complex. After the decomposition, reddish coloured irregular-shaped agglomerated CuNPs of size 30–80 nm were obtained (Salavati-Niasari et al. 2008). While Cu and Cu_2O NPs have been formed by this method using [bis(salicylidiminato)copper(II)], $[Cu(sal)_2]$, as metal precursor. $[Cu(sal)_2]$-oleylamine complex was heated at a high temperature and initially led to the formation of red-coloured CuNPs which on a later stage get changed into Cu_2O NPs after oxidation. Agglomerated Cu and Cu_2O NPs of size 8–10 nm were obtained by this method (Salavati-Niasari and Davar 2009).

Khalil et al. (2014) have prepared ZnO NPs of size 117 nm by thermal decomposition of binuclear zinc(II) curcumin complex. In another case, the synthesis of $ZnCO_3$ and ZnO NPs has also been investigated using this method by optimizing the reaction parameters such as the concentration of zinc and carbonate ions, flow rate of reagent addition and reactor temperature (Shamsipur et al. 2013). Multi-type nitrogen-doped TiO_2 NPs have also been synthesized by employing decomposition of a mixture of titanium hydroxide and urea at 400 °C for 2 h (Dong et al. 2009). In another experiment by Chin et al. (2010), the synthesis of TiO_2 NPs has been reported by decomposition of

titanium tetraisopropoxide (TTIP) in a tubular electric furnace at synthesis temperatures ranging 700–1300 °C and TTIP heating temperatures of 80–110 °C. An example of MNPs where the formation of $Co_{48}Pt_{52}$ NPs of size 7 nm has been carried out by the simultaneous reduction of platinum acetylacetonate and the thermal decomposition of cobalt tricarbonylnitrosyl [$Co(CO)_3(NO)$] in the presence of oleic acid and oleyl amine (Chen and Nikles 2002). The other example where Fe_2O_3 NPs with size range of 5–19 nm have already been synthesized by thermal decomposition of iron pentacarbonyl, $Fe(CO)_5$ in dioctyl ether solvent where oleic acid and oleylamine were used as surfactants (Frey et al. 2009). The ratio of precursors used, surfactants, solvent, reaction temperature and reaction time are the crucial factors to control the size and shape of MNPs.

3.3.4 Laser Ablation

It is a physical technique to generate NPs and is characterized by the absence of any counter-ion contamination and surface active molecules (Brust et al. 1995). There are two main problems faced by researchers while using laser ablation method. Firstly, due to post-ablation agglomeration, the particles coalesce with each other and form large clusters. Secondly, at higher laser fluence, large fragments are formed which limit the formation of small clusters (Kabashin and Meunier 2003). Laser ablation is a process where a solid target substance is ablated by laser of a particular wavelength in a gas or liquid medium. In this method, the control over the growth rate of NPs formation is manipulated by varying certain process parameters like wavelength of laser beam, duration of beam irradiation and time, pulse energy and pulse repetition, etc. (Amendola and Meneghetti 2013).

In a recent report, AgNPs have been developed by laser ablation technique where a pure Ag plate was ablated using a Q-switched Nd:YAG (neodymium-doped yttrium aluminium garnet; $Nd:Y_3Al_5O_{12}$) pulsed laser at a wavelength of 532 nm (360 mJ/pulse) with a pulse duration of 10 ns and 30 Hz repetition rate in two different media such as ethylene glycol and chitosan. The plate was ablated to laser beam for 30 min at room temperature which resulted in the formation of spherical-shaped AgNPs of size 22 and 10 nm respective to media used. The formation efficiency and stability of AgNPs synthesized in chitosan media were comparatively high as the chitosan molecules played a role in prevention of particle aggregations (Tajdidzadeh et al. 2014). AgNPs of nearly spherical and elliptical shape with 9–27 nm size have been formed by placing a pure Ag rod in aqueous media of double-distilled water and ablated for 3 h by a pulsed Nd:YAG laser beam of 1,064 nm operating at 40 mJ/pulse energy with 10 Hz repetition rate and 10 ns (Pandey et al. 2014).

AuNPs in the size range of 5–20 nm have been formed by laser ablation of Au foil located inside or outside the ionic liquids, 1-n-butyl-3-methylimidazolium tetrafluoroborate, 1-n-butyl-3-methylimidazolium hexafluorophosphate and 1-(3-cyanopropyl)-3-methylimidazolium bis (trifluoromethylsulfonyl)imide (Wender et al. 2011). The formation of CuNPs by laser ablation in pure water and aqueous solutions of 1,10-phenanthroline has been reported (Muniz-Miranda et al. 2012). Nano Zn particles of colloidal behaviour have been synthesized by this method where Zn target in distilled water was ablated by a laser beam and sodium dodecyl sulphate (SDS) was used as a surfactant to prevent particle agglomeration (Singh and Gopal 2008). Pulsed laser ablation method in liquid media has also been used for the formation of nano-sized Ti particles where Ti target present in water or ethanol was ablated using fibre laser doped with monomode Ytterbium (Boutinguiza et al. 2013).

The formation of magnetic Fe_2O_3 NPs ranging in size 50–110 nm has been reported where iron target in dimethylformide and SDS were ablated. The authors have also studied the effect of laser fluence on particle characteristics (Ismail et al. 2015). There are reports on the synthesis of other kind of MNPs like Co and Ni NPs by laser ablation in organic media of ethylene glycol. In

this experiment, pure Ni, $Ni_{50}Co_{50}$ alloy and Co metal plates have been used as respective solid targets for irradiation (Zhang and Lan 2008). A simplified way of synthesis of mercaptan acid-capped CdTe/CdSe (core/shell) type II QDs in aqueous dispersion has been known by a microwave-assisted approach. The CdTe/CdSe QDs obtained with a core/shell structure of high crystallinity exhibited an adjustable fluorescence emission by administering the changes in the thickness of the CdSe shell (Sai and Kong 2011).

The advantages of laser ablation technique involve no use of chemical reagents and simplicity of the procedure. The method is quite fast and effective and does not require several reaction steps as well as long processing time to carry out the reaction (Barcikowski and Compagnini 2013). Along with certain advantages, the same process has few drawbacks also. Concentration and size of NPs change with time as the number of pulsed laser beams increase. With the increase in laser shots, the density of NPs in solution was rised (Jafarabadi and Mahdieh 2013).

3.3.5 Chemical Reduction

Chemical method for the synthesis of NPs has been greatly employed. This method is relatively simple and easy to perform the synthesis of stable NPs in solution. Metal precursors, reducing agents and stabilizing agents are the three basic components used in any chemical method. For the synthesis of monodisperse and uniform-sized NPs, all the nuclei should be formed at the same time to acquire the same subsequent growth (Tran et al. 2013). Through the use of chemical reducing agents, control over the shape, size and size distribution of metal and metal oxide NPs is possible by easily manipulating the various process parameters viz. molar ratio of the reducing agent used to the molar ratio of metal precursor salt as well as the molar ratio of capping agent used to the molar ratio of metal precursor salt (Dang et al. 2011). The use of strong reducing agents such as borohydride leads to the formation of monodisperse small NPs, but the synthesis of large-sized NPs becomes uncontrolled. On the other hand, weak reducing agents like citrate are known to cause a slower reduction and produce small-sized NPs (Shirtcliffe et al. 1999). The stabilizing agents are used in the reaction to avoid an agglomeration of NPs formed during the reaction (El-Nour et al. 2010). The time duration, reaction temperature and pH conditions play a vital role in determining the size and shape of NPs during chemical synthesis (Mott et al. 2007).

Various reducing agents such as $NaBH_4$, ethylene glycol, glucose, citrate, ascorbate and elemental hydrogen and stabilizing agents such as polyvinyl alcohol (PVA), PVP and sodium oleate have been employed for the synthesis of AgNPs (Patil et al. 2011). SDS and citrate have also been reported for synthesis of AgNPs (Guzman et al. 2009). In Tollen's method, AgNPs of size 20–50 nm have been formed in a single-step process by the reduction of silver ammoniacal solution using saccharides like glucose, galactose and lactose as reducing agents (Panacek et al. 2006). The chemical reduction of Au salts by citrate anions to yield monodisperse water-soluble Au clusters of size 7–100 nm has been reported. The only requirement for this method is Au salt, water and tri-sodium citrate. Citrate acts as a reducing agent as well as a stabilizer. It acts as a stabilizing agent by forming a negative layer on the particles and thus preventing their aggregation (Verma et al. 2014). Another method is seed-mediated growth process where 2-mercaptosuccinic acid (MSA) has been used as a reducing agent in aqueous solution leading to the formation of quasi-spherical AuNPs (30–150 nm). MSA acts as a capping agent favouring the formation of monodisperse Au seeds (Niu et al. 2007). A study reports the formation of CuNPs using copper sulphate pentahydrate, $CuSO_4 \cdot 5H_2O$ as metal precursor salt and starch as capping agent where L-ascorbic acid acted as reducing agent. After heating, a colour change of the mixture from yellow to ocher was resulted. Cu and Cu_2O NPs of cubic shape with mean diameter 28.73 and 25.19 nm, respectively, were formed (Khan et al. 2015). In another case, L-ascorbic acid has been used as reducing agent as well as antioxidant to reduce

metal salt, $CuCl_2$ without the addition of any external capping agent or stabilizer. The reaction was carried out to reduce Cu^{2+} ions to metallic Cu as:

$$Cu^{2+} + C_6H_8O_6 \rightarrow Cu + C_6H_6O_6 + 2H^+ \quad (3.3)$$

Spherical-shaped CuNPs of average size less than 6 nm have been formed by this method (Li et al. 2013). Sodium borohydride has been used as chemical reducing agent along with polyethylene glycol (PEG) as capping agent for the reduction of $CuSO_4 \cdot 5H_2O$ where ascorbic acid acted as antioxidant for colloidal copper. From this reaction, CuNPs of less than 10 nm have been obtained at room temperature. Particle size was decreased as the concentration of reducing agent and the relative amount of capping agent used for the reaction were increased (Dang et al. 2011).

For the synthesis of ZnO NPs by chemical synthesis, most of the alcoholic media like ethanol, methanol and isopropanol are known. In alcoholic medium, the synthesis rate of NPs is slow and controllable (Sabir et al. 2014). Zinc acetate and zinc nitrate salts have been used as precursor for the formation of ZnO NPs. The development of Ni, Co and Fe_2O_3 NPs has been described through the rapid expansion of super critical fluid solutions coupled with chemical reduction method. For the synthesis of Ni and Co NPs, chloride salts of both the metals were expanded at room temperature and reduced by $NaBH_4$. Poly(vinyl propylene) has been used for NPs stabilization. Fe_2O_3 NPs have been synthesized from the reduction of $FeBr_3$ metal precursor by a reducing agent $LiB(C_2H_5)_3H$, while $NaBH_4$ was incapable of reducing iron ions. Poly (ethylene oxide) was used for particle stabilization (Sun et al. 1999).

The synthesis of semiconductor nanocrystals in water was started earlier than the synthesis in the organic phase. A variety of semiconductors are being used for synthesis of core–shell nanocrystals which mainly include the combination of II–VI and III–V type of semiconductor materials (Grieve et al. 2000). Monodisperse cadmium selenide (CdSe) QDs of size 2–2.3 nm with high quantum yield up to 76.57 % have been prepared by the aqueous precipitation method by adding Se precursors to Cd precursor solution under the maintained nitrogen atmosphere at magnetic stirring (Gao et al. 2013). The synthesis of CdS semiconductor NPs of II–VI type by the chemical precipitation method has been reported using cadmium salt and sodium sulphide along with the use of triethanolamine as a capping agent (Prabhu and Khadar 2005). The synthesis of cadmium telluride (CdTe) QDs has been reported in the literature from the precursor ions Cd^{2+} and Te^{2-} which react in the aqueous solvent in the presence of thiol ligands, thioglycolic acid (TGA) or mercaptopropionic acid (MPA) to nucleate the crystalline seeds (Gaponik et al. 2002). The dimensions of nanocrystals can be altered by varying the time of heating/growth from few minutes to hours. A very similar approach has been applied for the aqueous synthesis of zinc selenide (ZnSe) nanocrystals, as that for CdTe. The reaction was carried out at optimum pH by bubbling H_2Se gas through the aqueous media of the zinc salt and the thiol group containing stabilizing molecules like thioglycerol, TGA and 3-MPA by refluxing the reaction mixture for a few hours to attain nanocrystals growth (Shavel et al. 2004).

The organometallic synthesis of QDs in the high-temperature organic solvents is quiet easy and controllable. An organometallic synthesis of QDs includes mainly three components: precursor molecule, organic coordinating solvent and surfactant. Organometallic precursors comprise of metal alkyls or aryls (dimethylcadmium, diethylzinc, dibenzylmercury), whereas S, Se or Te sources are generally selected from trialkylphosphine chalcogenides (R_3PSe, R_3PTe with R¼octyl or butyl) or bistrimethylsilylchalcogenides e.g. $(Me_3Si)_2S$, abbreviated $(TMS)_2S$. The selection of suitable solvent is important as it influences the reactivity of precursors as well as growth kinetics (Farkhani and Valizadeh 2014). The synthesis of most important type of QDs (II–VI semiconductors) consists of rapid injection of semiconductor precursor molecule into constantly stirred solvents like

trioctylphosphine oxide (TOPO) or trioctylphosphine (TOP) as these solvents provide the most appropriate controlled conditions for the growth of nanocrystals (Hammer et al. 2007). Another facile method for the synthesis of CdTe QDs of size 3.2–6 nm involves the mixing of cadmium oxide with Te along with oleic acid, paraffin oil and TOP as solvents, and heating at a high temperature of 200 °C (Xing et al. 2008). Indium phosphide (InP) and indium arsenide (InAs) QDs have been synthesized under argon atmosphere at high temperature using different precursors like tris(trimethylsilyl)arsine ($TMSi_3As$) and the similar molecules TME_3V (E = Si, Ge; V = P, As) and their reaction kinetics were studied (Harris and Bawendi 2012). Another simplest, one-step method without the precursor injection for providing the heat up pathway to synthesize high-quality InP/ZnS nanocrystals consists of combination of both InP core and ZnS shell precursors (indium myristate; tris(trimethylsilyl) phosphine, P $(TMS)_3$; zinc stearate; dodecanethiol) at room temperature in 1-octadecene and heating of this mixture at 250–300 °C. The obtained nanocrystals emit in the range of 480–600 nm with a quantum yield of 50–70 % and excellent photostability (Li and Reiss 2008).

The only disadvantage of chemical reduction synthesis method is that it involves the use of some toxic chemicals which may cause harm to the users as well as environment. Moreover, the process is quiet costly as it takes into account the utility of expensive chemical substances.

3.3.6 Polyol Method

This is the versatile chemical synthetic method used to synthesize NPs with well-defined shape and controlled sizes. The polyol process uses a poly-alcohol like PEG which acts as a solvent to dissolve inorganic compounds due to their high dielectric constant and offers a wide operating temperature (25 °C to boiling point) due to their relatively high boiling points. The polyols also act as reducing as well as stabilizing agents to produce NPs from the metallic cationic precursor and prevent inter-particle aggregation (Laurent et al. 2008).

The polyol process is one such method in which large quantity of $AgNO_3$ solution is reduced with ethylene glycol in the presence of PVP (Sun and Xia 2002). An oleylamine-liquid paraffin system has been used for the formation of monodisperse AgNPs. Commonly used chemicals in this process are liquid paraffin, oleylamine and $AgNO_3$. The paraffin provides a temperature range of 300 °C and controls the particle size of AgNPs alone without changing the solvent (Chen et al. 2007). AuNPs of size range 75 ± 10 nm have also been prepared by reduction of Au ions in neat ethylene glycol. This reaction occurred without addition of any external reducing agent and it gets accelerated on addition of NaOH (Nalawade et al. 2012). The synthesis of CuNPs has also been done by polyol method using copper acetate as metal precursor, hydrazine as reductant, PVP as stabilizer under aerobic atmosphere (Dementeva and Rudoy 2012).

Three mixing strategies such as stirred batch, T-mixer and impinging free jets have been used to study their effect on the particle morphology of ZnO NPs synthesized via a polyol process (Hosni et al. 2015). The fascinating benefit of a polyol process is its capacity to produce hydrophilic Fe_2O_3 NPs of greater magnetization and controllable secondary structures in just a single step (Couto et al. 2007). For the formation and morphology evolution of a series of magnetic Fe_2O_3 NPs clusters and porous NPs, two polyols namely ethylene glycol and 1,2-propylene glycol were used as a solvent with different reductive abilities (Cheng et al. 2011).

3.3.7 Microemulsion

Microemulsions mainly consist of three components polar phase, non-polar phase and a surfactant. The microemulsions possess some specific properties like large interfacial area, ultra-low surface tension, high thermodynamic stability, and the ability to solubilize both

aqueous and oil based compounds. Two types of microemulsions are (a) oil-in-water microemulsion (o/w) which is formed when the droplets of oil are dispersed in the water and (b) water-in-oil microemulsion (w/o) consists of nano-sized water droplets dispersed in a continuous phase of oil. These microemulsions are further stabilized by the surfactant molecules present at the interface of polar and non-polar compounds. The water-in-oil microemulsion is also termed as reverse micelle because the surfactant molecules containing the polar part are attracted by the aqueous phase towards inside while the non-polar part of hydrocarbons is directed outside by the attraction of non-aqueous phase (Malik et al. 2012). The parameters affecting the size of nano-droplets include different kinds of stabilizing agents, content of precursor molecule, the continuous phase and the molar ratio of water to surfactant. Additionally, temperature, pressure, reagent concentration and types of salts have been found to affect the stability of microemulsions formed (Zielinska-Jurek et al. 2012).

AgNPs synthesis has been reported by a microemulsion technique using H_2 reducing agent in toluene supercritical CO_2 microemulsion system (Lu and An 2015). AuNPs have been prepared by the same method (Hernandez et al. 2004). CuNPs synthesis by the reduction of copper ions in $CuCl_2$ solution in triton X-100, n-hexanol and cyclohexane w/o microemulsion has been done using $NaBH_4$ as a reducing agent (Qi et al. 1997). ZnO NPs have been synthesized by a reverse microemulsion system of sodium bis (2-ethylhexyl)sulfosuccinate:glycerol:n-heptane (Yildirim and Durucan 2010). The synthesis of crystalline TiO_2 NPs of size 4.2 nm has been performed by water-in–oil-type microemulsion method where titanium tetrachloride was dissolved in organic phase and another reactant ammonium hydroxide in aqueous media (Keswani et al. 2010). Fe_2O_3 NPs have been prepared using w/o microemulsion using n-heptane as oil phase, water and AOT as the surfactant with $FeCl_3$ as a starting material and ammonium hydroxide as a precipitating agent (Wongwailikhit and Horwongsakul 2011).

3.3.8 Biological Synthesis

Recent trend has adopted the use of bacteria, fungus, actinomycetes, plant and plant parts for the synthesis of metal and metal oxide NPs. Biological approach is environmental friendly, non-toxic and relatively cheap. Also, this approach does not involve the use of any harmful chemicals as well as no energy intensive process is required for the synthesis purpose.

3.3.8.1 Bacteria-Mediated Synthesis

The use of micro-organisms for the NPs synthesis purpose is found to be easy, economical and eco-friendly. AgNPs have been synthesized intracellularly and extracellularly using Bacillus strain CS11. For this, $AgNO_3$ solution was added to the nutrient broth-containing bacterial biomass and incubated for 72 h at room temperature in the presence of light. The change in colour of the medium from pale yellow to brown has indicated the formation of AgNPs. The mechanism for the bioreduction of silver ion to AgNPs is still unclear. Although, it is considered that some enzymes like nitrate reductase secreted by the microbes are responsible for the reduction (Das et al. 2014). AgNPs can also be synthesized by adding $AgNO_3$ solution to the supernatant of bacterial cultures of *Bacillus subtilis*, *Lactobacillus acidophilus*, *Klebsiella pneumoniae*, *Escherichia coli*, *Enterobacter cloacae* and *Staphylococcus aureus*, etc. The extracellular metabolites excreted by the cultures reduce the silver ions into AgNPs in the presence of light (Minaeian et al. 2008).

The biosynthesis of AuNPs has been reported from *Pseudomonas aeruginosa* and *Rhodopseudomonas capsulate* whereby the cell free supernatant of these two strains is mixed with hydrogen tetrachloroaurate, indicating the colour change of solution to purple or red wine, further confirming the formation of AuNPs. The pH of the solution is the deciding factor for the shape and size of NPs. At pH 4 and 7, nanoplates and spherical NPs of size range 10–20 nm have been formed, respectively (Singh and Kundu 2013). Cubic AuNPs were developed when a filamentous cyanobacterium, *Plectonema boryanum*

UTEX 485 reacted with aqueous Au $(S_2O_3)_2^{3-}$ solution at 25–100 °C for 1 month and octahedral AuNPs were formed after reacting $AuCl_4^-$ at 200 °C for one day (Lengke et al. 2006). A microbial approach has been used for the synthesis of CuNPs by incubating $CuSO_4 \cdot 5H_2O$ solution with the cell pellet and cell-free supernatant of *Pseudomonas fluorescens*. Spherical- and hexagonal-shaped NPs of 49 nm were formed (Shantkriti and Rani 2014). The supernatant of another bacterial culture *Salmonella typhimurium* was incubated with aqueous solution of copper nitrate to form CuNPs of size 49 nm (Ghorbani et al. 2015). TiO_2 NPs (66–72 nm) have been synthesized by *B. subtilis* using titanium as a precursor (Kirthi et al. 2011). The strains of *Magnetospirillum magneticum* produce either Fe_3O_4 magnetic NPs in chains or Fe_3S_4 (greigite), while some other strains produce both types of NPs (Roh et al. 2001). Another facile and biocompatible route has been developed to synthesize CdSe QDs using *E. coli* cells as a matrix. QDs extracted from such cells showed a surface protein layer which has improved the biocompatibility of QDs (Yan et al. 2014).

3.3.8.2 Fungus-Mediated Synthesis

The use of fungal species has also been reported for the formation of AgNPs. The fungus-mediated formation of AgNPs is based on the mechanism that the fungal cells trap Ag ions on its surface followed by the reduction with the help of released enzymes. The fungal species *Aspergillus terreus* has also been reported earlier leading to formation of AgNPs by extracellular nicotinamide adenine dinucleotide dehydrogenase (NADH)-dependent reductase enzyme (Li et al. 2012a). Extracellular biosynthesis of AgNPs by the use of *Fusarium oxysporum* is based on the reduction of metal ions by nitrate-dependent reductase enzyme and shuttle quinone process (Duran et al. 2005). Fungi produce large amounts of AgNPs as compared to bacteria due to the secretion of a large number of proteins by a fungus.

Phanerochaete chrysosporium (fungal mycelium) was treated with $HAuCl_4$ under ambient conditions to form AuNPs within 90 min by the protein secreted by fungus itself. The extracellular and intracellular production of AuNPs was due to the secretion of enzymes lacase and ligninase by fungus, respectively (Sanghi et al. 2011). *Verticillium* species of fungus has also led to the formation of AuNPs by the reduction of aqueous $AuCl_4^-$ ions (Mukherjee et al. 2001). The enzymes present within the cell wall of fungi are known to reduce the ions. A species specific NADH-dependent reductase, released by *F. oxysporum* has also been used for the reduction of $AuCl_4^-$ ion to AuNPs (Mukherjee et al. 2002). Fungi, such as *Penicillium* sp. and *F. oxysporum* strains have also been reported to biosynthesize CuO and Cu_2S NPs. Another fungus known as *Stereum hirsutum* has been known for the formation of Cu and CuO NPs (Cuevas et al. 2015). The synthesis of Cu or CuO NPs can lead to different surface plasmon resonances (SPR) which are formed due to the strong coupling between incident electromagnetic radiation and surface plasmon in metal NPs. Spherical-shaped ZnO NPs of size range 54.8–82.6 nm have been synthesized extracellularly using the fungal strain of *A. terreus* (Baskar et al. 2013). *F. oxysporum* and *Verticiilium* species were able to form iron oxides mainly Fe_3O_4 by hydrolyzing the precursor ions extracellularly (Bharde et al. 2006). The fungus *F. oxysporum* has been reported to synthesize CdTe QDs extracellularly. Stabilizing agents were not required because the formed QDs have already been capped by a natural protein (Syed and Ahmad 2013).

3.3.8.3 Actinomycetes- and Yeast-Mediated Synthesis

AgNPs have been developed using soil actinomycetes namely *Streptomyces* sp. and *Rhodococcus* sp. (Abdeen et al. 2014; Saminathan 2015). *Thermomonospora*, an extremophilic actinomycete, was also found to reduce Au ions to AuNPs extracellularly. The harvested biomass was added to solution of chloroauric acid and kept in dark for the synthesis of monodisperse AuNPs whereby enzymatic processes were found to be responsible for the

reduction of metal ions and stabilization of AuNPs. The proteins secreted by actinomycetes biomass act as capping agents for the stabilization of AuNPs (Sastry et al. 2003). The biomass of other actinomycetes, *Streptomyces viridogens* has also been added to chloroauric acid solution, and colour of biomass changes to pink within 24 h indicated the formation of AuNPs within the cells. These synthesized AuNPs possess anti-bacterial activity against *S. aureus* and *E. coli* (Balagurunathan et al. 2011). Yeast cells have been reported to synthesize biocompatible CdTe QDs of size 2–3.6 nm with easily tunable florescence emission capacity. An extracellular growth pathway has been found responsible for the formation of the protein-capped CdTe QDs (Bao et al. 2010).

3.3.8.4 Plant-Mediated Synthesis

A variety of plant parts and their extracts have been used to synthesize AgNPs. The sun-dried mass of *Cinnamomum camphora* leaf extract has been reported to form spherical AgNPs. The polyol component and the water-soluble heterocyclic compounds present in the leaf extract could be responsible for the reduction of silver ions and their stabilization (Huang et al. 2007). The extracellular enzymatic synthesis of AgNPs has been obtained when geranium (*P. graveolens*) leaf extract was exposed to $AgNO_3$ solution. The terpenoids, proteins and other bio-organic compounds in leaf broth were the causal agents for the reduction of Ag ions and their stabilization (Shankar et al. 2003). The methanolic extract of *Eucalyptus* hybrid (safeda) was also found to synthesize AgNPs of 50–150 nm. The particles formed were stabilized by flavonoids and terpenoids of the plant extract (Dubey et al. 2009). *Syzygium cumini* leaf and seed extract has been reported to synthesize AgNPs due to the reduction of Ag ions by the soluble polar constituents present in the extracts (Kumar et al. 2010). Leaf extract of weed, *Lantana camara* at a concentration of 5, 10 and 15 % has been used to prepare AgNPs that showed strong anti-bacterial activity (Kumari et al. 2014a).

A perennial shrub, *Sesbania drummondii* seedlings have been explored for intracellular formation of monodisperse and spherical-shaped AuNPs (Sharma et al. 2007). The use of *Coriandrum sativum* leaf extract has also been known to reduce the aqueous solution of Au ions. The formed AuNPs (30 nm) showed stability for a month at room temperature in the solution (Rao 2011). Green tea (*Camellia sinensis*) has also been used to synthesize AuNPs (Vilchis-Nestora et al. 2008). Increasing the amount of tea extract used, NPs of spherical shape and bigger size were formed. The caffeine and theophylline present in tea extracts were found to be responsible for synthesis whereas the phenolic compounds were responsible for the stabilization of AuNPs. AuNPs of hexagonal and triangular shape with size range 200–500 nm have been synthesized using pear fruit extract. The bioreduction of chloroaurate ions to AuNPs was due to the presence of saccharides in the fruits (Ghodake et al. 2010). Dried clove buds (*Syzygium aromaticum*) solution has also been used to synthesize extracellular Au nanocrystals. The flavonoids present may be responsible for the bioreduction as well as stabilization of NPs (Raghunandan et al. 2010).

The aqueous solution of $CuSO_4 \cdot 5H_2O$ when treated with leaf extract of *Magnolia kobus*, has produced stable CuNPs of size range 40–100 nm (Lee et al. 2011). Stem latex of medicinal plant, *Euphorbia nivulia* has been used for the extracellular production of CuNPs. The terpenoids and peptides present in the latex act as stabilizing and capping agents for the formation of NPs (Valodkar et al. 2011). ZnO NPs were prepared from leaf extract of *Aloe vera* using zinc nitrate as metal salt precursor (Gunalan et al. 2012). Fe_3O_4 NPs have been synthesized using a fast, one-step and completely green biosynthetic method by the reduction of ferric chloride solution with the aqueous extract of brown seaweed (*Sargassum muticum*). The sulphated polysaccharides present in the seaweed have acted as the reducing agent and efficient stabilizer (Mahdavi et al. 2013). MnO_2 NPs were formed by the reduction of salt potassium permanganate using

leaf extract of plant *Kalopanax pictus* at room temperature (Moon et al. 2015).

3.4 Effect of Shape, Size and Surface Chemistry of NPs on Their Properties and Biological Behaviour

To study the effect of size, shape and surface chemistry on the properties of NPs, it is necessary to estimate the size, shape and morphology of particles through multi-scale characterization of NPs using high-throughput instruments. NPs shape and size are determined by scanning electron microscope (SEM), transmission electron microscope (TEM) and atomic force microscope (AFM). The hydrodynamic size and surface charge of nanomaterials are calculated by dynamic light scattering (DLS) and zeta potential. Other structural attributes of NPs are measured by spectroscopic techniques like UV–Vis spectroscopy, Fourier transform infra red spectroscopy (FTIR), mass spectroscopy and matrix-assisted laser desorption ionization (MALDI). A detailed description of characterization techniques used for measuring structural attributes of NPs is provided in Chap. 2.

Variation in shape, size, surface chemistry, morphology and surface charge of nanostructures tends to impart a great change in the properties of NPs and ultimately their behaviour in the biological systems. As mentioned above under the heading of "synthesis of metal NPs", it can be clearly observed that the use of different synthesis methods, synthesis parameters and use of different metal salts have an influence on the size, shape and morphology of nanomaterials. Few literature reports have described the influence of size of NPs on the properties which are mentioned in details in Chap. 7. The effect of differently shaped CdSe (rods, dots, branched and hyperbranched) on the morphology, surface characteristics and optical properties has been described. The aerogels formed from rod-shaped and branched QDs exhibit greater surface area whereas hyperbranched QDs exhibit lesser surface area. The rod-shaped and branched QDs possessed better porosity and strength (Yu and Brock 2008). Another independent study has been carried out to explain the effect of different-sized AuNPs on their absorption and scattering properties. Increase in the size of AuNPs from 20 to 80 nm has further increased the magnitude of extinction as well as the extinction scattering. The nanorods of AuNPs having smaller size show better cellular uptake as compared to nanoshells or nanospheres of AuNPs (Jain et al. 2006). The effect of particle size, shape and surface charge on therapeutic action of brain and retinal disease has been described. All of these factors play a role in deciding the in vivo fate of NPs to cross the biological barriers, stability inside the body, clearance by phagocytes, tendency of their binding to a target organ and ultimately penetration inside the cells (Jo et al. 2015). For the detailed study on this topic, reading of Chap. 7 is advisable. So, the designing of NPs structure and shape is a very critical step which should be kept in mind before depicting its role in imaging, therapeutics and other biomedical applications. The use of surface modifying agents to alter the behaviour of NPs in the biological milieu also affects the properties of NPs to a greater extent.

3.5 Medical Prospects of Metallic Nanoparticles

Out of plethora of applications, metallic NPs including MNPs and semiconductor NPs are versatile agents for utility in biomedical prospects such as diagnostics, cancer targeting, disease treatment, anti-microbial activity, tissue engineering and many more. Additionally, the nanotechnology-based approaches are also beneficial in diagnostic as well as therapy simultaneously. The term 'theranostics' has been explored for the unique properties of NPs possessing better penetration of therapeutic moieties and tracking within the body so as to allow a more efficient therapy with a reduced risk in comparison to conventional therapies.

3.5.1 Disease Diagnostics

3.5.1.1 Imaging

Imaging of live whole cells with the help of microscopic techniques gives information about the anatomical structures of cells and tissues required in diagnostics. A variety of NPs have been designed to absorb visible light in the near-infrared region (NIR) to be used for in vivo imaging of biological tissues. Imaging mainly includes computed tomography (CT), magnetic resonance imaging (MRI), optical imaging, positron-emission tomography (PET), photo-acoustic tomography (PAT), single-photon-emission computed tomography (SPECT) and ultrasound (Massoud and Gambhir 2003). The principle of MRI is based on nuclear magnetic resonance together with the relaxation of proton spins in a magnetic field which is used to visualize MNPs in the tissues (Brown and Semelka 2003). The contrast enhancement in MRI is produced due to the interaction between the contrast agents and neighbouring water protons, which is affected by intrinsic and external factors like density of protons and MRI pulse sequences. CT is a routinely used high-resolution medical imaging technique which provides 3D tomography knowledge of the internal structures on the basis of absorption of X-rays by the tissues.

Metal NPs, particularly Au and Ag have been found of wide applicability in diagnostics due to SPR effect and surface-enhanced Raman spectroscopy (SERS) properties (Kneipp et al. 2010). Such NPs have led to the development of nanoprobes used for imaging because of excellent features of size range (≤100 nm), enhanced surface area and different behaviours from their bulk counterpart (Na et al. 2009). The discrete gadolinium complexes conjugated to AgNPs (10 nm) have been prepared as contrast agents (Siddiqui et al. 2009). The two new complexes formed as $[Gd(DTPA\text{-}bisamido\ cysteine)]^{2-}$ and $[Gd(cystine–NTA)_2]^{3-}$ undergo chemisorption by thiol or disulfide groups to the particle surface to develop a novel contrast agent for MRI. Decahedral AgNPs have been used as sensor for targeted cell imaging based on fluorescence resonance energy transfer (FRET) phenomenon. Ag nanomaterials have the effect of metal-enhanced fluorescence (MEF) on nearby fluorophores, and due to this MEF effect, the emission intensity of fluorophores increases. Fluorophore-functionalized aptamers (Sgc8-FITC) bound to decahedral AgNPs show enhanced fluorescence intensity of FITC due to the presence of AgNPs. The developed sensor based on AgNPs was found to be highly sensitive and specific for target cell imaging (Li et al. 2015).

Kim et al. (2007) have developed PEG-coated AuNPs (30 nm) as a contrast agent for in vivo X-ray CT imaging. Intravenous injection of these coated AuNPs into hepatoma bearing rats showed a twofold high contrast between hepatoma and normal liver cells confirming the use of PEG-coated AuNPs as a CT contrast agent for hepatoma imaging. Earlier some problems of short imaging time due to fast clearance of contrast agents by kidneys were faced with the use of iodine based compounds in CT imaging. The use of AuNPs as contrast agent in CT imaging has overcome these limitations. In the same way, AuNPs functionalized with gadolinium chelates have been used as high-relaxivity MRI contrast agent (Moriggi et al. 2009).

The 80–90 nm-sized self-assembled Cu neodecanoate NPs have been reported for the first time as a contrast metal for near-infra red detection of sentinel lymph node using PAT (Pan et al. 2012). These NPs showed a sixfold increase in signal sensitivity when compared to blood, a natural absorber of light. The clinical applications of these CuNPs may replace sentinel lymph node biopsy in the near future. Another report described that red fluorescent ZnO NPs conjugated with Cu and a monoclonal antibody (TRC105) could serve as multimodality tumour imaging agents in applications of PET imaging and fluorescence imaging of tumour vasculature (Hong et al. 2015). The alloy NPs, FePt of 3, 6 and 12 nm in diameter have been developed as dual modality contrast agent in both MRI and CT imaging due to the excellent magnetic power and stability properties associated along with high capacity of X-ray absorption (Chou et al. 2010).

MNPs have also been used as MRI contrast agents because of their magnetism, nanoscale size, low toxicity and biocompatibility. Some of these NPs possess higher relaxivity, higher magnetization and different types of magnetism based on their core–shell structure and even functional aspects. Zeng et al. (2012) have demonstrated the use of ultra-small, water-soluble iron oxide NPs (Fe_3O_4, $ZnFe_2O_4$ and $NiFe_2O_4$ NPs) synthesized in aqueous solutions, as T1-weighted contrast agents for MRI. These ultra-small MNPs have possessed strong T1-weighted relaxation and weak T2 relaxation properties. In another approach, Walter et al. (2014) have shown the effect of size and composition of iron oxide NPs to tailor MRI. Iron oxide NPs of spherical, cubical and octopod shapes have been synthesized by thermal decomposition method. The spherical iron oxide NPs have displayed high in vitro and in vivo MRI properties at very low concentrations whereas cubical-shaped NPs showed positive contrast for T1 weighted images and negative contrast for T2 weighted images confirming the use of these iron oxide NPs as high contrast agents in MRI (Walter et al. 2014).

Semiconductor QDs serve as potential candidate in imaging for the diagnostic purposes as they have possessed the fascinating optical and electronic properties of intense brightness and stability against photo-bleaching. These semiconducting polymer NPs serve as contrast agents for PAT molecular imaging which can even produce stronger signals than AuNPs, thereby, permitting the whole-body lymph-node photo-acoustic mapping in living mice at a low systemic injection mass (Pu et al. 2014). Semiconductor CuS NPs have been reported for use in PAT molecular imaging to visualize the mouse brain after intracranial injection and also possess the potential for molecular imaging of breast cancer. The strong absorption at 1064 nm by CuS NPs has suggested the possibility of these candidates as contrast enhancement agents for PAT (Ku et al. 2012). Another functionalized QDs of [^{64}Cu]CuInS/ZnS have been synthesized with excellent radiochemical stability and controllable cerenkov luminescence. These agents can serve as an efficient PET and optical imaging agents (Guo et al. 2015). A water dispersible Si NPs of 2 nm mean diameter with quantum yield of 0.21 have been synthesized to serve as novel candidates for lifetime fluorescence imaging of living cells. These developed NPs also possess the characteristics of high photo-stability, pH stability, as well as non-toxic to biological entities (Wang et al. 2014b).

3.5.1.2 Cancer Detection

Cancer or tumour detection at an early stage may decrease the chances of tumour progression and helps to get successful treatment so as to provide quality life to patients. In order to detect or diagnose the tumour at initial stages, it is essential to detect certain tumour markers, macrophages or circulating tumour cells to have information of cancer screening and diagnosis. During early phases of disease, determination of cancer tissue-specific biomarkers at ultra-low levels requires numerous strategies which take into consideration the usage of various bio-nanocomposites with high content of specific and sensitive detection tags for signal tracing (Du et al. 2010). The nanotechnological approaches are appropriate to design certain functionalized nanoscale materials to play a real role in cancer diagnosis as compared to conventional chemotherapeutic agents.

Metallic NPs have been proven as one of the astonishing nanomaterials for cancer detection because of their size, shape, composition, easy preparation, light absorbance and scattering potential and size-dependent optical properties. Metal NPs particularly, Ag and Au have the capacity to scatter light in the wavelength of visible and NIR upon the excitation of their SPR. The scattering light intensity is highly sensitive to the size and aggregation of NPs. An attempt has already been made to use AgNPs-based SERS to analyze and screen human blood plasma to develop a simple and label-free blood test for oesophageal cancer detection which proved a great potential of these AgNPs for improving cancer detection and screening (Duo et al. 2014). A different study by Lin et al. (2011) has developed a promising, label-free, non-invasive

tool to detect and screen malignant cells for cancer by mixing blood plasma-isolated total serum proteins with AgNPs having SERS effect. Another novel functional carbon nanotube (CNT)/AgNP nanohybrid has been demonstrated as a trace tag for the ultra-sensitive detection of tumour markers by using single vessel in situ deposition of AgNPs on carboxylated CNTs and their subsequent functionalization with streptavidin (Lai et al. 2011).

Spherical-shaped AuNPs have been reported as optical probes for the detection of prostate cancer biomarkers using immunoassay. AuNPs of diameter 37 nm have been conjugated to anti-prostate specific antibodies for detection purpose (Liu et al. 2008). AuNPs (~35 nm) have been conjugated to monoclonal anti-epidermal growth factor receptor (EGFR) for the detection of oral epithelial live cancer cells. The differences in SPR scattering and absorption imaging between cancerous and non-cancerous cells have made the technique useful in cancer diagnostics (El-Sayed et al. 2005). Similarly, citrate-capped AuNPs have been used as candidates for the detection of early stage cancer through the blood test. AuNPs mixed with blood serum of cancer patients have formed protein corona on their surface due to adsorption of proteins from the blood serum. The quantification of immunoglobulin G (IgG) present in the protein corona attached on the surface of AuNPs shows increased concentration of IgG which further revealed that IgG has been formed in cancer patients as a mechanism of auto-defence by the immune systems of patients. This developed blood test through the use of AuNPs is quiet simple, low cost enabling the early stage tumour detection and risk assessment (Zheng et al. 2015). Novel bimetallic Ag–Au nanostructures have already been synthesized in the presence of deoxyribonucleic acid (DNA) which acted as SERS-active substrates and exhibited great enhancement signals to show response for the detection of carcinoembryonic antigen (Yang et al. 2009).

A colorimetric assay based on iodide responsive Cu–Au NPs has been constructed for highly sensitive detection of cancer cells. The developed bimetallic NPs platform possess the capacity to chemically absorb iodine as well as the ability to modify biomolecules which could help in colorimetric detection of target cancer cells by inducing a change in concentration of Cu–Au NPs (Ye et al. 2015). MNPs are highly sensitive and selective for diagnostic purposes. Also, problem of magnetic background does not exist with the use of these NPs as biological samples do not exhibit any virtual magnetic background. Monoclonal antibody coupled to fluorescent-magnetic-biotargeting multi-functional nanobioprobes has been developed for diagnosis as well as for isolation of single type of target tumour cancer cells from a mixed sample. These developed nanobioprobes serve to detect and isolate tumour cells even at an ultra-low concentration of 0.01 % in mixed sample within just 25 min with high sensitivity and specificity at an early stage (Song et al. 2011). Yuan et al. (2013) have also created photoactive core–shell Fe_3O_4@TiO_2 detection NPs conjugated with EGFR for high-resolution X-ray imaging of NPs for detection of cancer in HeLa cells. A rapid and sensitive nano-sensor based on conjugation of biotin-labelled aptamer with the streptavidin-coated iron oxide MNPs has been constructed for cancer detection. Aptamer possess the ability to specifically recognize and bind the target cancer cell whereas large surface area of MNPs can easily accommodate large number of aptamers that could help the clinicians to accurately identify the cancerous cells at single-cell level or molecular level (Bamrungsap et al. 2012).

The development of novel QDs protein microarray system has been reported for applications in detection of cancer markers. QDs offer the property of photo-stability and brightness whereas protein microarrays allow the quantification of particular proteins by low-cost, rapid and low sample volume enabling this multiplexed assay to be used as a powerful tool for cancer diagnostics as well as biomarker analysis (Zajac et al. 2007). The semiconductor NPs are used in diagnosis mainly due to the principle of electron transfer and energy transfer. A multiplexed detection system based on goat anti-mouse IgG secondary antibody conjugated to CdTe/CdS QDs have been synthesized for the

sensitive and selective detection of cancer biomarkers in two clinical cancer diagnostics such as sandwich and reverse phase immunoassays (Hu et al. 2010). Another very sensitive electrochemiluminescence (ECL) approach based on AuNPs-enhanced ECL of CdS nanocrystal film has been devised, which was further supplemented by magnetic separation for the detection of HL-60 (human promyelocytic leukaemia cells) (Zhang et al. 2012a). This approach was used to detect HL-60 cancer cells in a range of 20-1.0 × 10^6 cells/mL. Highly biocompatible and photoluminescent QDs of stable $CuInS_2/ZnS@SiO_2$ NPs were embedded into silane micelles for the development of $CuInS_2/ZnS@SiO_2$ NPs with NIR emission and quantum yield of 30-50 %. Holo-transferrin has also been bioconjugated to these NPs for targeted live cancer cell imaging by these NIR emitter and robust NPs (Foda et al. 2014).

3.5.2 Disease Therapy

3.5.2.1 Anti-microbial Activity

The anti-microbial agents are those that kill or dampen the growth of microbes such as bacteria, fungus, algae, etc. The emergence of infectious diseases poses a great threat to human health mainly occurring due to antibiotic resistant micro-organisms. Due to the overuse of antibiotics, micro-organisms become resistant to various commonly used anti-microbial agents. Nanotechnological advances are used to synthesize anti-microbial NPs with different shapes and sizes to control the bacterial growth to a benchmark level. NPs are seeker of great attention in various fields but mainly medicines as the functionality of NPs is based on particle size. The ability to easily manipulate or control the dimensions of NPs has created the opportunities for the development of new nanotechnology-based anti-microbial agents. NPs possessing anti-microbial activities are widely applicable in various biomedical applications such as their use as a material in wound dressings as well as for the prevention of microbial infections leading to outbreak of deadly diseases.

A variety of metallic NPs and metal oxides including Ag, Au, Cu, Ti and Zn are known to inhibit the growth of several species of bacteria, fungi and viruses. The inhibition of bacterial growth is influenced by factors such as the size of NPs, concentration used and their stability. Smaller sized NPs have been observed for more bacterial inhibition (Kumari et al. 2014a). The size of bacterial cell is in micrometre range and their membrane pores are in nanometre dimensions. Hence, use of NPs of size smaller than bacterial pores would be better choice to kill them. The small-sized metal NPs can cross the bacterial cell membrane and enter the cell to destroy the proteins thus leading to hampering of bacterial growth (Prabhu and Poulose 2012).

Krishnaraj et al. (2010) have checked the anti-microbial action of biosynthesized AgNPs from the leaf extract of *Acalypha indica* and reported that the synthesized NPs of size 20–30 nm at a minimum inhibitory concentration (MIC) of 10 µg/ml showed inhibitory activity against *E. coli* and *Vibrio cholera.* Similarly, AgNPs of variable shapes synthesized by *L. camara* LE showed strong anti-bacterial activity against *E. coli* at MIC of 50 µg/ml (Kumari et al. 2014a). Hydrophobic and cation-functionalized AuNPs have exhibited a strong bactericidal activity against both the Gram-negative and Gram-positive multiple drug resistant bacteria (Li et al. 2014). It has been demonstrated that the attachment of ligands and surface chemistry played a deterministic role in anti-microbial activity of these AuNPs. AuNPs and AgNPs have also been reported for anti-bacterial activity against *E. coli* and BCG bacteria. The changes in surface properties of AuNPs have exhibited a change in inhibitory activity of AuNPs. These AuNPs and AgNPs can act as anti-TB compounds for potential biomedical applications (Zhou et al. 2012). CuNPs also have great prospective to act as anti-microbial agents. The anti-microbial activity of CuNPs synthesized using polyol method has been evaluated against bacteria such as *Micrococcus luteus*, *S. aureus*, *E. coli*, *K. pneumoniae* and *P. aeruginosa*, and against fungus like *Aspergillus flavus*, *Aspergillus niger* and *Candida*

Table 3.1 Different types of metallic NPs showing anti-bacterial activity against broad spectrum of bacteria

Source or method of NPs synthesis	Type of NPs synthesized	Anti-bacterial activity against microbes (zone of inhibition in mm)	References
Tinospora cordifolia	AgNPs	*P. aeruginosa* (10–21)	Singh et al. (2004)
Ochrobactrum anthropi	AgNPs	*Salmonella typhi* (14), *Salmonella paratyphi* (15), *V. cholera* (16), and *S. aureus (15)*	Thomas et al. (2014)
Planomicrobium sp.	AgNPs	*B. subtilis* (17), *Klebsiella planticola* (14), *K. pneumonia* (15), *Serratia nematodiphila* (21), and *E. coli* (21).	Rajeshkumar and Malarkodi (2014)
Escherichia coli	AgNPs	*B. subtilis* (18), *K. pneumonia* (20), *E. coli* (15), *P. aeruginosa* (15), and *S. aureus* (13)	Veeraapandian et al. (2012)
Ananas comosus	AuNPs	*BCG and E. coli*	Zhou et al. (2012)
Galaxaura elongate	AuNPs	*S. aureus* (13), *E. coli* (17), *K. pneumonia* (16) and *P. aeruginosa* (13)	Abdel-Raouf et al. (2013)
Polyol method	CuNPs	*E. coli* (26) and *C. albicans* (23)	Ramyadevi et al. (2012)
Enterococcus faecalis	CuNPs	*E. coli* (25), *K. pneumonia* (18), and *S. aureus* (25)	Ashajyothi et al. (2014)
Nerium oleander	CuNPs	*S. typhi* (18), *B. subtilus* (14), *S. aureus* (13), *K. pneumoniae* (10), *E. coli* (10)	Gopinath et al. (2014)
Thermal decomposition	CuNPs	*S. aureus* and *P. aeruginosa*	Betancourt-Galindo et al. (2014)
Hibiscus subdariffa	ZnO NPs	*E. coli* and *S. aureus*	Bala et al. (2015)
Psidium guajava	TiO_2 NPs	*S. aureus* (25) and *E. coli* (23)	Santhoshkumar et al. (2014)
Sol–gel method	TiO_2 NPs	*S. aureus*, *E. coli* and *K. pneumonia*	Kedziora et al. (2012)
Laser ablation method	Fe_2O_3 NPs	*S. aureus, E. coli*, *P. aeruginosa* and *Serratia marcescens*	Ismail et al. (2015)
Lawsonia inermis and *Gardenia jasminoides*	Iron NPs	*E. coli*, *Salmonella enterica*, *Proteus mirabilis* and *S. aureus*	Naseem and Farrukh (2015)
Enterococcus sp.	CdS NPs	*Serratia nematodiphila*, *E. coli*, *Klebsiella planticola*, *Vibrio* sp. and *Planomicrobium* sp.	Rajeshkumar et al. (2014)
Klebsiella pneumoniae	CdS and ZnS NPs	*Streptococcus* sp., *S. aureus*, *Lactobacillus* sp., and *C. albicans*	Malarkodi et al. (2014)

albicans (Ramyadevi et al. 2012). MNPs and QDs have also been observed to play as anti-microbial agents with some surface modifications. NPs reported for anti-microbial activity are tabulated in Table 3.1.

The mechanistic action of anti-microbial activity of NPs is not clearly understood. It is hypothesized that NPs accumulate near the microbial cell membrane and get penetrated inside by membrane damage or through the formation of pits. After entering inside the bacterial cell membrane, NPs produce some free radicals or interact with many proteins present inside the bacterial cells and lead to enzyme inactivation. These events cause the distortion of internal environment of microbial cells and seem to be responsible for cellular death (Prabhu and Poulose 2012). The pictorial representation of anti-microbial mechanism of NPs is shown in Fig. 3.1.

3.5.2.2 Cancer Treatment

Most of the drugs and many methods like surgery or chemotherapy are used to fight with the cancerous cells. However, many of these are unable to reach to the cancer cells or decipher toxicity levels into the healthy cells (Sunderland et al. 2006). One of the basic causes for cancer to

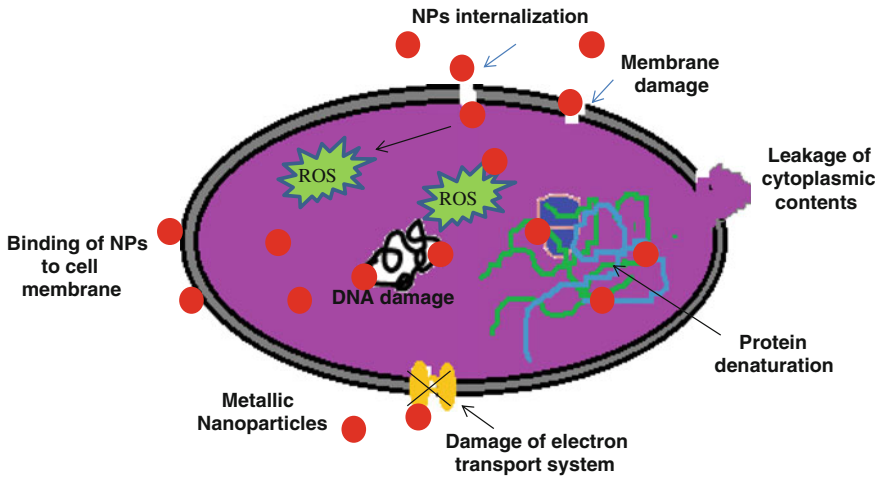

Fig. 3.1 Mechanistic action of anti-bacterial activity of metallic NPs

occur in the body is over expression and over activity of certain receptors, antigens, growth factors or hormones such as EGFR, vascular endothelial growth factor (VEGF), integrins, transferrin or folate receptors. The cancerous cells exhibit unique properties which can be exploited for detection and treatment by using different NPs. The treatment of cancer cells involves the targeting of specific biomarkers or antigens present on their surface, so that the cells apoptise at the same place rather than getting migrated to different places and causing damage to the normal body cells. Researchers are trying to design NPs in such a way so as to conjugate various active targeting moieties to modify the surface of nanomaterials. These efforts can make possible targeting to cancer cells through active penetration of NPs by binding to a ligand or any other active compound, through sieving mechanism in passive targeting and sometimes by using the magnetic shear forces to direct the NPs inside the body (Plank et al. 2003; Jain et al. 2005).

Metallic NPs possesses properties like selective nature, biocompatibility and smaller size to make them amenable for surface modifications so as to be used in cancer treatment. The small size of NPs enhances their surface area and thus serves to be more effective. AgNPs biosynthesized by honey bee extract possess anti-proliferative activity which revealed their competence against colon cancer cell line (Caco-2) at a concentration 39 µg/ml and showed 60 % of growth inhibition in comparison to naked AgNPs. AgNPs have been reported to suppress the levels of Bcl-2 and surviving genes (El-Deeb et al. 2015). Chitosan nanocarrier-mediated delivery of AgNPs to mammalian cells has generated oxidative stress through the formation of intracellular reactive oxygen species (ROS). Hence, nanocarriers led to apoptosis of human colon cancer cells and play an important role in cancer therapy (Sanpui et al. 2011). A nanocarrier 50 nm size made up of AgNPs, folate receptor, PEG, curcumin, Prussian blue and pemetrexed have been found to enter the cancerous cells. The folate receptors are specific and are over-expressed on epithelial cancer cells where AgNPs got attached to them. The whole nano-assembly was disintegrated on application of the electric field releasing the drug pemetrexed, and was found effective in killing cancerous cells (Soumya and Hela 2013). The cisplatin-tethered AuNPs have been reported to treat glioblastoma multiforme, the most difficult to treat brain tumour. The cisplatin possesses chemotherapeutic properties, whereas nanospheres cause DNA damage by inducing caspase pathway for the apoptosis of cells. On applying the radiations, Au emits ionizing photoelectrons and auger electrons which further act in

mutualism with cisplatin to reduce the number of tumour cells (Setua et al. 2014). AuNPs synthesized by green chemistry route using cocoa extract have shown NIR absorbance. The cell death was induced through the photo-thermal ablation of epidermoid carcinoma cells by these AuNPs, facilitating their use as photo-thermal therapeutic agents (Fazal et al. 2014).

CuO NPs have caused the greater cytotoxicity to A549 cell lines (human lung adenocarcinoma) as compared to their bulk counterparts. CuO NPs have caused cellular death through autophagic pathway as the autophagic biomarker named LC3 II was found to be increased in A549 cells upon their exposure to CuO NPs (Sun et al. 2012). CuNPs synthesized by using leaf extract of *Ficus religiosa* have been proved as anti-cancer chemotherapeutic agents against A549 cells. The apoptotic effect of CuNPs is mediated through the generation of ROS and further causing the disruption of mitochondrial membrane (Sankar et al. 2014). There are also reports describing the anti-cancer activities of ZnO NPs against few mammalian cell lines viz. human hepatocellular carcinoma (HepG2), A549 cells, and human bronchial epithelial cells (BEAS-2B) by the induction of apoptosis in cancer cells through the generation of ROS effect (Akhtar et al. 2012). ZnO NPs biosynthesized by aqueous extract of brown seaweed, *Sargassum muticum* have also shown cytotoxic effects against murine cell lines. The activation of certain caspases has triggered the cell apoptosis and facilitated the role of ZnO NPs as cancer therapeutic agents (Namvar et al. 2015).

MNPs serve as promising agents for the treatment of various tumours. In an attempt towards the use of these MNPs for cancer therapy, anti-EGFR antibody was combined with plasmonic MNPs and has been checked against non-small cell lung cancer (NSCLC) over-expressed EGFR. Anti-EGFR antibody has caused the cellular death expressing EGFR through inhibiting the EGFR-mediated signal cascade and inducing apoptosis of the cells. While EGFR-null NSCLC cells did not show any response (Yokoyama et al. 2011). Johannsen et al. (2007) have given an injection of iron oxide MNPs at a particular dosage for 1 h once in a week for a period of two months to the patients having recurrent prostate cancer and found that NPs (20 nm) could easily enter the cancer cells and produced heat under magnetic fields of 50–100 kHz responsible for causing photo-thermal death of cancer cells. The super-paramagnetic iron oxide nanoparticle (SPION) micelles have been synergized with β-lapachone (β-lap), a novel anti-cancer drug and observed ten times greater ROS stress in β-lap-exposed cells treated with SPION-micelles as compared to cells treated with β-lap alone, resulting in increased cell death. These SPION-micelles along with ROS generating drugs can serve as novel NPs for the cancer therapy (Huang et al. 2013).

Fluorescent silica shell-coated CdSe and CdTe QD NPs have been used for the treatment of mice melanoma cells. These QDs can rapidly convert light energy into heat and found to be responsible for the photo-thermal therapy of cancer (Chu et al. 2012). In the similar way, water dispersible copper selenide (Cu_2Se) nanocrystals of size 16 nm have been developed which exhibited strong NIR optical absorption and produced photo-thermal heating. After laser irradiation at 33 W/cm^2, injected Cu_2Se QDs led to destruction of human colorectal cancer cells within 5 min of exposure due to photo-thermal heating (Hessel et al. 2011).

3.5.2.3 Treatment of Other Diseases

Metallic NPs have been used in administration of drug due to their properties like small size, longer retention in the body and ability to penetrate the cell membrane with drug encapsulated in the core. AgNPs play a deterministic job to treat diabetes. In an attempt to prove AgNPs as a beneficial candidate to lower down the blood glucose level, streptozotocin (STZ) has been induced in rats to make them diabetic and then AgNPs at a dose of 10 mg/kg was orally administered which resulted in reduction of 68.2 % in the blood glucose level. AgNPs could also increase the serum insulin level by 3 % in the diabetic mice in comparison to diabetic mice treated with insulin. The glucokinase activity was enhanced by 25.8 % and there was a significant

increase in the expression of insulin receptor A and GLUT-2 in the diabetic rats elucidating the role of AgNPs as anti-diabetic agent (Alkaladi et al. 2014). AuNPs prepared using plant extract of *Gymnemasylvestre R. Br* (an anti-diabetic plant) have been given to alloxan-induced diabetic wistar albino rats and their activity was evaluated. AuNPs given at a concentration of 0.5 mg/kg body weight showed decrease in blood glucose level, reduction in cholesterol, triglycerides and low-density lipoprotein-c levels and normal levels of glycosylated haemoglobin in the diabetic mice (Karthick et al. 2014). Oral administration of ZnO NPs has also shown their anti-diabetic efficacy in STZ-induced type I and type III diabetes by increasing the secretion of insulin and decreasing the level of blood glucose (Umrani and Paknikar 2014).

In Alzheimer's disease, the amyloid protein builds up in the spaces between nerve cells, thereby inhibiting the connections between the neurons. The effects of bare AuNPs and carboxyl conjugated AuNPs (negatively charged) have been observed where NPs acted as nano-chaperones to assist repression and redirection of the amyloid fibrillization (Liao et al. 2012). A complex of hyaluronate-AuNPs/tocilizumab (HA-AuNP/TCZ) has been used to treat rheumatoid arthritis (RA). AuNPs bind to VEGF, whereas TCZ is immunosuppressive in nature which acts against interleukin-6 receptor and HA has lubricating properties (Lee et al. 2014).

QDs offer a wide variety of advantages like good optical properties, minimal photo-bleaching and narrow range of fluorescence peaks. The glucose oxidase conjugated with phosphorescent Mn-doped ZnS quantum dots have been used for sensing glucose. They catalyzed the oxidation of glucose and led to the production of hydrogen peroxide. The hydrogen peroxide quenches the phosphorescence of Mn-doped ZnS (Wu et al. 2010). In a manner to reduce the pathogenesis of Alzheimer's disease, it was aimed to reduce the production of amyloid protein by ribonucleic acid (RNA) interference. The fluorescent CdSe/ZnS QDs have been surface modified with PEG. The negatively charged small interfering RNAs (siRNAs) were then electrostatically adsorbed on QDs. The siRNAs have targeted β-secretase (BACE1) and reduced the accumulation of amyloid protein that has further reduced the chances of Alzheimer's disease (Li et al. 2012b).

3.5.2.4 Radiotherapy

The intensity of the ionizing radiations falling on the tissue undergoes a variety of molecular processes like Crompton effect and Auger effect. These effects create a change in the state of electrons and releases energy for the damage of living cells. Water is the main component of the cells and when the cells are exposed to these radiations, aqueous free radicals are formed which further react with cellular components like proteins, DNA, and RNA and hinder normal metabolic processes of the cell. This occurs in both diseased as well as normal cells. So, approaches are being developed which may target and destroy only the diseased cell and render normal cells to be harmless by the development of non-toxic radioprotectors (Nair et al. 2001; Upadhyay et al. 2005).

AgNPs intricated with alpha-lipoic acid (an antioxidant molecule) and stabilized using 1 % pluronic F-127 have exhibited free radical scavenging action revealed by 2,2-diphenyl-1-picrylhydrazyl (DPPH) assays. The anti-inflammatory activity has been speculated in paw models of edema in mice. Use of AgNPs-lipoic acid complex has protected the mice from weight loss when exposed to gamma radiation. The complex was also effective for tumour growth delay when given to the mice before any exposure to the gamma radiation. Their antioxidant, radio-protecting and anti-inflammatory properties revealed their role in protecting normal tissues (Ramachandran and Nair 2011). The effect of AgNPs and their interaction with gamma radiation (6 meV) in breast cancer has been studied. NPs serve as photo-absorbing agents and enhance the proficiency of radiowaves in cancer therapy. Their mode of action relies on the fact that AgNPs have high-mass energy absorption coefficient which in turn generate free radicals to damage cancerous cells by DNA denaturation. Their usage has

helped in detecting and targeting the cancer cell simultaneously (Salih 2013).

Au has an outstanding effect in absorbing X-rays. AuNPs hold many properties like inertness, biocompatibility and low osmolality. Mice treated with AuNPs and radiation (30 Gy) showed 50 % long-term tumour-free survival whereas the death of all the mice treated with radiation alone was observed (Hainfeld et al. 2008). AuNPs of size range 57–346 nm have been prepared by controlled reduction method. AuNPs of 57 nm in size reduced the dose effectiveness of radiation by 21 % and thus are used as dose enhancer (Kamiar et al. 2013). Similarly in another study, rats bearing glioma have been estimated for the effectiveness of AuNPs of sizes 1.9 and 15 nm given at a concentration of 50 mg/ml with energy radiations of 88 keV. It was found that rats receiving a combinational therapy of 15 nm AuNPs and irradiation had greater survival rate in comparison to the ones having irradiation therapy alone (Bobyk et al. 2013). Iron–gold core–shell (Fe@Au) MNPs could be used as a tool for imaging as well as targeting the tumour area by applying the magnetic field. Fe@Au NPs of average size of 70 nm were examined in human breast cancer cell line (MCF-7). It was found that the malignant cells treated with NPs have increased the effectiveness of the radiation, thereby causing the survival of only 33 % cells. These MNPs did not show any cytotoxic effects (Manjili et al. 2014). Human prostate cancer grown in male mice has been treated with iron oxide MNPs. 5.5 mg Fe/cm^3 dosage was given for 24 h and exposed to alternating magnetic field. The combination of iron oxide MNPs and radiation therapy has been found to have an enhanced effect on the tumour than the single agent therapy at the same dosage (Attaluri et al. 2015).

Iodine (^{131}I)-doped CuS NPs [(CuS/^{131}I) NPs] functionalized with PEG have been used for radiotherapy and photo-thermal therapy as CuS NPs absorb in NIR region and ^{131}I provide radioactivity. Developed nano-complex can be used to treat metastatic tumours (Yi et al. 2015). Similarly, tungsten sulphide (WS_2) QDs have been used as dual-model image-guided photo-thermal therapy along with radiotherapy (Yong et al. 2015).

3.5.2.5 Gene Therapy

Nanotechnology offers a promising technique in the area of gene delivery for therapeutics purposes. NPs used for carrying genes to specific target regions in the body serve as important gene delivery vehicles. Earlier, the viral vectors were used to carry genes to the target organism but the use of viral vectors possesses certain limitations. Compared to viral gene delivery approaches, non-viral gene delivery systems have the supplementary advantages of being less immunogenic, ability to incorporate larger genes, easy and inexpensive to produce at large scale in relation to viral systems (Zhang et al. 2011). The overall ability of NPs to function as non-viral gene delivery vectors depends upon certain factors like properties of NPs such as shape, size, morphology and surface charge (Khalil et al. 2006).

Excellent optical properties as well as anti-microbial activities of AgNPs make them potential therapeutic agents for cancer treatment, wound healing and bioimaging. AgNPs are easy to form, have ease of control over their size and shape along with ease of its surface modifications. Hence, these AgNPs can find a space for their utility in other biomedical applications like gene therapy. In a report, AgNPs prepared by greener route have further been surface modified using chitosan-g-polyacrylamide. Plasmid DNA (pDNA) was bound to AgNPs to form AgNPs-pDNA complex. The transfection ability of AgNPs in HeLa and A549 cells has been enhanced by immobilization of RGDS (Arg-Gly-Asp-Ser) tetra-peptide confirming the therapeutic efficacy of developed biofunctionalized AgNPs as non-viral gene delivery carriers (Sarkar et al. 2015). AuNPs can also serve as feasible candidates for carrying siRNAs and genes to body cells due to their ease of synthesis, good biocompatibility and monodispersity. Charge reversal AuNPs have successfully delivered siRNA and pDNA to cancer cells. The

delivered siRNA has caused the silencing of a lamin protein present in nuclear envelop. Charge reversed AuNPs acted as potential vectors for the effective delivery of nuclear genes to cancer cells for gene therapy (Guo et al. 2010). Nanocapsules formed from polyethyleneimine (PEI)-coated SiO_2 NPs as shell and Fe_3O_4 as core have also been used to deliver siRNAs to HeLa cells which led to the down regulation of target proteins for cancer therapy (Zhang et al. 2012b).

Anirudhan and Rejeena (2014) have developed a complex of MNPs synthesized using aminated β-cyclodextrin-modified-carboxylated cobalt/nanocellulose composite (ACDC-Co/NCC) for carrying pDNA into alveolar epithelial A549 lung tumour cells. Here, nanocellulose acted as a biotemplate for the incorporation of NPs. The transfection efficiency of 88.2 % at high dose of DNA has documented the role of magnetic Co/NCC as efficient gene delivery agents for cancer therapy. Multi-functional hollow manganese oxide (MnO_2) NPs have been surface functionalized using 3,4-dihydroxy-L-phenylalanine and used for carrying siRNAs for therapeutic action against targeted cancer cells (Bae et al. 2011). Photostable QDs NPs serve as suitable candidates for delivery of genes or siRNAs. But the use of QDs is limited for the purpose of biomedical imaging and drug/gene targeting due to their toxicity issues as most of the QDs are composed of cadmium, tellurium and selenium (Su et al. 2009). CdSe/ZnS semiconductor QDs have been used to deliver siRNAs for gene silencing of BACE-1 in human neuroblastoma cell (SK-N-SH) as well as for the reduction of β-amyloid in nerve cells. The resulted nano-complex has inhibited BACE-1 gene associated with Alzheimer's disease. Such gene delivery by the use of nanocarrier semiconductor QDs may serve to treat neurodegenerative disease (Li et al. 2012b). DNA-templated CdS semiconductor nanocrystals have exhibited a gene transfection efficiency of 32 % for gene delivery to live cells (Gao and Ma 2012).

3.5.2.6 Targeted Delivery and Controlled Drug Release

The development of therapeutic carriers is of utmost importance that possesses the potential to deliver high-drug payload to the target organs. The design and synthesis of metal and metal oxide NPs can easily be tailored to produce NPs of narrow size distribution. These NPs can encapsulate high amount of drugs for their delivery to the diseased site. The use of NPs as drug delivery vehicles may solve the common problems like poor drug solubility in aqueous media and in vivo short half-life of drug that are generally associated with the traditional drug delivery systems. In an attempt to use NPs as drug delivery vectors, researchers have tried to encapsulate drugs in NPs but the major concern behind the use of these NPs as delivery vehicles arises from their cytotoxicity. Research throughout the global world is being carried out to develop novel delivery vehicles based on these NPs with reduced or minimal cytotoxicity.

Metal NPs are greatly employed in the drug delivery applications as they have large surface area which can be easily modified to attach various ligands or specific biomarkers for cell targeting. An anti-cancer drug doxorubicin (DOX) has been encapsulated in folic acid (FA) protected AgNPs (23 ± 2 nm) for its delivery to cancer cells. FA helps in the targeted delivery to cancer cells as these cells express folate receptors on their surface. After 8 h of incubation with DOX-containing AgNPs, the cancer cells underwent death due to release of DOX from NPs (Wang et al. 2012). Similarly, glutathione-stabilized AuNPs have been used as drug delivery agents for the targeted delivery of chemotherapeutic platinum-containing drugs (cisplatin, oxaliplatin and carboplatin) to neuropilin (1) receptors of prostate cancer cells (Kumar et al. 2014). Du et al. (2014) has also developed DNA–DOX conjugates of AuNPs as a specific and effective therapeutic agent for neuroblastoma.

MNPs of Fe_3O_4 coated with PVA have been encapsulated with DOX and showed up to 45 % of adsorbed drug release in 80 h confirming the role of MNPs as efficient drug delivery vectors (Kayal and Ramanujan 2010). Iron oxide MNPs (8-10 nm) coated with antracyclinic antibiotic violamycine B1 has been tested for its anti-tumour activity against the breast adenocarcinoma cell line MCF-7. The drug-loaded NPs were internalized into cell cytoplasm by endocytosis and induced apoptosis in the tumour cells (Marcu et al. 2013). Another kind of MNPs of mesoporous cobalt ferrite ($CoFe_2O_4$) decorated with FA has been encapsulated with methotrexate and DOX (anti-cancer drugs). The drug-loaded NPs exhibited cytotoxicity and induced apoptosis in HeLa cells demonstrating their role as drug delivery vehicles (Mohapatra et al. 2011). Multi-functional SiO_2 NPs have been surface modified with PEG and functionalized with adamantine and FA. Release of encapsulated drug, DOX has been triggered by acidic endosomal pH after the endocytosis of NPs. This has demonstrated the utility of these NPs in controlled and targeting drug release (Zhang et al. 2012b). QDs of CdTe stabilized by glutathione have been encapsulated with DOX and further decorated with FA for targeted delivery to HeLa cells. Such QDs have released DOX at a target site as FA helped in recognition of folate receptors present on cancerous cells (Chen et al. 2014b).

3.5.3 Tissue Engineering

Tissue engineering or regenerative medicine lays stress on recent technological developments to make tissue functional in such a way that it repairs or replaces the tissues already worn out due to some injury or disease. Nowadays, the alteration in cell behaviour like adhesion, locomotion, contraction and cytoskeletal movements is being carried out by the nanomaterials which have in turn increased their usage in regeneration and orthopaedic repair. The nanofibrous structures have proved to be well-known material to bring out the changes in bone in accordance to the scaffold material used (Nair and Laurencin 2008).

The Ag-coated catheter has been developed where inert ceramic zeolite is used as a source to bind the Ag ions on its surface. A comparison between standard catheters and Ag-coated catheters has been done with respect to the infection in the blood stream. It was found that the infection rate is less in Ag-coated catheters than standard catheters (Wong and Liu 2010). In joint athroplasty, infections from many types of resistant bacteria remain a major problem. The dentures are mainly made up of polymethylmethacrylate (PMMA) and possess rough surface which facilitate the easy adherence of bacteria. In vitro anti-bacterial and cytotoxicity study of PMMA bone cement loaded with metallic AgNPs, and PMMA bone cement loaded with gentamicin has been carried out. AgNPs-loaded form of PMMA showed bactericidal activity against *S. epidermidis*, methicillin-resistant *S. epidermidis* and methicillin-resistant *S. aureus* while the gentamicin cement was not efficient (Alt et al. 2004). The nanofibres of TiO_2 have been impregnated with AgNPs and hydroxyapatite. Their strong anti-bacterial property against *E. coli* and *S. aureus* suggested it an effective implant material (Sheikh et al. 2010).

During the treatment of root canal, it is important to remove the bacteria present over there, so the material used for endodontic should have some inbuilt anti-microbial property. Gutta-percha is one of the frequently used materials for filling the root cavity. The gutta-percha encrusted with AgNPs has proven to be successful against bacteria like *Enterococcus faecalis, S. aureus* and *E. coli* (Correa et al. 2015). A hybrid of AuNPs deposited on material similar to extracellular matrix (ECM) scaffold has been made and tested for cardiac tissue engineering. The cardiac cells cultured in scaffolds showed regeneration of the cardiac patches and AuNPs have increased the conductance and lessened the fibroblast proliferation (Shevach et al. 2014). AuNPs–hydrogel complex has been used for bone regeneration. The complex promotes proliferation, viability and osteogenic differentiation of human-derived adipose stem cells.

AuNPs–hydrogel system can act as an implant material for the engineering of defected bone tissues (Heo et al. 2014). The hydroxyapatite-copper NPs have been synthesized and further modified with PEG-400 for use in bone implant. Their anti-bacterial activity was found to be enhanced against Gram-positive and Gram-negative bacteria. This material was safe against primary osteoprogenitor cells of rat and documented their usefulness in bone transplant (Sahithi et al. 2010). A nanofibrous scaffold of polylactide acid (PLA), hydroxyapatite NPs and super-paramagnetic γ-Fe_2O_3 NPs have been synthesized. The rabbit lumbar transverse defects were treated with this scaffold. Under the effect of magnetic field, the MNPs produced large amount of magnetic force in the scaffold which led to enhanced production of osteocalcin. The defect in rabbit was found to be healed and led to the formation of the new ECM required for bone repair (Meng et al. 2013).

Surface hydrophobicity can be increased by adding metallic NPs to the organic material and thereby the adherence to biomolecules can be reduced. For this purpose, metal oxide NPs (TiO_2 and Fe_2O_3) have been used on PMMA resin. The synthesized hybrid metal oxides-alginate-containing PMMA resin has been used to perform anti-microbial assays and proved them a boon material in dentistry (Acosta-Torres et al. 2011). Dental resins are the accessory restorative materials used to fill the tooth cavities. The optical properties of the resin should be similar to the natural tooth. The variety, shape, size determines the colour of resin based on the principle of light like absorption, scattering and reflection (Lim and Lee 2007). A dental resin has been doped with CdSe/ZnS core–shell QDs. The laser-induced fluorescence technique has been used to check the fluorescence emitted by the resin. It was found that the use of CdSe/ZnS core–shell QDs tailored the fluorescence of the resin which could closely match to the fluorescent properties of the natural teeth (Alves et al. 2010). In an attempt to treat the damage in eye by laser, bone marrow-derived stem cells labelled with QD have been introduced into the vitreous of mice. The tissue repair caused by the cells through differentiation of the retinal cells, endothelial cells and pericytes was monitored by QD (Wang et al. 2010).

3.5.4 Wound Healing and Skin Repair

Wound healing is a complex process involving various cell and tissue lineages. The process of healing mainly occurs through phases including homeostasis, inflammation, angiogenesis and ultimately epithelization and dermal remodelling. These phases occur in sequence following one after the other but may also overlap in time. The wounds are categorized into few types such as acute wound, chronic wound, burn wound, diabetic wound, etc. Acute wounds are those which require a short-time period to heal whereas chronic wounds are those where healing is delayed or wounds are difficult to heal which takes several months to even years for healing. The healing and tissue repair process depends upon various factors like age of the patient, type of wound, nutritional status, wound size and depth. A wide variety of nanomaterials have applicability in wound healing dressings in these days.

Ag has been known as a material of wound healing from the long past historical ages. In the modern times, AgNPs have been used in wound dressings due to their extraordinary features of anti-microbial activity along with large surface area to volume ratio. The in vivo acute skin wound healing activity of AgNPs in mice has resulted in rapid healing as compared to standard drugs (Akila and Nanda 2014). Even AgNPs have been used for the treatment of burn wounds. The topical application of AgNPs on wounded mice skin has shown better healing efficacy than marketed formulations (Kaler et al. 2014). The use of AgNPs for wound healing is beneficial as it helps in reducing inflammation as well as modulates cytokine production required for faster healing due to anti-inflammatory action of AgNPs (Tian et al. 2007).

AuNPs synthesized phytochemically have been deposited in hydrocolloid membrane for healing of cutaneous wounds within 15 days.

The application of this material has enhanced collagen expression and resulted in a decrease in matrix metalloproteinase expression. Also an increase in VEGF and superoxide dismutase (SOD) was found which tend to accelerate wound healing (Kim et al. 2015). Other kind of metal oxide NPs like ZnO NPs has been used in composite wound dressings along with chitin hydrogels (Sudheesh Kumar et al. 2013) as well as alginate hydrogels (Mohandas et al. 2015). These wound dressings revealed faster healing by an increase in collagen deposition and keratinocytes infiltration around the wound. There are also reports on skin excision wound healing activity of CuO NPs (Sankar et al. 2015) and TiO_2 NPs (Sankar et al. 2014) in wistar rats due to their anti-microbial nature. The results indicated the faster wound contraction along with increased rate of epithelization, fibroblast formation and collagen deposition in the wounded skin. In an independent study, the bacterial cellulose incorporated with Fe_3O_4 MNPs has been used for treatment of chronic wounds. The nanocomposites have been found to be biocompatible to human adipose stem cells in terms of viability, cytotoxicity, proliferation and cellular morphology (Galateanu et al. 2015).

3.5.5 Theranostics

Theranostics is an emerging field in nanomedicine which takes advantage of NPs for the dual purpose of imaging and therapy of diseases. The nano-platforms have the capacity to load the molecules which carry imaging and therapeutic functions. These multi-functional nanostructures used for disease diagnosis, drug delivery, and to monitor the response of a given therapy will attract the dawning era of personalized medicine. Researchers throughout the world are engaged in the field of theranostics to construct these kinds of function integrated new agents. To develop newer nano-based theranostics agents, it is needed to understand the surface chemistry of NPs so as to easily conjugate or load the other moieties having pharmaceutical role.

Metallic NPs play a great job in theranostics due to the convenience to manipulate their size and shape. Moreover, some of them possess the fluorescent properties used for imaging and properties to generate oxidative stress due to which these can act as anti-cancer agents for therapeutic purpose playing the dual role in theranostics. Mukherjee et al. (2014) have reported that AgNPs biosynthesized using methanolic leaf extract of *Olax scandens* showed red fluorescence. The synthesized Ag nanoconjugates have been found to be biocompatible towards normal cell lines and showed anti-cancer activity against different cancer cell lines. The authors have also reported that the red fluorescence of these AgNPs could be used as diagnostic tool for cancer detection.

Advances in nanotechnology have led its way to produce multi-functional hollow Au nanospheres which can act to generate photo-acoustic signals and also help to induce photo-thermal ablation for therapeutics. Au nanospheres conjugated to RGD (Arg-Gly-Asp) peptide for targeting to integrin receptors that are highly expressed on glioma and angiogenic blood vessels have shown that photo-thermal ablation therapy has increased the survival rate of tumour bearing mice (Lu et al. 2011). AuNPs with PEG surface modification and then combined with radiotherapy have possessed diagnostic and therapeutic potential for sarcoma. PEG-AuNPs in combination with radiotherapy have enhanced CT imaging whereas radiotherapy has helped to induce tumour tissue damage by increasing unrepaired DNA damage. This study has suggested that AuNPs can potentially improve target imaging and radiosensitization of tumour while minimizing dose to normal tissues thus providing more chances of survival to animals under experimentation (Joh et al. 2013). Zhang et al. (2015) have prepared high-density CuNPs which have provided fourfold higher signals as PAT contrast agents in NIR region than that of blood. The $\alpha_v\beta_3$-

targeted CuNPs have effectively delivered Sn 2 lipase-labile fumagillin-prodrug, a potent anti-angiogenic therapy, under in vivo conditions. This has set an example of a systemically targeted drug delivery therapy with a PAT agent.

MNPs are a generation of advanced NPs which act both as imaging as well as therapy playing a role in theranostics. Wang et al. (2014a) have developed a system based on iron oxide NPs for photodynamic therapy (PDT) and imaging of head and neck squamous cell carcinoma. PDT is an alternate treatment to various cancers other than chemotherapeutic agents and involves the activation of photosensitizer through the use of light of a specific wavelength which further interacts with molecular oxygen to produce singlet oxygen and ROS. These species can easily lead to tumour death mediated by apoptosis and necrosis. Iron oxide NPs were first conjugated with a fibronectin-mimetic peptide (Fmp), specific to integrin β1 and then combined with a PDT drug, Pc 4. Targeted Fmp-IO-Pc4 NPs have induced greater inhibition of tumour cells as compared to non-targeted IO-Pc 4 NPs in which iron oxide NPs were not conjugated to Fmp. This developed system of nano-therapeutics has great potential to serve as MRI contrast enhancement agent due to the presence of iron oxide NPs whereas the presence of PDT drug helps in therapy of cancer cells. Another prior art report describes the formation of multilayered water-soluble MNPs coated with β-cyclodextrin and F127 polymer and encapsulated with anti-cancer drug, curcumin. This has shown good stability, enhanced cellular uptake and sustained drug release. The developed nano-formulation has been shown to exhibit haemo-compatibility and hyperthermia which can act as potential candidates as MRI contrast enhancer as well as drug delivery agents for cancer therapy (Yallapu et al. 2011).

Semiconductor QDs are well known for the applications of theranostics as they help in cancer targeting and imaging in the living cells or animals. ZnS-capped CdS luminescent QDs have been encapsulated with an ABC triblock copolymer consisted of a polybutylacrylate segment, a polyethylacrylate segment and a polymethacrylic acid segment. Developed system was further linked to tumour-targeting ligand and peptide Tat or polyarginine for multi-functional applications. In vivo targeting of these multi-functional NPs to prostate cancer has shown that QDs accumulate at the cancer site by increased permeability, retention at tumour site and also by specific binding of peptide antibody to the biomarkers present on cancer cell surface. Very sensitive and multicolor fluorescence imaging of cancer cells due to targeted QDs probes have raised the opportunities for multiplexed imaging of molecular targets under in vivo conditions (Gao et al. 2004). Ag_2S QDs have been prepared by the reaction of $AgNO_3$ and Na_2S (Chen et al. 2014a). They have covalently conjugated tumour-targeting RGD tripeptide and anti-cancer drug, DOX to form Ag_2S-DOX-cRGD. Ag_2S-DOX-cRGD showed effective tumour inhibition in both the cell culture and in vivo animal studies. These developed nanoconjugates can effectively be used as imaging as visible nano-therapeutics.

3.6 Toxicity Issues Related to the Use of Nanomaterials

The intended use of nanomaterials is increasing day by day in the products of daily life from household to human health. Yet there is only a little knowledge on the toxicity of these NPs and their long-term impact on the health of living beings (Aillon et al. 2009). Unfortunately, no strict regulatory laws or guidelines are defined or followed to determine the particular methodology and risk assessment tools for toxicity measurement of nanostructures. Due to very small dimensions, NPs are capable of easy penetration inside the bodies and are able to cross various biological barriers so as to enter the cells and tissues of the body (Kumar et al. 2012). Since the properties and toxicity levels of bulk molecules from which the nanomaterials are being synthesized are well understood but there is a complete lack of information on how the properties and toxicological nature of these materials change at nanoscale dimensions. Also it is not easy to

determine at what concentration dosage and which size the nanoscale materials exhibit different toxicity behaviour (Sharifi et al. 2012). Most of the published work describes the synthesis, characterization and wide applications of these nanocompounds in the biomedical area. Only a few studies examine the toxicity and risk assessment of these NPs. The consideration of nanotoxicology is a matter of serious concern in the near future as the exposure of NPs to the workers and end users may tend to have lethal effects on their biological systems. Briefly, a critical issue concerning in vitro and in vivo toxicity of emerging nanomaterials as well as the current progress on their safety is discussed below.

In a study, the toxicity of metal and metal oxide NPs of different sizes has been determined where AgNPs (20 nm), AgNPs (200 nm) and TiO_2 NPs (21 nm) have been exposed to human testicular embryonic carcinoma cells and primary mouse testicular cells. Ag20 and Ag200 were reported more cytotoxic and cytostatic compared to TiO_2-NPs. They have caused apoptosis, necrosis and decreased proliferation in a concentration and time-dependent manner. Ag20 and Ag200 NPs have affected the mouse testicular cells to a greater extent as compared to human testicular cells at same concentration (Asare et al. 2012). The toxicity of Ag ions and AgNPs (70 nm) towards bacterial cells (*E. coli* and *S. aureus*) and human cells (human mesenchymal stem cells (hMSCs) and peripheral blood mononuclear cells (T-lymphocytes and monocytes) at a same concentration have been examined. Cytotoxicity of Ag ions at a concentration more than 1 ppm was observed on monocytes in an increasing and dose-dependent manner whereas AgNPs at a concentration of 30 ppm or more showed an increase in cytotoxicity. On exposure to Ag ion concentration of above 1.5 ppm, T-cell viability was affected whereas no effect on its viability was found by exposure of AgNPs. Similarly, Ag ions have more toxicity effect on bacterial cells as compared to AgNPs at same concentration (Greulich et al. 2012). The effect of AgNPs of different sizes (10, 20, 40, 60 and 80 nm) has been reported on bacteria, yeast, algae, crustaceans and mammalian cells. Smaller sized AgNPs have induced greater toxicity as compared to bigger sized particles. The reason for increased toxicity of smaller sized AgNPs could be due to more release of Ag and thus more bioavailability of Ag which can produce ROS effect in the cells (Ivask et al. 2014).

AuNPs of size 5 and 15 nm have been studied for toxicity analysis on mouse fibroblast cell lines after 72 h of exposure. The results suggested that 5 nm-sized AuNPs used at concentration (≥50 μm) were cytotoxic whereas no significant cytotoxicity was seen with exposure to 15 nm AuNPs. These 4 nm-sized AuNPs played a role in damage of cytoskeletal organization of cells (Coradeghini et al. 2013). The toxicity of 4 nm-sized Au NPs at different concentrations and incubation periods has been assessed in neural progenitor cells, human umbilical vein endothelial cells, and PC12 rat pheochromocytoma cells to study the parameters like cell viability, morphology and functionality, ROS generation and cytoskeleton organization. AuNPs at a concentration higher than 200 nm have reduced the cell viability as a result of ROS generation. Exposure of cells to 10 nm concentration did not show significant effect on any of cellular parameters (Soenen et al. 2012a).

CuO NPs have been found cytotoxic determined under in vitro conditions against human bronchial epithelial cells (HBEC) and lung adenocarcinoma cells (A549 cells). In a dose-dependent manner, CuO NPs exposure to cells has reduced the cell viability, increased lactate dehydrogenase release and increased ROS and IL-8 (Jing et al. 2015). The toxicity of ZnO NPs at different concentrations of 5–25 μg/ml in HBEC has been determined to check the cell viability after 24 h of exposure (Heng et al. 2010). Similarly, sub-acute toxicity of ZnO NPs in rats has been conducted where ZnO NPs were given at a dose of 10 mg/kg body weight for 5 consecutive days. A minor change in rat tissues was noted whereas no change in exploratory behaviour of rats was found (Ben-Slama et al. 2015). Intraperitoneal injection of TiO_2 NPs at a concentration dose of 0, 324, 648, 972, 1296, 1944 or 2592 mg/kg body weight of mice was

given to assess the acute toxicity and the treatment mice were observed for passive behaviour, loss of appetite, tremor and lethargy (Chen et al. 2009). The toxicity of MNPs like Fe_2O_3 NPs (Mahmoudi et al. 2009; Naqvi et al. 2010; Soenen et al. 2012b) and cobalt oxide NPs (Cho et al. 2012) have been reported to be based on their size, shape and concentration.

CdSe/ZnS QDs showed greater accumulation and toxicity to the amphipod *Leptocheirus plumulosus* (Jackson et al. 2012). Factors responsible for the toxicity of QDs include the release of heavy metal ions and formation of ROS. Size and surface chemistry of NPs have also affected their toxicological behaviour inside the living systems. SiO_2 NPs having size of 15 or 46 nm showed reduction in cell viability of human lung cancer cells after an exposure of 48 h at concentrations between 10 and 100 µg/ml (Lin et al. 2006). The oral administration of SiO_2 NPs (10–15 nm) has caused significant variation in levels of mice albumin, total protein, cholesterol, triglyceride, high- and low-density lipoproteins as well as change in enzyme activity. Apart from this, SiO_2 NPs showed toxic effects on liver, lungs, testis and kidney of mice (Hassankhani et al. 2015). Metal and metal oxide NPs, as well as QDs may or may not impart toxicity to humans, bacteria and other living beings depending upon their size, shape, surface properties and concentration. Therefore, efforts should be made to develop safe NPs for human benefits.

3.7 Conclusions

This chapter has described the synthesis of metal NPs (Au and Ag), metal oxide NPs (Cu, Fe, Zn, Mn, Ti) and fluorescent nanomaterials (QDs). A large number of synthesis methods are followed for the formation of NPs which include physical, chemical and biological (green) methods. Generally in the recent times, researchers are more convinced by biological approaches for the development of nanostructures as compared to the conventional physical and chemical methods because biological approaches are eco-friendly, inexpensive and lesser time and energy consuming. These nanomaterials possess unique physical, chemical, optical, mechanical and electrical properties making the utility of such NPs in wide spheres of life especially biomedical field. The size, shape, morphology and surface chemistry of NPs have tendency to alter the properties of NPs and ultimately their behaviour in the biological systems. NPs play a deterministic role in disease diagnostics, therapy, tissue engineering and theranostics. Apart from innumerable benefits of NPs, there are certain toxicity concerns behind the use of these metallic NPs under in vitro and in vivo conditions which need to be minimized to realize the full potential of nanomaterials for the betterment of human life.

Acknowledgements The authors are highly grateful to Director for providing immense facilities. We pay our great gratitude towards Council of Scientific and Industrial Research, New Delhi for financial assistance. RS is highly thankful to UGC for providing senior research fellowship. Academy of Scientific Innovations and Research, New Delhi is duly acknowledged.

References

Abdeen S, Geo S, Sukanya S et al (2014) Biosynthesis of silver nanoparticles from actinomycetes for therapeutic applications. Int J Nano Dimens 5(2):155–162

Abdel-Raouf N, Al-Enazi NM, Ibraheem IBM (2013) Green biosynthesis of gold nanoparticles using *Galaxaura elongate* and characterization of their antibacterial activity. Arab J Chem (In press). doi:10.1016/j.arabjc.2013.11.044

Abulizi A, Yang GH, Okitsu K et al (2014) Synthesis of MnO_2 nanoparticles from sonochemical reduction of MnO_4 in water under different pH conditions. Ultrason Sonochem 2:1629–1634

Acosta-Torres LS, López-Marín LM, Núñez-Anita RE et al (2011) Biocompatible metal-oxide nanoparticles: nanotechnology improvement of conventional prosthetic acrylic resins. J Nanomater 2011:8. doi:10.1155/2011/941561

Aillon KL, Xie Y, El-Gendy N et al (2009) Effects of nanomaterial physicochemical properties on in vivo toxicity. Adv Drug Delivery Rev 61:457–466

Akhtar MJ, Ahamed M, Kumar S et al (2012) Zinc oxide nanoparticles selectively induce apoptosis in human cancer cells through reactive oxygen species. Int J Nanomedicine 7:845–857

Akila S, Nanda A (2014) *In-vivo* wound healing activity of silver nanoparticles: An investigation. IJSR 3 (7):1208–1212

Alkaladi A, Abdelazim AM, Afifi M (2014) Antidiabetic activity of zinc oxide and silver nanoparticles on streptozotocin-induced diabetic rats. Int J Mol Sci 15:2015–2023

Alt V, Bechert T, Steinrücke P et al (2004) An *in vitro* assessment of the antibacterial properties and cytotoxicity of nanoparticulate silver bone cement. Biomater 25(18):4383–4391

Alves LP, Pilla V, Murgo DOA et al (2010) Core–shell quantum dots tailor the fluorescence of dental resin composites. J Dent 3(8):149–152

Amendola V, Meneghetti M (2013) What controls the composition and the structure of nanomaterials generated by laser ablation in liquid solution? Phys Chem Chem Phys 15:3027–3046

Anand V, Srivastava VC (2015) Zinc oxide nanoparticles synthesis by electrochemical method: optimization of parameters for maximization of productivity and characterization. J Alloys Compn 636:288–292

Anandgaonker P, Kulkarni G, Gaikwad S et al. (2015) Synthesis of TiO_2 nanoparticles by electrochemical method and their antibacterial application. Arab J Chem (In press). doi:10.1016/j.arabjc.2014.12.015

Anirudhan TS, Rejeena SR (2014) Aminated β-cyclodextrin-modified-carboxylated magnetic cobalt/nanocellulose composite for tumor-targeted gene delivery. J Appl Chem 2014:10. doi:10.1155/2014/184153

Asare N, Instanes C, Sandberg WJ et al (2012) Cytotoxic and genotoxic effects of silver nanoparticles in testicular cells. Toxicol 291:65–72

Ashajyothi C, Jahanara K, Chandrakanth RK (2014) Biosynthesis and characterization of copper nanoparticles from *Enterococcus faecalis*. Int J Pharm Bio Sci 5:204–211

Attaluri A, Kandala SK, Wabler M et al (2015) Magnetic nanoparticle hyperthermia enhances radiation therapy: A study in mouse models of human prostate cancer. Int J Hyperthermia 31(4):359–374

Bae KH, Lee K, Kim C et al (2011) Surface functionalized hollow manganese oxide nanoparticles for cancer targeted siRNA delivery and magnetic resonance imaging. Biomater 32:176–184

Bakrania SD, Rathore GK, Wooldridge MS (2009) An investigation of the thermal decomposition of gold acetate. J Therm Anal Calorim 95(1):117–122

Bala N, Saha S, Chakraborty M et al (2015) Green synthesis of zinc oxide nanoparticles using *Hibiscus subdariffa* leaf extract: effect of temperature on synthesis, anti-bacterial activity and anti-diabetic activity. RSC Adv 5:4993–5003

Balagurunathan R, Radhakrishnan M, Rajendran RB et al (2011) Biosynthesis of gold nanoparticles by actinomycete *Streptomyces viridogens* strain HM10. Indian J Biochem Biophys 48(5):331–335

Bamrungsap S, Chen T, Shukoor MI et al (2012) Pattern recognition of cancer cells using aptamer-conjugated magnetic nanoparticles. ACS Nano 6(5):3974–3981

Bao H, Hao N, Yang Y et al (2010) Biosynthesis of biocompatible cadmium telluride quantum dots using yeast cells. Nano Res 3:481–489

Barcikowski S, Compagnini G (2013) Advanced nanoparticle generation and excitation by lasers in liquids. Phys Chem Chem Phys 15:3022–3026

Baskar G, Chandhuru J, Fahad KS et al (2013) Mycological synthesis, characterization and antifungal activity of zinc oxide nanoparticles. Asian J Pharm Tech 3(4):142–146

Ben-Slama I, Amara S, Mrad I et al (2015) Sub-acute oral toxicity of zinc oxide nanoparticles in male rats. J Nanomed Nanotechnol 6:284. doi:10.4172/2157-7439.1000284

Betancourt-Galindo R, Reyes-Rodriguez PY, Puente-Urbina BA et al (2014) Synthesis of copper nanoparticles by thermal decomposition and their antimicrobial properties. J Nanomater 2014:5. doi:10.1155/2014/980545

Bharde A, Rautaray D, Bansal V et al (2006) Extracellular biosynthesis of magnetite using fungi. Small 2:135–141

Bhattacharya D, Rajinder G (2005) Nanotechnology and potential of microorganisms. Crit Rev Biotechnol 25:199–204

Bobyk L, Edouard M, Deman P et al (2013) Photoactivation of gold nanoparticles for glioma treatment. Nanomed 9(7):1089–1097

Boutinguiza M, del Val J, Riveiro A et al (2013) Synthesis of titanium oxide nanoparticles by ytterbium fiber laser ablation. Phys Procedia 41:787–793

Brown MA, Semelka RC (eds) (2003) MRI: basic principles and applications. Wiley-Liss, New York

Brust M, Fink J, Bethell D et al (1995) Synthesis and reactions of functionalised gold nanoparticles Chem Commun 16:1655–1656

Chen M, Feng YG, Wang X et al. (2007) Silver nanoparticles capped by oleylamine: formation, growth, and self-organization. Langmuir 23:5296–5304

Chen M, Nikles DE (2002) Synthesis of spherical FePd and CoPt nanoparticles. J Appl Phys 91:8477–8479

Chen W, Cai W, Zhang L et al (2001) Sonochemical processes and formation of gold nanoparticles within pores of mesoporous silica. J Colloid Interface Sci 238(2):291–295

Chen J, Dong X, Zhao J et al (2009) *In vivo* acute toxicity of titanium dioxide nanoparticles to mice after intraperitioneal injection. J Appl Toxicol 29:330–337

Chen H, Li B, Zhang M et al (2014a) Characterization of tumor-targeting Ag_2S quantum dots for cancer imaging and therapy *in vivo*. Nanoscale 6:12580–12590

Chen X, Tang Y, Cai B et al (2014b) One-pot synthesis of multifunctional GSH–CdTe quantum dots for targeted drug delivery. Nanotechnol 25(23):235101

Cheng C, Xu F, Gu H (2011) Facile synthesis and morphology evolution of magnetic iron oxide nanoparticles in different polyol processes. New J Chem 35:1072–1079

Chin S, Park E, Kim M et al (2010) Photocatalytic degradation of methylene blue with TiO_2 nanoparticles prepared by a thermal decomposition process. Powder Technol 201(2):171–176

Cho WS, Dart K, Nowakowska DJ et al (2012) Adjuvanticity and toxicity of cobalt oxide nanoparticles as an alternative vaccine adjuvant. Nanomed (Lond) 7(10):1495–1505

Chou SW, Shau YH, Wu PC et al (2010) *In vitro* and *in vivo* studies of FePt nanoparticles for dual modal CT/MRI molecular imaging. J Am Chem Soc 132:13270–13278

Chu M, Pan X, Zhang D et al (2012) The therapeutic efficacy of CdTe and CdSe quantum dots for photothermal cancer therapy. Biomater 33:7071–7083

Coradeghini R, Gioria S, García CP et al (2013) Size-dependent toxicity and cell interaction mechanisms of gold nanoparticles on mouse fibroblasts. Toxicol Lett 217(3):205–216

Correa JM, Mori M, Sanches HL et al (2015) silver nanoparticles in dental biomaterials. Int J Biomater 2015:9

Couto GG, Kleinb JJ, Schreiner WH et al (2007) Nickel nanoparticles obtained by a modified polyol process: synthesis, characterization, and magnetic properties. J Colloid Interface Sci 311:461–468

Cuevas R, Durán N, Diez MC et al (2015) Extracellular biosynthesis of copper and copper oxide nanoparticles by *Stereum hirsutum*, a native white-rot fungus from chilean forests. J Nanomater 2015:7

Dang TMD, Le TTT, Blanc EF et al (2011) Synthesis and optical properties of copper nanoparticles prepared by a chemical reduction method. Adv Nat Sci Nanosci Nanotechnol 2:15009–15012

Das VL, Thomas R, Varghese RT et al (2014) Extracellular synthesis of silver nanoparticles by the Bacillus strain CS 11 isolated from industrialized area. 3. Biotech 4(2):121–126

Dementeva OV, Rudoy VM (2012) Copper nanoparticles synthesized by the polyol method and their oxidation in polar dispersion media: the influence of chloride and acetate ions. Colloid J 74(6):668–674

Dhas NA, Raj CP, Gedanken A (1998) Synthesis, characterization, and properties of metallic copper nanoparticles. Chem Mater 10:1446–1452

Dong F, Zhao W, Wu Z et al (2009) Band structure and visible light photocatalytic activity of multi-type nitrogen doped TiO_2 nanoparticles prepared by thermal decomposition. J Hazard Mater 162:763–770

Du D, Zou ZX, Shin Y et al (2010) Sensitive immunosensor for cancer biomarker based on dual signal amplification strategy of graphene sheets and multienzyme functionalized carbon nanospheres. Anal Chem 82:2989–2995

Du YQ, Yang XX, Li WL et al (2014) A cancer-targeted drug delivery system developed with gold nanoparticle mediated DNA–doxorubicin conjugates. RSC Adv 4:34830–34835

Dubey M, Bhadauria S, Kushwah B (2009) Green synthesis of nanosilver particles from extract of Eucalyptus hybrida (safeda) leaf. Dig J Nanomater Biostruct 4:537–543

Duo L, Shangyuan F, Hao H et al (2014) Label-free detection of blood plasma using silver nanoparticle based surface-enhanced Raman spectroscopy for esophageal cancer screening. J Biomed Nanotechnol 10(3):478–484

Duran N, Marcato PD, Alves OL et al (2005) Mechanistic aspects of biosynthesis of silver nanoparticles by several *Fusarium oxysporum* strains. J Nanobiotechnol 3:8

El-Deeb NM, El-Sherbiny IM, El-Aassara MR et al (2015) Novel trend in colon cancer therapy using silver nanoparticles synthesized by honey bee. J Nanomed Nanotechnol 6:265. doi:10.4172/2157-7439.1000265

El-sayed IH, Huang X, El-sayed MA (2005) Surface plasmon resonance scattering and absorption of anti-EGFR antibody conjugated gold nanoparticles in cancer diagnostics: Applications in oral cancer. Nano Lett 5(5):829–834

Farkhani SM, Valizadeh A (2014) Review: three synthesis methods of CdX (X = Se, S or Te) quantum dots. IET Nanobiotechnol 8(2):59–76

Fazal S, Jayasree A, Sasidharan S et al (2014) Green synthesis of anisotropic gold nanoparticles for photothermal therapy of cancer. ACS Appl Mater Interfaces 6:8080–8089

Foda MF, Huang L, Shao F et al (2014) Biocompatible and highly luminescent near-infrared $CuInS_2$/ZnS quantum dots embedded silica beads for cancer cell imaging. ACS Appl Mater Interfaces 6:2011–2017

Frey NA, Peng S, Cheng K et al (2009) Magnetic nanoparticles: Synthesis, functionalization, and applications in bioimaging and magnetic energy storage. Chem Soc Rev 38(9):2532–2542

Galateanu B, Bunea M-C, Stanescu P (2015) *In vitro* studies of bacterial cellulose and magnetic nanoparticles smart nanocomposites for efficient chronic wounds healing. Stem Cells Int 2015:10

Gao L, Ma N (2012) DNA-templated semiconductor nanocrystal growth for controlled DNA packing and gene delivery. ACS Nano 6:689–695

Gao X, Cui Y, Levenson RM et al (2004) *In vivo* cancer targeting and imaging with semiconductor quantum dots. Nature Biotechnol 22(8):969–976

Gao B, Shen C, Yuan S et al (2013) Synthesis of highly emissive CdSe quantum dots by aqueous precipitation method. J Nanomater 2013:7

Gaponik N, Talapin DV, Rogach AL (2002) Thiolcapping of CdTe nanocrystals: an alternative to organometallic synthetic routes. J Phys Chem B 106:7177–7185

Gericke M, Pinches A (2006) Biological synthesis of metal nanoparticles. Hydrometallurgy 83:132–140

Ghodake GS, Deshpande NG, Lee YP et al (2010) Pear fruit extract-assisted room-temperature biosynthesis of gold nanoplates. Colloids Surf B Biointerfaces 75:584–589

Ghorbani HR, Mehr FP, Poor AK (2015) Extracellular synthesis of copper nanoparticles using culture supernatants of *Salmonella typhimurium*. Orient J Chem 31(1):527–529

Gong C, Hart DP (1998) Ultrasound induced cavitation and sonochemical yields. J Acoust Soc Am 104:1–16

Gopinath M, Subbaiya R, Selvam MM et al (2014) Synthesis of copper nanoparticles from nerium oleander leaf aqueous extract and its antibacterial activity. Int J Curr Microbiol App Sci 3(9):814–818

Greulich C, Braun D, Peetsch A et al (2012) The toxic effect of silver ions and silver nanoparticles towards bacteria and human cells occurs in the same concentration range. RSC Adv 2:6981–6987

Grieve K, Mulvaney P, Grieser F (2000) Synthesis and electronic properties of semiconductor nanoparticles/quantum dots. Curr Opin Colloid Interface Sci 5:168–172

Gunalan S, Sivaraj R, Rajendran V (2012) Green synthesized ZnO nanoparticles against bacterial and fungal pathogens. Prog Nat Sci Mater Int 22(6):693–700

Guo S, Huang Y, Jiang Q et al (2010) Enhanced gene delivery and siRNA silencing by gold nanoparticles coated with charge-reversal polyelectrolyte. ACS Nano 4(9):5505–5511

Guo W, Sun X, Jacobson O et al (2015) Intrinsically radioactive [64Cu]CuInS/ZnS quantum dots for PET and optical imaging: improved radiochemical stability and controllable cerenkov luminescence. ACS Nano 9 (1):488–495

Guzman MG, Dille J, Godet S (2009) Synthesis of silver nanoparticles by chemical reduction method and their antibacterial activity. Int J Chem Biomol Eng 2 (3):104–111

Hainfeld JF, Dilmanian FA, Slatkin DN et al (2008) Radiotherapy enhancement with gold nanoparticles. J Phram Pharmacol 60(8):977–985

Hammer NI, Emrick T, Barnes MD (2007) Quantum dots coordinated with conjugated organic ligands: new nanomaterials with novel photophysics. Nanoscale Res Lett 2:282–290

Harris DK, Bawendi MG (2012) Improved precursor chemistry for the synthesis of iii–v quantum dots. J Am Chem Soc 134(50):20211–20213

Hassankhani R, Esmaeillou M, Tehrani AS et al (2015) In vivo toxicity of orally administrated silicon dioxide nanoparticles in healthy adult mice. Environ Sci Pollut Res 22(2):1127–1132

Heng BC, Zhao X, Xiong S et al (2010) Toxicity of zinc oxide (ZnO) nanoparticles on human bronchial epithelial cells (BEAS-2B) is accentuated by oxidative stress. Food Chem Toxicol 48(6):1762–1766

Heo DN, Ko WK, Bae MS et al (2014) Enhanced bone regeneration with a gold nanoparticle–hydrogel complex. J Mater Chem B 2:1584–1593

Hernandez J, Solla-Gullon J, Herrero E (2004) Gold nanoparticles synthesized in a water-in-oil microemulsion: electrochemical characterization and effect of the surface structure on the oxygen reduction reaction. J Electroanal Chem 574:185–196

Hessel CM, Pattani VP, Rasch M et al (2011) Copper selenide nanocrystals for photothermal therapy. Nano Lett 11:2560–2566

Hong H, Wang F, Zhang Y et al (2015) Red fluorescent zinc oxide nanoparticle: a novel platform for cancer targeting. ACS Appl Mater Interfaces 7:3373–3381

Hosni M, Farhat S, Amar MB et al (2015) Mixing strategies for zinc oxide nanoparticle synthesis via a polyol process. AIChE J 61(5):1708–1721

Hu M, Yan J, He Y et al (2010) Ultrasensitive, multiplexed detection of cancer biomarkers directly in serum by using a quantum dot-based microfluidic protein chip. ACS Nano 4(1):488–494

Huang J, Li Q, Sun D et al (2007) Biosynthesis of silver and gold nanoparticles by novel sundried *Cinnamomum camphora* leaf. Nanotechnol 18:105104–105114

Huang G, Chen H, Dong Y et al (2013) Superparamagnetic iron oxide nanoparticles: Amplifying ROS stress to improve anticancer drug efficacy. Theranostics 3 (2):116–126

Hyeon T (2003) Chemical synthesis of magnetic nanoparticles. Chem Commun 8:927–934

Ibrahim RK, Ahmed SS, Naje AN et al. (2013) Synthesis of silver nanoparticles by electrochemical method. Indian J Appl Res 3(5). doi:10.15373/2249555X

Iravani S, Korbekandi H, Mirmohammadi SV et al (2014) Synthesis of silver nanoparticles: Chemical, physical and biological methods. Res Pharm Sci 9(6):385–406

Ismail RA, Sulaiman GM, Abdulrahman SA et al (2015) Antibacterial activity of magnetic iron oxide nanoparticles synthesized by laser ablation in liquid. Mater Sci Eng, C 53(1):286–297

Ivask A, Kurvet I, Kasemets K et al (2014) Size-dependent toxicity of silver nanoparticles to bacteria, yeast, algae, crustaceans and mammalian cells in vitro. PLoS ONE 9(7):e102108

Jackson BP, Bugge D, Ranville JF et al (2012) Bioavailability, toxicity, and bioaccumulation of quantum dot nanoparticles to the amphipod *Leptocheirus plumulosus*. Environ Sci Technol 46(10):5550–5556

Jadhav S, Gaikwad S, Nimse M et al (2011) Copper oxide nanoparticles: Synthesis, characterization and their antibacterial activity. J Clust Sci 22:121–129

Jafarabadi MA, Mahdieh MH (2013) Evaluation of crater width in nanosecond laser ablation of Ti in liquids and the effect of light absorption by ablated nano-particles. Int J Opt Photonics 7:105–112

Jain TK, Morales MA, Sahoo SK et al (2005) Iron oxide nanoparticles for sustained delivery of anticancer agents. Mol Pharm 2:194–205

Jain PK, Lee KS, El-Sayed IH et al (2006) Calculated absorption and scattering properties of gold nanoparticles of different size, shape, and composition: Applications in biological imaging and biomedicine. J Phys Chem B 110:7238–7248

Jing X, Park JH, Peters TM et al (2015) Toxicity of copper oxide nanoparticles in lung epithelial cells exposed at the air–liquid interface compared with *in vivo* assessment. Toxicol In Vitro 29(3):502–511

Jo DH, Kim JH, Lee TG et al (2015) Size, surface charge, and shape determine therapeutic effects of nanoparticles on brain and retinal diseases. Nanomedicine 11(7):1603–1611

Joh DY, Kao GD, Murty S et al (2013) Theranostic gold nanoparticles modified for durable systemic circulation effectively and safely enhance the radiation

therapy of human sarcoma cells and tumors. Transl Oncol 6(6):722–731
Johannsen M, Gneveckow U, Thiesen B et al (2007) Thermotherapy of prostate cancer using magnetic nanoparticles: Feasibility, imaging, and three-dimensional temperature distribution. Eur Urol 52(6):1653–1661
Kabashin V, Meunier M (2003) Synthesis of colloidal nanoparticles during femtosecond laser ablation of gold in water. J Appl Phys 94:7941–7943
Kaler A, Mittal AK, Katariya M et al (2014) An investigation of *in vivo* wound healing activity of biologically synthesized silver nanoparticle. J Nanopart Res 16:2605–2615
Kamiar A, Ghotalou R, Valizadeh H (2013) Preparation, physicochemical characterization and performance evaluation of gold nanoparticles in radiotherapy. Adv Pharm Bull 3(2):425–428
Karthick V, Kumar G, Dhas TS et al (2014) Effect of biologically synthesized gold nanoparticles onalloxan-induced diabetic rats—An *in vivo* approach. Colloids Surf B Biointerfaces 122:505–511
Kayal S, Ramanujan RV (2010) Doxorubicin loaded PVA coated iron oxide nanoparticles for targeted drug delivery. Mater Sci Eng, C 30(3):484–490
Kedziora A, Strek W, Kepinski L et al (2012) Synthesis and antibacterial activity of novel titanium dioxide doped with silver. J Sol-Gel Sci Technol 62:79–86
Keswani RK, Ghodke H, Sarkar D et al (2010) Room temperature synthesis of titanium dioxide nanoparticles of different phases in water in oil microemulsion. Colloids Surf A Physicochem Eng Aspects 369:75–81
Khalil IA, Kogure K, Akita H et al (2006) Uptake pathways and subsequent intracellular trafficking in nonviral gene delivery. Pharmacol Rev 58:32–45
Khalil MI, Al-Qunaibit MM, Al-zahem AM et al (2014) Synthesis and characterization of ZnO nanoparticles by thermal decomposition of a curcumin zinc complex. Arab J Chem 7(6):1178–1184
Khan A, Rashid A, Younas R et al (2015) A chemical reduction approach to the synthesis of copper nanoparticles. Int Nano Lett. doi:10.1007/s40089-015-0163-6
Khodashenas B, Ghorbani HR (2015) Synthesis of silver nanoparticles with different shapes. Arab J Chem. doi:10.1016/j.arabjc.2014.12.014
El-Nour KMA, Eftaiha AA, Al-Warthan A et al (2010) Synthesis and applications of silver nanoparticles. Arab J Chem 3:135–140
Kim D, Park S, Lee JH et al (2007) Antibiofouling polymer-coated gold nanoparticles as a contrast agent for in vivo X-ray computed tomography imaging. J Am Chem Soc 129:7661–7665
Kirthi AV, Rahuman AA, Rajakumar G et al (2011) Biosynthesis of titanium dioxide nanoparticles using bacterium *Bacillus subtilis*. Mater Lett 65:2745–2747
Kim JE, Lee J, Jang M et al (2015) Accelerated healing of cutaneous wounds using phytochemically stabilized gold nanoparticle deposited hydrocolloid membranes. Biomater Sci 3:509–519
Kneipp J, Kneipp H, Wittig B et al (2010) Novel optical nanosensors for probing and imaging live cells. Nanomedicine 6(2):214–226
Korbekandi H, Ashari Z, Iravani S et al (2013) Optimization of biological synthesis of silver nanoparticles using *Fusarium oxysporum*. IJPR 12(3):289–298
Krishnaraj C, Jagan EG, Rajasekar S et al (2010) Synthesis of silver nanoparticles using *Acalypha indica* leaf extracts and its antibacterial activity against water borne pathogens. Colloid Surf B Biointerfaces 76(1):50–56
Ku G, Zhou M, Song S et al (2012) Copper sulfide nanoparticles as a new class of photoacoustic contrast agent for deep tissue imaging at 1064 nm. ACS Nano 6(8):7489–7496
Kumar K, Yadav SC, Yadav SK (2010) *Syzygium cumini* leaf and seed extract mediated biosynthesis of silver nanoparticles and their characterization. J Chem Technol Biotechnol 85:1301–1309
Kumar V, Kumari A, Guleria P et al (2012) Evaluating the toxicity of selected types of nanochemicals. In: Whitacre DM (ed) Reviews of environmental contamination and toxicology, vol 215. Springer, New York, pp 39–121
Kumar A, Huo S, Zhang X et al (2014) Neuropilin-1-targeted gold nanoparticles enhance therapeutic efficacy of platinum (iv) drug for prostate cancer treatment. ACS Nano 8(5):4205–4220
Kumari A, Guliani A, Singla R et al (2014a) Silver nanoparticles synthesised using plant extracts show strong antibacterial activity. IET Nanobiotechnol 9 (3):142–152
Kumari A, Singla R, Guliani A et al (2014b) Nanoencapsulation for drug delivery. EXCLI J 13:265–286
Lai G, Wu J, Ju H et al (2011) Streptavidin-functionalized silver-nanoparticle-enriched carbon nanotube tag for ultrasensitive multiplexed detection of tumor markers. Adv Funct Mater 21:2938–2943
Laurent S, Forge D, Port M et al (2008) Magnetic iron oxide nanoparticles: synthesis, stabilization, vectorization, physicochemical characterizations, and biological applications. Chem Rev 108(6):2064–2110
Lee DK, Kang YS (2004) Synthesis of silver nanocrystallites by a new thermal decomposition method and their characterization. ETRI J 26(3):252–256
Lee HJ, Lee G, Jang NR et al (2011) Biological synthesis of copper nanoparticles using plant extract. Nanotechnol 1:371–374
Lee E, Piao L, Kim J (2012) Synthesis of silver nanoparticles from the decomposition of silver(I) [bis(alkylthio)methylene]malonate complexes. Bull Korean Chem Soc 33(1):60–64
Lee H, Lee MY, Bhang SH et al (2014) Hyaluronate gold nanoparticle/tocilizumab complex for the treatment of rheumatoid arthritis. ACS Nano 8(5):4790–4798
Lengke MF, Fleet ME, Southam G (2006) Morphology of gold nanoparticles synthesized by filamentous cyanobacteria from gold(I)-thiosulfate and gold(III)-chloride complexes. Langmuir 22(6):2780–2787

Li L, Reiss P (2008) One-pot synthesis of highly luminescent InP/ZnS nanocrystals without precursor injection. J Am Chem Soc 130:11588–11589

Li Y, Wu Y, Ong BS (2005) Facile synthesis of silver nanoparticles useful for fabrication of high-conductivity elements for printed electronics. J Am Chem Soc 127:3266–3267

Li G, He D, Qian Y et al (2012a) Fungus-mediated green synthesis of silver nanoparticles using *Aspergillus terreus*. Int J Mol Sci 13:466–476

Li S, Liu Z, Ji F et al (2012b) Delivery of quantum dot-siRNA nanoplexes in SK-N-SH cells for BACE1 gene silencing and intracellular imaging. Mol Ther Nucleic Acids 1:e20. doi:10.1038/mtna.2012.11

Li M, Xiang K, Luo G et al (2013) Preparation of monodispersed copper nanoparticles by an environmentally friendly chemical reduction. Chin J Chem 31:1285–1289

Li X, Robinson SM, Gupta A et al (2014) Functional gold nanoparticles as potent antimicrobial agents against multi-drug-resistant bacteria. ACS Nano 8(10):10682–10686

Li H, Hu H, Xu D (2015) Silver decahedral nanoparticles-enhanced fluorescence resonance energy transfer sensor for specific cell imaging. Anal Chem 87:3826–3833

Liao YH, Chang YJ, Yoshiike Y et al (2012) Negatively charged gold nanoparticles inhibit Alzheimer's amyloid-β fibrillization, induce fibril dissociation, and mitigate neurotoxicity. Small 8(23):3631–3639

Lim YK, Lee YK (2007) Fluorescent emission of varied shades of resin composites. Dent Mater 23:1262–1268

Lin W, Huang YW, Zhou XD et al (2006) *In vitro* toxicity of silica nanoparticles in human lung cancer cells. Toxicol Appl Pharmacol 217(3):252–259

Lin J, Chen R, Feng S et al (2011) A novel blood plasma analysis technique combining membrane electrophoresis with silver nanoparticle-based SERS spectroscopy for potential applications in noninvasive cancer detection. Nanomedicine 7:655–663

Liu X, Dai Q, Austin L et al (2008) One-step homogeneous immunoassay for cancer biomarker detection using gold nanoparticle probes coupled with dynamic light scattering. J Am Chem Soc 130(9):2780–2782

Lu L, An X (2015) Silver nanoparticles synthesis using H_2 as reducing agent in toluene–supercritical CO_2 microemulsion. J Supercrit Fluids 99:29–37

Lu W, Melancon MP, Xiong C et al (2011) Effects of photoacoustic imaging and photothermal ablation therapy mediated by targeted hollow gold nanospheres in an orthotopic mouse xenograft model of glioma. Cancer Res 71:6116–6121

Ma H, Yin B, Wang S et al (2004) Synthesis of silver and gold nanoparticles by a novel electrochemical method. ChemPhysChem 5:68–75

Mahdavi M, Namvar F, Ahmad MB et al (2013) Green biosynthesis and characterization of magnetic iron oxide (Fe_3O_4) nanoparticles using seaweed (*Sargassum muticum*) aqueous extract. Molecules 18:5954–5964

Mahmoudi M, Simchi A, Milani AS et al (2009) Cell toxicity of superparamagnetic iron oxide nanoparticles. J Colloid Interface Sci 336(2):510–518

Makarov VV, Love AJ, Sinitsyna OV et al (2014) Green nanotechnologies: Synthesis of metal nanoparticles using plants. Acta Naturae 6(1):35–44

Malarkodi C, Rajeshkumar S, Paulkumar K et al (2014) Biosynthesis and antimicrobial activity of semiconductor nanoparticles against oral pathogens. Bioinorg Chem Appl 2014:10

Malik MA, Wani MY, Hashim MA (2012) Microemulsion method: a novel route to synthesize organic and inorganic nanomaterials:1st nano update. Arab J Chem 5(4):397–417

Manjili HK, Naderi-Manesh H, Mashhadikhan M et al (2014) The effect of iron- gold core shell magnetic nanoparticles on the sensitization of breast cancer cells to irradiation. JPS 5(2):85

Mann S (ed) (1996) Biomimetic materials chemistry. VCH Publishers, New York

Marcu A, Pop S, Dumitrache F et al (2013) Magnetic iron oxide nanoparticles as drug delivery system in breast cancer. Appl Surf Sci 281:60–66

Massoud TF, Gambhir SS (2003) Molecular imaging in living subjects: seeing fundamental biological processes in a new light. Genes Dev 17:545–580

Meng J, Xiao B, Zhang Y et al (2013) Super-paramagnetic responsive nanofibrous scaffolds under static magnetic field enhance osteogenesis for bone repair *in vivo*. Sci Rep 3. doi: 10.1038/srep0265

Minaeian S, Shahverdi AR, Nohi AS et al (2008) Extracellular biosynthesis of silver nanoparticles by some bacteria. JSIAU 17(66):1–4

Mody VV, Siwale R, Singh A et al (2010) Introduction to metallic nanoparticles. J Pharm Bioall Sci 2(4):282–289

Mohandas A, Sudheesh Kumar PT, Raja B et al (2015) Exploration of alginate hydrogel/nano zinc oxide composite bandages for infected wounds. Int J Nanomed 10:53–66

Mohapatra S, Rout SR, Maiti S et al (2011) Monodisperse mesoporous cobalt ferrite nanoparticles: synthesis and application in targeted delivery of antitumor drugs. J Mater Chem 21:9185–9193

Moon SA, Salunke BK, Alkotaini B et al (2015) Biological synthesis of manganese dioxide nanoparticles by *Kalopanax pictus* plant extract. IET Nanobiotechnol 9(4):220–225

Moriggi L, Cannizzo C, Dumas E et al (2009) Gold nanoparticles functionalized with gadolinium chelates as high-relaxivity MRI contrast agents. J Am Chem Soc 131:10828–10829

Mott D, Galkowski J, Wang L et al (2007) Synthesis of size-controlled and shaped copper nanoparticles. Langmuir 23:5740–5745

Mukherjee P, Ahmad A, Mandal D et al (2001) Bioreduction of AuCl(4)(-) ions by the fungus, *Verticillium* sp. and surface trapping of the gold nanoparticles. Angew Chem Int Ed Engl 40(19):3585–3588

Mukherjee P, Senapati S, Mandal D et al (2002) Extracellular synthesis of gold nanoparticles by the

fungus *Fusarium oxysporum*. Chem Bio Chem 3: 461–463
Mukherjee S, Chowdhury D, Kotcherlakota R et al (2014) Potential theranostics application of bio-synthesized silver nanoparticles (4-in-1 system). Theranostics 4 (3):316–335
Muniz-Miranda M, Gellini C, Simonelli A et al (2012) Characterization of copper nanoparticles obtained by laser ablation in liquids. Appl Phys A 110(4):829–833
Na HB, Song IC, Hyeon T (2009) Inorganic nanoparticles for MRI contrast agents. Adv Mater 21:2133–2148
Nair LS, Laurencin CT (2008) Nanofibers and nanoparticles for orthopaedic surgery applications. J Bone Joint Surg Am 90(Suppl 1):128–131
Nair CKK, Parida DK, Nomura T (2001) Radioprotectors in radiotherapy. J Rad Res 42:21–37
Nalawade P, Mukherjee T, Kapoor S (2012) High-yield synthesis of multispiked gold nanoparticles: characterization and catalytic reactions. Colloids Surf A Physicochem Eng Aspects 396:336–340
Namvar F, Rahman HS, Mohamad R et al (2015) cytotoxic effects of biosynthesized zinc oxide nanoparticles on murine cell lines. Evid Based Complement Alternat Med 2015:11
Naqvi S, Samim M, Abdin MZ et al (2010) Concentration-dependent toxicity of iron oxide nanoparticles mediated by increased oxidative stress. Int J Nanomed 5:983–989
Naseem T, Farrukh MA (2015) Antibacterial activity of green synthesis of iron nanoparticles using *Lawsonia inermis* and *Gardenia jasminoides* leaves extract. J Chem 2015:7
Niu J, Zhu T, Liu Z (2007) One-step seed-mediated growth of 30–150 nm quasispherical gold nanoparticles with 2-mercaptosuccinic acid as a new reducing agent. Nanotechnol 18:1–7
Okitsu K, Ashokkumar M, Grieser F (2005) Sonochemical synthesis of gold nanoparticles: Effects of ultrasound frequency. J Phys Chem B 109(44):20673–20675
Pan D, Cai X, Yalaz C et al (2012) Photoacoustic sentinel lymph node imaging with self-assembled copper neodecanoate nanoparticles. ACS Nano 6(2):1260–1267
Panacek A, Kvitek L, Prucek R et al (2006) Silver colloid nanoparticles: Synthesis, characterization, and their antibacterial activity. J Phys Chem B 110:16248–16253
Pandey JK, Swarnkar RK, Soumya KK et al (2014) Silver nanoparticles synthesized by pulsed laser ablation: as a potent antibacterial agent for human enteropathogenic gram-positive and gram-negative bacterial strains. Appl Biochem Biotechnol 174:1021–1031
Patil HB, Borse SV, Patil DR et al (2011) Synthesis of silver nanoparticles by microbial method and their characterization. Arch Phys Res 2(3):153–158
Pholnak C, Sirisathitkul C, Danworaphong S et al (2013) Sonochemical synthesis of zinc oxide nanoparticles using an ultrasonic homogenizer. Ferroelectrics 455 (1):15–20
Plank C, Scherer F, Schillinger U et al (2003) Magnetofection: Enhancing and targeting gene delivery with superparamagnetic nanoparticles and magnetic fields. J Liposome Res 13:29–32
Prabhu RR, Khadar MA (2005) Characterization of chemically synthesized CdS nanoparticles. J Phys 65 (5):801–807
Prabhu S, Poulose EK (2012) Silver nanoparticles: Mechanism of antimicrobial action, synthesis, medical applications, and toxicity effects. Int Nano Lett 2: 32–42
Pu K, Shuhendler AJ, Jokerst JV et al (2014) Semiconducting polymer nanoparticles as photoacoustic molecular imaging probes in living mice. Nature Nanotechnol 9:233–239
Qi L, Ma J, Shen J (1997) Synthesis of copper nanoparticles in nonionic water-in-oil microemulsions. J Colloid Interface Sci 186(2):498–500
Raghunandan D, Bedre MD, Basavaraja S et al (2010) Rapid biosynthesis of irregular shaped gold nanoparticles from macerated aqueous extracellular dried clove buds (*Syzygium aromaticum*) solution. Colloids Surf B Biointerfaces 79:235–240
Rajeshkumar S, Malarkodi C (2014) *In vitro* antibacterial activity and mechanism of silver nanoparticles against foodborne pathogens. Bioinorg Chem Appl 2014:10
Rajeshkumar S, Ponnanikajamideen M, Malarkodi C et al (2014) Microbe-mediated synthesis of antimicrobial semiconductor nanoparticles by marine bacteria. J Nanostruct Chem 4:96
Ramachandran L, Nair CKK (2011) Therapeutic potentials of silver nanoparticle complex of α-lipoic acid. Nanomater Nanotechnol 1(2):17–24
Ramyadevi J, Jeyasubramanian K, Marikani A et al (2012) Synthesis and antimicrobial activity of copper nanoparticles. Mater Lett 71:114–116
Rao SV (2011) Picosecond nonlinear optical studies of gold nanoparticles synthesised using coriander leaves (*Coriandrum sativum*). J Mod Optics 58(12):1024–1029
Roh Y, Lauf RJ, McMillan AD et al (2001) Microbial synthesis and the characterization of metal-substituted magnetites. Solid State Commun 118:529–534
Rosarin FS, Mirunalini S (2011) Nobel metallic nanoparticles with novel biomedical properties. J Bioanal Biomed 3:085–091
Sabir S, Arshad M, Chaudhari SK (2014) Zinc oxide nanoparticles for revolutionizing agriculture: synthesis and applications. The Scientific World J 2014:8
Sahithi K, Swetha M, Prabaharan M et al (2010) Synthesis and characterization of nanoscale-hydroxyapatite-copper for antimicrobial activity towards bonetissue engineering applications. J Biomed Nanotechnol 6(4):333–339
Sai LM, Kong XY (2011) Microwave-assisted synthesis of water-dispersed CdTe/CdSe core/shell type II quantum dots. Nanoscale Res Lett 6:399
Saito G, Hosokai S, Tsubota M et al (2011) Synthesis of copper/copper oxide nanoparticles by solution plasma. J Appl Phys 110(2):023302–023306

Salavati-Niasari M, Davar F (2009) Synthesis of copper and copper(I) oxide nanoparticles by thermal decomposition of a new precursor. Mater Lett 63:441–443

Salavati-Niasari M, Davar F, Mir N (2008) Synthesis and characterization of metallic copper nanoparticles via thermal decomposition. Polyhedron 27:3514–3518

Salih NA (2013) The enhancement of breast cancer radiotherapy by using silver nanoparticles with 6 MeV gamma photons. Adv Phys Theor Appl 26:10–14

Salkar RA, Jeevanandam P, Aruna ST et al (1999) The sonochemical preparation of amorphous silver nanoparticles. J Mater Chem 9:1333–1335

Saminathan K (2015) Biosynthesis of silver nanoparticles using soil Actinomycetes *Streptomyces sp*. Int J Curr Microbiol App Sci 4(3):1073–1083

Sanghi R, Verma P, Puri S (2011) Enzymatic formation of gold nanoparticles using *Phanerochaete Chrysosporium*. Adv Chem Eng Sci 1:154–162

Sankar R, Maheswari R, Karthik S et al (2014) Anticancer activity of *Ficus religiosa* engineered copper oxide nanoparticles. Mater Sci Eng C Mater Biol Appl 1 (44):234–239

Sankar R, Baskaran A, Shivashangari KS et al (2015) Inhibition of pathogenic bacterial growth on excision wound by green synthesized copper oxide nanoparticles leads to accelerated wound healing activity in Wistar Albino rats. J Mater Sci Mater Med 26(7):214

Sanpui P, Chattopadhyay A, Ghosh SS (2011) Induction of apoptosis in cancer cells at low silver nanoparticle concentrations using chitosan nanocarrier. ACS Appl Mater Interfaces 3:218–228

Santhoshkumar T, Rahuman AA, Jayaseelan C et al (2014) Green synthesis of titanium dioxide nanoparticles using *Psidium guajava* extract and its antibacterial and antioxidant properties. Asian Pac J Trop Dis 12:968–976

Sarkar K, Banerjee SL, Kundu PP et al (2015) Biofunctionalized surface-modified silver nanoparticles for gene delivery. J Mater Chem B 3:5266–5276

Sastry M, Ahmad A, Khan MI et al (2003) Biosynthesis of metal nanoparticles using fungi and actinomycetes. Curr Sci 85(2):162–170

Senapati S (2005) Biosynthesis and immobilization of nanoparticles and their applications. PhD thesis, University of Pune

Setua S, Ouberai M, Piccirillo SG et al (2014) Cisplatin-tethered gold nanospheres for multimodal chemo-radiotherapy of glioblastoma. Nanoscale 6 (18):10865–10873

Shamsipur M, Pourmortazavi SM, Hajimirsadeghi SM et al (2013) Facile synthesis of zinc carbonate and zinc oxide nanoparticles via direct carbonation and thermal decomposition. Ceramics Int 39:819–827

Shankar SS, Absar A, Murali S (2003) Geranium leaf assisted biosynthesis of silver nanoparticles. Biotechnol Prog 19:1627–1631

Shantkriti S, Rani P (2014) Biological synthesis of copper nanoparticles using *Pseudomonas fluorescens*. Int J Curr Microbiol App Sci 3(9):374–383

Sharifi S, Behzadi S, Laurent S et al (2012) Toxicity of nanomaterials. Chem Soc Rev 41:2323–2343

Sharma NC, Sahi SV, Nath S et al (2007) Synthesis of plant-mediated gold nanoparticles and catalytic role of biomatrix-embedded nanomaterials. Environ Sci Technol 41(14):5137–5142

Shavel A, Gaponik N, Eychmuller A (2004) Efficient UV-blue photoluminescing thiol-stabilized water-soluble alloyed ZnSe(S) nanocrystals. J Phys Chem B 108:5905–5908

Sheikh FA, Barakat NA, Kanjwal MA et al (2010) Electrospun titanium dioxide nanofibers containing hydroxyapatite and silver nanoparticles as future implant materials. J Mater Sci Mater Med 21 (9):2551–2559

Shevach M, Fleischer S, Shapira A et al (2014) Gold nanoparticle decellularized matrix hybrids for cardiac tissue engineering. Nano Lett 14(10):5792–5796

Shirtcliffe N, Nickel U, Schneider S (1999) Reproducible preparation of silver sols with small particle size using borohydride reduction: for use as nuclei for preparation of larger particles. J Colloid Interface Sci 211 (1):122–129

Siddiqui TS, Jani A, Williams F et al (2009) Lanthanide complexes on Ag nanoparticles: designing contrast agents for magnetic resonance imaging. J Colloid Interface Sci 337:88–96

Singh SC, Gopal R (2008) Synthesis of colloidal zinc oxide nanoparticles by pulsed laser ablation in aqueous media. Physica E 40:724–730

Singh PK, Kundu S (2013) Biosynthesis of gold nanoparticles using bacteria. Proc Natl Acad Sci India Sect B Biol Sci 84(2):331–336

Singh K, Panghal M, Kadyan S et al (2004) Antibacterial activity of synthesized silver nanoparticles from tinospora cordifolia against multi drug resistant strains of pseudomonas aeruginosa isolated from burn patients. J Nanomed Nanotechnol 5:2

Soenen SJ, Manshian B, Montenegro JM et al (2012a) Cytotoxic effects of gold nanoparticles: a multiparametric study. ACS Nano 6(7):5767–5783

Soenen SJ, De Cuyper M, De Smedt SC et al (2012b) Investigating the toxic effects of iron oxide nanoparticles. Methods Enzymol 509:195–224

Song EQ, Hu J, Wen CY et al (2011) Fluorescent-magnetic-biotargeting multifunctional nanobioprobes for detecting and isolating multiple types of tumor cells. ACS Nano 5(2):761–770

Soumya RS, Hela PG (2013) Nano silver based targeted drug delivery for treatment of cancer. Der Pharmacia Lettre 5(4):189–197

Su Y, He Y, Lu H et al (2009) The cytotoxicity of cadmium based, aqueous phase—synthesized, quantum dots and itsmodulation by surface coating. Biomater 30(1):19–25

Sudheesh Kumar PT, Lakshmanan VK, Raj M et al (2013) Evaluation of wound healing potential of β-chitin hydrogel/nano zinc oxide composite bandage. Pharm Res 30:523–537

Sun Y, Xia Y (2002) Large-scale synthesis of uniform silver nanowires through a soft, self-seeding, polyol process. Adv Mater 14:833–837

Sun YP, Rollins HW, Guduru R (1999) Preparations of nickel, cobalt, and iron nanoparticles through the rapid expansion of supercritical fluid solutions (RESS) and chemical reduction. Chem Mater 11:7–9

Sun T, Yan Y, Zhao Z et al (2012) Copper oxide nanoparticles induce autophagic cell death in A549 cells. PLoS ONE 7(8):e43442. doi:10.1371/journal.pone.0043442

Sunderland CJ, Steiert M, Talmadge JE et al (2006) Targeted nanoparticles for detecting and treating cancer. Drug Dev Res 67:70–93

Syed A, Ahmad A (2013) Extracellular biosynthesis of CdTe quantum dots by the fungus Fusarium oxysporum and their anti-bacterial activity. Spectrochim Acta A Mol Biomol Spectrosc 106:41–47

Tajdidzadeh M, Azmi BZ, Yunus WMM et al (2014) Synthesis of silver nanoparticles dispersed in various aqueous media using laser ablation. The Scientific World J 2014:7

Thakkar KN, Mhatre SS, Parikh RY (2010) Biological synthesis of metallic nanoparticles. Nanomedicine 6:257–262

Theivasanthi T, Alagar M (2011) Nano sized copper particles by electrolytic synthesis and characterizations. Int J Phys Sci 6(15):3662–3671

Thomas R, Park IK, Jeong YY (2013) Magnetic iron oxide nanoparticles for multimodal imaging and therapy of cancer. Int J Mol Sci 14(8):15910–15930

Thomas R, Janardhanan A, Varghese RT et al (2014) Antibacterial properties of silver nanoparticles synthesized by marine *Ochrobactrum* sp. Braz J Microbiol 45:1221–1227

Tian J, Wong KKY, Ho CM et al (2007) Topical delivery of silver nanoparticles promotes wound healing. ChemMedChem 2:129–136

Tran QH, Nguyen VQ, Le AT (2013) Silver nanoparticles: synthesis, properties, toxicology, applications and perspectives. Adv Nat Sci Nanosci Nanotechnol 4:1–20

Tripathi A, Chandrasekaran N, Raichur AM et al (2009) Process variables in biomimetic synthesis of silver nanoparticles by aqueous extract of *Azadirachta indica* (Neem) leaves. J Biomed Nanotechnol 5:93–98

Umrani RD, Paknikar KM (2014) Zinc oxide nanoparticles show antidiabetic activity in streptozotocin-induced Type 1 and 2 diabetic rats. Nanomedicine (Lond) 9(1):89–104

Upadhyay SN, Dwarakanath BS, Ravindranath T (2005) Chemical radioprotectors. Defence Sci J 55:403–425

Valodkar M, Jadeja RN, Thounaojam MC et al (2011) Biocompatible synthesis of peptide capped copper nanoparticles and their biological effect on tumor cells. Mater Chem Phys 128:83–89

Veeraapandian S, Sawant SN, Doble M (2012) Antibacterial and antioxidant activity of protein capped silver and gold nanoparticles synthesized with *Escherichia coli*. J Biomed Nanotechnol 8:1400148

Verma HN, Singh P, Chavan RM (2014) Gold nanoparticle: synthesis and characterization. Vet World 7 (2):72–77

Vilchis-Nestora R, Sanchez-Mendietaa V, Camacho-Lopeza MA et al (2008) Optical properties of Au and Ag nanoparticles using *Camellia Sinensis* extract. Mater Lett 62:3103–3105

Walter A, Billotey C, Garofalo A et al (2014) Mastering the Shape and composition of dendronized iron oxide nanoparticles to tailor magnetic resonance imaging and hyperthermia. Chem Mater 26:5252–5264

Wang YQ, Chen SG, Tang XH et al (2001) Mesoporous titanium dioxide: sonochemical synthesis and application in dye-sensitized solar cells. J Mater Chem 11:521–526

Wang HC, Brown J, Alayon H et al (2010) Transplantation of quantum dot-labelled bone marrow-derived stem cells into the vitreous of mice with laser-induced retinal injury: survival, integration and differentiation. Vision Res 50:665–673

Wang Y, Newell BB, Irudayaraj J (2012) Folic acid protected silver nanocarriers for targeted drug delivery. J Biomed Nanotechnol 8:751–759

Wang D, Fei B, Halig LV et al (2014a) Targeted iron-oxide nanoparticle for photodynamic therapy and imaging of head and neck cancer. ACS Nano 8 (7):6620–6632

Wang J, Ye DX, Liang GH et al (2014b) One-step synthesis of water-dispersible silicon nanoparticles and their use in fluorescence lifetime imaging of living cells. J Mater Chem B 2:4338–4345

Wei L, Lu J, Xu H et al (2015) Silver nanoparticles: synthesis, properties, and therapeutic applications. Drug Discov Today 20(5):595–601

Wender H, Andreazza ML, Correia RRB et al (2011) Synthesis of gold nanoparticles by laser ablation of an Au foil inside and outside ionic liquids. Nanoscale 3:1240–1245

Wong KKY, Liu X (2010) Silver nanoparticles—the real "silver bullet" in clinical medicine? Med Chem Commun 1:125–131

Wongwailikhit K, Horwongsakul S (2011) The preparation of iron (III) oxide nanoparticles using w/o microemulsion. Mater Lett 65(17–18):2820–2822

Wu P, He Y, Wang HF et al (2010) Conjugation of glucose oxidase onto Mn-doped ZnS quantum dots for phosphorescent sensing of glucose in biological fluids. Anal Chem 82(4):1427–1433

Xing B, Li WW, Sun K (2008) A novel synthesis of high quality CdTe quantum dots with good thermal stability. Mater Lett 62:3178–3180

Yallapu MM, Othman SF, Curtis ET et al (2011) Multi-functional magnetic nanoparticles for magnetic resonance imaging and cancer therapy. Biomater 32:1890–1905

Yan Z, Qian J, Gu Y et al (2014) Green biosynthesis of biocompatible CdSe quantum dots in living *Escherichia coli* cells. Mater Res Express 1:015401

Yang L, Chen G, Wang J et al (2009) Sunlight-induced formation of silver-gold bimetallic nanostructures on

DNA template for highly active surface enhanced Raman scattering substrates and application in TNT/tumor marker detection. J Mater Chem 19:6849–6856

Ye X, Shi H, He X et al (2015) Iodide-responsive Cu−Au nanoparticle-based colorimetric platform for ultrasensitive detection of target cancer cells. Anal Chem 87:7141–7147

Yi X, Yang K, Liang C et al (2015) Imaging-guided combined photothermal and radiotherapy to treat subcutaneous and metastatic tumors using iodine-131-doped copper sulfide nanoparticles. Adv Func Mater 25:4689–4699

Yildirim OA, Durucan C (2010) Synthesis of zinc oxide nanoparticles elaborated by microemulsion method. J Alloys Compd 506:944–949

Yin B, Ma H, Wang S et al (2003) Electrochemical synthesis of silver nanoparticles under protection of poly(*N*-vinylpyrrolidone). J Phys Chem B 107:8898–8904

Yokoyama T, Tam J, Kuroda S et al (2011) EGFR-targeted hybrid plasmonic magnetic nanoparticles synergistically induce autophagy and apoptosis in non-small cell lung cancer cells. PLoS ONE 6(11): e25507

Yong Y, Cheng X, Bao T et al (2015) Tungsten sulfide quantum dots as multifunctional nanotheranostics for *in vivo* dFual-modal image-guided photothermal/radiotherapy synergistic therapy. ACS Nano. doi:10.1021/acsnano.5b05825

Yu H, Brock SL (2008) Effects of nanoparticle shape on the morphology and properties of porous cdse assemblies (aerogels). ACS Nano 2(8):1563–1570

Yuan Y, Chen S, Paunesku T et al (2013) Epidermal growth factor receptor targeted nuclear delivery and high-resolution whole cell X-ray imaging of Fe3O4@-TiO2 nanoparticles in cancer cells. ACS Nano 7 (12):10502–10517

Zajac A, Song D, Qian W et al (2007) Protein microarrays and quantum dot probes for early cancer detection. Colloid Surf B Biointerfaces 58(2):309–314

Zamborini FP, Bao L, Dasari R (2012) Nanoparticles in measurement science. Anal Chem 84(2):541–576

Zeng L, Ren W, Zheng J et al (2012) Ultrasmall water-soluble metal-iron oxide nanoparticles as T1-weighted contrast agents for magnetic resonance imaging. Phys Chem Chem Phys 14:2631–2636

Zhang J, Lan CQ (2008) Nickel and cobalt nanoparticles produced by laser ablation of solids in organic solution. Mater Lett 62(10–11):1521–1524

Zhang J, Lei Y, Dhaliwal A et al (2011) Protein-polymer nanoparticles for nonviral gene delivery. Biomacromol 12:1006–1014

Zhang L, Wang T, Li L et al (2012a) Multifunctional fluorescent-magnetic polyethyleneimine functionalized Fe_3O_4–mesoporous silica yolk–shell nanocapsules for siRNA delivery. Chem Commun 48:8706–8708

Zhang Q, Liu F, Nguyen KT et al (2012b) Multifunctional mesoporous silica nanoparticles for cancer-targeted and controlled drug delivery. Adv Func Mater 22:5144–5156

Zhang R, Pan D, Cai X et al (2015) $\alpha_v\beta_3$-targeted copper nanoparticles incorporating an Sn 2 lipase-labile fumagillin prodrug for photoacoustic neovascular imaging and treatment. Theranostics 5(2):124–133

Zheng T, Pierre-Pierre N, Yan X et al (2015) Gold nanoparticle-enabled blood test for early stage cancer detection and risk assessment. ACS Appl Mater Interfaces 7(12):6819–6827

Zhou Y, Kong Y, Kundu S et al (2012) Antibacterial activities of gold and silver nanoparticles against *Escherichia coli* and Bacillus Calmette- Guérin. J Nanobiotechnol 10:19

Zhu J, Liu S, Palchik O et al (2000) Shape-controlled synthesis of silver nanoparticles by pulse sonoelectrochemical methods. Langmuir 16:6396–6399

Zielińska-Jurek A, Reszczyńska J, Grabowska E et al (2012) Nanoparticles preparation using microemulsion systems. In: Najjar RE (ed) Microemulsions—an introduction to properties and applications. InTech Publisher, Rijeka, Croatia

Liposomal and Phytosomal Formulations

4

Anika Guliani, Rubbel Singla, Avnesh Kumari and Sudesh Kumar Yadav

Abstract

Liposomes and phytosomes are kind of nanoparticles (NPs) which serve as an imperative tool for the delivery of various bioactive molecules. The molecules possessing lesser water solubility, bioavailability and retention time are encapsulated into both of these formulations. More specifically, liposomes can encapsulate both hydrophobic as well as hydrophilic molecules. While phytosomes contain only plant-based molecules having poor solubility in biological media like flavanones and terpenes. The various advantages of liposomes and phytosomes like biocompatibility, nontoxicity, ease to administer, decrease in dosage and increase in retention time make them potent vehicles for the drug delivery of various molecules. These nanoformulations find potential applications for delivery of various bioactive molecules, in tissue regeneration and as antimicrobials. This chapter highlights the importance of liposomes and phytosomes, methods of their preparation, mechanism of their action and applications.

Keywords

Liposomes · Phytosomes · Bioactive molecule · Drug delivery · Antioxidant

A. Guliani · R. Singla · A. Kumari · S.K. Yadav
Department of Biotechnology, Council of Scientific and Industrial Research-Institute of Himalayan Bioresource Technology, Palampur 176061, Himachal Pradesh, India

A. Guliani · R. Singla · S.K. Yadav
Academy of Scientific and Innovative Research, New Delhi, India

S.K. Yadav (✉)
Department of Biotechnology, Center of Innovative and Applied Bioprocessing (CIAB), Mohali 160071, Punjab, India
e-mail: skyt@rediffmail.com; sudesh@ciab.res.in

© Springer Science+Business Media Singapore 2016

S.K. Yadav (ed.), *Nanoscale Materials in Targeted Drug Delivery, Theragnosis and Tissue Regeneration*, DOI 10.1007/978-981-10-0818-4_4

Contents

4.1 Introduction

The elementary meaning of formulation means combining the various components together in a proper structure or relationship. The delivery of active component at target site is mainly governed by the composition of formulation at an optimum concentration. In this respect, nanoformulations have been widely explored for the delivery of active components to increase their efficacy and minimise toxicity associated with molecules. The effectiveness of water soluble compounds is limited because they are poorly absorbed by the body. These compounds cannot retain themselves for long into the gastrointestinal tract as they get excreted out very easily. Due to their hydrophilic nature, these molecules are unable to cross the lipid bilayer. To make these water soluble molecules available to the body, these compounds are integrated with phospholipids which help them to cross the lipid bilayer (Karimi et al. 2015a). The incorporated material is protected from degradation by most external factors and microbes of the intestine (Amin and Bhat 2012). The bioavailability of the molecules is achieved by crossing of the material through plasma membrane and dissipation of molecules in the tract and finally ingression into the blood (Manach et al. 2004). Two of the most common nanoformulations which have been discussed in detail in the literature are based on liposomal and phytosomal formulations. The liposomal formulation defines liposomes as artificially prepared minuscule bubbles comprised of phospholipids just in a similar manner as that of cell membranes. The term 'liposome' was first coined by Dr. Alec D Bangham in 1961 which consists of two words 'lipo' and 'soma' with the meaning of fat and body, respectively. Liposomes are spherical vesicles made up of cholesterol and phospholipids. The phosphatidylethanolamine, phosphatidylcholine (PC), phosphatidyl glycerol and phosphatidyl serine are the major phospholipids which have been used for the formation of liposomes (Dua et al. 2012). The phospholipids being amphipathic in nature possess both the hydrophobic and hydrophilic characters and thereby serve as potential carriers of drugs. The phospholipids in aqueous media form a thermodynamically stable closed structure resulting into a bilayer. The bilayer contains hydrophilic head groups facing out towards the aqueous phase whereas the hydrophobic tails orient inwards away from the aqueous media. The core is formed in the centre of the spherical bilayer which is an aqueous compartment by virtue of which it can carry water soluble molecules like peptides, enzymes, antibiotics, anticancer agents and hormones into it while the bilayer can encapsulate

the hydrophobic molecules (Akbarzadeh et al. 2013). The drug molecules encapsulated in the liposomes have to be released out before metabolism and excretion in the body, rendering high therapeutic effect. The stability, diffusion of the proteins as well as the encapsulated molecules along with their functions, clearance of liposome from the body circulation depends upon the viscosity (fluidity) of the membrane which is further determined by its phospholipid composition or the lipid packaging (Drummond et al. 1999; Muramatsu et al. 1999). The unsaturated phospholipids contribute towards the permeable and less stable nature of lipid bilayer while the saturated phospholipids form a rigid and impermeable lipid bilayer (Marripati et al. 2014). The surface charge, lipid composition, size and use of different synthetic methods for the preparation of liposomes are responsible for different properties of liposome. The advantages of using liposomes as therapeutic carriers involve (a) its suitability for different hydrophilic, hydrophobic and amphipathic drugs with increased therapeutic effect and efficacy, (b) sustained release, (c) ease of surface modifications with specific ligands for targeted delivery, (d) increased retention time (RT) in the blood, (e) ease of administration by various routes and (f) biodegradability, nontoxicity and biocompatibility (Kaur et al. 2013). However, few major drawbacks viz., chemical instability of phospholipids due to hydrolysis and oxidation, high cost of production, short half life, low thermal stability, minimal uptake of large sized liposomes in reticuloendothelial system (RES), leakage and fusion possess serious constraints for their use as a suitable delivery agent (Bhai et al. 2012).

Similarly, another formulation 'phytosome' is formed by conjugation of two words in which 'phyto' means plant and 'some' means cell like (Kareparamban et al. 2012). It has long been known that several plant secondary metabolites viz., phenolics, glycosides and flavonoids possess potential benefits to animals. Phytosomes are the modified versions of herbal products and have better properties in terms of absorption, therapy, bioavailability and solubility (Gunasekaran et al. 2014). The phytosomes confer many advantages like increase in the solubility of polar compounds, absorption rate and decrease in the dosage of the drug. The phytochemical compounds loaded into phytosomes are more stable than their pure forms. Most of the phytosomes are prepared from phosphatidylcholine (PC) which in synergy with the hepatoprotective molecule aids in better protection of the liver. The use of phytosomes augments the bioavailability of encapsulated molecule and can be used for dermal as well as transdermal delivery of the molecule. (Bhattacharya 2009; Athira et al. 2014; Pawar and Bhangale 2015).

Keeping in view all the advantages and disadvantages of liposomes and phytosomes, this chapter describes their types, different methods of synthesis, surface modifications, behaviour in biological system, properties and applications in medical field. There are numerous applications of liposomes and phytosomes but here the main focus is laid on the medicinal aspects of molecules encapsulated into liposomes and phytosomes.

4.2 Types of Liposomes

The size of liposomes can vary from few nanometers (nm) to micrometres (μm). Liposomes can be broadly classified into two different categories viz., based on drug delivery systems and structural parameters.

4.2.1 Liposomes Based on Drug Delivery Systems

The liposomal membrane is generally composed of natural compounds as found in the membrane of the living organisms and can be modified synthetically. By modification of these membrane ingredients, different types of liposomes like conventional, stealth, active and charged can be synthesised.

The conventional liposomes (first generation liposomes) are mainly made up of neutral phosphatidylcholine or negatively charged phosphatidylserine phospholipids and cholesterol. These vesicles were first evolved for the drug delivery with fast removal from the blood circulation and less RT. These suffered from the disadvantage of leaky endothelium effect i.e. leakage of the drug or the substance entrapped within the liposomes. Though these can mimic plasma membrane to a greater extent, the macrophages treat them as foreign bodies. Due to this reason, these conventional liposomes were further modified to second generation liposomes with appropriate surface modifications (Shaheen et al. 2006).

The second generation liposomes or stealth liposomes are also known as sterically stabilised liposomes. These are covalently attached with long hydrocarbon chains or coated with some synthetic polymers like polyethylene glycol (PEG). The coating further produced stealth effect and increased the half life in the blood and reduced the process of opsonisation in the body. Such liposomes aided in better stabilisation and protection for the drugs entrapped (Immordino et al. 2006).

Active liposomes are the vesicles which provide selective, sustained and controlled release of the entrapped molecules. Such liposomes travel along the media for longer time before their contents are being released. These liposomes are known to be both temperature and pH sensitive with the added advantage of being cell specific and hence can be used for targeted as well as triggered release of the components. The target specificity can be achieved by attaching the specific ligands like lectins, antibodies and oligosaccharides on the liposomal surface (Gomez-Hens and Fernández-Romero 2006).

Charged liposomes (cationic and anionic in nature), also termed as lipoplexes are the vesicles integrated with the charged phospholipids. These are subjected to integrate with oppositely charged macromolecules like DNA, proteins and form a covalent bond (Lipid–DNA complex). The molecules having high molecular weight can also be internalised by these liposomes (Gomez-Hens and Fernández-Romero 2006).

4.2.2 Liposomes Based on Structural Parameters

On the basis of structural parameters, the liposomes are classified into three major classes (Kant et al. 2012) viz., unilamellar, made up of aqueous core surrounded by a single layer of phospholipids of 20–1000 nm; oligolamellar, here the aqueous core is enclosed within lipid bilayers of 10–12 concentric rings of 0.1–0.5 μm; and multilamellar liposomes (MLV), here the unilamellar liposomes form a concentric layer of lipids one after the other forming a multilamellar liposome of >0.5 μm. The unilamellar liposomes are again classified into small unilamellar vesicles (SUV, generally of 20–40 nm), medium unilamellar vesicles (MUV, varies from 40 to 80 nm in size) and large unilamellar vesicles (LUV, differs largely from 100 to 1000 nm). In MLVs, the water content is separated by different number of lipid bilayers in a different fashion and resembles an onion structure.

4.3 Methods of Preparation of Liposomes

Various methods are employed for the synthesis of liposomes and their choice depends upon different parameters like physicochemical properties of the material to be entrapped as well as of liposomal material, the polydispersity and shelf life of the vesicles to be synthesised, medium in which liposomes are disseminated, concentration of encapsulated drug and its toxicity level (Mozafari et al. 2008). The synthesis of drug/molecule loaded liposome involves mainly two mechanisms, passive and active drug loading. Figure 4.1 depicts the various methodologies used for the synthesis of liposomes.

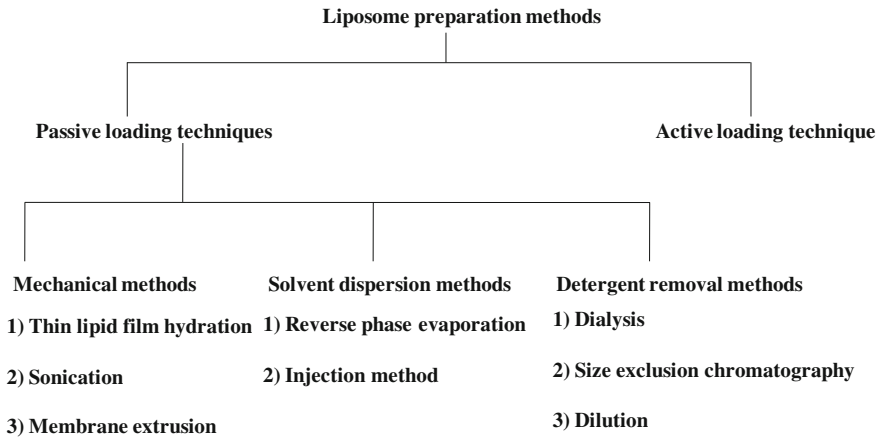

Fig. 4.1 Flow chart representing different preparation methodologies for the synthesis of liposomes

4.3.1 Passive Drug Loading/ Encapsulation

Passive drug loading is the technique in which the drug is encapsulated simultaneously during the formation of liposome vesicles. In passive loading, any molecule irrespective of its shape, charge and molecular mass can be loaded into the aqueous part or in the hydrophobic layer of liposomes. The attraction and repulsion between phospholipids of bilayer and encapsulated drug can affect the loading magnitude as increase or decrease (Barenholz 1996). Passive drug loading can be again classified into three different methods viz., mechanical, solvent dispersion and detergent removal.

4.3.1.1 Mechanical Method

This method is further classified into (1) thin lipid film hydration, (2) sonication and (3) membrane extrusion. In thin lipid film hydration method, the basic steps involved are hydration of lipids, hydration with agitation followed by sizing of the vesicles formed into a homogeneous solution (Wagner and Vorauer-Uhl 2011). This method deals with the procedure where lipids are immersed in an organic solvent to form a homogeneous mixture. Generally, chloroform or chloroform: methanol mixtures, tertiary butanol, cyclohexane are the few organic solvents being used. These solvents are used in concentration of about 10–20 mg lipid/ml of organic solvent. Once the lipids are well mixed with the solvent, a thin film of lipids is obtained by solvent evaporation. The dry nitrogen or argon gases are used to evaporate little amount of the organic solvent in a closed hood while large amount of solvent is removed using a rotatory evaporator. The lipid film so formed is further dried from the residual solvent by keeping the flask overnight in a vacuum pump (Dua et al. 2012). The dry lipid film formed is then hydrated by adding the buffer and agitating it for sometime. This step is done at a temperature above the gel-liquid crystal transition temperature (T_c) of the lipids. Depending upon the solubility of the molecules to be encapsulated, these are dissolved accordingly into the organic solvent or the aqueous buffer. This method is generally applied for the formation of MLV. The hydrated film is further downsized using various techniques like sonication and extrusion. This method has certain drawbacks such as low encapsulation efficiency and heterogeneity in size distribution (Bangham et al. 1974). Liposomes prepared using this method have been used for the encapsulation of celecoxib, nabumetone (Moghimipour and Handali 2012; Senthilkumar et al. 2012), paclitaxel (Huang et al. 2010), cisplatin (Kroon et al. 2005), gentamycin (Rukholm et al. 2006). Drug encapsulated liposomes have shown more effectiveness as compared to pure drugs.

Sonication is one of the most broadly used methods with the employment of ultrasonics. The use of ultrasonics is a tool to prepare liposomes for the encapsulation of active biomolecules. In this procedure, liposomal dispersion or MLVs are sonicated with a probe. Usually two different types of sonication techniques such as probe and bath sonication are employed. In probe sonication, liposomal dispersion remains in direct contact with the probe of sonicator. The amount of energy applied is very high. The vessel containing liposomal dispersion must be placed in an ice bath as huge amount of heat energy is produced. The disadvantages of probe sonication include low encapsulation, degradation of encapsulated molecule, metal erosion from probe's tip and the presence of MLVs along with SUVs (Riaz 1996). In bath sonication, the tube in which liposomes are present is placed in bath sonicator. This method provides better protection of liposomes from generated heat as compared to probe sonication (Akbarzadeh et al. 2013). Liposomes enclosing chondroitin sulphate (Craciunescu et al. 2014), 1-oleoyl-2-[12-[(7-nitro-2-1,3-benzoxadiazole-4-yl)amino]dodecanoyl]-sn-glycero-3 phospho choline (Lapinski et al. 2007), eicosapentaenoic acid and docosahexaenoic acid (Hadian et al. 2014), and 5-fluorouracil (Costa and Moraes 2003) have been prepared by this technique.

The membrane extrusion is one of the most accepted techniques for the reduction of liposomal size as well as to obtain LUVs. Extrusion is the process of passing the solution through a series of filters with decreasing pore size under a low pressure (Olson et al. 1979). The method is applicable for a variety of lipid mixtures and is quiet rapid and can work out with MLVs directly. MLVs encounter several limitations like large diameter, low entrapment and batch-to-batch variation during its preparation. The extrusion method deals well with all the aforementioned problems. In this method, under very limited amount of pressure, MLVs are forced through filters of definite pore size. By passing through the filter pores, the layers of MLVs deform and then breaking and resealing of the membranes take place. On repetition of cycle through filter membrane, liposomal population of similar mean diameter is formed with homogeneous nature (Hope et al. 1993). Liposomes entrapping cyclo (l-tyrosyl- l-prolyl) (Kilian et al. 2011), linoleic acid (Jung et al. 2015), 1-oleoyl-2-[12-[(7-nitro-2-1,3-benzoxadiazol-4-yl)amino]dodecanoyl]-sn-glycero-3-phosphocholine (Lapinski et al. 2007), and 5-fluorouracil (Costa and Moraes 2003) have been synthesised by extrusion method.

4.3.1.2 Solvent Dispersion

In this method, the lipids dissolved in organic solvent are brought in contact with aqueous phase containing the drug. At the interface, the lipids align themselves and form a bilayer (Himanshu et al. 2011). The solvent dispersion method is further divided into two types; reverse phase evaporation and injection (ethanol and ether) methods.

The reverse phase evaporation method aims at encapsulating high amount of water soluble molecules into liposomes with high aqueous concentration to lipid ratio. The method is based on the formation of inverted micelles. The lipids dissolved in an organic solvent like diethyl ether or a mixture of chloroform and water (w/o emulsion) are sonicated. The water soluble compounds get dissolved in aqueous phase while amphipathic molecules are dissolved in organic solvent. The rotatory evaporator is used to form a viscous gel by removing organic solvent under reduced pressure. The slow removal of organic solvents continuously converts this viscous gel into liposomal formulation (Meurre et al. 2008). At some critical point, the collapsing of gel disrupts the original orientation of inverted micelles and surplus amount of phospholipids in the surrounding leads to creation of a bilayer around the left over micelles forming a complete liposome (Turanek et al. 2003). In a medium of low ionic strength, an entrapment efficiency of 65 % can be achieved. The disadvantage of this method is that the molecules to be entrapped should be present in contact with organic solvent, therefore; very brittle molecules cannot be encapsulated. Sometimes, the sonication period may alter DNA helix if it has been encapsulated for gene delivery into liposomes or may also denature the

encapsulated proteins (Batzri and Korn 1973; Szoka and Papahadjopoulos 1978). Liposomes made up of 5-fluorouracil (Costa and Moraes 2003), diminazene aceturate (Oliveira et al. 2014), polyethylenimine/oligonucleotide (Ko and Bickel 2012), ferritin, albumin, insulin and alkaline phosphatase (Szoka and Papahadjopoulos 1978) have been synthesised by this method.

The injection method is further of two kinds namely ethanol and ether injection. This process is suitable for the formation of MLVs. The lipids are dissolved in ethanol/ether and then added to excess of aqueous buffer. If proper mixing of lipids does not happen with ethanol, a heterogeneous (30–110 nm) population of liposomes is obtained. The removal of entire ethanol from the solution is a complicated task as it forms azeotrope with water. In contrast, ether is immiscible with water, so it can be removed by gentle heating. The ether injection is much more time consuming than ethanol injection method (Batzri and Korn 1973; Deamer and Bangham 1976; Schieren et al. 1978). The ether injection method forms liposomal formulation with enhanced encapsulation efficiency. A modified version of ethanol method has been developed and named as inkjet method. This method controls the particle size and forms homogeneous population of liposomes (Hauschild et al. 2005). The chaos mastic gum (Gortzi et al. 2014), celestrol (Song et al. 2011), beclomethasone dipropionate and cytarabine (Jaafar-Maalej et al. 2010) and atenolol (Karn et al. 2011) have been entrapped using this method.

4.3.1.3 Detergent Removal

In this method of liposomal preparation, lipids in the micellar system are solubilised with the help of detergents like bile salts or alkylglycosides. The final concentration of detergents to be added should have high critical micellar concentration (CMC). All kinds of lipids below their transition temperature could be used for liposome formation (Shaheen et al. 2006). Only few of detergents viz., sodium cholate, sodium deoxycholate, alkyl glycoside and triton-X 100 are the most suitable for use in this method. The detergents are highly soluble in aqueous as well as organic media; thereby equilibrium is established between detergent molecules in water and lipids in micelles. The removal of detergents causes the formation of lipid bilayer. Faster the removal, smaller is the size of formed vesicles. The concentration of lipids and detergents used as well as the chemical nature of detergents decide the shape (unilamellar, oligolamellar and multilamellar) and size of formed liposomes (Wagner and Vorauer-Uhl 2011). The detergent removal from detergent-phospholipid mixtures is achieved by following approaches viz., dialysis, gel permeation chromatography and dilution.

The dialysis method was first reported by Kagawa and Racker in 1971. The detergents at their CMCs are used for solubilisation of lipids. After this, detergent is removed by dialysis. The dialysis bag containing mixture of lipids and detergents is kept in detergent free buffers. As the detergent gets detached, liposomes are formed (Shaheen et al. 2006). The cholate and/or deoxycholate are removed by dialysis from the mixture of protein–lipid which then leads to formation of vesicles containing proteins (Szoka 1980). This method is reproducible and produces a homogeneous population of vesicles (Bhai et al. 2012).

The size exclusion chromatography came into existence since long and is a well defined method for the separation of vesicles on the basis of their size (Holzer et al. 2009). By this technique, the detergent gets depleted. There are various latex molecules like Sephadex G-50, Sepharose 2B-6B and sephacryl S200-S1000 which are generally employed for the packing of column in gel filtration. The column prepared is pre-treated with empty liposomal solution so as to form a layer as these beads adsorb some amount of lipids onto them. The liposomes percolate through the interstitial spaces formed between the beads in accordance to their size. The liposomes thus separated out from the detergent monomers very efficiently when the flow rate is kept slow (Shaheen et al. 2006). Sometimes, the detergent is pre-removed from liposomes by dialysis and is then further subjected to gel exclusion chromatography to narrow down the size distribution.

Another method of detergent removal involves dialysis. The micellar solution containing phospholipids and detergent is diluted with buffer. Because of dilution, size of micelles and polydispersity of solution are greatly enhanced by virtue of which a spontaneous change occurs and monodisperse vesicles are formed (Akbarzadeh et al. 2013).

4.3.2 Active Drug Loading/ Encapsulation

In this mechanism of drug loading, drug molecules are encapsulated into vesicles which are already formed in nature. The empty liposome and solution containing drugs are merged together and incubated until a homogeneous solution is formed by diffusion of drug. The lipid bilayer is completely permeable for drugs to diffuse into liposome vesicles until an equilibrium stage is achieved inside and outside of liposomes. The amount of lipid bilayer decides how much and up to what extent a hydrophobic drug can enter (Brandl and Massing 2007; Li et al. 2007). The hydrophilic drugs remain into polar heads of vesicular bilayer but amphiphilic molecules suffer from a difficulty of retaining inside liposomes because they pervade very quickly from lipid bilayer. This technique holds good for weak amphipathic drugs which can cross the lipid bilayer in a neutral state (Li et al. 2007). Irinotecan hydrochloride (CPT-11) liposomes have been prepared by active loading technique. The lipids soybean phospholipids/cholesterol or hydrogenated natural soybean phospholipids/cholesterol have been dissolved in chloroform and prepared by sonication technique. The preformed liposomes and CPT-11 solution were kept for 10 min at 60 °C and the drug was encapsulated into it (Wei et al. 2013). In another study, liposomes of polystyrene$_{310}$-*b*-poly (acrylic acid)$_{36}$ have been prepared in which an anticancer drug doxorubicin was loaded actively. The permeability of liposomal wall was increased by use of plasticizer like dioxane. An acidic pH inside the vesicles was found to increase loading of drug by 10 times because the decrease in pH helped in concentrating the drug into liposomes (Choucair et al. 2005).

4.4 Methods of Preparation of Phytosomes

Methods employed for the synthesis of phytosomes deal with supercritical fluids, solvent evaporation and antisolvent precipitation techniques.

4.4.1 Supercritical Fluids

By the use of supercritical fluids (SCFs) method, particles of different size ranging from 5 to 200 nm can be prepared. Various SCFs have been employed for enhancing the solubility status and bioavailability of entrapped molecules viz., supercritical antisolvent method, antisolvent process, rapid expansion of supercritical solutions, solution enhanced dispersion by supercritical fluids (SEDS) and gas antisolvent technique (GAS) (Singh et al. 2014). In GAS, the supercritical antisolvent is poured individually to phospholipid and drug till a pressure of 10 mPa is reached. In SEDS, antisolvent and solution containing drug as well as phospholipids is kept in a precipitation unit under a reduced pressure of carbon dioxide. As compared to GAS, there is loss of crystallinity in SEDS method (Khan et al. 2013).

4.4.2 Solvent Evaporation

In this technique, the organic solvent contains both the drug and lipid together in the flask. The organic solvents used are ethanol and tetrahydrofuran. The reaction mixture is kept at an optimum time interval and temperature so that maximum drug entrapment can be achieved in the phytosomes formed. The organic solvent is then removed under reduced pressure via rotatory evaporator (Singh et al. 2014). Nimesulide is a potent drug but its use is limited because of its poor aqueous solubility, less bioavailability and

poor absorption. The phospholipid complex has been formed by dissolving the nimesulide and PC in dichloromethane (DCM) and their phytosomes have been formed (Semalty and Tanwar 2013). Curcumin (Gupta and Dixit 2011), luteolin-phospholipid complex (Sabzichi et al. 2014) mitomycin C-soybean (Hou et al. 2013) and embelin (Pathan and Bhandari 2011) loaded into PC phytosomes have also been prepared by this method.

4.4.3 Antisolvent Precipitation Technique

The basic principle is same as that of solvent technique. The only difference is that a solvent like n-hexane is used to precipitate out the conjugate of lipid and drug from the organic solvent in which they are dissolved. The solvent is then removed and is vacuum dried (Patel et al. 2009). Naringenin-PC phytosomes has been prepared by dissolving both of these into DCM and was further precipitated by adding n-hexane (Semalty et al. 2010b). Ellagic acid, an antioxidant was formulated with PC by this technique (Murugan et al. 2009).

4.5 Mechanism of Liposome and Phytosome Formation

Lipids by virtue of which liposomes are synthesised possess both hydrophilic as well as hydrophobic characters or are amphipathic. Two chains of fatty acid containing 10–24 carbon atoms with 0–6 double bonds per chain are known to complete the hydrophilic tail of lipids. The polarity of molecule is due to phosphoric acid moiety joined to a water molecule. On interaction with solvent, hydrophilic and hydrophobic parts of lipids reorient and then organise themselves into an ordered structure. If water is the solvent, then polar heads organise themselves towards aqueous environment and shields the inner hydrophobic core (Mansoori et al. 2012). It could be explained by citing an example of CMC of dipalmitoyl phosphatidyl choline. CMC value of dipalmitoyl phosphatidyl choline in water is 4.6×10^{-10} M, indicating its affinity for the hydrophobic environment while the free energy for transference from water to micelle is 15.3 kcal/mol. The large difference between free energy of water and hydrophobic environment explains the thermodynamic basis for formation of lipid bilayer i.e. by the assembly of lipids. The aggregated structure formed has the highest stability and lowest energy (Kant et al. 2012).

On the other hand, phytosomes are formed by stoichiometry reaction of natural phospholipids and natural plant product in a solvent of non-polar nature (Bombardelli et al. 1989). The formation of hydrogen bonds occurs between heads of phospholipids and functional groups of substrate as both are polar in nature. In addition to their lipophilic nature, they have a sharp melting point, soluble in non-polar solvents and can dissolve themselves in fats. Phytosomes when dissolved in water organise themselves into micelle like orientation (Karatas and Turhan 2015). Spectroscopic techniques are used to detect molecules attached to the head of membrane via chemical bonds (Bombardelli 1991; Bombardelli and Spelta 1991). For example, in catechindistearylphosphatidylcholine conjugate, hydrogen bonds have been formed between flavones (OH) and PC (PO_4^-) (Semalty et al. 2010a). PC can be determined by spectroscopic studies when compared to pure molecules. The signal for fatty acids remains unaltered. The long chain hydrocarbons surround the biomolecules, thereby forming a lipophilic layer protecting the polar parts of molecule and allow them to dissolve in solvents of low polarity (Bombardelli and Mustich 1991).

4.6 PhysicoChemical Characterisation of Liposomal and Phytosomal Formulations

The biological properties of liposomes and phytosomes have been determined by studying kinetics as well as dynamics of encapsulated materials in animal models (Franco and

Bombardelli 1998). Liposomal and phytosomal formulations offer much greater bioavailability and solubility than pure compounds (Dubey et al. 2007). There are many factors like size, type of encapsulated molecules; permeability and composition of the formulation are responsible to determine the behaviour of liposomes and phytosomes in biological media. Therefore, the physical characterisation is very important before their administration (Jain 2001). Various techniques used for characterisation of liposomes and phytosomes are scanning electron microscopy, atomic force microscopy, transmission electron microscopy, cryo-TEM, dynamic light scattering, measuring polydispersity index and zeta potential, and fourier transform infra-red spectroscopy. These techniques have been discussed in detail in Chap. 2. Few other techniques more precisely used for characterisation of liposomes and phytosomes are stated below.

Cryo-TEM is a technique widely accepted for understanding of materials which are quite complex (Almgren et al. 1996). This technique holds good advantage for characterisation of liposomes as these contain both hydrophobic as well as hydrophilic molecules into them. This technique helps in understanding the morphology of liposomes as well as changes which occur after encapsulation of molecules (Davidsen et al. 2005). The solution containing the sample is coated on grid which is further blotted by filter paper to remove excess of the sample and then vitrified by plunging into ethane or liquid nitrogen. The vitrified grid is placed on cryo-holder to visualise liposomal structure (Almgren et al. 2000). The rapid freezing is advantageous as it prevents the ice crystal formation and conserves the drugs or proteins encapsulated in their native form without any distortion. Thereby the details of sample morphology delivered by this technique are obtained in true form (Bibi et al. 2011).

Differential scanning calorimetry (DSC) is a very sensitive thermodynamic technique used to determine the hydrated phospholipid membranes and their transition temperature (T_c) (Chiu and Prenner 2011). This technique reveals how the chemical structure of lipids gets transformed to the thermodynamic behaviour, thus contributing to a change in their phases i.e. liquid-crystalline changes. The phase behaviour is important in determining fluidity, permeability, fusion and binding of molecules at membrane (Mozafari and Mortazavi 2005). It helps to determine the physicochemical parameters as well as stability of liposomes (Demetzos 2008). The basic principle that lies behind this technique is that it contains two cells where one cell acts as a reference cell while other as sample cell. The temperature of both the cells is raised uniformly by the power compensation unit. If a change occurs in the phase transition of sample, temperature of sample cell gets altered. Due to this, sample cell suffers from a temperature lag. Finally, the value of power which keeps both the cells at same temperature is measured. The excess heat capacity is calculated by the extra amount of heat required by sample cell to be at the same temperature as that of reference cell. A graph of heat capacity vs temperature can be obtained and finally T_c and changes in enthalpy are calculated (Chiu and Prenner 2011). As liposomes are amphipathic in nature, they undergo changes at a temperature below their melting point. These changes are contributed by number of factors like length of hydrocarbon chain, presence of acyl and methyl groups, polarity of molecule and ionic strength (Taylor and Morris 1995). All these factors change T_c of liposomes. It has been found that low phase transition temperature holds a good place for liposomes to act as a good delivery vehicle for molecules whose release rate is intended to be faster (Betz et al. 2005). Phytosomes of diosmin (a flavanoid) encapsulated into soybean phospholipids (Freag et al. 2013), mitomycin C into soybean phosphatidylcholine (Hou et al. 2013) have also been assessed for their thermal behaviour using DSC.

Nuclear magnetic resonance (NMR) is another technique used to exploit the fluidity and lamellarity of liposomes. It reveals about physical nature of molecules and how do they affect the phospholipid bilayer. This technique enables the estimation of soluble molecules being encapsulated and does not determine the non-soluble part of molecule (Peleg-Shulman et al. 2001). NMR is used to study the order of

chain, sugar backbone and phosphate groups of phospholipid bilayer. The lamellarity in terms of number of lipid bilayers surrounding the core can be evaluated by comparing the intensity of signals of outer layer and total signals (Yamauchi et al. 2007). The naringenin–phospholipid complex phytosomes have been characterised using NMR which showed their interaction with each other (Semalty et al. 2010b). NMR spectroscopy of embelin and embelin complexed with soya phosphatidylcholine has shown that phenylhydroxyl part of embelin was complexed with lipid (Pathan and Bhandari 2011).

4.7 Surface Modifications of Liposomes and Phytosomes

Liposomes have been used in various imaging and diagnostic techniques. The conventional liposomes possess very short half life and are considered as foreign antigens due to which they are easily cleared from reticuloendothelial system (RES) of body and experience opsonisation (Immordino et al. 2006). Thus, a need was felt to modify the surface of liposomes so that they will have a better half life and long RT in blood stream. Numerous approaches have been employed to change the size and surface charge of liposomes. The stepping stone towards making liposomes stealth in nature was their modification by use of natural polymers like pullulans and dextrans (gangliosides) which were then surmounted by PEG (Nag and Awasthi 2013). After surface binding, PEG did not provide any further space for binding of opsonins on to liposomes, thereby, preventing liposomal removal by RES (Drummond et al. 1999). The cholesteryl–PEG has also been used where PEG was anchored to cholesterol. The use of cholesterol increases hydrophilicity and stabilises liposomal membrane (Kirby et al. 1980). Liposomes coated with mucin (sugar chain) have been prepared for the delivery of insulin by virtue of which insulin was prevented from degradation in gastrointestinal tract, thus increased its stability and resulted in slow and sustained release (Iwanaga et al. 1997). To increase RT of calcitonin in body, the surface charge of liposomes was amended using carbopol (negative charge) and chitosan (positive charge). The carbopol has imparted negative charge and provided a better adherence to liposomes (Takeuchi et al. 2003). The liposomes coated with polydopamine have also provided mucoadhesivity for internalisation of a lipophilic compound from the surface of cells (Lynge et al. 2011). Oral administration of eudragit S-100 coated atenolol liposomes has paved a way for better residence time and bioavailability of drug. They have possessed a bigger size than uncoated liposomes and better encapsulation efficiency (Karn et al. 2011).

The surface modification of phytosomes can be attained by applying their surface with some hydrophilic, mucoadhesives or stabilising agents like surfactants (Tiwari et al. 2012). The surface coatings bring a change in zeta potential i.e. overall charge, hydrophobicity, and their mucilage and protein adsorption activity which plays an important role in the uptake of phytosomes. The phytochemicals lack good absorption and RT in gastrointestinal tract (Gunasekaran et al. 2014). For this purpose, mitomycin C loaded into soybean phosphatidylcholine phytosomes has been surface modified using folate-PEG so as to have targeted delivery and improved therapy in HeLa cells. The surface modified phytosomes have shown enhanced cellular uptake and better anticancer activity (Li et al. 2014).

4.8 Targeting Mechanism of Liposomes and Phytosomes

4.8.1 Active Targeting

Active targeting is the targeting of cells by knowing specific receptors present on their surface and by the expression of specific proteins of cells. This is generally done to reduce the off-target effects. The active targeting aims to move liposomes to the desired organ, either it is a cell or a tissue; before its contents are released. The surface is modified in such a way that liposome moving towards target forms a lock and key so that it can be restricted at the target site

only (Cirli and Hasirci 2004). To attain this, various surface modifications of liposomes are being done. Liposomes for active targeting are attached with various moieties like antibodies, ligands and peptides (Byrne et al. 2008). Further, the use of some external factors like light, laser, ultrasound and local environment near the targeted tissue also help to release the contents from liposomes only at tumor site (Pitt and Husseini 2008). Liposomes which are pH and heat sensitive have been coated with antibodies for active targeting. Photosensitivity is one of the parameters exploited for targeted release of molecules from liposomes. Photosensitive liposomes have been prepared by joining photolabile lipids and retinoids into lipid bilayer. On exposure to gamma rays or ultraviolet rays, these photosensitive components destabilise the liposomal membrane and causes release of contents (Miller et al. 2000). A similar example was found when gold NPs were embedded into liposomes and release of calcein was seen in human retinal pigment epithelial cells. The gold NPs absorb light energy upon exposure to UV rays, and cause a thermal change in lipid bilayer, which further releases calcein into cells. No release was seen without exposure to UV rays (Paasonen et al. 2010). pH sensitive liposomes are another type of liposomes that has been constructed to enhance the intracellular delivery of bioactive molecules. The fact lies that they are stable at pH 7 and when exposed to some acidic environment, they get disrupted and thus release the aqueous contents. Liposomes made up of PC and oleyl alcohol loaded with cytosine β-D-arabinofuranoside (araC) have been examined against KB cell lines for intracellular delivery of molecules. KB (epidermal carcinoma) cells express folate receptors on them, thus liposomes were targeted onto cells. The results showed that araC was released into cells approximately 17 times higher as compared to non pH sensitive liposomes (Sudimack et al. 2002). Gelonin, is a well-known antitumor molecule which arrests ribosomes, thus truncating the synthesis of protein. It suffers from a major drawback that it cannot pass through plasma membrane. If it does so, it gets break down within endosomes. Thus, gelonin along with listeriolysin O (helps in flee of gelonin from endosomes to cytosol) have been encapsulated into pH sensitive liposomes. They were checked against B16 melanoma cell line and showed remarkable cytotoxic effects of gelonin as compared to gelonin alone and gelonin encapsulated without listeriolysin O (Provoda et al. 2003). For active targeting, another strategy has been investigated that involved binding of some specific ligands on the surface of liposomes. pH sensitive liposomes made up of 1,2-dioleoyl-sn-glycero-3-phosphoethanolamine and oleic acid have been coated with anti-H-2K^k antibody and showed better effectiveness in releasing their contents than the ones which did not possess antibody on their surface (Connor and Huang 1986). Anti-BCG (bacillus calmatte-guerin) antibodies were attached on liposomes modified with succinylated polyglycidol for better internalisation. These liposomes have been examined against mouse carcinoma expressing BCG on them. These liposomes have been found to recognise their target cells and transferred their content to cytoplasm (Mizoue et al. 2002). The surface functionalised phytosomes of mitomycin C with folate-PEG have been targeted to HeLA cell and showed better efficacy under in vitro as well as in vivo conditions (Li et al. 2014).

4.8.2 Passive Targeting

Passive targeting is the delivery of drug molecules into body dependent upon the longevity of desired molecule in the systemic circulation and its accumulation at pathological site. It aims at normal distribution of liposomes in body in accordance to their own fate. The tumor blood vessels have leaky nature due to which various nanosized drug delivery vehicles enter the interstitial space after crossing endothelium lining of cells. The normal endothelium has size range of 5–10 nm while it varies from 100 to 780 nm depending upon different cancer types (Haley and Frenkel 2008). In solid tumors, there is very less amount of proper lymphatic clearance leading to accretion of nano-vehicles and

macromolecules at tumor site. This occurrence is termed as enhanced permeability and retention (EPR) effect that is an important strategy used for targeting of liposomes at tumor spot (Torchilin 2011). Small molecules possessing the low molecular weight stays for longer duration at tumor site. The targeting of drugs is a major issue which is totally dependent on patho-physiological properties of the tumor spot and is termed as passive drug targeting (Deshpande et al. 2013). The more number of times blood passes through target, more is the EPR effect and it increases the interaction of liposomes with target cell (Torchilin 2010). The amassing of liposomes is dependent upon the size of endothelial walls and capillaries, thus the size of liposomes should be less than 400 nm (Danhier et al. 2010). Doxorubicin loaded liposomes have been coated with polyvinyl alcohol and hydroxypropyl methylcellulose and therefore, depicted higher drug dose at tumor spots in tumor exhibiting rats (Takeuchi et al. 2001). Liposomes containing anti-TB (tuberculosis) drug has been administered intravenously and found effective against extra-pulmonary TB treatment compared to free drug (Pinheiro et al. 2011). Phytosomes loaded with luteolin can sensitise MDA-MB 231 (breast cancer cells) to doxorubicin and thus helps in passive targeting of drug towards these cells (Sabzichi et al. 2014). Luteolin inhibits Nrf2 pathway and sensitises the agents possessing chemotherapeutic properties.

4.9 Medical Applications of Liposomes and Phytosomes

The liposomal applications are widely exploited in research, industry, pharmacology and medicine depending upon the types of drugs and molecules encapsulated into them. With the advances in liposomal design, these are widely used as carriers in diagnostics, imaging and tissue regeneration, as a tool in drug delivery and in prevention of body from the attack of microbes because of slow release of encapsulated molecules from them. The phytosomes of various molecules possessing antioxidant and anticancer potentials have been explored for their drug delivery.

4.9.1 Diagnostics and Imaging

Nowadays, liposomes are engineered in such a way that they can effectively deliver drug and various imaging agents to diseased site to be further detected by imaging systems (Petersen et al. 2012). The passive targeting of liposomes is being exploited for the delivery of imaging agents to liver and spleen. Liposomes containing aqueous contrasting agents are used to assess the differences between tumor and non-tumor tissue and are further detected by computational tomography (CT) (Seltzer 1988). Ultrasound imaging and magnetic resonance imaging (MRI) are important tools for diagnostics and are done by liposomes filled with gas. The gas in these liposomes is able to reflect sound waves thus contributing to Doppler's effect. Adzamli et al. (1990) have successfully used 1,2-distearoyl-sn-glycero-3-phosphocholine liposomes encapsulating gas for echocardiography. The gas bubbles as contrast agent helps in sensitisation of liposomes to ultrasounds. The liposomes become highly echogenic because the gas provides oscillatory effects to liposomes on application of some external acoustic waves (Kheirolomoom et al. 2007). Several iodinated contrast agents have been trapped into liposomes and are used for CT. During CT, the contrast agents opacify liver and spleen tissues (Seltzer et al. 1988). Liposomes made on the basis of various agglutination tests TB/M card test and TB screen tests have been used for the detection of antigen or anti-glycolipid antibodies (Bisen et al. 2005). An assembly of liposomes has been prepared by attaching non-covalently linked DNA in solution. These liposomes on interaction with complementary strands of DNA form aggregates. These aggregates then get disintegrated on heating and show very critical thermal change which helps in the detection of single nucleotide polymorphism (Jakobsen and Vogel

2009). Various contrasting agents have been inserted into paramagnetic liposomes and are employed for in vitro and in vivo imaging. MRI active liposomes have been prepared by adding gadolinium (Gd) as contrast agents into lipid bilayer or by inserting contrast agents into the aqueous core of liposomes and these are used for tracking of cells (Oliver et al. 2006). Kabalka et al. (1988) reported that liposomes containing Gd cause an ample amount of increase in MRI signal intensity and holds a good place for imaging liver, spleen, bone marrow and all other organs which have an increased macrophage activity in them. The encapsulation of MRI agent Gd into liposomes core, and its development as antibody targeted liposomes have been made for imaging purpose (Ayyagari et al. 2006; Erdogan et al. 2006). Surface of liposomes have been modified with arginine-glycine-aspartate (RGD) tripeptides and targeted towards the walls of cancer cell of tumor bearing mice. MRI in combination with fluorescence microscopy has been used to image angiogenesis of these cells which was detected by enhanced expression of $\alpha_2\beta_2$ integrins (Mulder et al. 2005). ^{99}Tc-labelled liposomes have been used in replacement of red blood cells and in detection of some internal bleeding sites and internal clotting sites. These liposomes have been reported as safe for use and have higher efficiency (Torchilin 1995).

4.9.2 Drug Delivery

There are many drugs used to treat cancer but they are non specific in nature and sometimes kill the nearby healthy cells (Sunderland et al. 2006). Cancer cells possess several unique properties and exploiting these properties liposomes can be emerged as an important nanomaterial for the delivery of various molecules. Liposomes have a wide regime in encapsulating and delivering anticancer drugs. Various drugs like doxorubicin, methotrexate and cisplatin are less soluble in water but have high anticancer activities. These drugs have been encapsulated into liposomes. The liposomes have a long circulation time and are used for both active and passive targeting of anticancer drugs (Franciullino and Ciccolini 2009). Doxorubicin HCl encapsulated into liposomes is the first commercialised product that came into existence in 1995 for cancer treatment (Bogner et al. 1994). The inclusion of antitumor drugs into liposomes has caused a decrease in the concentration of drug and thereby, reduced the toxicity of free drug in blood stream. Due to increase in vasculature size of blood capillaries, liposomes get accumulated at tumor site. Melphalan and methotrexate, anticancer drugs attached to rac-1,2-dioleoylglycerol have been entrapped into liposomes made up of PC and phosphatidylinositol and evaluated under in vitro conditions. Liposomes containing methotrexate have helped in overcoming the resistance of tumor cells to drug i.e. multiple drug resistance effect (Vodovozova et al. 2008). Cisplatin, an anticancer drug possesses a great potential to treat head, neck and various kinds of solid tumors. The drug has been encapsulated into phospholipid bilayer of liposomes and tested in ovarian carcinoma cell line which shows improved cytotoxicity as compared to pure drug. This was explained on the fact that drug encapsulated in the shell of liposomes was protected from disintegration by enzymes and hence demonstrated a better efficacy (Kroon et al. 2005). Various liposomes encapsulating doxorubicin, daunorubicin and cytarabine have been used to cure metastatic ovarian cancer, acute myeloid leukaemia and leukaemia with meningeal spread, respectively (Glantz et al. 1999; Latagliata et al. 2008; Markman et al. 2010). The human ovarian cancer developed in nude mice model has been treated with paclitaxel loaded liposomes whose surface was modified with RGD peptide had shown inhibition in growth of tumor cells (Zhao et al. 2009).

There are various polyphenols whose bioavailability has been improved by exploiting the likeness of phenolics to phospholipids. Due to this, a conjugate of precise stoichiometry is formed with the capacity to cross biological membranes and is soluble in intestinal layer. So, phytosomes of various polyphenols have been prepared (Kidd 2009). Compared to the conventional plant extracts and their products,

phytosomes have been found to be better in efficacy as well as in therapy (Tedesco et al. 2004). Silymarin is an important molecule having a wide potential in hepatoprotectivity. But its use is limited because of its low bioavailability, absorption and solubility. To overcome the above said problems, its phytosome has been prepared. An adduct of silymarin has been formed with phospholipids (La Grange et al. 1999). By the use of silymarin phytosomes, rat foetuses were protected against ethanol-induced toxicity (Busby et al. 2002), the broiler chicks were also found to be safe against aflatoxin B1 (Tedesco et al. 2004) and the serum ferritin levels got reduced in the chronic hepatitis C patients (Bares et al. 2008). The increase in solubility can be accounted on the basis of binding of silymarin to the polar head of phospholipids (Bilia et al. 2014). Silibin, an antioxidant isolated from milk thistle is a polyphenol flavonolignan. It is an active constituent of silymarin. The prostate cancer patients were treated with silibin phytosomes to check its level in blood and tissues. The patients were administered with silibin phytosomes for 20 days before the operation which showed that oral dose of silibin had achieved its higher concentration in blood (Flaig et al. 2010). The comparative effect of silibin and its phytosomes has been checked in humans by an oral administration of a dose of 360 mg. Phytosomal silibin was observed to be absorbed at 4–6 times higher than non-phytosomal silibin. Silibin phytosomes lower the enzymes level produced by liver and resulted in improvement of symptoms of cirrhosis and hepatitis caused by viruses (Kidd 2009).

Curcumin is a polyphenol derivatised from turmeric. It has the potential to fight against cancer and aid in chemotherapy. The bioavailability and poor absorption limits the use of curcumin. The phytosomes prepared were given to mice through gavage and showed higher level of curcumin in rat plasma and liver as compared to non-phytosomal curcumin (Marczylo et al. 2007; Shehzad et al. 2010). The phytosomes of curcumin were checked for their transdermal penetration. The phytosomal curcumin showed 60 % increase in distribution than pure curcumin (Zaveri et al. 2011). The phytosomal curcumin showed better bioavailability in topical formulation proving its better anti-ageing and antioxidant properties (Gupta and Dixit 2011).

Catechins are present in green tea and possess different properties like cardioprotectivity, neuroprotectivity, antioxidant and anticancer activity in nature (Kidd 2009). However, their low bioavailability limits its translation into clinics. The decaffeinated catechin extract and the one in phytosomes were checked and after 6 h, phytosomal catechin concentration in blood was found to be almost double than pure extract (Barzaghi et al. 1990). A phytosome carrying catechin more than 400 mg is good enough to stop atherosclerosis and angiogenesis and it blocks vascular endothelial growth factors (Neuhaus et al. 2004). A dose of 135 mg/day catechins administered for two weeks in humans, revealed that vitamin D and poly unsaturated fatty acids (PUFA) levels in blood rises which make RBCs less prone towards oxidation (Pietta et al. 1998).

The grape seed extract being antioxidant in nature has been used to form phytosomes. A dose of 110 mg/day of phytosome given for 30 days revealed the enhanced level of α-tocopherol in RBCs in addition to higher PUFA levels. It has been found that these phytosomes reduce the oxidative stress in body (Wang et al. 2008). These phytosomes have been found to enhance the pumping of heart, and increase prostacyclins into blood circulation. Phytosomes bind to lumens of endothelial cells, and render protection from oxidative stress (Carini et al. 2001). The phytosomes prepared from different phytoconstituents are tabulated in Table 4.1.

4.9.3 Tissue Regeneration

Tissue engineering or regenerative medicine lays stress on recent technological developments to make tissues functional in such a way that it repairs or replaces the tissue already worn out due to some injury or disease. Nowadays, the alterations in cell behaviour like adhesion, locomotion, contraction and cytoskeletal movements are being carried out by nanomaterials which

Table 4.1 List of phytosomes prepared

Phytosome	Phytoconstituent (source)	Uses	References
Silybin	*Silymarin marianum* (Milk thistle)	Hepatoprotective, antioxidant	Kidd and Head (2005)
Curcumin	*Curcuma longa*	Antioxidant, anti-inflammatory, anticancer	Marczylo et al. (2007)
Ginkgo	*Ginkgo biloba*	Antioxidant, neurocognitive	Naik et al. (2006)
Green tea catechin	*Camellia sinensis*	Neuroprotectant, cardioprotectant, helps in weight loss	Pietta et al. (1998)
Quercetin	Fruits, vegetables	Antioxidant, antimicrobial, anticancer	Rasaie et al. (2014)
Ginseng	Panax ginseng	Immunomodulator	Karimi et al. (2015b)
Naringenin	*Citrus paradise, Lycopersicum esculentum*	Antitumor, anti-estrogenic	Semalty et al. (2010b)
Resveratrol	Mulberry, peanuts, grapes	Antioxidant, anti-ageing, neuroprotective	Ma et al. (2014)
Grape seed	*Vitis vinifera*	Antioxidant, nutraceutical	Kidd (2009)

have in turn increased their usage in regeneration and orthopaedic repair. The nanofibrous structures have proved to be well-known material to bring changes in bone in accordance to the scaffold material used (Nair and Laurencin 2008). Gene transfer by means of liposomes is an effective measure for regeneration of both dermal as well as epidermal tissue layers of skin. The biological as well as chemical structures of liposomes contribute to their regenerative properties (Jeschke et al. 2005). Injectable thermo-liposome hydrogels contain crosslinking agents which act as scaffold for regeneration of bones or repair of wounded skin tissues. The crosslinking agents kept in polymer solution cannot diffuse out of thermo-liposomes at room temperature. Whenever there is an injury, the temperature rises at the wound site because of inflammation. The rise in temperature causes transformation from sol to gel form and causes release of crosslinking agents (Sudahakar et al. 2015).

In rats, repair of tooth sockets has been evaluated by administrating liposomes containing various growth factors like insulin growth factor and platelet derived growth factor and a mixture of both the growth factors. The production of osteocalcin and vascular endothelial growth factor has confirmed the enhancement in repair of socket bone (Abreu et al. 2013). Liposome encasing buflomedil hydrochloride has been topically applied to wounds in normal and ischemic mice. These have ameliorated the healing process in both the groups of mice. The regeneration has been confirmed by neovascularisation and formation of epithelium at wounded site (Roesken et al. 2000). The human mesenchymal stem cells have been cultured with liposomal magnetic particles with a magnet placed with them. Under the effect of magnetic field, these cells were found to form multilayered cell sheets and were layered on ischemic tissues of nude mice. While for control, the magnetised cell was administered via conventional needle method. These sheets have demonstrated an increment in angiogenesis as well as in preserving the tissues in ischemia (less amount of apoptosis) as compared to control (Ishii et al. 2011).

Dihydroquercetin (plant flavonoid), an antioxidant in conjugation with glycine has been encapsulated into lecithin liposomes and was assessed against healing of burns. The antioxidants did not allow the rise in any reactive oxygen species in cells and thus the same level of proteins, uric acid and α-tocopherol is maintained. This formulation was found to be attributed towards reduction of inflammation, necrosis and deepened the formation of oil glands and hair follicles at burnt site (Naumova and Potselueva 2010).

4.9.4 Antimicrobial Activity

There are several types of antimicrobial agents being used to kill various kinds of pathogens like bacteria, fungi, virus, nematodes and actinomycetes. They have high therapeutic index but their improper dosage at delivery site may cause various side effects like irritation, inflammation, peeling of skin and reduction in natural flora of body. To minimise the abovementioned side effects, antimicrobial agents have been encapsulated into liposomes (Zhang et al. 2010). The mechanism of their entry is endocytosis through which they get internalised and release their contents to inactivate the infections caused by microorganism (Zhang et al. 2008). *Pseudomonas aeruginosa* is the causative agent for cystic fibrosis. The liposomal formulation containing gentamycin has been examined for minimum inhibitory concentration (MIC) and was found to be more potent than free gentamycin. The reason for its better efficacy was due to enhanced penetration of liposome containing gentamycin into bacterial cells (Rukholm et al. 2006). Similar results have been found for LUV liposomes containing ceftazidime and cefepime (Torres et al. 2012). The MIC of various organisms like *Staphylococcus aureus*, *Klebsiella* sp. and *Escherichia coli* has been checked by liposomes containing a cyclic dipeptide named as cyclo(L-tyrosyl-L-prolyl) (cyclo(Tyr-Pro)). These liposomal formulations were found to be more effective than free drugs and also trounce over bacterial resistance (Kilian et al. 2011).

The plant extract of *Origanum dictamnus* encapsulated into liposomes has been seen for its antimicrobial activity against *Candida albicans* and was more effective than pure methanolic extract (Gortzi et al. 2007). Magallanes et al. (1993) have encapsulated aminoglycoside antibiotics like gentamycin and streptomycin and used to cure mice and pigs infected with *Brucella* sp. Liposomal linolenic acid formulation has increased bacterial cell death and showed better in vivo effects in gastritis ulcers caused by *Helicobacter pylori* (Jung et al. 2015). The human skin dermis provides a surface for fixation of *Pseudomonas aeruginosa* on to it. The liposomes containing amikacin, ciprofloxacin or polymyxin B has been used to treat such skin surfaces; helping in elimination of all the attached microbes and thereby cleaning the whole skin dermis (Trafny et al. 1999).

4.10 Conclusions

Both liposomes and phytosomes are made up of phospholipids and can encapsulate wide variety of molecules into them. Despite possessing common features like decrease in dosage and enhanced RT, they are unique to one another. The phytosomes formation occurs at molecular level by joining two molecules such as PC and polyphenol. The molecule in phytosomes is said to be very near to PC as it forms a quasi-stable bond and thus the molecule entrapped forms an integral part of membrane. The molecule thus marked as lipid as well as water soluble, thus helps in the transport from watery environment of intestine to cell membrane of enterocytes which is lipophilic in nature. The liposomes are spherical bodies formed of hundreds of phospholipids in which a molecule is entrapped into the core of sphere. The molecule does not form any bonds rather it is physically entrapped. The phytosomes hold a promising place in oral delivery of molecules and have better absorption while it does not hold good for liposomes. The liposomes and phytosomes serve as potent delivery systems by increasing the therapeutic index of encapsulated molecules. These formulations are developed as they are safer in use than existing drugs. Thus, these formulations can serve as better targeting agents and can deliver encapsulated drugs at specific sites, thereby proving promising candidates in various medical fields for enhancing health regimen of an individual.

Acknowledgments We are grateful to Director, CSIR-IHBT for providing valuable suggestions. Financial assistance in the form of project grant BSC-112 from the Council of Scientific and Industrial Research (CSIR), Government of India is truly acknowledged. AG and RS are thankful to Academy of Scientific and Innovative Research (AcSIR).

References

Abreu FA, Ferreira CL, Silva GA et al (2013) Effect of PDGF-BB, IGF-I growth factors and their combination carried by liposomes in tooth socket healing. Braz Dent J 24:299–307

Adzamli IK, Seltzer SE, Slifkin M et al (1990) Production and characterization of improved liposomes containing radiographic contrast media. Invest Radiol 25:1217–1223

Akbarzadeh A, Rezaei-Sadabady R, Davaran S et al (2013) Liposome: classification, preparation, and applications. Nanoscale Res Lett 8:1–9

Almgren M, Edwards K, Gustafsson J (1996) Cryotransmission electron microscopy of thin vitrified samples. Curr Opin Colloid Interface Sci 1:270–278

Almgren M, Edwards K, Karlsson G (2000) Cryo transmission electron microscopy of liposomes and related structures. Colloid Surface A 174:3–21

Amin T, Bhat SV (2012) A review on phytosome technology as a novel approach to improve the bioavailability of nutraceuticals. IJOART 1:43–57

Athira PP, Aswathy P, Nair Athira J et al (2014) Exploring potential of Planterosome as a novel Drug delivery system. Reviewing decades of research. Int Res J Pharma 5:254–258

Ayyagari AL, Zhang X, Ghaghada KB et al (2006) Long circulating liposomal contrast agents for magnetic resonance imaging. Magn Reson Med 55:1023–1029

Bangham AD, Hill HW, Miller NGA (1974) Preparation and use of liposomes as models of biological membranes. In: Korn ED (ed) Methods in membrane biology, vol 1. Springer, US, pp 1–68

Barenholz Y (1996) Optimization of amphiphile-based colloidal carriers. In: Barenholz Y, Lasic DD (eds) Handbook of Nonmedical Applications of Liposomes, vol 3. CRC Press, Boca Raton, p 101

Bares JM, Berger J, Nelson JE et al (2008) Silybin treatment is associated with reduction in serum ferritin in patients with chronic hepatitis C. J Clin Gastroenterol 42:937–944

Barzaghi N, Crema F, Gatti G et al (1990) Pharmacokinetic studies on IdB 1016, a silybin- phosphatidylcholine complex, in healthy human subjects. Eur J Drug Metab Pharmacokinet 15:333–338

Batzri S, Korn ED (1973) Single bilayer liposomes prepared without sonication. Biochim Biophy Acta 298:1015–1019

Betz G, Aeppli A, Menshutina N et al (2005) *In vivo* comparison of various liposome formulations for cosmetic application. Int J Pharm 296:44–54

Bhai SA, Yadav V, Mamatha Y et al (2012) Liposomes an overview. JPSI 1:13–21

Bhattacharya S (2009) Phytosomes: The new technology for enhancement of bioavailability of botanicals and nutraceuticals. Int J Health Res 2:2–25

Bibi S, Kaura R, Henriksen-Laceya M et al (2011) Microscopy imaging of liposomes: From coverslips to environmental SEM. Int J Pharm 417:138–150

Bilia AR, Isacchi B, Righeschi C et al (2014) Flavonoids loaded in nanocarriers: an opportunity to increase oral bioavailability and bioefficacy. Food Nutr Sci 5:1212–1227

Bisen PS, Prasad GBKS, Zacharia A et al (2005) Liposomes in diagnosis of tuberculosis. Adv Biomed Res 381–400

Bogner JR, Kronawitter U, Rolinski B et al (1994) Liposomal doxorubicin in the treatment of advanced AIDS related Kaposi sarcoma. J Acquir Immune Defic Syndr 7:463–468

Bombardelli E (1991) Phytosome: A new cosmetic delivery system. Boll Chim Farm 130:431–438

Bombardelli E, Mustich G (1991) Bilobalide phospholipid complex, their uses and formulation containing them. U.S. Patent US EPO-275005

Bombardelli E, Spelta M (1991) Phospholipid-polyphenol complexes: a new concept in skin care ingredients. Cosmet Toiletr 106:69–76

Bombardelli E, Curri SB, Della RL et al (1989) Complexes between phospholipids and vegetal derivatives of biological interest. Fitoterapia 60:1–9

Brandl M, Massing U (2007) Vesicular phospholipid gels. In: Gregoriadis G (ed) Liposome technology liposome preparation and related technique, 3rd edn. Informa Healthcare Inc, USA, pp 241–260

Busby A, La Grange L, Edwards J et al (2002) The use of a silymarin/phospholipid compound as a fetoprotectant from ethanol-induced behavioral deficits. J Herb Pharmacother 2:39–47

Byrne JD, Betancourt T, Brannon-Peppas L (2008) Active targeting schemes for nanoparticle systems in cancer therapeutics. Adv Drug Del Rev 60:1615–1626

Carini M, Stefani R, Aldini G et al (2001) Procyanidins from Vitis vinifera seeds inhibit the respiratory burst of activated human neutrophils after lysosomal enzyme release. Planta Med 67:714–717

Chiu MH, Prenner EJ (2011) Differential scanning calorimetry: An invaluable tool for a detailed thermodynamic characterization of macromolecules and their interactions. J Pharm Bioallied Sci 3:39–59

Choucair A, Soo PL, Eisenberg A (2005) Active loading and tunable release of doxorubicin from block copolymer vesicles. Langmuir 21:9308–9313

Cirli OO, Hasirci V (2004) UV-induced drug release from photoactive REV sensitized by suprofen. J Control Rel 96:85–96

Connor J, Huang L (1986) pH-sensitive immunoliposomes as an efficient and target-specific carrier for antitumor drugs. Cancer Res 46:3431–3435

Costa CAM, Moraes AM (2003) Encapsulation of 5-fluorouracil in liposomes for topical administration. Acta Sci Technol 25:53–56

Craciunescu O, Gaspar A, Trif M et al (2014) Preparation and characterization of a collagen-liposome-chondroitin sulfate matrix with potential application for inflammatory disorders treatment. J Nanomater 2014:1–9

Danhier F, Feron O, Preat V (2010) To exploit the tumor microenvironment: Passive and active tumor targeting

of nanocarriers for anticancer drug delivery. J Control Rel 148:135–146

Davidsen J, Rosenkrands I, Christensen D et al (2005) Characterization of cationic liposomes based on dimethyldioctadecylammonium and synthetic cord factor from *M. tuberculosis* (trehalose 6,6'-dibehenate)-a novel adjuvant inducing both strong CMI and antibody responses. Biochim Biophys Acta 1718:22–31

Deamer D, Bangham AD (1976) Large volume liposomes by an ether vaporization method. Biochim Biophys Acta 443:629–634

Demetzos C (2008) Differential Scanning Calorimetry (DSC): a tool to study the thermal behavior of lipid bilayers and liposomal stability. J Liposome Res 18:159–173

Deshpande PP, Biswas S, Torchilin VP (2013) Current trends in the use of liposomes for tumor targeting. Nanomedicine NBM 8:1509–1528

Drummond DC, Meyer O, Hong K et al (1999) Optimizing liposomes for delivery of chemotherapeutic agents to solid tumors. Pharmacol Rev 51:691–743

Dua JS, Rana AC, Bhandari AK (2012) Liposome: methods of preparation and applications. IJPSR 3:14–20

Dubey D, Shrivastava S, Kapoor S (2007) Phytosome: a novel dosage structure

Erdogan S, Roby A, Sawant R et al (2006) Gadolinium-loaded polychelating polymer-containing cancer cell-specific immunoliposomes. J Liposome Res 16:45–55

Flaig TW, Glode M, Gustafson D et al (2010) A study of high-dose oral silybin-phytosome followed by prostatectomy in patients with localized prostate cancer. Prostate 70:848–855

Franciullino R, Ciccolini J (2009) Liposome-encapsulated anticancer drugs: still waiting for the magic bullet? Curr Med Chem 16:4361–43771

Franco PG, Bombardelli E (1998) Complex coppouns of bioflavonoids with phospholipids, their preparation and uses and pharmaceutical and cosmetic compositions containing them. U.S. Patent EPO 275005

Freag MS, Elnaggar YSR, Abdallah Ossama Y (2013) Lyophilized phytosomal nanocarriers as platforms for enhanced diosmin delivery: Optimization and *ex vivo* permeation. Int J Nanomed 8:2385–2397

Glantz MJ, LaFollette S, Jaeckle KA et al (1999) Randomized trial of a slow-release versus a standard formulation of cytarabine for the intrathecal treatment of lymphomatous meningitis. J Clin Oncol 17:3110–3116

Gomez-Hens A, Fernández-Romero JM (2006) Analytical methods for the control of liposomal delivery systems. Trends Analyt Chem 25:167–178

Gortzi O, Lala S, Chinou I et al (2007) Evaluation of the antimicrobial and antioxidant activities of *origanum dictamnus* extracts before and after encapsulation in liposomes. Molecules 12:932–945

Gortzi O, Athanasiadis V, Lalas S et al (2014) Study of antioxidant and antimicrobial activity of chios mastic gum fractions (neutral, acidic) before and after encapsulation in liposomes. J Food Process Technol 5:355

Gunasekaran T, Haile T, Nigusse T et al (2014) Nanotechnology: an effective tool for enhancing bioavailability and bioactivity of phytomedicine. Asian Pac J Trop Biomed 4:S1–S7

Gupta NK, Dixit VK (2011) Bioavailability enhancement of curcumin by complexation with phosphatidyl choline. J Pharm Sci 100:1987–1995

Hadian Z, Sahari MA, Moghimi HR et al (2014) Formulation, characterization and optimization of liposomes containing eicosapentaenoic and docosahexaenoic acids: a methodology approach. Iran J Pharm Res 13:393–404

Haley B, Frenkel E (2008) Nanoparticles for drug delivery in cancer treatment. Urol Oncol 26:57–64

Hauschild S, Lipprandt U, Rumplecker A et al (2005) Direct preparation and loading of lipid and polymer vesicles using inkjets. Small 1:1177–1180

Himanshu A, Sitasharan P, Singhai AK (2011) Liposomes as drug carriers. IJPLS 2:945–951

Holzer M, Barnert S, Momm J et al (2009) Preparative size exclusion chromatography combined with detergent removal as a versatile tool to prepare unilamellar and spherical liposomes of highly uniform size distribution. J Chromatogr A 1216:5838–5848

Hope MJ, Nayar R, Mayer LD et al (1993) Reduction of liposome size and preparation of unilamellar vesicles by extrusion techniques. In Gregoriadis (ed) Liposome Technology 3rd edn. CRC Press, Boca Raton, pp 123–$_{139}$

Hou Z, Li Y, Huang Y et al (2013) Phytosomes loaded with mitomycin C-soybean phosphatidylcholine complex developed for drug delivery. Mol Pharmaceutics 10:90–101

Huang Y, Chen XM, Zhao BX, Ke XY, Zhao BJ, Zhao X, Wang Y, Zhang X, Zhang Q (2010) Antiangiogenic activity of sterically stabilized liposomes containing paclitaxel (SSL-PTX): *in vitro* and *in vivo*. AAPS PharmSciTech 2:752–759

Immordino ML, Dosio F, Cattel L (2006) Stealth liposomes: review of the basic science, rationale, and clinical applications, existing and potential. Int J Nanomedicine 1:297–315

Ishii M, Shibata R, Numaguchi Y et al (2011) Enhanced angiogenesis by transplantation of mesenchymal stem cell sheet created by a novel magnetic tissue engineering method. Arterioscler Thromb Vasc Biol 31:2210–2215

Iwanaga K, Ono S, Narioka Kohji et al (1997) Oral delivery of insulin by using surface coating liposomes Improvement of stability of insulin in GI tract. Int J Pharm 157:73–80

Jaafar-Maalej C, Diab R, Andrieu V et al (2010) Ethanol injection method for hydrophilic and lipophilic drug-loaded liposome preparation. J Liposome Res 20:228–243

Jain NK (ed) (2001) Controlled and novel drug delivery. CBS, New Delhi

Jakobsen U, Vogel S (2009) DNA controlled assembly of liposomes in diagnostics. Methods Enzymol 464:233–248

Jeschke MG, Sandmann G, Finnerty CC (2005) The structure and composition of liposomes can affect skin regeneration, morphology and growth factor expression in acute wounds. Gene Ther 12:1718–1724

Jung SW, Thamphiwatana S, Zhang L et al (2015) Mechanism of antibacterial activity of liposomal linolenic acid against Helicobacter pylori. PLoS ONE 10:e0116519

Kabalka GW, Buonocore E, Hubner K et al (1988) Gadolinium-labeled liposomes containing paramagnetic amphipathic agents: targeted MRI contrast agents for the liver. Magn Reson Med 8:89–95

Kant S, Kumar S, Prashar B (2012) A complete review on: liposomes. IRJP 3:10–16

Karatas A, Turhan F (2015) Phyto-phospholipid complexes as drug delivery system for herbal extracts/molecules. Turk J Pharm Sci 12:93–102

Kareparamban JA, Nikam PH, Jadhav AP et al (2012) Phytosome: a novel revolution in herbal drugs. IJRPC 2:299–310

Karimi M, Ghanbharzadeh B, Hamishekhar H et al (2015a) Phytosome and liposome: the beneficial encapsulation systems in drug delivery and food application. App Food Biotechnol 2:17–27

Karimi N, Ghanbarzadeh M, Hamishehkar H et al (2015b) Phytosome as novel delivery system for nutraceutical materials. Int J Curr Microbiol App Sci 4:152–159

Karn PR, Vanic Z, Pepic I et al (2011) Mucoadhesive liposomal delivery systems: the choice of coating material. Drug Dev Ind Pharm 37:482–488

Kaur L, Kaur P, Khan MU (2013) Liposome as a drug carrier—a review. IJRPC 3:121–128

Khan J, Alexander A, Ajazuddin et al (2013) Recent advances and future prospects of phyto-phospholipid complexation technique for improving pharmacokinetic profile of plant actives. J Control Rel 168:50–60

Kheirolomoom A, Dayton PA, Lum AF et al (2007) Acoustically-active microbubbles conjugated to liposomes: Characterization of a proposed drug delivery vehicle. J Control Rel 118:275–284

Kidd PM (2009) Bioavailability and activity of phytosome complexes from botanical polyphenols: The silymarin, curcumin, green tea, and grape seed extracts. Altern Med Rev 14:226–246

Kidd Parris, Head Kathleen (2005) A review of the bioavailability and clinical efficacy of milk thistle phytosome: a silybin-phosphatidylcholine complex (siliphos). Alt Med Rev 10:193–203

Kilian G, Tshanga SS, Oidu B et al (2011) Antimicrobial activity of liposome encapsulated cyclo (l-tyrosyl-l-prolyl). Pharmazie 66:421–423

Kirby C, Clarke J, Gregoriadis G (1980) Effect of the cholesterol content of small unilamellar liposomes on their stability *in vivo* and *in vitro*. Biochem J 186:591–598

Ko YT, Bickel U (2012) Liposome-encapsulated Polyethylenimine/Oligonucleotide polyplexes prepared by reverse-phase evaporation technique. AAPS PharmSciTech 13:373–378

Kroon A, Staffhorst RWHM, Kruijff BD et al (2005) Cisplatin nanocapsules. Methods Enzymol 391:118–125

La Grange L, Wang M, Watkins R et al (1999) Protective effects of the flavonoid mixture, silymarin, on fetal rat brain and liver. J Ethnopharmacol 65:53–61

Lapinski MM, Castro-Forero A, Greiner AJ et al (2007) Comparison of liposomes formed by sonication and extrusion: Rotational and translational diffusion of an embedded chromophore. Langmuir 23:11677–11683

Latagliata R, Breccia M, Fazi P et al (2008) Liposomal daunorubicin versus standard daunorubicin: Long term follow-up of the GIMEMA GSI 103 AMLE randomized trial in patients older than 60 years with acute myelogenous leukaemia. Br J Haematol 143:681–689

Li C, Deng YJ, Cui JX (2007) Prepraration of liposomes and oily formulations by freeze drying of monophase solutions. In: Gregoriadis G (ed) Liposome technology liposome preparation and related technique, 3rd edn. Informa Healthcare Inc, USA, pp 35–54

Li Y, Wu H, Jia M et al (2014) Therapeutic effect of folate-targeted and PEGylated phytosomes loaded with a mitomycin C-soybeanphosphatidyhlcholine complex. Mol Pharm 11:3017–3026

Lynge ME, Ogaki R, Laursen AO et al (2011) Polydopamine/liposome coatings and their interaction with myoblast cells. ACS Appl Mater Interfaces 3:2142–2147

Ma T, Tan MS, Yu JT et al (2014) Resveratrol as a therapeutic agent for alzheimer's disease. Biomed Res Int 2014:350516

Magallanes M, Dijkstra J, Fierer J (1993) Liposome incorporated ciprofloxacin in treatment of murine salmonellosis. Antimicrob Agents Chemother 37:2293–2297

Manach C, Scalbert A, Morand C (2004) Polyphenols: food sources and bioavailability. Am J Clin Nutr 79:727–747

Mansoori MA, Agrawal S, Jawade S et al (2012) A review on liposome. IJARPB 2:453–464

Marczylo TH, Verschoyle RD, Cooke DN et al (2007) Comparison of systemic availability of curcumin with that of curcumin formulated with phosphatidylcholine. Cancer Chemother Pharmacol 60:171–177

Markman M, Moon J, Wilczynski S et al (2010) Single agent carboplatin versus carboplatin plus pegylated liposomal doxorubicin in recurrent ovarian cancer: final survival results of a SWOG (S0200) phase 3 randomized trial. Gynecol Oncol 116:323–325

Marripati S, Umasankar K, Reddy PJ (2014) A review on liposomes. IJRPNS 3:159–169

Meurre LA, Foster NR, Dehghani F (2008) Conventional and dense gas techniques for the production of liposomes: a review. AAPS PharmSciTech 9:798–809

Miller CR, Clapp PJ, O'Brien DF (2000) Visible light-induced destabilization of endocytosed liposomes. FEBS Lett 46:52–56

Mizoue T, Horibe T, Maruyama K (2002) Targetability and intracellular delivery of anti-BCG antibody-modified, pH sensitive fusogenic immunoliposomes to tumor cells. Int J Pharm 237:129–137

Moghimipour E, Handali S (2012) Utilization of thin film method for preparation of celecoxib loaded liposomes. Adv Pharm Bull 2:93–98

Mozafari MR, Mortazavi MS (eds) (2005) Nanoliposomes: from fundamentals to recent developments. Trafford Publishing Ltd, Oxford, UK

Mozafari MR, Johnson C, Hatziantoniou S et al (2008) Nanoliposomes and their applications in food nanotechnology. J Liposome Res 18:309–327

Mulder WJ, Strijkers GJ, Habets JW et al (2005) MR molecular imaging and fluorescence microscopy for identification of activated tumor endothelium using abimodal lipidic nanoparticle. FASEB J 19:2008–2010

Muramatsu K, Maitani Y, Takayama K et al (1999) The relationship between the rigidity of the liposomal membrane and the absorption of insulin after nasal administration of liposomes modified with an enhancer containing insulin in rabbits. Drug Dev Ind Pharm 10:1099–1105

Murugan V, Mukherjee K, Maiti K et al (2009) Enhanced oral bioavailability and antioxidant profile of ellagic acid by phospholipids. J Agric Food Chem 57:4559–4565

Nag OK, Awasthi V (2013) Surface engineering of liposomes for stealth behavior. Pharmaceutics 5:542–569

Naik SR, Pilgaonkar VW, Panda VS (2006) Evaluation of antioxidant activity of *Ginkgo biloba* phytosomes in rat brain. Phytother Res 20:1013–1016

Nair LS, Laurencin CT (2008) Nanofibers and nanoparticles for orthopaedic surgery applications. J Bone Joint Surg Am 90:128–131

Naumova A, Potselueva MM (2010) Liposomal form of dihydroquercetin contributes to skin regeneration after thermal burns. Cell tissue Biol 4:240–244

Neuhaus T, Pabst S, Stier S et al (2004) Inhibition of the vascular-endothelial growth actor induced intracellular signalling and mitogenesis of humanendothelial cells by epigallocatechin-3 gallate. Eur J Pharmacol 483:223–227

Oliveira CB, Rigo LA, Rosa LD et al (2014) Liposomes produced by reverse phase evaporation: *In vitro* and *in vivo* efficacy of diminazene aceturate against *Trypanosoma evansi*. Parasitology 141:761–769

Oliver M, Ahmad A, Kamaly N (2006) MAGfect: a novel liposome formulation for MRI labelling and visualization of cells. Org Biomol Chem 4:3489–3497

Olson F, Hunt CA, Szoka EC et al (1979) Preparation of liposomes of defined size distribution by extrusion through polycarbonate membranes. Biochim Biophys Acta 557:9–23

Paasonen L, Sipila T, Subrizi A et al (2010) Gold-embedded photosensitive liposomes for drug delivery: triggering mechanism and intracellular release. J Control Rel 147:136–143

Patel J, Patel R, Khambholja K et al (2009) An overview of phytosomes as an advanced herbal drug delivery system. Asian J Pharm Sci 4:363–371

Pathan RA, Bhandari U (2011) Preparation & characterization of embelin–phospholipid complex as effective drug delivery tool. J Incl Phenom Macrocycl Chem 69:139–147

Pawar HA, Bhangale BD (2015) Phytosome as a novel biomedicine: a microencapsulated drug delivery system. J Bioanal Biomed 7:6–12

Peleg-Shulman T, Gibson D, Cohen R et al (2001) Characterization of sterically stabilized cisplatin liposomes by nuclear magnetic resonance. Biochim Biophys Acta 1510:278–291

Petersen AL, Hansen AE, Gabizon A (2012) Liposome imaging agents in personalized medicine. Adv Drug Deliv Rev 64:1417–1435

Pietta P, Simonetti P, Gardana C (1998) Relationship between rate and extent of catechin absorption and plasma antioxidant status. Biochem Mol Biol Int 46:895–903

Pinheiro M, Lucio M, Lima JL et al (2011) Liposomes as drug delivery systems for the treatment of TB. Nanomedicine. NBM 6:1413–1428

Pitt WG, Husseini GA (2008) Ultrasound in drug and gene delivery. Adv Drug Deliv Rev 60:1095–1096

Provoda CJ, Stier EM, Lee KD (2003) Tumor cell killing enabled by listeriolysin O-liposome-mediated delivery of the protein toxin gelonin. J Biol Chem 278:35102–35108

Rasaie S, Ghanbarzadeh S, Mohammadi M et al (2014) Nano phytosomes of quercetin: a promising formulation for fortification of food products with antioxidants. Pharma Sci 20:96–101

Riaz M (1996) Liposome preparation method. Pak J Pharm Sci 9:65–77

Roesken F, Uhl E, Curri SB et al (2000) Acceleration of wound healing by topical drug delivery *via* liposomes. Langenbecks Arch Surg 385:42–49

Rukholm G, Mugabe C, Azghani AO et al (2006) Antibacterial activity of liposomal gentamicin against *Pseudomonas aeruginosa*: a time–kill study. Int J Antimicrob Agents 27:247–252

Sabzichi M, Hamishehkar H, Ramezani F et al (2014) Luteolin loaded phytosomes sensitize human breast carcinoma MDA MB 231 cells to doxorubicin by suppressing Nrf2 mediated signalling. Asian Pac J Cancer Prev 15:5311–5316

Schieren H, Rudolph S, Findelstein M et al (1978) Comparison of large unilamellar vesicles prepared by a petroleum ether vaporization method with multilamellar vesicles: ESR, diffusion and entrapment analyses. Biochim Biophys Acta 542:137–153

Seltzer SE (1988) Contrast-carrying liposomes. Current status. Invest Radiol 23:S122–S125

Seltzer SE, Swensson RG, Judy PF et al (1988) Size discrimination in computed tomographic images.

Effects of feature contrast and display window. Invest Radiol 23:455–462
Semalty A, Tanwar YS (2013) Nimuslide phosphatidylcholine complex for improvement of solubility and dissolution. Amer J Drug Disc Devel 3:225–234
Semalty A, Semalty M, Rawat MSM et al (2010a) Supramolecular phospholipidspolyphenolics interactions: the phytosome strategy to improve the bioavailability of phytochemicals. Fitoterapia 81:6–14
Semalty A, Semalty M, Singh D, Rawat MSM (2010b) Preparation and characterization of phospholipid complexes of naringenin for effective drug delivery. J Incl Phenom Macrocycl Chem 67:253–260
Senthilkumar KL, Ezhilmuthu RP, Praveen P (2012) Preparation and characterization of nabumetone liposomes. Int J Life Sci Biotechnol Pharm Res 1:81–86
Shaheen SM, Shakil Ahmed FR, Hossen MN et al (2006) Liposome as a carrier for advanced drug delivery. Pak J Biol Sci 9:1181–1191
Shehzad A, Khan S, Shehzad O et al (2010) Curcumin therapeutic promises and bioavailability in colorectal cancer. Drugs Today (Barc) 46:523–532
Singh RP, Parpani S, Narke R et al (2014) Phytosome: Recent advance research for novel drug delivery system. Asian J Pharmaceut Res Health Care 2:15–29
Song J, Shi F, Zhang Z et al (2011) Formulation and evaluation of celastrol-loaded liposomes. Molecules 16:7880–7892
Sudahakar CK, Upadhyay N, Verma A et al (2015) Nanomedicine and tissue engineering. In: Thomas S, Grohens Y, Ninan N (eds) Nanotechnology applications for tissue engineering. William Andrew, USA, pp 1–20
Sudimack JJ, Guo W, Tjarks W et al (2002) A novel pH-sensitive liposome formulation containing oleyl alcohol. Biochim Biophys Acta 1564:31–37
Sunderland CJ, Steiert M, Talmadge JE et al (2006) Targeted nanoparticles for detecting and treating cancer. Drug Dev Res 67:70–93
Szoka F (1980) Comparative properties and methods of preparation of lipid vesicles (liposomes). Ann Rev Biophys Bioeng 9:467–508
Szoka F Jr, Papahadjopoulos D (1978) Procedure for preparation of liposomes with large internal aqueous space and high capture by reverse-phase evaporation. Proc Natl Acad Sci 75:4194–4198
Takeuchi H, Kojima H, Yamamoto H et al (2001) Passive targeting of doxorubicin with polymer coated liposomes in tumor bearing rats. Biol Pharm Bull 24:795–799
Takeuchi H, Matsui Y, Yamamoto H et al (2003) Mucoadhesive properties of carbopol or chitosan-coated liposomes and their effectiveness in the oral administration of calcitonin to rats. J Control Rel 86:235–242
Taylor KMG, Morris RM (1995) Thermal analysis of phase transition behaviour in liposomes. Thermochim Acta 248:289–301
Tedesco D, Steidler S, Galletti S, Tameni M, Sonzogni O, Ravarotto L (2004) Efficacy of silymarin-phospholipid complex in reducing the toxicity of aflatoxin B1 in broiler chicks. Poult Sci 11:1839–1843
Tiwari G, Tiwari R, Sriwastawa B et al (2012) Drug delivery systems: An updated review. Int J Pharm Investig 2:2–11
Torchilin VP (ed) (1995) Handbook of Targeted Delivery of Imaging Agents. CRC Press, Boca Raton
Torchilin V (2010) Passive and active drug targeting: Drug delivery to tumors as an example. Handb Exp Pharmacol 197:3–53
Torchilin V (2011) Tumor delivery of macromolecular drugs based on the EPR effect. Adv Drug Deliv Rev 63:131–135
Torres IM, Bento EB, Almeida Lda C et al (2012) Preparation, characterization and *in vitro* antimicrobial activity of liposomal ceftazidime and cefepime against *Pseudomonas aeruginosa* strains. Braz J Microbiol 43:984–992
Trafny EA, Antos-Bielska M, Grzybowski J (1999) Antibacterial activity of liposome-encapsulated antibiotics against *Pseudomonas aeruginosa* attached to the matrix of human dermis. J Microencapsul 16:419–429
Turanek J, Kasna A, Zaluska D et al (2003) Preparation of sterile liposomes by proliposome-liposome method. Methods Enzymol 367:111–125
Vodovozova EL, Kuznetsova NR, Kadykov VA et al (2008) Liposomes as nanocarriers of lipid-conjugated antitumor drugs melphalan and methotrexate. Nanotechnol Russ 3:228–239
Wagner A, Vorauer-Uhl K (2011) Liposome technology for industrial purposes. J Drug Deliv 2011:591325
Wang JS, Luo H, Wang P et al (2008) Validation of green tea polyphenol biomarkers in a phase II human intervention trial. Food Chem Toxicol 46:232–240
Wei H, Song J, Li H et al (2013) Active loading liposomal irinotecan hydrochloride: Preparation, *in vitro* and *in vivo* evaluation. Asian J Pharm Sci 8:303–311
Yamauchi M, Tsutsumi K, Abe M et al (2007) Release of drugs from liposomes varies with particle size. Biol Pharm Bull 5:963–966
Zaveri M, Gajjar H, Kanaki N et al (2011) Preparation and evaluation of drug phospholipid complex for increasing transdermal penetration of phytoconstituents. IJIPLS 1:80–93
Zhang L, Gu FX, Chan JM et al (2008) Nanoparticles in medicine: Therapeutic applications and developments. Clin Pharmacol Ther 83:761–769
Zhang L, Porfattanangku D, Hu CM (2010) Development of nanoparticles for antimicrobial drug delivery. Curr Med Chem 17:585–594
Zhao H, Wang JC, Sun QS et al (2009) RGD-based strategies for improving antitumor activity of paclitaxel-loaded liposomes in nude mice xenografted with human ovarian cancer. J Drug Target 17:10–18

Nanocellulose and Nanocomposites

5

Rubbel Singla, Anika Guliani, Avnesh Kumari and Sudesh Kumar Yadav

Abstract

Nanocellulose is a class of fascinating bio-based nanomaterials with dimensions from few nanometers up to several micrometers depending upon the type of cellulosic fibers obtained from the source. Cellulose is a biopolymer present in huge amounts in the biosphere that mainly include the cell walls of green plants, bacteria, fungi, and tunicates. The isolation of nanocellulosic fibers is done by various methods like enzymatic methods, chemical methods, and chemical combined with mechanical methods. A large number of parameters like methodology used for isolation, source of cellulose, age, and reaction parameters affect the physicochemical properties of nanocellulose. Nanocellulose show unique features like biocompatibility, abundance in nature, high thermal stability, great mechanical, chemical, and physical properties which make them a suitable candidate for applicability as reinforcing agents in nanocomposites formation. The nanocellulose also plays a great role in drug delivery, tissue engineering, and repair of organs. This chapter mainly deals with detailed description of nanocellulose, types, sources, and methodologies opted for isolation, properties, and surface modifications. The applications of nanocellulose in the medical are also covered to make nanocellulose as a potential candidate to serve humankind.

Keywords

Nanocellulose · Nanocomposites · Drug delivery · Tissue engineering · Antibacterial

R. Singla · A. Guliani · A. Kumari · S.K. Yadav
Department of Biotechnology, Council of Scientific and Industrial Research-Institute of Himalayan Bioresource Technology, Palampur 176061, Himachal Pradesh, India

R. Singla · A. Guliani · A. Kumari · S.K. Yadav
Academy of Scientific and Innovative Research, New Delhi, India

S.K. Yadav (✉)
Department of Biotechnology, Center of Innovative and Applied Bioprocessing (CIAB), Mohali 160071, Punjab, India
e-mail: skyt@rediffmail.com; sudesh@ciab.res.in

© Springer Science+Business Media Singapore 2016

S.K. Yadav (ed.), *Nanoscale Materials in Targeted Drug Delivery, Theragnosis and Tissue Regeneration*, DOI 10.1007/978-981-10-0818-4_5

Contents

5.1 Introduction

Cellulose is the most widely abundant, inexhaustible, and renewable source present on this global earth with an annual biomass production of about 7.5×10^{10} tons (Habibi et al. 2010). Cellulose is a primary component of cell walls of green plants such as woods, reeds, grasses, stalks, and other vegetations (Alemdar and Sain 2008). It is also present in various other forms of living entities like bacteria, fungi, actinomycetes, and tunicates. In the old past history, cellulose was used in the form of cellulosic fibers or its derivatives for a great spectra of applications in daily life as it is inexhaustible natural biopolymer possessing wide efficacies which include its utility in paper formation, textiles, explosives, dietary fibers, and many more (Habibi et al. 2010). Natural plant fibers mainly contain cellulose, hemicelluloses, starch, and lignin. Removal of lignin, hemicelluloses and pectins like impurities is required from the original plant source by appropriate processing method to obtain pure cellulosic fibers (Siro and Plackett 2010). The content, quality, and other properties of fibers depend on various factors such as type of fiber, origin, size, maturity, and processing methods used for the isolation of fibers (Bledzki and Gassan 1999). Despite the chemical composition, properties of natural fibers are strongly influenced by factors that may differ among different parts of the plant as well as among different plants.

Recently, a new class of cellulosic biomaterials has been introduced named as nanocellulose. The term "nanocellulose" is an example of one dimensional nanoparticles (NPs) used to describe elongated crystalline rod-like cellulose NPs having at least one dimension in the nano (10^{-9} m) range (Siro and Plackett 2010). Nanocellulose is also named as cellulose nanocrystals (CNCs), nanowhiskers, cellulose nanofibers (CNFs), nanorods, and cellulose microcrystals depending on their dimensions and aspect ratio (length/diameter). A variety of methods are known to obtain pure nanocellulose from the original source, viz, chemical method, enzymatic method, and chemomechanical method. All these methods help to remove the noncellulosic impurities from the source of cellulose. The treatment by any of these methods is generally followed by acid hydrolysis to break the bonds between amorphous and crystalline regions of cellulose fibers to convert it into micro or nanoscale dimension (Brinchi et al. 2013). In comparison to natural cellulose fibers, the growing interest in the preparation of nanoscale

cellulosic particles is due to the remarkable features induced by nanosize effect as well as renewable nature of nanocellulose. The nanocellulose possesses unsurpassed physical and chemical properties such as high aspect ratio (l/d), environmental benign nature, high sustainability, abundant availability, low density, low energy consumption, inherent renewability, high tensile strength, more flexibility, good mechanical, electrical and thermal properties, biodegradability and biocompatibility (Roohani et al. 2008; Siro and Plackett 2010).

Due to the above-mentioned properties, nanocellulose have been used in diverse significant applications, including antimicrobial films, pharmaceutical, drug delivery, biomedical implants, biosensing, paper making, electronics, catalysis, and nanocomposite formation, tissue engineering and many more (Duran et al. 2011). The surface modification of nanocellulose is possible due to the presence of large number of OH^- on its surface (Habibi et al. 2010). A large number of chemical methods such as acetylation, oxidation, silylation, non-covalent modification and grafting have been reported to alter the chemical functional groups on the surface of nanocellulose to make them successfully well designed for the attachment of any active moiety or ligand (Habibi 2014). A lot of research has been done worldwide on the use of nanocellulose for the formation of nanocomposites because one can exploit the high stiffness of nanocellulosic fibers for reinforcement. Despite this, a variety of metal nanoparticles like gold, silver, and copper have also been used as dispersed phase or fillers in the formation of bionanocomposites with cellulose fibers as matrix, due to their different properties being small size and homogenous size distribution as compared to bulk counterpart (Thomas et al. 2007). The bionanocomposites are of potential use in a wide range of applications such as medical, optical, water treatment, sensors, textile, and energy conversion, cosmetics, and electronics (Kalia et al. 2011).

In view of the fascinating properties of nanocellulose, the contents of current book chapter are designed in such a manner to provide a detailed description on this topic. The chapter deals with the structure and morphology of cellulose, its sources, methods of nanocellulose isolation, its types based on source and dimensions, properties of nanocellulose, the vital factors affecting nanocellulosic properties, surface modifications, and ultimately the applications in nanocomposites formation. The chapter also throws light on the biomedical applications of nanocellulose like drug delivery and tissue engineering.

5.2 Structure and Morphology of Cellulose

Cellulose is a long homopolysaccharide consisting of D-glucose units with repeating units of cellobiose, where two glucose molecules are joined through a β-1,4 glycosidic linkage. Cellulose possesses a complicated architecture of β-D-glucopyranose rings representing a $^4C_1$ chair conformation (Klemm et al. 2005). The −OH functional groups present on the surface of cellulose are oriented in an equatorial plane of the ring form, whereas the hydrogen atoms are present in the axial positions. This structure of cellulose is stabilized by an intramolecular hydrogen bonding extending from O(3′)-H hydroxyl group to the O(5) ring oxygen of the next unit across the glycosidic linkage and from the O(2)-H hydroxyl to the O(6′) hydroxyl of the next residue (Habibi et al. 2010). The degree of polymerization of cellulosic chains depends on the source of cellulose. It is observed that wood cellulose contain approximately 10,000 glucopyranose units while cotton cellulose has 15,000 units (Sjostrom 1993).

In nature, the cellulose is present as a main component in plant cell wall and help to provide mechanical strengths to plants. In plants, the cellulose does not exist as an individual entity but many chains of cellulose fibers assemble together (Somerville 2006). In general, 36 individual cellulose molecules assemble with one another via van der Waals forces and hydrogen bonds to form larger units known as protofibrils or elementary fibrils (Williamson et al. 2002). These protofibrils are further packed into larger

microfibrils which in turn assemble to form cellulose fibers (Moon et al. 2011). These cellulose microfibrils are made up of two major parts consisting of highly ordered cellulose crystalline structure as well as randomly oriented amorphous part. The cellulose microfibrils in the cell wall are also surrounded by nanocellulosic compounds such as lignin and hemicelluloses. The isolation of highly pure crystalline cellulose referred as nanocellulosic crystals, deals with the deconstruction of this highly crystalline structure by removal of lignin and hemicelluloses from the cell wall by adopting a proper methodology in a combination of mechanical, chemical and/or enzymatic treatments (Alemdar and Sain 2008). Some bacterial cells and tunicate have also been known to form cellulose in pure forms only. Natural cellulose mainly exists in the form of cellulose I with its two allomorphs Iα and Iβ. The occurrence of these allomorphs in different ratios is highly dependent on the type of plant species from which the cellulose is extracted (Eichhorn et al. 2010). The bacterial cellulose is usually rich in Iα whereas tunicates cellulose contain high content of Iβ form (Nishiyama et al. 2002).

5.3 Sources of Cellulose

Cellulose occurs in nature in wide variety of sources that include green plants, viz, woody vegetations, stalks, reeds, and agricultural biomass. Other sources of polymeric cellulose comprise bacteria, fungi, tunicates, and actinomycetes. Green vegetation contain lignins, hemicelluloses, and starch residues along with long cellulose fibers having diameter 5–50 nm and length up to several micrometers. Cellulose fibers of plant origin can be categorized based on the plant species and plant parts. The different types of plants and plant parts like leaves (cantala, abaca, pineapple, sisal, date palm, and banana); seeds (cotton); fruits (oil palm, coir, kapok); straw/agricultural biomass (rice husk, wheat, sorghum, barley, soy hulls); bast (flax, ramie, hemp, jute); grass (alfa-alfa, bamboo, bagasse) are rich in cellulose (Williams and Wool 2000; Torres and Diaz 2004). The bacterial cells (*Acetobacter, Agrobacterium, Alcaligenes, Pseudomonas, Rhizobium, or Sarcina*) and tunicates (*Ciona intestinalis, Ascidia sp., Halocynthia roretzi and Styela plicata*) synthesize cellulose in the pure forms and also in the nanocellulosic forms (Keskh 2014; Zhao and Li 2014). Nanocellulose in the forms of CNFs/CNCs have been extracted from various sources including corncob (Silverio et al. 2013), cotton (Xiong et al. 2012), wheat straw and soy hulls (Alemdar and Sain 2008), bamboo culm (Nguyen et al. 2013), bamboo wood pulp (Brito et al. 2012), curaua (Correa et al. 2010), wood (Stelte and Sanadi 2009), agave (Rosli et al. 2013), algae (Imai et al. 2003), bacteria (Olsson et al. 2010), and tunicates (Iwamoto et al. 2011). The isolation of nanocellulose from different sources requires an intense amount of further work. A brief information regarding the sources from which different forms of nanocellulose has been isolated along with the size, shape, and morphology is presented in tabular form (Table 5.1).

5.4 Types of Nanocellulose

Nanocellulose is categorized into various kinds based on their dimensions and sources. The dimensions of nanocellulose vary depending upon the raw material used and processing methods opted. Microfibrillated cellulose (MFCs), cellulose nanocrystals (CNCs), and bacterial nanocellulose (BNCs) are the different types of nanocellulose known.

5.4.1 Microfibrillated Cellulose (MFCs)

Microfibrillated cellulose is also known as cellulose microfibrils, microfibers, microfibrillar cellulose, nanofibrillar cellulose, as well as cellulose nanofibers (Siro and Plackett 2010). These fibers contain aggregates of many microfibrils having both the crystalline and amorphous parts

Table 5.1 List of different forms of nanocellulose, their sources, methodology of isolation, dimensions, and morphology

Source of cellulose	Form of extracted nanocellulose	Pretreatment method	Acid used for hydrolysis	Mechanical treatment	Dimensions and morphology	References
Bamboo culm	Microfibrillated cellulose	Chemical pretreatment	64 % sulfuric acid	–	20–40 nm, long cylindrical fibers	Nguyen et al. (2013)
Banana rachis	Cellulose microfibrils	Hydrogen peroxide/organosol	80 % acetic + 70 % nitric acid	Homogenization	5 nm width, long slender fibrils	Zuluaga et al. (2007)
Wheat straw and soy hulls	Cellulose nanofibers	Chemical pretreatment	Hydrochloric acid	Cryocrushing + homogenization	Wheat straw 10–80 nm, soy hulls 20–120 nm, individualized long fibers	Alemdar and Sain (2008)
Soybean	Cellulose nanofibers	Chemical pretreatment	Hydrochloric acid	Beating and defibrillation	50–100 nm diameter, long length up to several micrometers	Wang and Sain (2007)
Banana fibers	Cellulose nanofibers	Steam explosion and chemical pretreatment	Oxalic acid	Mechanical stirring	Long fibrils of diameter 1 μm	Deepa et al. (2011)
Banana fibers	Nanofibril whiskers	Steam explosion followed by chemical pretreatment	5, 7, 9, and 11 % Oxalic acid	Mechanical stirring	4–4 nm diameter and 200–250 nm length	Cherian et al. (2008)
Okra fibers	Cellulose nanocrystals	Chemical pretreatment	64 % sulfuric acid	Sonication	Diameter of 9.8 μm having length up to several μm, long individualizing fibers	Fortunati et al. (2013b)
Agave angustifolia	Cellulose nanocrystals	Chemical pretreatment	60 % sulfuric acid	–	8–15 nm diameter with 170-500 nm length	Rosli et al. (2013)
Capim Dourado	Cellulose nanocrystals	Chemical pretreatment	65 % sulfuric acid	Homogenization	4.5 nm width and 300 nm length	Siqueira et al. (2010b)
Corn cob	Cellulose nanocrystals	Chemical pretreatment	Sulfuric acid	Ultrasonication	Needle shaped having 210.8 ± 44.2 nm length and 4.15 ± 1.08 nm width	Silverio et al. (2013)
Cotton fibers	Microcrystalline cellulose (MCC) and nanocrystalline cellulose (NCC)	Chemical pretreatment	Nitric acid (68 % w/w) and hydrochloric acid (37 % w/w)	Ultrasonication	49 μm sized MCC and 35 nm NCC	Xiong et al. (2012)
Palm oil fruit	Cellulose nanofibers	Chemical pretreatment	64 wt% sulfuric acid	Ultrasonic homogenization	1–3.5 nm thickness	Fahma et al. (2010)
Gluconacetobacter xylinus	Bacterial cellulose nanofibers	Treatment with NaOH	–	–	5.6–12.7 nm crystal size of uniaxial long ribbon shaped fibrils	Sheykhnazari et al. (2011)
Acetobacter xylinum	Bacterial nanocellulose	–	–	–	Sphere like morphology of 60–80 nm width	Goelzer et al. (2009)

of cellulose and exist in a rigid network like structure (Lu et al. 2008). MFCs possess high aspect ratio with an average width of 20–60 nm and length up to several micrometers generally 10 μm (Krassig 1993). The microfibers are synthesized in plants during the biosynthesis of cellulose. Their diameters vary depending upon the source of origin of cellulose.

5.4.2 Cellulose Nanocrystals (CNCs)

Cellulose nanocrystal is a term used to designate cellulose NPs that are prepared from natural source of cellulose by acid hydrolysis method. CNCs are also known as nanowhiskers which are elongated, cylindrical and rod like in morphology with widths of 5–70 nm and lengths of 100 nm to several micrometers (Silverio et al. 2013). These CNCs are shorter and thinner than cellulose microfibers. This rod-like form of crystalline nanocellulose is obtained when all the noncellulosic polysaccharide impurities have been removed from the fibril surface and also after the cleavage of amorphous parts of cellulose (Kargarzadeh et al. 2012). CNCs form dispersions in aqueous mixtures as well as organic solvents but show particle aggregations in highly hydrophobic solutions.

5.4.3 Bacterial Nanocellulose (BNCs)

In comparison to plant species, the biosynthesis of extracellular cellulose takes place in many bacterial species such as *Rhizobium*, *Acetabacter*, *Agrobacterium*, *Pseudomonas,* and many more. Even other microbial sources like fungi and actinomycetes also form cellulose. The biocellulose formed from microbial sources possess diameter in the range of 20–100 nm, whereas length of 100–300 nm depending upon the cultivation conditions, type of microbial strain used, and bioreactor used. BNCs are form of pure cellulose made by self-assembly of cellulose fibrils secreted in the media (Klemm et al. 2011).

5.5 Preparation Methodologies of Nanocellulose

Since cellulose fibers present in cell walls provide great tensile strength to plant fibers, there isolation from cell wall is necessary to exactly get information about the properties of fibers in the form of either MFCs or nanocellulosic crystals (CNCs), so as to use them for a particular application. The preparation methods involve the pretreatment (chemical and enzymatic), acid hydrolysis, mechanical treatment, and a combination of chemical and mechanical methods.

5.5.1 Pretreatment

Pretreatment is a general method followed to isolate CNCs/CNFs from the natural fibers. It involves the use of enzymatic as well as chemical approach to extract nanocellulose. The main objective behind the use of pretreatment enzymatic and chemical agents is to remove all the components of cell wall other than cellulose. The removal of lignin, hemicelluloses, starch, wax and oils is necessary to obtain pure cellulosic nanocrystals.

5.5.1.1 Chemical Pretreatment

The chemical pretreatment consists of applications of a large number of chemical agents to remove noncellulosic components from the plant cell walls. The wax from the plant material is removed using a mixture of hexane/ethanol/water in soxhlet apparatus. The complex of lignin/hemicelluloses and pectins is removed by the treatment of alkali agents like sodium hydroxide or potassium hydroxide. These lignin and hemicelluloses are solubilized in alkali agents at high temperature (Abdel-Halim 2014). The removal of phenolic compounds or chromophore pigments is required for bleaching of the fibers that involve the treatment of bleaching agents. Bleaching is done by the use of acidified sodium hypochlorite solution (NaOCl) at high temperature (Nguyen et al. 2013). The bleaching

or delignification can also be obtained by a chlorine free method which involve the heating of cellulosic pulp in a mixture of hydrogen peroxide and tetraacetylethylenediamine (Rosa et al. 2012). Thus, the chemical pretreatment helps in almost complete removal of noncellulosic components like lignin, pectins, and hemicelluloses to leave behind only pure cellulose. Alkali treatments is needed to be given in a controlled manner to avoid cellulose degradation and to make sure that hydrolysis occurs only at the fiber surface to obtain fibers in their intact form (Wang and Sain 2007).

Instead of bleaching and alkali pretreatment, chemical oxidative treatment is also given to fibers with the purpose to solve the problem of fiber aggregation arising due to the presence of −OH groups on the surface of native cellulose. These −OH groups are converted to carboxylate and aldehyde functional groups by 2,2,6,6-tetramethylpiperidine-1-oxyl (TEMPO) mediated oxidation process (Saito and Isogai 2005). The oxidation induces negative charge at fiber surface which is responsible for fiber repulsion further leading to fibrillation. The TEMPO mediated oxidation process is very fast as compared to other chemical pretreatments and form uniform CNCs dispersion in water without having any chances of aggregation (Qian et al. 2012). A study has also reported the comparison of CNCs obtained from bamboo, softwood, and cotton linters by TEMPO mediated oxidation followed by ultrasonication (Qian et al. 2012).

The only disadvantage behind the use of chemical treatment for the isolation of CNCs/CNFs is the employment of highly toxic chemical agents. The usage of such chemicals may sometimes be not human and environmental friendly. Sometimes, the treatment procedure also involves the application of high temperature which is an energy consuming process.

5.5.1.2 Enzymatic Pretreatment

The enzymatic pretreatment is generally given to already bleached cellulose in order to obtain nanocrystalline cellulose. It is not possible in nature to degrade cellulose by using a single enzyme but it requires a set of cellulases to break cellulose. The enzyme cellobiohydrolases is further categorized into type A- and B-cellulases and also known as exoglucanases (Henriksson et al. 2007). These cellobiohydrolases are able to hydrolyze the highly crystalline cellulose at the chain endings. Another enzyme known as endoglucanase is responsible for degrading the amorphous regions of cellulose (Siro and Plackett 2010). Most systems use a combination of the cellobiohydrolases and endoglucanases to allow MFCs disintegration. In general, it is also recommended to use cellulases and hemicellulases together as a synergistic effect to remove hemicelluloses and also facilitate cellulose hydrolysis (Siqueira et al. 2010b). The resulted MFCs obtained after the enzymatic pretreatment show a more favorable structure with a greater aspect ratio. Campos et al. (2013) has used a combination of hemicellulases/pectinase and endoglucanase to isolate CNFs from curaua and sugarcane bagasse fibers.

The enzymatic route for the isolation of synthesis offers the potential for higher yields, higher selectivity, lower energy costs, and milder operating conditions other than chemical processes. The enzymatic treatment is environmental friendly as compared to chemical method of treatment but facing the difficulty in its application due to high cost of enzymes, and long processing time required for cellulose degradation (Pedersen and Meyer 2010).

5.5.2 Acid Hydrolysis

Acid hydrolysis is used to break the polysaccharides into monomeric units. In this case, the isolation of CNCs of highly crystalline nature can be obtained by removing the amorphous part of cellulose (Rosli et al. 2013). The removal of disorderly arranged amorphous regions, acid hydrolysis is imparted to pretreated fibers. Majorly, sulphuric acid and hydrochloric acid are the two good options for acid hydrolysis of fibers (Braun and Dorgan 2009; Fortunati et al. 2013b). Oxalic acid and nitric acid can also be used to form crystalline nanocellulose (Deepa et al. 2011; Xiong et al. 2012). Hydrochloric acid

impart neutral charge on the fiber surface with lesser water dispersibility, whereas sulphuric acid treatment provides negative charge to cellulose suspension allowing its better dispersion ability in aqueous media and also impart greater stability (Rosli et al. 2013).

The acid hydrolysis is generally given at high temperature of around 45 °C for a variable time period depending upon the source of cellulose and requirement of desirable dimensions of CNCs/CNFs. Reaction time is a critical parameter to be considered during hydrolysis. The long reaction time of hydrolysis results in almost complete degradation of cellulosic amorphous regions (Kargarzadeh et al. 2012). Insufficiently short hydrolysis time produces large sized undispersible fibers and lead to their aggregations. Acid treatment after a particular time period does not have further impact on reducing the nanocellulose dimensions. In a study, the effect of hydrolysis conditions have been shown on the morphology and crystallinity of CNCs isolated from kenaf fibers (Kargarzadeh et al. 2012).

5.5.3 Mechanical Treatment

A purely mechanical method is used to develop fine fibers. Several methods which come under mechanical treatment are named as high-pressure homogenization, grinding, cryocrushing, and sonication. The only disadvantage behind the use of mechanical method of treatment is the requirement of high energy consumption.

5.5.3.1 High-Pressure Homogenization

It is a conventional technique used to isolate nanocellulose with simplicity, high efficiency, and without the requirement of toxic organic solvents. This technique can easily be used for scaling up the procedure for extraction of fine fibrillated cellulose from cellulosic biomass. In this process, the wood pulp or cellulose slurry is passed through a narrow homogenization gap at a very high pressure and at high velocity. During the successive and rapid opening and closing of valve, the fibers undergo disintegration by shearing and impact forces (Karadag et al. 2014). The mechanical treatment is responsible for irreversible changes in the fiber structure by altering the morphology and size (Nakagaito and Yano 2004). The number of homogenization passes determines the size range of obtained nanofibers. There is a great problem for the extraction of nanocellulose by this method as cellulose is insoluble in water and most of the organic solvents due to which it can clog the valves of homogenizer. The valve clogging leads to nonuniform refining of nanocellulose (Kaushik and Singh 2011). Using the refining and high-pressure homogenization method, nanocellulose has been isolated from sugarcane bagasse (Li et al. 2012) and cotton (Wang et al. 2015).

5.5.3.2 Grinding

Commercial grinders with disks of modified designs are available commercially for the extraction of cellulose in the micro or nano form. In this procedure, the cellulose slurry is passed through a static grind stone and rotating grind stone revolving at 1500 rpm. The multilayered microfibers of cellulose present in cell walls and their hydrogen bonds are broken by the impact of shearing forces generated by grind stone to form nanofibrillated cellulose from the pulp (Siro and Plackett 2010). The isolation of CNFs of 15 nm diameter from wood has been obtained by using mechanical treatment through grinding (Abe et al. 2007). The disintegration of fiber into submicron-sized fibers requires only 3 passes through grinder whereas 5 passes of grinding produce fibers of nano size range. As compared to homogenization process, the mechanical treatment using grinder requires comparatively lesser number of passes to MFCs (Lavoine et al. 2012).

5.5.3.3 Cryocrushing

In this process of mechanical treatment, the fibers are first frozen using liquid nitrogen to form ice crystals within the cell wall. These ice crystals

exert high pressure on the cell wall when high-impact shear forces are applied on the frozen fibers during crushing. The pressure developed will lead to damage of cell wall and ultimately release of CNFs (Wang and Sain 2007). Cryocrushing method has been applied to extract MFCs from wheat straw and soy hulls (Alemdar and Sain 2008) where 60 % of fibers were of diameter 30–40 nm and length up to several thousand nanometers.

5.5.3.4 Sonication

Ultrasonication is a reliable and powerful technique and requires use of high intensity ultrasonic waves for the formation, expansion and collapse of gas bubbles. A high temperature up to 5000 °C and pressures of greater than 500 atm is produced near the implosion site and immediate surroundings of the liquid sample. Higher is the temperature, better is the fibrillation of cellulose fibers. A larger distance between the tip of sonication probe and the beaker containing cellulose suspension is not favorable for the disintegration of fibers from cellulose cell wall (Wang and Cheng 2009). The process of sonication is generally followed after the chemical treatment of raw or natural fibers for nanocellulose extraction.

5.5.4 Combined Chemical and Mechanical Approach

Chemical combined with mechanical approach is generally followed these days for the isolation of nanocellulose. In this approach, first the natural fibers undergo chemical pretreatment which is then followed by mechanical treatment using sonication or homogenization. Using this approach, the drawbacks associated with individual chemical or mechanical method are minimized. CNFs isolation from soybean source has been done by such chemomechanical approach where mechanical treatment (refining and beating) was given after complete chemical treatment (Wang and Sain 2007). Similarly, the extraction of cellulose microfibrils from potato tuber using the same methodology in which chemical pretreatment was given initially and then followed by 15 passes of homogenization (Dufresne et al. 2000).

5.6 Multiscale Characterizations

A large number of high throughput instruments and techniques are employed for the characterization of CNCs/CNFs. The shape, size and morphology of these nanocellulosic fibers extracted from variable sources using different preparation methodologies is examined by microscopic techniques like transmission electron microscopy (TEM), scanning electron microscopy (SEM) and atomic force microscopy (AFM). The surface topography of fibers is generally examined through SEM which reveals the smoothness or roughness of the outer surface of fibers. TEM clearly examines the shape and size of CNCs/CNFs. AFM mainly helps to know the 3-D structure of fibers. Another technique known as dynamic light scattering (DLS) determines the hydrodynamic diameter of fibers as well as surface charge (Yadav et al. 2014). The estimation of surface charge is necessary to know the tendency of aggregation or flocculation of nanocellulose suspension in water. CNCs having negative surface charge do not agglomerate while positively charged fibers do not disperse in aqueous media and get easily flocculate (Fahma et al. 2010). Apart from the morphological examination, a number of other structural attributes of nanocellulose are decided on the basis of their crystallinity index, surface functional groups, thermal stability, mechanical strength and viscosity.

Fourier transform infrared (FTIR) spectroscopy is used to examine the chemical composition of fibers before and after each step of chemical treatment to know whether the noncellulosic impurities like lignins, pectins and hemicelluloses have been removed from the raw fibers by estimation of change in transmittance intensity of corresponding peaks at a particular

wavenumber (Nguyen et al. 2013). The thermal properties of nanocellulose are determined by thermogravimetric analysis (TGA). The technique works on the principle where the physical and chemical properties of the substances are measured as a function of increase in temperature or time (Xiong et al. 2012). A sample of known weight is kept in the sample pan of the instrument and is heated at a particular temperature. A loss in weight of sample is measured. On the basis of weight loss at a particular temperature, thermostability of the sample can be estimated. Differential scanning calorimetry (DSC) is another technique also used to determine the thermal degradation of CNCs/CNFs.

X-ray diffraction (XRD) technique is used to analyze the degree of crystallinity of nanocellulose. The nanocellulosic sample before and after acid hydrolysis is analyzed through XRD. The curve showing the peak at a particular 2-theta value denotes the % crystallinity in the sample. In case of nanocellulose, a sharp peak around 22.5° designates the crystalline region and a broad peak at 15–18° designates the presence of amorphous regions of cellulose (Abe and Yano 2009). Another important property of cellulose microfibrils is mechanical behavior. Tensile testing is the technique used to measure the tensile strength, Young's modulus, and elasticity of the fibers. The tensile tester measures the elongation at break and also the stress/strain ratio which determines that how much force is required to break a sample of particular area (Wang and Sain 2007).

Another valuable property of CNCs is degree of polymerization and viscosity which is calculated by using viscometer. Preparation of microcrystalline cellulose from cotton fibers has shown that degree of polymerization decreases during the formation of microcrystalline cellulose from 1200 to 219 indicating the effect of chemical treatments on degree of polymerization for the extraction of the same (Xiong et al. 2012). The rheological properties of CNFs solutions are also characterized by rheometer that measures the viscoelastic behavior of dispersions. The rheology is a study of flow and deformation of matter in liquid state under applied forces (Hardelin et al. 2013).

5.7 Physicochemical Properties

Nanocellulose is a biomaterial of advanced research as it holds certain physical, chemical and biological properties. Nanocellulose show diverse characteristics which are quite different from the bulk traditional materials such as biocompatibility, biodegradability, surface chemistry, surface charge, geometrical dimensions, crystallinity index, mechanical properties, and high surface area to volume ratio.

The surface properties of nanocellulose are due to the structural chemistry of nanocellulose. In a view of structure of cellulose as already explained above, cellulose is a high molecular weight polymeric compound composed of β-1,4-anhydro-D-glucopyranose repeating units which do not lie in the structural planes but adopt a chair conformation. The great structural chemistry of nanocellulose is imparted by the presence of hydroxyl groups at carbons 2, 3, and 6 which have the tendency to readily form hydrogen bonds. These bonds play an important role in fibrillar and semicrystalline packing of nanocellulose which determine the fascinating physical properties of the CNCs/CNFs (Habibi et al. 2010). Another important property of nanocellulose is the surface charge. CNCs carry negative charge on their surface due to the presence of the sulfate ester groups. Later groups are introduced during sulfuric acid hydrolysis on the surface of CNCs via a process of condensation esterification occurring between surface −OH groups and a H_2SO_4 molecule. Due to the existence of negative charge on CNCs surface, these materials find a space in certain biomedical applications like adsorption of enzymes/proteins (Lin and Dufresne 2014).

Nanocellulose show astonishing properties having high surface area due to the dimensions in the nano scale range. The nanocellulose isolated from biological sources is quite biodegradable,

hemocompatible and biocompatible (Lin and Dufresne 2014). Nanocellulose is highly porous, and water insoluble having hygroscopic nature which can absorb humidity or moisture. Nanocellulose has high water uptake capacity measured as the degree of swelling. Bacterial cellulose have greater tendency to absorb more water as compared to nanocellulose obtained from other sources. CNFs films possess the oxygen barrier properties making them highly applicable for food packaging materials. The oxygen transmission rate of CNCs films increases with an increase in relative humidity (Miettinen et al. 2014). The nanocellulose possesses high dielectric properties and is used as an insulator in electrical industries. The dielectric constant is influenced by moisture content, length of fibers, presence of noncellulosic components, degree of polymerization and fiber density (Bras et al. 2015). The nanocellulosic films show remarkable optical transparency due to which CNFs hold a place for utility in optical devices. The orientation and alignment of CNFs form suitable ordered structures. During the formation of solid films, the casting of nanocellulosic dispersions on a solid support is done where NPs can maintain their alignment to form iridescent structures with chiral nematic ordering (Edgar and Gray 2001). These developed films possess the tendency to reflect polarized light at a particular wavelength which is further dependent on the pitch of liquid crystals (Dufresne 2013). The high aspect ratio, cylindrical shape, flexibility, and rigidity of CNCs lead to their optical effects in the aqueous suspensions.

CNCs/CNFs have been used as reinforcing agents or as fillers due to their strong mechanical properties. The improvement in Young's modulus is responsible for better mechanical behavior or tensile strength of CNCs. Due to the excellent tensile strength; CNCs play a great role in nanocomposites formation. Bacterial nanocellulose has greater tensile strength as compared to plant nanocellulose. This may be due to the presence of substantial amount of pellicular proteins that are secreted by bacterial cell and bind together the cellulose microfibrils (George et al. 2005). Another important property of nanocellulose fibers is high thermostability. The thermal stability increases upon chemical and mechanical treatments to the raw fibers. The high thermostability of CNCs makes them appropriate candidates for utility in thermoplastic nanocomposites (Alemdar and Sain 2008). The degree of crystallinity or crystalline index is another valuable property of nanocellulose. The crystallinity of nanocellulose determines the morphology of CNCs/CNFs. Crystallinity index of CNCs increases after removal of noncellulosic components from the natural fibers by using pretreatment methods.

5.8 Factors Affecting Nanocellulose

A vast number of factors are known to affect the dimensions, morphology, surface chemistry and properties of nanocellulose. The major factor is the source from which nanocellulose is extracted play a vital role. The dimensions of nanocellulose are determined by the original source of cellulose. Apart from the bacterial sources, the cellulose isolated from all other sources is obtained in micrometer dimensions and requires further purification and treatments to produce in nanoscale range (Alemdar and Sain 2008). For example, cellulose microfibrils isolated from banana rachis by applying combined chemical and mechanical (sonication) method has been obtained in the form of individualized or associated fiber bundles of 5 nm width (Zuluaga et al. 2007). On the other hand, CNCs extracted from bacterial culture of *Acetobacter xylinus* followed by enzymatic hydrolysis using cellulose enzyme were 100–300 nm in length and 10–15 nm in diameter (George et al. 2011). Moreover, the age of source, climate conditions, and maturity level has also affected the dimensions of nanocellulose.

The chemical, enzymatic or mechanical method used has an impact on the dimensions of CNCs. A study has reported the comparison of properties of CNCs and cellulose nanofibrils isolated from three different sources (bacteria, wood, and tunicates) by applying acidic, enzymatic, mechanical, and oxidative approaches.

The results described that size, aspect ratio and other characteristics properties of CNCs and nanofibrils are tuned by varying the source and hydrolysis techniques (Sacui et al. 2014). During the purification process, concentration and type of reagents used, reaction temperature, time duration, pH of the culture media and many more lead to variations in the dimensions and morphology of nanocellulose. Two different reports have described the isolation of CNFs from rice and wheat straw and studied the effect of acid used, its concentration and time duration on the size, morphology and other properties of CNFs (Nasri-Nasrabadi et al. 2014a; Shamsabadi et al. 2015). Surface charge of nanocellulose can be controlled through optimization of acid hydrolysis parameters such as type of acid used (sulfuric acid, hydrochloric acid, nitric acid, and a combination thereof), concentration of the acid used, temperature and time period for which hydrolysis is carried out. The surface charge of CNCs/CNFs also has also affected the properties to a greater extent. The introduction of negatively charged sulfate groups on the cellulosic crystals could reduce the thermostability. The presence of negative surface charge increases the suspension stability of nanocellulose while decreasing the chances of agglomeration or fiber aggregation.

Surface chemistry or tendency of surface modifications has been affected by the presence of hydroxyl groups on the structure of CNCs. The hydroxyl group at C-6 can react ten times faster than OH groups present at C-2 and C-3, while the reactivity of the hydroxyl group on C-2 position was found to be twice than that of C-3 position (Habibi 2014). The ability to surface modification is thus manifested by the chemical conversions of these hydroxyl functional groups. The size, shape and high surface area of nanocellulose influences the properties in aqueous media, for example, the optical characteristics, stability and rheology of their suspensions. Rheological parameters of CNCs are also influenced by properties such as liquid crystallinity, ordering, and gelation properties (George and Sabapathi 2015).

The original source of cellulose and degree of swelling also affects the mechanical properties of CNCs. As a result of the internal stress produced by swelling, the intermolecular bonds break which are responsible for holding the fibers together (Saheb and Jog 1999). Due to swelling, the degree of order within the fiber is reduced contributing toward decreasing mechanical properties. The dimension of cellulose microfibrils has been found to be significantly affected the mechanical properties. The longitudinal modulus of pulp CNFs has been reported to be 81 ± 12 GPa (Cheng et al. 2009), whereas the Young's modulus of BNC was 114 GPa (Hsieh et al. 2008). Another important property of crystallinity index is also affected by various factors such as source, and method used for fiber isolation. Alkali treatment plays a major role to determine the mechanical as well as crystalline properties of nanocellulose (Das and Chakraborty 2008). BNC have greater degree of crystallinity as compared to cellulose isolated from other sources. The degree of crystallinity further affects the oxygen transfer rate. The relatively low oxygen transfer rate has been attributed to the higher degree of crystallinity of CNFs and the higher fibrillation of the materials.

5.9 Surface Chemical Modifications

Since nanocellulose is highly hydrophilic in nature, a problem is faced due to its nonuniform dispersion in various nonpolar media. The researchers are interested in surface modifications of nanocellulose to enhance its compatibility with different types of matrices. Nanocellulose has great ability for surface modifications by the reactions of various types of chemical moieties with the hydroxyl groups present on its surface. The tendency of surface modifications makes them suitable candidates for nanocomposites formation. A variety of methods are known through which the surface of nanocellulose is being modified which are described in detail as ahead.

5.9.1 Non-covalent Surface Modification

This is the method where non-covalent attachment or adsorption of surfactants or oppositely charged molecules is achieved on the surface of nanocellulose. Surfactants are the molecules used to reduce the surface tension when used at very low concentrations. The use of surfactants such as mono- and di-esters of phosphoric acid bearing alkylphenol tails was introduced by Heux et al. (2000) for improving the dispersion ability of CNCs in the nonpolar solvents. The interactions mainly take place through van der Walls forces, hydrogen bonding, hydrophilic affinity, or electrostatic attractions with the surface moieties of nanocellulose (Habibi 2014). Another approach used for non-covalent surface modification of CNCs is by the attachment of cationic surfactants. As the surface of CNCs contain anionic charged moieties at neutral pH, the modification with cationic surfactants is done to improve hydrophobic character of CNCs (Kaboorani and Riedl 2015). In this case, hexadecyltrimethylammonium bromide used is a tetra substituted ammonium cationic surfactant containing charged quaternary nitrogen and a long straight alkyl chain of 16 carbon atoms that has induced a high degree of hydrophobicity to CNCs. Similarly, an entirely bio-derived poly lactide acid (PLA)-carbohydrate copolymer has been used to modify the surface of BNC by the interactions through hydrogen bonding in order to increase the mechanical properties of nanocomposites (Lee et al. 2012).

5.9.2 Silylation

The silylation procedure is used to chemically modify CNCs surface with the hydrophobic compounds to enhance their interactions with the polymer matrices (George and Sabapathi 2015). Silane coupling agents such as chlorosilanes and alkoxysilanes serve to modify the hydroxyl groups present on the surface of nanocellulose to improve its hydrophobic behavior. In a study, CNCs have been silylated using 3-isocyanatepropyltriethoxysilane (IPTS) where triethoxysilane moiety was grafted onto CNCs surface offering good miscibility of silylated CNCs with silicon rubber and further increased its reinforcing capacity (Yu et al. 2015). Similar experiment has described the silylation of cellulose microfibrils extracted from sugar beet pulp using isopropyl dimethylchlorosilane. The silylated microfibrils showed flocculation in the dispersion of tetrahydrofuran when the degree of substitution was smaller than 0.1 whereas homogenous dispersion was resulted between 0.1 and 0.4 degree of substitution. Silylation has resulted in increased flexibility of microfibrils (Gousse et al. 2004). In another case, either CNCs or NFCs have been coupled with 3-aminopropyltriethoxysilane which resulted in enhancement of their compatibility with PLA responsible for improving the mechanical strength of nanocomposites (Frone et al. 2011).

5.9.3 Acetylation

It is one of the useful methods of surface alteration of nanocellulose and is mainly applied to reduce the hygroscopic nature or moisture absorption potential of cellulose fibers. Acetylation of fibers is a common method for esterification reactions. Degree of acetylation has a crucial impact on the physical properties of fibers while maintaining their morphology as such. Acetylation occurs through the substitution of hydroxyl groups by acetyl moiety by treating the fibers with a mixture of dry acetic anhydride and acetic acid along with the use of sulfuric or perchloric acid as catalysts (Habibi 2014). A study reported the surface acetylation of cellulose whiskers using alkyenyl succinic anhydride and described that acetylated whiskers maintained their morphological features along with crystallinity. But the whiskers were more readily dispersible in less polar solvents (Yuan et al. 2006). Similarly, CNCs of cotton fiber have been acetylated by a single step method using acetic anhydride in anhydrous phosphoric acid system of solvents. Acetylated CNCs have possessed the greater

ability to disperse and also increased the reinforcing potential of PLA sheets (Yan et al. 2013).

5.9.4 Oxidation

TEMPO mediated oxidation is an effective and simple to implement conversion of primary hydroxyl alcohols into aldehydes, ketones and carboxylic acids. Commonly, the reaction involves the usage of a nitroxyl radical, TEMPO along with NaBr and NaOCl. The reaction is carried out by dissolving catalytic amounts of TEMPO and NaBr in polysaccharide solutions generally at pH of 10–11. Oxidation reaction is initiated by the addition of NaClO solution as a primary oxidizing agent (Isogai et al. 2011). In a study, TEMPO oxidized CNCs from olive stones have been used to develop chitosan nanocomposites. These TEMPO-CNCs have increased the mechanical strength of nanocomposites and showed higher dissolution rate in simulated body fluids (Abou-Zeid et al. 2015). Similarly, a comparative study has been reported in which TEMPO oxidized CNCs isolated from bamboo, soft wood and cotton linters have been characterized (Qian et al. 2012). TEMPO oxidation has been applied to scaffold of bacterial cellulose nanofibers. The oxidation has imparted few new functions to scaffold used for tissue engineering applications without any significant alteration in the morphology, fiber diameter, and also the tensile strength (Luo et al. 2013).

5.9.5 Polymer Grafting

Grafting of polymers on the surface of nanocellulose can be achieved by two different approaches namely 'grafting onto' and 'grafting from'. The first approach of grafting onto deals with the attachment of polymers onto the surface of CNCs/CNFs in the presence of coupling agent. In this method, high density of grafting is not possible to achieve due to steric hindrance of polymer matrices. But the properties of material formed by this method can be easily controlled as the polymer characterization is possible before grafting (Missoum et al. 2013). In the second approach, polymer chains are grown in situ from the surface of nanocellulose by hydroxyl groups initiated polymerization. It is difficult to control the properties of grafted molecules but the grafting density can be increased by this approach (Islam et al. 2013). A study presented the grafting of poly(acrylic acid) onto cellulose microfibers where vinyl-terminated ethoxy silane was deposited onto fiber surface in the presence of potassium persulfate which acted as initiator of polymerization reaction. The grafting process was resulted in 3 times more water absorption by grafted cellulose microfibers (Loría-Bastarrachea et al. 2002). Similarly, CNCs have been grafted by surface-initiated polymerization of 4-vinylpyridine with ceric(IV) ammonium nitrate as initiator. The grafting reaction has provided controlled stability, wettability and dispersibility to CNCs in nonpolar solvents (Kan et al. 2013). In another study, surface of CNCs have been modified by grafting from PLA by ring-opening polymerization so as to improve the compatibility of CNCs and hydrophobic polymers (Peltzer et al. 2014). The grafting of poly (3-hydroxybutyrate) onto the bacterial cellulose has been reported where laccase was taken as grafting tool. The grafting has caused an increase in mechanical strength as well as hydrophilic characteristics of composite (Iqbal et al. 2014).

5.10 Nanocomposites Formation

Nanocellulose find a great role as a reinforcing agent or filler in the formation of nanocomposites as it possesses extraordinary properties of great tensile strength, thermal behavior, ease of surface modifications, and many more. These properties make nanocellulose a suitable candidate for potentiality in nanocomposites development (Siqueira et al. 2010a). Nanocomposites are solid materials which incorporate nano-sized particles into the matrix of material. Nanocomposites generally composed of different constituents, i.e., dispersed phase or fillers, interfacial region and dispersion matrix. The matrix is that phase in which nano sized filler particles are incorporated.

Commonly, nanocomposites have unique characteristics as compared to conventional composites mainly due to their large surface area to volume ratio and nanometric size effect (Mariano et al. 2014). In the nanocomposites formation, nanocellulose may have the potential to act either as matrix or fillers. The use of natural fibers like cellulose fibers is seeking attention in nanocomposites formation these days due to their cheapness, environmental friendly nature, and tendency to be recycled along with comparative mechanical properties (Kalia et al. 2011). Nanocomposites are mainly classified into natural and synthetic nanocomposites based on the constituents used. A wide variety of studies have designed for the formation of nanocomposites using nanocellulose for utility in multiple applications. A list of nanocomposites of nanocellulose is given in (Table 5.2) which describes the kind of dispersed matrix and type of fillers used in nanocomposites along with their application.

5.11 Applications of Nanocellulose and Nanocomposites in Biomedical

Nanocellulose and its nanocomposites play a great part in biomedical applications such as disease diagnostics, drug delivery for disease therapy, antibacterial activity, tissue engineering including wound healing and repair of damaged organs. The role of nanocellulose in biomedical field is attributed mainly to its biodegradable, cytocompatible, and hemocompatible nature. Some of the biomedical applications of nanocellulose and nanocomposites are discussed below.

5.11.1 Diagnostics

Polymeric materials like cellulose have been used as a support for various medical and diagnostic applications. The advantages of hydrophilicity, nontoxic nature and ease of surface modification with chemical reactivity make them suitable for diagnostic purpose (Pelton 2009). In a study, nanofibrillated cellulose have been isolated from wood by chemical and mechanical treatments and further oxidized by TEMPO mediated oxidation reaction. The oxidized nanofibrillated cellulose was then activated by EDC/NHS coupling. Then bovine serum albumin (BSA) and anti-human IgG was conjugated to the chemically activated nanocellulose fibers which acted as a platform for the immunoassays and diagnostics (Orelma et al. 2012).

In a report, it has been described that fluorescein-5′-isothiocyanate (FITC) was covalently attached to cellulose nanocrystals which will act as a technique to fluorescently label cellulose nanocrystals for bioassay and bio-imaging applications (Dong and Roman 2007). Similarly, cellulose nanofibrils have also been modified with luminescent carbon dots as an attempt to develop a nanocomposites system for bio-imaging (Junka et al. 2014). In a recent study, cellulose nanoparticles have been used as a biodegradable contrast agent in photoacoustic signaling in live mice models of ovarian cancer. The use of cellulose nanoparticles as a contrast agent in optical imaging may serve as a better agent in biomedical imaging (Jokerst et al. 2014).

5.11.2 Drug Delivery

Drug delivery system is a known program which deals with the release of drugs at an appropriate time, to specific targeted organ and in a specified amount of needed drug. Cellulose has been used as a tablet coating when blended with various drug excipients in the pharmaceutical industry (Jackson et al. 2011). The potential of use of different forms of nanocellulose such as CNCs, CNFs, BNCs and cellulose microfibrils as a carrier for drug delivery by binding and releasing drugs to a target organ have been referred in the literature. The fascinating properties of nanocellulose which are utilized in view of nanocellulose as a drug delivery carrier are porosity, network like structure, biocompatibility, nontoxic nature, low cost, and easy to obtain in nature (Trovatti et al. 2011).

Table 5.2 Nanocomposites of nanocellulose and their functions

Reinforcing material	Matrix used	Surface modification (if any)	Applications/functions	References
Titania nanoparticles along with drugs	Cellulose nanofibers	–	In transdermal drug delivery and as wound dressings	Galkina et al. (2015)
Chitin nanocrystals	Bacterial cellulose	–	Antibacterial applications	Butchosa et al. (2013)
Bacterial cellulose nanofibers	Natural rubber	Polystyrene coated bacterial cellulose	For increasing mechanical strength of natural rubber	Trovatti et al. 2013
Polyaniline	Bacterial cellulose nanofibers	–	Supercapacitor electrodes	Wang et al. (2012)
Cellulose nanofibers	Sodium caseinate protein films	–	Food packaging materials	Pereda et al. (2011)
Palladium nanoparticles	Bacterial cellulose nanofibers	–	Catalyst in chemical reactions	Zhou et al. (2012)
Collagen	Nanocellulose fibers	Oxidation to dialdehyde nanofibers	As wound dressing and tissue engineering scaffold	Lu et al. (2014)
Silver nanoparticles	Microcrystalline cellulose		Antimicrobial films	Vivekanandhan et al. (2012)
Cellulose nanocrystals	Polyurethane film	–	To increase the mechanical strength of films	Cao et al. (2009)
Nanocellulose	Poly lactide acid (PLA)	Glycidyl methacrylate grafting of cellulose nanofibers	To enhance the thermal resistance of nanocomposites	Pracella et al. (2014)
Cellulose fibers	PLA and ethylene-vinyl acetate-glycidyl Methacrylate	–	To improve the thermal, rheological and biodegradation properties of nanocomposites	Fortunati et al. (2013a)
Flax cellulose nanocrystals	Starch-based film	–	To increase mechanical strength and water resistance of starch based materials	Cao et al. (2008)
Cellulose nanocrystals	PLA films	Polyethylene grafting of cellulose nanocrystals	Scaffolds for tissue engineering	Zhang et al. (2015)
Soy cellulose microfibers	Soy protein film	–	Increased mechanical strength at elevated humidity levels	Chan et al. (2014)
Electrospun cellulose nanofibers	Soybean protein films	–	Increased the mechanical strength and young's modulus of protein films	Chen and Liu (2008)
Silk fibroin	Bacterial cellulose	–	Scaffold for tissue regeneration	Barud et al. (2015)
Cellulose nanocrystals	Chitosan polymer	Functionalization of cellulose with methyl adipoyl chloride	Enhanced mechanical strength and decreased hydrophillicity of chitosan	De Mesquita et al. (2012)
Silver nanoparticles + bacterial cellulose nanocrystals	Polyvinyl alcohol (PVA)	–	To augment the properties of PVA films	George et al. (2012)
Ag–Pd alloy nanoparticles	Cellulose nanocrystals	TEMPO mediated carboxylation of cellulose	Labels for electrical detection of DNA hybrids	Liu et al. (2011)

The biopolymeric bacterial cellulose has been used as a model carrier of serum albumins. The bacterial cellulose showed controlled drug loading and release. This has suggested that this hydrophilic, biocompatible material may serve as an innovative drug delivery vehicle (Müller et al. 2013). In another report, nanocrystalline cellulose (NCCs) has been surface modified by cetyl trimethylammonium bromide (CTAB) and loaded with hydrophobic anticancer drugs namely docetaxel, paclitaxel, and etoposide. NCCs showed the controlled release of drugs over a period of 2 days along with cellular uptake by binding to KU-7 (bladder cancer cells) which confirmed the potential of NCCs as novel drug delivery vehicles (Jackson et al. 2011). Similarly, bacterial cellulose has been used as a new drug delivery system where cellulose was loaded with berberine hydrochloride and berberine sulphate. The drug release was found to be lowest in simulated gastric fluid whereas highest release in simulated intestinal fluid. This has depicted that bacterial cellulose act as a carrier for sustained drug release (Huang et al. 2013).

The development of a dual drug delivery system was based on the pH and electro responsive characteristics of bacterial cellulose nanofibers along with sodium alginate hydrogel (nf-BC/SA). The developed hybrid hydrogel was loaded with a model drug ibuprofen. nf-BC/SA hybrid hydrogels may serve as novel promising candidates for dual controlled drug delivery systems (Shi et al. 2014). Nanocomposites of cellulose nanofibers and titania nanoparticles have also been reported for drug delivery in dermal applications. The nanocomposites was loaded with drugs like diclofenac sodium, penicillamine-D and phosphomycin. The major advantage of using titanium nanoparticles in this system was that titania has acted as binding agent between cellulose and drugs. The developed system showed the long term release profile of drugs based on different release kinetics highly depending on the type of medicine used in the nanocomposites. The developed drug delivery system may serve as anesthetics, analgesics, and wound dressing materials (Galkina et al. 2015).

5.11.3 Tissue Engineering

Nanocellulose has been used in tissue engineering applications due to its great mechanical strength, biocompatibility and inherent nontoxic nature. The high oxygen transfer rate, ease of preparation as well as surface modification, porosity, suitable viscosity and elasticity properties of nanocellulose hydrogels are extensively employed as 3D scaffold. Osteoarthritis is a disease of synovial joints due to defects in soft tissues that causes pain and loss of function. Tissue engineering may provide an artificial functional cartilage for the repair and regeneration of defected soft tissues (Elisseeff et al. 2002). To repair and regenerate cartilages, nanocomposites of porous starch/CNFs have been used for tissue engineering (Nasri-Nasrabadi et al. 2014b). Starch based films have great potential for tissue engineering as a biomaterial scaffold. CNFs have been incorporated in the starch to improve its mechanical strength, hydrophilicity, porosity and degradation rate in the living systems. The use of this biomaterial nanocomposite as a cell scaffold has increased the attachment and proliferation rate of rabbit chondrocytes (Nasri-Nasrabadi et al. 2014b). Bacterial cellulose has served as a potential scaffold for cartilage tissue engineering and supported the proliferation of human chondrocytes (Svensson et al. 2005).

Role of bacterial cellulose-collagen nanocomposites has been described in bone tissue engineering. Collagen is supposed to provide cell adhesion and enhanced cell proliferation, whereas bacterial cellulose has network structure to provide mechanical strength and barrier properties required for scaffold materials. In this case, osteogenic cells have been cultured to observe the effect of this nanocomposite on cell adhesion, proliferation and morphology. The material has allowed the formation of osteoblastic phenotype under in vitro conditions beneficial for bone tissue engineering (Saska et al. 2012). The preparation of electrospun hydroxyethyl CNFs with the coating of calcium phosphate has shown the pronounced cellular attachment and proliferation of osteosarcoma

cells, thereby, confirming the role of these nanocomposites as promising candidates for bone tissue engineering (Chahal et al. 2015).

Bionanocomposites of hyaluronic acid/CNCs has promoted the proliferative activity of human adipose derived stem cells confirming the role of this material for tissue engineering in biomedical applications (Domingues et al. 2015). Bacterial cellulose has also been used as a material in tissue engineering of cornea. Corneal disease is common ophthalmic disease present in clinical patients. The lack of corneal donors is a problem faced in the transplantation of cornea. The development of biomaterials for tissue engineering of cornea may provide the solution to this disease. Bacterial cellulose used in this regard has shown the potential to support the growth and proliferative activity of human corneal stromal cells due to its high water holding capacity as well as biocompatibility. Bacterial cellulose may be used as a scaffold for corneal tissue engineering (Hui et al. 2009).

5.11.4 Wound Repair

Wound/injury repair of skin or any other tissue requires the materials possessing tendency to provide moist environment to the wounded organ. The moisture provided by the wound dressing helps to promote the ulcer healing and also reduces pain of the patients. The wound dressing should have strong mechanical strength and should also be easy to apply and easy to remove without causing any damage to newly developed epithelium. Nanocellulose wound dressings possess all the features required for optimum wound dressing. The nanocellulose possesses high water uptake capacity, high mechanical strength, biodegradability and cytocompatibility. In this attempt, various reports have described the applicability of nanocellulose as a biomaterial for wound healing. Antibacterial silver nanoparticles/bacterial cellulose nanocomposites gel membranes have been used as wound dressing biomaterial. These nanocomposites have reduced the inflammation and pronounced the wound healing under both in vitro and in vivo systems (Wu et al. 2014). BNC has also played a role as wound dressing upon its incorporation with antiseptic drug octenidine to provide antibacterial activity. The drug loaded BNCs were found to be highly biocompatible in human keratinocytes suggesting their role in treatment of chronic wounds (Moritz et al. 2014).

Nanocomposite of bacterial cellulose–hyaluronan has also shown the potential for the treatment of severe skin injury. These nanocomposites films have shown the growth of human fibroblast cells and have also been tested for wound healing in wistar rats which showed healing in shortest time (Li et al. 2015). Bacterial cellulose isolated from *Gluconacetobacter xylinus* by multilayer fermentation method has also been used for skin tissue repair. The use of this material as a wound dressing has resulted in significant tissue regeneration and capillary formation in the wounded region showing faster and better signs of healing (Fu et al. 2012). Similarly, nanocomposites of bacterial cellulose and kaolin have been developed for wound healing purpose. Kaolin is a blood clotting factor which has been incorporated into bacterial cellulose to provide combination of short term and long term wound healing materials (Wanna et al. 2013). Bacterial cellulose–chitosan nanocomposites membranes have also been prepared for the wound healing application. The chitosan is antibacterial in nature, promote the migration as well as proliferation of fibroblast cells and further help in deposition of collagen III in the deformed skin area, thus accelerating repair of injured tissue (Lin et al. 2013).

5.11.5 Antimicrobial Activity

Nanocellulose does not show any antimicrobial activity. But the nanoscale cellulose finds a proper space in the treatment of wounds or in tissue engineering applications due to its water or moisture retaining capacity. As it keeps the wounded tissue moist, there are quite high chances of bacterial infection. To avoid the high risk of microbial infection, the antimicrobial nanocomposites have been developed.

Nanocomposites containing bacterial cellulose and silver nanoparticles have been developed which showed antibacterial activity against gram negative and gram positive bacteria (Barud et al. 2011). Similarly, nanocomposites of bacterial cellulose nanofibers and chitin nanocrystals have shown bactericidal activity (Butchosa et al. 2013). Zinc-oxide–silver NPs have been incorporated into CNCs possessing bactericidal activity (Azizi et al. 2013). Also, antibacterial nanocomposites of bacterial cellulose/poly (2-aminoethyl methacrylate) have been developed (Figueiredo et al. 2015). Bacterial cellulose-titanium dioxide nanocomposites have been reported for antibacterial activity against *E. coli* (Khan et al. 2015).

5.12 Conclusions

Cellulose is a fascinating biopolymer of great demand and is present in great abundance on global earth including green woody plants, agricultural biomass, bacteria, fungi, actinomycetes, and tunicates. Nanocellulose extracted from these sources by applying different isolation procedures possesses various self-sufficient astonishing properties different from the natural cellulose. Due to these properties, nanocellulose find a better space in wide applications such as biomedical field, drug delivery, tissue engineering, nanocomposites formation, automobile industry, digital display formation, textile industry, foods and pharmaceuticals area. There is further a scope to carry out high-end research on this subject matter to find alternative ways to modify the surface of nanocellulose so as to make it suitable for other applications where nanocellulose could act as a dispersed matrix or reinforcing agent.

Acknowledgements The authors are highly grateful to Director for providing immense facilities. We pay our great gratitude toward Council of Scientific and Industrial Research, New Delhi for financial assistance. RS is highly thankful to UGC for providing senior research fellowship. Academy of Scientific and Innovative Research, New Delhi is duly acknowledged.

References

Abdel-Halim ES (2014) Chemical modification of cellulose extracted from sugarcane bagasse: preparation of hydroxyethyl cellulose. Arab J Chem 7:362–371

Abe K, Iwamoto S, Yano H (2007) Obtaining cellulose nanofibers with a uniform width of 15 nm from wood. Biomacromolecules 8:3276–3278

Abe K, Yano H (2009) Comparison of the characteristics of cellulose microfibril aggregates of wood, rice straw and potato tuber. Cellulose 16:1017–1023

Abou-Zeid RE, Hassan EA, Bettaieb F et al (2015) Use of cellulose and oxidized cellulose nanocrystals from olive stones in chitosan bionanocomposites. J Nanomater 2015. doi:10.1155/2015/687490

Alemdar A, Sain M (2008) Isolation and characterization of nanofibers from agricultural residues–Wheat straw and soy hulls. Bioresour Technol 99:1664–1671

Azizi S, Ahmad MBH, Hussein MZ et al (2013) Synthesis, antibacterial and thermal studies of cellulose nanocrystal stabilized ZnO-Ag heterostructure nanoparticles. Molecules 18:6269–6280

Barud HO, Barud HDS, Cavicchioli M et al (2015) Preparation and characterization of a bacterial cellulose/silk fibroin sponge scaffold for tissue regeneration. Carbohydr Polym 128:41–51

Barud HS, Regiani T, Marques RF et al (2011) Antimicrobial bacterial cellulose-silver nanoparticles composite membranes. J Nanomater 2011. doi:10.1155/2011/721631

Bledzki AK, Gassan J (1999) Composites reinforced with cellulose based fibres. Prog Polym Sci 24:221–274

Bras DL, Stromme M, Mihranyan A (2015) Characterization of dielectric properties of nanocellulose from wood and algae for electrical insulator applications. J Phys Chem B 119:5911–5917

Braun B, Dorgan JR (2009) Single-step method for the isolation and surface functionalization of cellulosic nanowhiskers. Biomacromolecules 10:334–341

Brinchi L, Cotana F, Fortunati E et al (2013) Production of nanocrystalline cellulose from lignocellulosic biomass: technology and applications. Carbohydr Polym 94:154–169

Brito BSL, Pereira FV, Putaux JL et al (2012) Preparation, morphology and structure of cellulose nanocrystals from bamboo fibers. Cellulose 19:1527–1536

Butchosa N, Brown C, Larsson PT et al (2013) Nanocomposites of bacterial cellulose nanofibers and chitin nanocrystals: fabrication, characterization and bactericidal activity. Green Chem 15:3404–3413

Cao X, Chen Y, Chang PR, Muir AD et al (2008) Starch-based nanocomposites reinforced with flax cellulose nanocrystals. Express Polym Lett 2(7):502–510

Cao X, Habibi Y, Lucia LA (2009) One-pot polymerization, surface grafting, and processing of waterborne polyurethane-cellulose nanocrystal nanocomposites. J Mater Chem 19(38):7137–7145

Chahal S, Hussain FSJ, Kumar A et al (2015) Electrospun hydroxyethyl cellulose nanofibers functionalized with calcium phosphate coating for bone tissue engineering. RSC Adv 5:29497–29504

Chan R, Lim LT, Barbut S et al (2014) Extrusion and characterization of soy protein film incorporated with soy cellulose microfibers. Int Polym Process 29(4):467–476

Chen G, Liu H (2008) Electrospun cellulose nanofiber reinforced soybean protein isolate composite film. J Appl Polym Sci 110(2):641–646

Cheng Q, Wang S, Harper DP (2009) Effects of process and source on elastic modulus of single cellulose fibrils evaluated by atomic force microscopy. Compos Part A 40:583–588

Cherian BM, Pothan LA, Nguyen-Chung T et al (2008) A novel method for the synthesis of cellulose nanofibril whiskers from banana fibers and characterization. J Agric Food Chem 56:5617–5627

Correa AC, Teixeira EDM, Pessan LA et al (2010) Cellulose nanofibers from curaua fibers. Cellulose 17:1183–1192

Das M, Chakraborty D (2008) Evaluation of improvement of physical and mechanical properties of bamboo fibers due to alkali treatment. J Appl Polym 107:522–527

de Campos A, Correa AC, Cannella D et al (2013) Obtaining nanofibers from curaua and sugarcane bagasse fibers using enzymatic hydrolysis followed by sonication. Cellulose 20:1491–1500

de Mesquita JP, Donnici CL, Teixeira IF et al (2012) Bio-based nanocomposites obtained through covalent linkage between chitosan and cellulose nanocrystals. Carbohydr Polym 90(1):210–217

Deepa B, Abraham E, Cherian BM et al (2011) Structure, morphology and thermal characteristics of banana nano fibers obtained by steam explosion. Bioresource Technol 102:1988–1997

Domingues RM, Silva M, Gershovich P et al (2015) Development of injectable hyaluronic acid/cellulose nanocrystals bionanocomposite hydrogels for tissue engineering applications. Bioconjug Chem 26:1571–1581

Dong S, Roman M (2007) Fluorescently labeled cellulose nanocrystals for bioimaging applications. J Am Chem Soc 129:13810–13811

Dufresne A (2013) Nanocellulose: a new ageless bionanomaterial. Mater Today 16(6):220–227

Dufresne A, Dupeyre D, Vignon MR (2000) Cellulose microfibrils from potato tuber cells: processing and characterization of starch–cellulose microfibril composites. J Appl Polym Sci 76:2080–2092

Duran N, Lemes AP, Duran M et al (2011) A minireview of cellulose nanocrystals and its potential integration as co-product in bioethanol production. J Chil Chem Soc 56:672–677

Edgar CD, Gray DG (2001) Induced circular dichroism of chiral nematic cellulose films. Cellulose 8:5–12

Eichhorn SJ, Dufresne A, Aranguren M et al (2010) Review: current international research into cellulose nanofibres and nanocomposites. J Mater Sci 45:1–33

Elisseeff JH, Lee A, Kleinman HK et al (2002) Biological response of chondrocytes to hydrogels. In: Sipe JD, Kelley CA, McNichol LA (eds) Reparative medicine: growing tissues and organs, vol 961. New York Academy of Science, New York, pp 118–122

Fahma F, Iwamoto S, Hori N et al (2010) Isolation, preparation, and characterization of nanofibers from oil palm empty-fruit-bunch (OPEFB). Cellulose 17:977–985

Figueiredo AR, Figueiredo AG, Silva NH et al (2015) Antimicrobial bacterial cellulose nanocomposites prepared by in situ polymerization of 2-aminoethyl methacrylate. Carbohydr Polym 123:443–453

Fortunati E, Puglia D, Kenny JM et al (2013a) Effect of ethylene-co-vinyl acetate-glycidylmethacrylate and cellulose microfibers on the thermal, rheological and biodegradation properties of poly (lactic acid) based systems. Polym Degrad Stability 98(12):2742–2751

Fortunati E, Puglia D, Monti M et al (2013b) Cellulose nanocrystals extracted from okra fibers in PVA nanocomposites. J Appl Polym Sci 128:3220–3230

Frone AN, Berlioz S, Chailan JF (2011) Cellulose fiber-reinforced polylactic acid. Polym Compos 32:976–985

Fu L, Zhang Y, Li C (2012) Skin tissue repair materials from bacterial cellulose by a multilayer fermentation method. J Mater Chem 22:12349–12357

Galkina OL, Ivanov VK, Agafonov AV (2015) Cellulose nanofiber–titania nanocomposites as potential drug delivery systems for dermal applications. J Mater Chem B 3:1688–1698

George J, Ramana KV, Bawa AS (2011) Bacterial cellulose nanocrystals exhibiting high thermal stability and their polymer nanocomposites. Int J Biol Macromol 48:50–57

George J, Ramana KV, Sabapathy SN et al (2005) Physico-mechanical properties of chemically treated bacterial (Acetobacter xylinum) cellulose membrane. World J Microbiol Biotechnol 21:1323–1327

George J, Sabapathi S (2015) Cellulose nanocrystals: synthesis, functional properties, and applications. Nanotechnol Sci Appl 8:45–54

George J, Sajeevkumar VA, Ramana KV et al (2012) Augmented properties of PVA hybrid nanocomposites containing cellulose nanocrystals and silver nanoparticles. J Mater Chem 22(42):22433–22439

Goelzer FDE, Faria-Tischer PCS, Vitorino JC et al (2009) Production and characterization of nanospheres of bacterial cellulose from Acetobacter xylinum from processed rice bark. Mater Sci Eng, C 29:546–551

Gousse C, Chanzy H, Cerrada ML et al (2004) Surface silylation of cellulose microfibrils: preparation and rheological properties. Polymer 45:1569–1575

Habibi Y (2014) Key advances in the chemical modification of nanocelluloses. Chem Soc Rev 43:1519–1542

Habibi Y, Lucia LA, Rojas OJ (2010) Cellulose nanocrystals: chemistry, self-assembly, and applications. Chem Rev 110:3479–3500

Hardelin L, Perzon E, Hagstrom B et al (2013) Influence of molecular weight and rheological behavior on electrospinning cellulose nanofibers from ionic liquids. J Appl Polym Sci 130:2303–2310

Henriksson M, Henriksson G, Berglund LA et al (2007) An environmentally friendly method for enzyme-assisted preparation of microfibrillated cellulose (MFC) nanofibers. Eur Polym J 43:3434–3441

Heux L, Chauve G, Bonini C (2000) Nonflocculating and chiral-nematic self-ordering of cellulose microcrystals suspensions in nonpolar solvents. Langmuir 16:8210–8212

Hsieh Y-C, Yano H, Nogi M et al (2008) An estimation of the young's modulus of bacterial cellulose filaments. Cellulose 15:507–513

Huang L, Chen X, Nguyen TX et al (2013) Nano-cellulose 3D-networks as controlled-release drug carriers. J Mater Chem B 1:2976–2984

Hui J, Yuanyuan J, Jiao W et al (2009) Potentiality of bacterial cellulose as the scaffold of tissue engineering of cornea. In: Biomedical engineering and informatics, BMEI'09: 2nd international conference. IEEE, pp 1–5

Imai T, Putaux JL, Sugiyama J (2003) Geometric phase analysis of lattice images from algal cellulose microfibrils. Polymer 44:1871–1879

Iqbal HM, Kyazze G, Tron T et al (2014) Laccase-assisted grafting of poly (3-hydroxybutyrate) onto the bacterial cellulose as backbone polymer: development and characterisation. Carbohydr Polym 113:131–137

Islam MT, Alam MM, Zoccola M (2013) Review on modification of nanocellulose for application in composites. Int J Innovative Res Sci Engand Technol 2(10):5451

Isogai A, Saito T, Fukuzumi H (2011) TEMPO-oxidized cellulose nanofibers. Nanoscale 3:71–85

Iwamoto S, Isogai A, Iwata T (2011) Structure and mechanical properties of wet-spun fibers made from natural cellulose nanofibers. Biomacromolecules 12:831–836

Jackson JK, Letchford K, Wasserman BZ (2011) The use of nanocrystalline cellulose for the binding and controlled release of drugs. Inter J Nanomed 6:321

Jokerst JV, Van de Sompel D, Bohndiek SE et al (2014) Cellulose nanoparticles are a biodegradable photoacoustic contrast agent for use in living mice. Photoacoustics 2:119–127

Junka K, Guo J, Filpponen I et al (2014) Modification of cellulose nanofibrils with luminescent carbon dots. Biomacromolecules 15:876–881

Kaboorani A, Riedl B (2015) Surface modification of cellulose nanocrystals (CNC) by a cationic surfactant. Ind Crops Prod 65:45–55

Kalia S, Dufresne A, Cherian BM et al (2011) Cellulose-based bio-and nanocomposites: a review. Int J Polym Sci 2011. doi:10.1155/2011/837875

Kan KH, Li J, Wijesekera K et al (2013) Polymer-grafted cellulose nanocrystals as pH-responsive reversible flocculants. Biomacromolecules 14:3130–3139

Karadag A, Ozcelik B, Huang Q (2014) Quercetin nanosuspensions produced by high-pressure homogenization. J Agric Food Chem 62:1852–1859

Kargarzadeh H, Ahmad I, Abdullah I et al (2012) Effects of hydrolysis conditions on the morphology, crystallinity, and thermal stability of cellulose nanocrystals extracted from Kenaf bast fibers. Cellulose 19:855–866

Kaushik A, Singh M (2011) Isolation and characterization of cellulose nanofibrils from wheat straw using steam explosion coupled with high shear homogenization. Carbohydr Res 346:76–85

Keshk SMAS (2014) Bacterial cellulose production and its industrial applications. J Bioprocess Biotech 4:150–160

Khan S, Ul-Islam M, Khattak WA et al (2015) Bacterial cellulose-titanium dioxide nanocomposites: nanostructural characteristics, antibacterial mechanism, and biocompatibility. Cellulose 22:565–579

Klemm D, Heublein B, Fink HP et al (2005) Cellulose: fascinating biopolymer and sustainable raw material. Angew Chem Int Ed 44:3358–3393

Klemm D, Kramer F, Moritz S et al (2011) Nanocelluloses: a new family of nature-based materials. Angew Chem Int Ed 50:5438–5466

Krassig HA (ed) (1993) Cellulose-structure, accessibility and reactivity. Gordon and Breach Science Publishers, Yverdon, Switzerland, pp 307–314

Lavoine N, Desloges I, Dufresne A et al (2012) Microfibrillated cellulose—its barrier properties and applications in cellulosic materials: a review. Carbohydr Polym 90:735–764

Lee KY, Tang M, Williams CK et al (2012) Carbohydrate derived copoly (lactide) as the compatibilizer for bacterial cellulose reinforced polylactide nanocomposites. Compos Sci Technol 72:1646–1650

Li J, Wei X, Wanga Q et al (2012) Homogeneous isolation of nanocellulose from sugarcane bagasse by high pressure homogenization. Carbohydr Polym 90:1609–1613

Li Y, Jiang H, Zheng W et al (2015) Bacterial cellulose–hyaluronan nanocomposite biomaterials as wound dressings for severe skin injury repair. J Mater Chem B 3:3498–3507

Lin N, Dufresne A (2014) Nanocellulose in biomedicine: current status and future prospect. Eur Polym J 59:302–325

Lin WC, Lien CC, Yeh HJ et al (2013) Bacterial cellulose and bacterial cellulose–chitosan membranes for wound dressing applications. Carbohydr Polym 94:603–611

Liu D, Chen X, Yue Y et al (2011) Structure and rheology of nanocrystalline cellulose. Carbohydr Polym 84:316–322

Loría-Bastarrachea MI, Carrillo-Escalante HJ, Aguilar-Vega MJ (2002) Grafting of poly (acrylic acid) onto cellulosic microfibers and continuous cellulose filaments and characterization. J Appl Polym Sci 83:386–393

Lu J, Askeland P, Drzal LT (2008) Surface modification of microfibrillated cellulose for epoxy composite applications. Polymer 49:1285–1296

Lu T, Li Q, Chen W et al (2014) Composite aerogels based on dialdehyde nanocellulose and collagen for potential applications as wound dressing and tissue engineering scaffold. Compos Sci Technol 94:132–138

Luo H, Xiong G, Hu D et al (2013) Characterization of TEMPO-oxidized bacterial cellulose scaffolds for tissue engineering applications. Mater Chem Phys 143:373–379

Mariano M, El Kissi N, Dufresne A (2014) Cellulose nanocrystals and related nanocomposites: review of some properties and challenges. J Polym Sci B: Polym Phys 52:791–806

Miettinen A, Chinga-Carrasco G, Kataja M (2014) Three-dimensional microstructural properties of nanofibrillated cellulose films. Int J Mol Sci 15:6423–6440

Missoum K, Belgacem MN, Bras J (2013) Nanofibrillated cellulose surface modification: a review. Materials 6:1745–1766

Moon RJ, Martini A, Nairn J et al (2011) Cellulose nanomaterials review: structure, properties and nanocomposites. J Chem Soc Rev 40:3941–3994

Moritz S, Wiegand C, Wesarg F et al (2014) Active wound dressings based on bacterial nanocellulose as drug delivery system for octenidine. Int J Pharm 471:45–55

Müller A, Ni Z, Hessler N et al (2013) The biopolymer bacterial nanocellulose as drug delivery system: investigation of drug loading and release using the model protein albumin. J Pharm Sci 102:579–592

Nakagaito AN, Yano H (2004) The effect of morphological changes from pulp fiber towards nano-scale fibrillated cellulose on the mechanical properties of high-strength plant fiber based composites. Appl Phys A-Mater Sci Process 78:547–552

Nasri-Nasrabadi B, Behzad T, Bagheri R (2014a) Extraction and characterization of rice straw cellulose nanofibers by an optimized chemomechanical method. J Appl Polym Sci 131:40063–40070

Nasri-Nasrabadi B, Mehrasa M, Rafienia M et al (2014b) Porous starch/cellulose nanofibers composite prepared by salt leaching technique for tissue engineering. Carbohydr Polym 108:232–238

Nguyen HD, Mai TTT, Nguyen NB et al (2013) A novel method for preparing microfibrillated cellulose from bamboo fibers. Adv Nat Sci Nanosci Nanotechnol 4:015016

Nishiyama Y, Sugiyama J, Chanzy H (2002) Crystal structure and hydrogen-bonding system in cellulose Iβ from synchrotron X-ray and neutron fiber diffraction. J Am Chem Soc 124:9074–9082

Olsson RT, Kraemer R, Rubio AL et al (2010) Extraction of microfibrils from bacterial cellulose networks for electrospinning of anisotropic biohybrid fiber yarns. Macromolecules 43:4201–4209

Orelma H, Filpponen I, Johansson LS et al (2012) Surface functionalized nanofibrillar cellulose (NFC) film as a platform for immunoassays and diagnostics. Biointerphases 7(1):61. doi:10.1007/s13758-012-0061-7

Pedersen M, Meyer AS (2010) Lignocellulose pretreatment severity-relating pH to biomatrix opening. New Biotechnol 27:739–750

Pelton R (2009) Bioactive paper provides a low-cost platform for diagnostics. Trac-Trend Anal Chem 28:925–942

Peltzer M, Pei A, Zhou Q et al (2014) Surface modification of cellulose nanocrystals by grafting with poly (lactic acid). Polym Int 63:1056–1062

Pereda M, Amica G, Rácz I et al (2011) Structure and properties of nanocomposite films based on sodium caseinate and nanocellulose fibers. J Food Eng 103 (1):76–83

Pracella M, Haque MMU, Puglia D (2014) Morphology and properties tuning of PLA/cellulose nanocrystals bio-nanocomposites by means of reactive functionalization and blending with PVAc. Polymer 55 (16):3720–3728

Qian Y, Qin Z, Vu NM et al (2012) Comparison of nanocrystals from TEMPO oxidation of bamboo, softwood, and cotton linter fibers with ultrasonic-assisted process. BioRes 7:4952–4964

Roohani M, Habibi Y, Belgacem NM et al (2008) Cellulose whiskers reinforced polyvinyl alcohol copolymers nanocomposites. J Eur Polym 44:2489–2498

Rosa SM, Rehman N, de Miranda MIG et al (2012) Chlorine-free extraction of cellulose from rice husk and whisker isolation. Carbohydr Polym 87:1131–1138

Rosli NA, Ahmad I, Abdullah I (2013) Isolation and characterization of cellulose nanocrystals from Agave angustifolia fibre. BioRes 8:1893–1908

Sacui IA, Nieuwendaal RC, Burnett DJ et al (2014) Comparison of the properties of cellulose nanocrystals and cellulose nanofibrils isolated from bacteria, tunicate, and wood processed using acid, enzymatic, mechanical, and oxidative methods. ACS Appl Mater Interfaces 6(9):6127–6138

Saheb DN, Jog JP (1999) Natural fiber polymer composites: a review. Adv Polym Technol 18:351–363

Saito T, Isogai A (2005) Ion-exchange behavior of carboxylate groups in fibrous cellulose oxidized by the TEMPO mediated system. Carbohydr Polym 61:183–190

Saska S, Teixeira LN, de Oliveira PT et al (2012) Bacterial cellulose-collagen nanocomposite for bone tissue engineering. J Mater Chem 22(41):22102–22112

Shamsabadi MA, Behzad T, Bagheri R (2015) Optimization of acid hydrolysis conditions to improve cellulose nanofibers extraction from wheat straw. Fiber Polym 16:579–584

Sheykhnazari S, Tabarsa T, Ashori A et al (2011) Bacterial synthesized cellulose nanofibers; effects of

growth times and culture mediums on the structural characteristics. Carbohydr Polym 86:1187–1191
Shi X, Zheng Y, Wang G et al (2014) pH-and electro-response characteristics of bacterial cellulose nanofiber/sodium alginate hybrid hydrogels for dual controlled drug delivery. RSC Adv 4:47056–47065
Silverio HA, Neto WPF, Dantas NO et al (2013) Extraction and characterization of cellulose nanocrystals from corncob for application as reinforcing agent in nanocomposites. Ind Crop Prod 44:427–436
Siqueira G, Bras J, Dufresne A (2010a) Cellulosic bionanocomposites: a review of preparation, properties and applications. Polymers 2:728–765
Siqueira G, Tapin-Lingua S, Bras J et al (2010b) Morphological investigation of nanoparticles obtained from combined mechanical shearing, and enzymatic and acid hydrolysis of sisal fibers. Cellulose 17:1147–1158
Siro I, Plackett D (2010) Microfibrillated cellulose and new nanocomposite materials: a review. Cellulose 17:459–494
Sjostrom E (ed) (1993) Wood chemistry: fundamentals and application. Academic Press Inc., San Diego, USA
Somerville C (2006) Cellulose synthesis in higher plants. Annu Rev Cell Dev Biol 22:53–78
Stelte W, Sanadi AR (2009) Preparation and characterization of cellulose nanofibers from two commercial hardwood and softwood pulps. Ind Eng Chem Res 48:11211–11219
Svensson A, Nicklasson E, Harrah T et al (2005) Bacterial cellulose as a potential scaffold for tissue engineering of cartilage. Biomaterials 26:419–431
Thomas V, Namdeo M, Murali Mohan Y et al (2007) Review on polymer, hydrogel and microgel metal nanocomposites: a facile nanotechnological approach. J Macromol Sci A-Pure Appl Chem 45:107–119
Torres FG, Diaz RM (2004) Morphological characterization of natural fibre reinforced thermoplastics (NFRTP) processed by extrusion, compression and rotational moulding. Polym Polym Compos 12:705–718
Trovatti E, Silva NH, Duarte IF et al (2011) Biocellulose membranes as supports for dermal release of lidocaine. Biomacromolecules 12:4162–4168
Trovatti E, Carvalho AJ, Ribeiro SJ et al (2013) Simple green approach to reinforce natural rubber with bacterial cellulose nanofibers. Biomacromolecules 14:2667–2674
Vivekanandhan S, Christensen L, Misra M et al (2012) Green process for impregnation of silver nanoparticles into microcrystalline cellulose and their antimicrobial bionanocomposite films. J Biomater Nanobiotechnol 3. doi:10.4236/jbnb.2012.33035
Wang B, Sain M (2007) Dispersion of soybean stock-based nanofiber in a plastic matrix. Polym Int 56:538–546
Wang H, Zhu E, Yang J et al (2012) Bacterial cellulose nanofiber-supported polyaniline nanocomposites with flake-shaped morphology as supercapacitor electrodes. J Phys Chem C 116(24):13013–13019
Wang S, Cheng Q (2009) A novel process to isolate fibrils from cellulose fibers by high-intensity ultrasonication, part 1: process optimization. J Appl Polym Sci 113:1270–1275
Wang Y, Wei X, Li J et al (2015) Study on nanocellulose by high pressure homogenization in homogeneous isolation. Fiber Polym 16:572–578
Wanna D, Alam C, Toivola DM et al (2013) Bacterial cellulose–kaolin nanocomposites for application as biomedical wound healing materials. Adv Nat Sci Nanosci Nanotechnol 4:045002
Williams GI, Wool RP (2000) Composites from natural fibers and soy oil resins. Appl Compos Mater 7:421–432
Williamson RE, Burn JE, Hocart CH (2002) Towards the mechanism of cellulose synthesis. Trends Plant Sci 7:461–467
Wu J, Zheng Y, Wen X et al (2014) Silver nanoparticle/bacterial cellulose gel membranes for antibacterial wound dressing: investigation in vitro and in vivo. Biomed Mater 9:035005
Xiong R, Zhang X, Tian D et al (2012) Comparing microcrystalline with spherical nanocrystalline cellulose from waste cotton fabrics. Cellulose 19:1189–1198
Yadav R, Kumar D, Kumari A et al (2014) Encapsulation of catechin and epicatechin on BSA NPs improved their stability and antioxidant potential. EXCLI J 13:331–346
Yan M, Li S, Zhang M et al (2013) Characterization of surface acetylated nanocrystalline cellulose by single-step method. BioRes 8:6330–6341
Yu HY, Chen R, Chen GY et al (2015) Silylation of cellulose nanocrystals and their reinforcement of commercial silicone rubber. J Nanopart Res 17:1–3
Yuan H, Nishiyama Y, Wada M et al (2006) Surface acylation of cellulose whiskers by drying aqueous emulsion. Biomacromolecules 7:696–700
Zhang C, Salick MR, Cordie TM et al (2015) Incorporation of poly (ethylene glycol) grafted cellulose nanocrystals in poly (lactic acid) electrospun nanocomposite fibers as potential scaffolds for bone tissue engineering. Mater Sci Eng, C 49:463–471
Zhao Y, Li J (2014) Excellent chemical and material cellulose from tunicates: diversity in cellulose production yield and chemical and morphological structures from different tunicate species. Cellulose 21:3427–3441
Zhou P, Wang H, Yang J et al (2012) Bacteria cellulose nanofibers supported palladium (0) nanocomposite and its catalysis evaluation in Heck reaction. Ind Eng Chem Res 51(16):5743–5748
Zuluaga R, Putaux JL, Mondragon ARI et al (2007) Cellulose microfibrils from banana farming residues: isolation and characterization. Cellulose 14:585–592

Theragnosis: Nanoparticles as a Tool for Simultaneous Therapy and Diagnosis

6

Shanka Walia and Amitabha Acharya

Abstract

Theragnostic NPs give new hope in simultaneous diagnosis and therapy of a disease at curable stage. Theragnosis is the fundamental requirement of personalized medicine. For successful theragnosis applications, the imaging agents and drugs should be efficiently delivered, resulting in adequate imaging signal or drug concentration in the targeted disease site. The selection of NPs for imaging, diagnosis and therapy was based on their biomimetic features with higher surface to volume ratio of the nanomaterials. The essential properties of nanomedicines involve early and precise diagnosis of clinical conditions providing an efficient treatment without secondary effects. Thus, nanotheragnostic probes are much better than conventional treatments where the diagnosis and therapy are way apart from each other. This chapter briefs about the recent advancement of nanotheragnosis research with future scope and associated hurdles.

Keywords

Theragnositic NPs · Optical imaging · MRI · PET/SPECT · Contrasting agents · Trimodal imaging · Chemotherapy · Nanotoxicity

S. Walia · A. Acharya (✉)
Department of Biotechnology, Council of Scientific and Industrial Research-Institute of Himalayan Bioresource Technology, Palampur 176061, Himachal Pradesh, India
e-mail: amitabhachem@gmail.com
amitabha@ihbt.res.in

S. Walia · A. Acharya
Academy of Scientific and Innovative Research, New Delhi, India

© Springer Science+Business Media Singapore 2016

S.K. Yadav (ed.), *Nanoscale Materials in Targeted Drug Delivery, Theragnosis and Tissue Regeneration*, DOI 10.1007/978-981-10-0818-4_6

Contents

6.1 Introduction

In present era, early and effective diagnosis of severe diseases like cancer, HIV-AIDS, diabetes, etc., is an essential requirement. Delayed, defective diagnosis and nonspecific targeted delivery of drugs are some of the major drawbacks of conventional techniques of preclinical examination and disease treatment (Krishanan 2010; Choi et al. 2012). However, the development of such a diagnostic probe which can overcome these limitations in clinical world had still remained a dream. Research has played an important role in this aspect, and a new concept "theragnosis" came into origin. Theragnosis lead to the recognition of a specific disease and therapeutic efficacy of drug and its targeted delivery to the disease site. Theragnosis is a modern technique with dual property of imaging and treatment of a specific disease. Theragnosis encompassed two different applications on same platform resulting in the identification and curing of disease using single probe. The arrival of nanoparticles (NPs) in the medical field fulfilled the dream of the target-specific treatments with rapid efficacy and also development of diagnosis and treatment probe simultaneously (Janib et al. 2010; Bwatanglang et al. 2014). The synthesis of materials at nanoscale level changes their physical as well as chemical properties. The size of the NPs is in the range of series of biomolecules viz., proteins (1–20 nm), deoxyribonucleic acid (DNA, <diameter 2 nm), cell membrane (<6–10 nm), virus (<20 nm), hemoglobin (<5 nm), etc. (Acharya 2013). The selection of NPs for imaging, diagnosis, and therapy was based on such biomimetic features with higher surface to volume ratio of these nanomaterials (Pison et al. 2006; Yezhelyev et al. 2006). The essential properties of nanomedicines involve early and precise diagnosis of clinical conditions providing an efficient treatment without secondary effects. These requirements can be customize at nanoscale level (Sanvicens and Marco 2008; Salvador-Morales et al. 2009).

Though there are many achievements made by the scientists in medicinal world, the conflict on disease is still unsettled. The recognition of different dreadful diseases and their effect on different patients is the main reason behind this war. This led researcher to believe that each patient required disease specific therapy based on the differences in genetic factors, physical conditions, and

environmental factors. The entire knowledge about disease and patient is required for this approach (personalized medicine). The in vivo imaging techniques for noninvasive diagnosis act as a powerful tool in monitoring the disease site and biological situation of body (Lee et al. 2012). The traditional imaging techniques in the clinic include optical imaging, magnetic resonance imaging (MRI), computed tomography (CT), ultrasound (US), and positron emission tomography (PET) or single photon emission computed tomography (SPECT). The high spatial resolution is the characteristic feature of primarily morphological/anatomical imaging technologies, such as CT, MRI (with contrast agents injected at millimolar blood concentrations), and US. However, they also contribute to the limitation of not being able to detect diseases until tissue structural changes (for example, growth of a tumor) are large enough to be detected by the imaging modality. Primarily molecular imaging modalities, such as optical imaging, PET, and SPECT (with radiotracers injected at nanomolar blood concentrations), offer the potential to detect molecular and cellular changes of diseases (for example, before the tumor is large enough to cause structural changes). However, these modalities suffer from a poor spatial resolution (Willmann et al. 2008). The innovative wave of multimodal imaging brought new hope in imaging the disease site with high sensitivity and spatial resolution. The team work of Townsend and colleagues in collaboration with Siemens Medical led to the invention of first fused PET/CT instrument in 1988 and commercialized in 2001. This gave an innovation to the combination of PET/MRI, in which PET due to its high sensitivity can scan the tissue of interest in very short time by reducing the volume of targeted tissue. This can be now imaged by high resolution MRI (Ell 2006; Cherry et al. 2008; Jarrett et al. 2008; Jennings and Long 2009). The rise of these new hybrid technology attracted researchers in designing and development of such probes for clinical benefit. In this aspect, nanoscale multimodal imaging probe plays an important role as they can hold two or more imaging agents. Simultaneously, these overcome the limitations of single imaging probe providing full details of the target site via targeted delivery. There is class of inorganic NPs which behave as imaging agents such as iron oxide (IO) for MRI, gold NPs (AuNPs) for CT, and quantum dots (QDs) for optical imaging. The multimodal imaging probes can be developed by combining these imaging agents via conjugation or co-encapsulation. The organic NPs like liposomes, micelles, polymeric NPs, etc., also play an important role in the integration of these imaging probes in the interior or on their surfaces (Jennings and Long 2009; Louie 2010). Recently, trimodal imaging probes by combining radiometal chelates, such as ^{64}Cu-1,4,7,10-tetraazacyclododecane-1, 4,7,10-tetraacetic acid (DOTA) and Indium (^{111}In)-DOTA, to dual MRI/optical probes for PET/optical/MRI have also been designed (Xie et al. 2010a). The combination of different imaging modalities are expected to have many advantages like more precise and detailed information, high sensitivity, and spatial resolution and these are expected to compensate each other's drawbacks. But for the development of such an imaging probe, one should take into account the rational selection based on sensitivity and concentration of the imaging agent to be used (viz., PET or near-infrared fluorescence (NIRF) agents can be used in extremely low concentrations, while MR and CT agents need relatively high concentrations), probhition of the overlapping of advantages and overcome the weak points of each selected imaging modality to increase the efficiency of the multimodal probe. This is the reason that the imaging modalities with high sensitivity (PET, optical, etc.) are frequently combined with other imaging modalities with high spatial resolution (MR, CT, etc.) (Willmann et al. 2008; Jennings and Long 2009). Here in this chapter, detailed discussions have been included in nanoparticles-based single and multimodal imaging agents with special reference to theragnosis concept.

6.2 Nanomaterials in Disease Diagnosis and Therapy

The origin of NPs and their applications in medicine have revolutionized the twentieth century. NPs provide various facilities in medical field

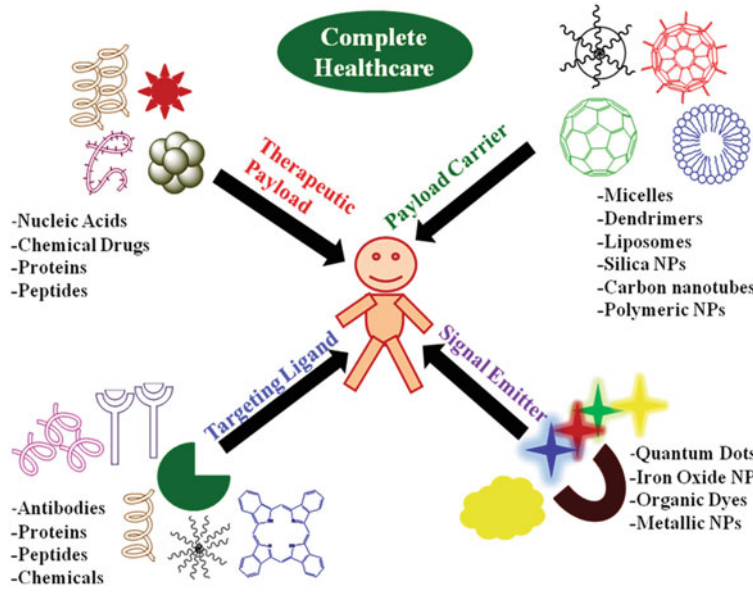

Fig. 6.1 Nanomaterials for simultaneous disease diagnosis and therapy

ranging from diagnosis to therapies (Taton 2002). Nanotechnology at its infant stage was studied because of its physicochemical properties, but now they have entered the commercial world (Murray et al. 2000; Mazzola 2003; Paull et al. 2003). The selection of theragnostic NPs is dependent on four components viz., signal emitter, therapeutic payload, payload carrier, and targeting ligand (Fig. 6.1). The signal emitter emits signals physically or by absorbing energy from external sources. The therapeutic payload can be chemotherapeutic drugs, or nucleic acids, such as DNA and small interfering ribonucleic acid (siRNA). The payload carrier can be polymeric matrix with multiple functional groups on which signal emitters or therapeutic payloads can be conjugated. The targeting ligand attached on the NP surface can be utilized for recognizing specific disease marker on the target cell, facilitating the delivery and specific interactions of theragnostic NP to the targeted cells or tissues (Fang and Zhang 2010). The details of the different payload carriers have been discussed in next sections.

6.2.1 Metallic Nanoparticles

The metallic NPs are used at large scale for biomedical applications because of their unique physicochemical properties due to the presence of large amount of high energy surface atoms than in the bulk material (Valden et al. 1998; El-Sayed 2001). The well-known metallic NPs in the field of pharmaceutics are silver (Ag), gold (Au), iron oxide (IO), titanium dioxide (TiO_2), copper (Cu), zinc oxide (ZnO), etc. These are used especially in cancer treatment, biosensing, and imaging drug delivery (Nikalje 2015). Their synthesis involves different wet chemical methods among which the use of excess of reducing agents like sodium citrate or sodium borohydride (Creighton et al. 1979; Panigrahi et al. 2004), use of mesityl derivatives for the synthesis of Ag, Au, and Cu NPs (Bunge et al. 2003) are most common. Nowadays, green approaches are also applied for the synthesis of metallic NPs (Makarov et al. 2014). This point has been discussed in detail in Chap. 3.

6.2.2 Quantum Dots

QDs are fluorescent semiconductor nanocrystals having optical properties. These fluorescent semiconductor nanocrystals, contain an inorganic core, and sometimes shell, and an organic, biocompatible coating. They are very small in size ranging from 5 to 50 nm. QDs exhibit higher

photostability, extinction coefficient, and quantum yield, and can also provide broadband absorption, narrow and tunable emission spectra, and multivalent ligand conjugation as compared to conventional organic fluorophores (Gao et al. 2004; Kim et al. 2004; Smith et al. 2004). QDs provide information of biochemical processes and cancer metastases in living animals (Akerman et al. 2002; Gao et al. 2004; Cai et al. 2006). QDs with appropriate size (10–30 nm) and fluorescence of near-infrared (NIR) emission viz., InAs/ZnS (Choi et al. 2009), $InAs_xP_{1-x}$/InP/ZnSe (Kim et al. 2005), CdTe/CdSe (Kim et al. 2004), and Cu–In–Se (Allen and Bawendi 2008) have extensively been used for sentinel lymph node mapping (Kim et al. 2004, 2005; Ohnishi et al. 2005; Parungo et al. 2005; Zimmer et al. 2006; Frangioni et al. 2007; Knapp et al. 2007). These fluorescent NPs can also be modified to target living organisms by conjugating them with small molecules, peptides, proteins, or antibodies (Han et al. 2001; Cai et al. 2006; Nie et al. 2007). In a recent work done by Hu et al. (2015) NIR-II Ag_2S QD has been used for theragnositic purposes. For clinical use they have first coated these NPs with biocompatible poly (maleic-anhydride-*alt*-1-octadecene) polyethylene glycol and then a therapeutic drug, doxorubicin (DOX), was loaded inside polyethylene glycol (PEG)/silver sulfide QDs. The NIR-II QDs allow deep tissue imaging and further help in the evaluation of therapeutic drug. QDs are toxic due to the presence of toxic elements (e.g., In, As, Cd or Te), and their in vivo stability is a challenge for their development (Ballou et al. 2007). However, the stability can be improved by coating the QDs with biomolecules like proteins, nucleic acids, antibodies, peptides, and aptamers resulting in the formation of biocompatible QDs. This strategy might increase their possibility to be used in bioimaging purposes. In the near future, the QDs should be used for diagnosis including ultrasensitive detection of various biomarkers, in vivo targeted imaging and drug delivery (Zhou et al. 2015a).

6.2.3 Silica NPs

The pharmaceutical drugs used for the treatment of diseases like chemotherapy of cancer are based on conventional antitumor drugs which causes adverse effect on normal tissues. Thus to overcome this major drawback, approaches were used to design biocompatible targeted drug delivery models which should transport the required amount of drug to the affected part of the body with controlled and sustained release (Slowing et al. 2008). Silica is one the most appropriate candidate for this purpose due to its biocompatibility, suitable size, thermal stability, and reactive surface which allows these to be surface functionalized with other groups (Mader et al. 2008). The honeycomb-like structure of mesoporous silica nanospheres allows the reactants to absorb through the pores of silica shell (Burns et al. 2009). The silica nanospheres can act as biosensors, biomarkers, theragnostic, and drug delivery agents in conjugation with Ag, Au, and other metallic NPs, fluorescent NPs, proteins, drugs, etc. (Hirsch et al. 2006; Walia and Acharya 2015).

6.2.4 Carbon Nanotubes

Carbon nanotubes (CNTs) first came into account in 1991. CNTs are allotropes of carbon single-walled or multiwalled cylindrical tubes in which different therapeutic and diagnostic agents can be accommodated easily. The diameter of CNTs is typically between 1 and 100 nm (Zhu et al. 2002). The hydrophobic nature of CNTs allows them to bind nonspecfically with plasma proteins. The surface modification of CNTs has been done by oxidation or conjugation to hydrophilic organic molecules to make them water soluble (Tasis et al. 2003). These water soluble CNTs shows amazing strength, electrical properties, and thermal conductivities, which hold great promise in biomedical research (Kolosnjaj et al. 2007). The in vivo studies on

mice have been done by many researchers to understand the biodistribution and translocation of CNTs in animal model though contradictory views regarding their toxicity inhibit their biomedical applications (Wu et al. 2010).

6.2.5 Dendrimers

Dendrimers have wide range of applications in the field of catalysis, optics, electronics, and biomedicine. The biomedical applications of dendrimers are dependent on their non-immunogenecity and biocompatibility. This led to the synthesis of dendrimer conjugated organic and inorganic NPs (Jang et al. 2009; Medina and El-Sayed 2009). The dendrimer encapsulated NPs are generally synthesized by fast reduction and nucleation chemistry with a size range of 5 nm (Crooks et al. 2001). Some other methods include thermotreatment, ultraviolet (UV)-irradiation, laser ablation, or g-ray irradiation. The amine terminated polyamidoamine (PAMAM) dendrimers are commonly used for the synthesis of dendrimer-coated Au NPs (Shen and Shi 2010). Similar strategies were also applied for the synthesis of Ag NPs-entrapped dendrimers (Shi et al. 2008). The biomedical applications of NPs conjugated dendrimers are related to the NPs entrapped in the dendrimer. They also bear higher electron density than cellular system, and hence can also be used as biomarkers (Shen and Shi 2010). The pioneer group of Bulte et al. (2002) in their three different studies used dendrimers modified with iron oxide NPs (IONPs) for the detection of olfactory ensheathing cells which ensheath the axons of the olfactory receptor neurons (Barnett and Riddell 2004), grafted into the rat spinal cord in vivo (Lee et al. 2004), and also to track murine and human skin stem/progenitor cells (Tunici et al. 2006). Further MR imaging was also done using these dendrimers to analyze stem cells in vivo (Bulte et al. 2002).

6.2.6 Micelles

Micelles are another class of organic NPs. They are collidal NPs with hydrophilic shell and hydrophobic core. Tumors, inflammation, infarction, and lesions having leaky vasculature structure help in the entry of the micelles. They are novel carrier for water insoluble drugs, gene delivery, and diagnostic imaging probes (Torchilin 2007; Movassaghian et al. 2015). The biocompatibility, stability at in vivo and in vitro systems, ability to solubilize a variety of poorly soluble drugs, and the ability to accumulate in the target area are some of its unique characteristic properties which have attracted the researchers (Movassaghian et al. 2015). Lin et al. (2013) investigated the ability of paclitaxel (PTX) micelles as a theragnostic probe for imaging and chemotherapy of bladder cancer. The mice carrying patient-derived xenografts were taken to analyze antitumor efficacy. Zhou et al. (2015b) reported the solvent-evaporation method for the encapsulation of super paramagnetic iron oxide nanoparticles (SPIONs) inside polyethylene glycol-*block*-polycaprolactone and modified these with a NIR fluorescent probe, Cy5.5, and glioma-targeting ligand lactoferrin. The in vivo results suggested that these micelles are suitable candidate for MRI/optical imaging. The MRI images showed their long-term stability at tumor site. It was also helpful during and after the surgery as fluorescent probe can be helpful in discriminating the tumor surroundings.

6.2.7 Liposomes

Liposomes are the most prominent carriers for delivery of hydrophobic and hydrophilic drugs, diagnostic agents, peptides, antibodies, hormones, and macromolecules after encapsulation by the lipid membranes (Choi and Frangioni 2010). Liposomes came into existence by the ability of self forming enclosed lipid bilayer upon hydration (Samad et al. 2007). However, they suffer from poor mechanical stability which can be improved by coating them with biodegradable coatings viz., PEG and further proteins, oligosaccharides, add on to their targeted approach (Langer 1998). It has been found that liposomes-encapsulated agents have prolonged circulation as compared to bare NPs. In this

context, Zheng et al. (2007) demonstrated the in vivo behavior of a liposome-encapsulated iohexol (1-*N*,3-*N*-bis(2,3-dihydroxypropyl)-5-[*N*-(2,3-dihydroxypropyl)acetamido]-2,4,6-triiodobenzene-1,3-dicarboxamide) as computed tomography (CT) agent and gadoteridol [Gadolinium (III) cation (Gd^{3+})] as magnetic resonance (MR) agent for diagnostic applications. This liposome-based dual CT/MR probe make it a promising agent for bioimaging applications because of its prolonged retention and simultaneous CT and MR signal enhancement in in vivo system. Similarly, De Leo et al. (2014) also reported the encapsulation of hydrophobic QDs in the phospholipid bilayers of liposomes via micelle to vesicle transition approach and reported increment of optical characteristics of QDs.

6.3 Different Imaging Modalities

Molecular imaging plays an important role in patient health management and curing of disease. It is one of the most challenging areas of science which is growing rapidly. Molecular imaging is a kind of facility to 'see' within the living human body which leads to the treatment of disease by understanding its biological complexities. It involves the noninvasive study of biological processes in vivo at the cellular and molecular level. The key role for chemists is to design the imaging agents that make molecular processes visible, quantifiable and traceable over time, aiming to probe molecular abnormalities. The key is to scrutinize the molecular abnormalities that are the basis of disease rather than to image the end effects of these molecular alterations, i.e., earlier detection and characterization of disease, earlier and direct molecular assessment of treatment effects, and a more fundamental understanding of the disease process. Various imaging modalities (e.g., PET, SPECT, MRI, optical, and US) can be used to assess specific molecular targets. Certain modalities are well suited for some applications, but very poorly suited for other applications. As no imaging modality that can provide information on all aspects of structure and function, the research on a subject using multiple imaging modalities is clearly attractive (Jennings and Long 2009).

6.3.1 Optical Imaging Systems

Optical imaging is one of the fascinating tools for the diagnosis of disease that uses NIR light to assess optical properties of tissues and might help in the detection of many critical diseases. The major advantages of in vivo optical imaging is that it does not use radioactive component and can detect imaging agents in picomolar to nanomolar concentration ranges (Herranz and Ruibal 2012). The noninvasive imaging, high sensitivity, cost-effectiveness, nonionizing, and real-time imaging are the features of in vivo optical imaging. These inimitable characteristics attracted the interest of many researchers. Soft tissues can be easily distinguished from one another due to the wide variety of ways different tissues absorb and scatter light (Weissleder and Pittet 2008). There are different optical imaging agents available like green fluorescent proteins, organic dyes, etc. They have advantages viz., fine visibility, efficiently emitting internal fluorophore, high absorption, and longer emission wavelength which are very helpful in biological imaging of DNA, amino acids, etc. (Tsien 1998; Gonçalves 2009). Although it has lot of unique features but still share some drawbacks like light scattering, autofluorescence, and absorption by adjacent tissues, water, and lipids from in vivo systems; therefore, optical imaging for in vivo systems has many limitations, in particular owing to small penetration depths (typically, 1 cm). They have not proved very successful where long-term imaging of small biomolecule is required (Medintz et al. 2005). So there is a need of such optical imaging agents which can cope up these limitations. However, some advanced techniques have been developed to overcome these limitations (viz., fluorescence, bioluminescence, diffused optical tomography, and optical coherence tomography) (Weissleder and Pittet 2008). The development of QDs brought a new hope in the world of optical imaging. The unique

size, photostability, high fluorescence intensity, and broad emission spectra ranging from UV to infrared region differ them from conventional fluorescent organic dyes (Zhou et al. 2015a). They had vast applications for both in vitro and in vivo studies including NIR imaging, targeted fluorescence, life-time imaging, multimodal imaging of tumors, proteins, DNA, siRNA, etc. (Zhou et al. 2015a). Bruchez et al. (1998) reported dual-colored silica-coated CdSe/CdS QDs for dual-colored imaging of mouse fibroblast. The green and red-emitting QDs were used to differentiate nuclei and actin filaments of mouse fibroblast. Dubertret et al. (2002) also used phospholipid-encapsulated QDs for the imaging of Xenopus embryogenesis. In the near future, the clinical diagnosis can be improved and developed by the applications of different fluorescent QDs.

6.3.2 Magnetic Resonance Imaging (MRI)

MRI is an excellent diagnostic tool used in hospitals for detection of diseases. It is used to investigate the anatomical, physiological, and even molecular state of the internal system of the body. The imaging of soft tissues with high contrast, high spatial resolution, and deep penetration is done using radio waves and magnetic field in MRI. The spatial resolution can be increased up to 10–100 μm, depending on the power of the magnetic field. For human body imaging, it is generally restricted to approximately 1 mm. The 3-Tesla magnetic field strength of MRI machines is quite efficient in providing detailed information at anatomical level, but due to low sensitivity their use at molecular level is not much explored. Therefore, to overcome the low sensitivity of MRI, various exogenous MRI contrast agents (IO, and Gd, etc.) have been synthesized and/or under development (Key and Leary 2014). The two main well-known imaging sequences are spin-echo and inversion recovery, which results in the improvements in the signal-to-noise ratio, contrast resolution, and imaging time. The clinical MRI imaging technique mainly focused on multislice, multiecho spin-echo imaging because it is less time-consuming technique. A standard spin-echo examination is the combination of one set of spin-lattice relaxation time (T_1)-weighted images (short repetition time [TR]) and one set of spin–spin relaxation time (T_2)-weighted images (long TR) (Scherzinger and Hendee 1986). The relaxation rates can be modified using MRI contrast agents, such as Gd chelators, which enhance the positive signal on T_1-weighted images, while T_2 agents, such as superparamagnetic iron oxide nanoparticles (SPION)-based contrast agents, decrease the signal intensity on T_2-weighted images (Thomas et al. 2013). There are many examples of such contrasting agents which improve the imaging of tissues and organs that are under diagnosis. Yang et al. (2011) reported a water soluble SPION-based nanocarrier. The in vitro studies revealed that the cellular uptake was higher when SPION were attached to tumor-targeting ligand as compared to bare tumor-targeting ligand. Chen et al. (2014b) reported folic acid-conjugated manganese oxide (MnO) NPs for efficient imaging of tiny brain gliomas in vivo. The SPIONs also showed efficiency toward stem cell labeling and tracking (Li et al. 2013). Along with such excellent properties, these contrast agents also suffer from some limitations including poor signal-to-noise ratio, low sensitivity, relatively long acquisition time, and requirement of expensive equipment (Thomas et al. 2013).

6.3.3 Computed Tomography (CT)

CT uses X-ray beam for the diagnosis and imaging of tissues with high spatial resolution. In CT, the images of thin slice of patient are recorded using a beam of X-rays. The different tomographic images have been produced from the X-ray images taken from different angles of the scanned area of an object or patient. The detectors of CT absorb X-rays that have passed through different tissues and differentiate the various tissues by detecting the difference in tissue density. CT is considered to be more efficient than conventional X-rays in

terms of greater contrast resolution, cross-sectional modality. Further this technique also eliminates problems of superimposition of overlying structures to a much greater extent. The information collected from the attenuation of the X-ray beam by the tissues is converted by the detectors into an arbitrary scale (Hounsfield units [HU]). The different tissues having different densities will result in variable HU values. For example bones, fats, air, and water have different electron densities and thus absorbs X-rays at different values. Bone or calcification (the abnormal deposition of calcium in soft tissues) is the most attenuating and are given a value of +1,000 HU, whereas air, the least attenuating, is given a value of −1,000 HU. The values are converted to a grayscale image and assigned a brightness level with the highest numbers in white and the lowest numbers in black. When interpreting CT examinations, the range (window width) and mean value (window level) of density units are selected to optimize visualization of different tissue densities of interest. Tissues of densities outside of the range selected will not be visible and will be either totally black or totally white. Standard settings can be selected to display variably lung, bone, or soft tissue, as required (Weissleder 2002; Barentsz et al. 2006). The contrast agents used in CT are commonly low molecular weight resulting in the rapid clearance from the body. In contrast to these agents, macromolecules and NPs of high molecular weight like gold, iodine and bismuth retained in the blood for longer time. The NPs thus can be used as vascular CT contrast agents because of its prolonged retention in blood pool. The AuNPs have gained much attention for their use as contrasting agent in CT (Cormode et al. 2009). The Au NPs have many advantages like biocompatibility, very high absorption coefficient, targeting ability toward cancer via enhanced permeability and retention (EPR) effect, and it also provides enhanced X-ray attenuation and contrast. All these properties made them suitable candidate for contrast agent in CT (Giljohann et al. 2010). Also micelles and liposomes, and polymer-based NPs are promising CT contrast agents (Lusic and Grinstaff 2013; Cormode et al. 2014).

6.3.4 Ultrasound (US)

Ultrasound is an imaging tool which uses sound waves for diagnosis of disease. It records the visualize structure present underneath the skin, resulting from the returned echoes of sound waves from internal organs that are beamed inside the body. The sound waves (N20 kHz) are emitted by transducer which is paced against the skin. The sound waves echoed by different tissues provide information to construct a shadow picture. It is commonly used to visualize the interface between solid- and liquid-filled spaces. US comprises many advantages like its low cost, speed, simplicity, and safety which make it the most common clinical imaging modalities (Massoud and Gambhir 2003). US contrast agents can improve imaging by introducing a material with different acoustic properties from that of tissues, such as gas (Blomley et al. 2001). NPs-based US contrasting agents play an important role. The echogenic poly(lactic-*co*-glycolic acid) (PLGA) NPs are efficiently used as contrasting agent in US-based gene delivery systems (Figueiredo and Esenaliev 2012). Larina et al. (2005) reported the in vivo studies of enhanced delivery of chemotherapeutic drugs when US is used in combination with polysterene NPs.

6.3.5 Nuclear Imaging

Nuclear imaging is the technique based on detection of radioisotopes that emit one or two gamma rays or positrons. It includes noninvasive imaging modalities such as PET and SPECT. Both the techniques are powerful imaging tool because of their specificity, sensitivity, and fast detection time. The isotopes used in PET are ^{68}Ga, ^{76}Br, technetium-94 m (^{94m}Tc), ^{11}C, ^{13}N, ^{15}O, ^{18}F, and ^{64}Cu, whereas SPECT is dependent upon gamma-emitting heavy radioisotopes such as ^{123}I, technetium-99m (^{99m}Tc), ^{133}Xe (Cassidy and Radda 2005). The noninvasive diagnosis of tumors by PET and SPECT in which radionuclides are combined with molecular tracers is

quite common imaging technique nowadays. For example, Fludeoxyglucose [^{18}F]FDG is used for the PET imaging of various cancers, while Iodine-123 fluoropropyl [^{123}I]-FP-CIT is a SPECT biomarker for dopamine transporter (Pimlott and Sutherland 2011). PET is ten times more sensitive than SPECT, however, in other fields SPECT is better than PET as it enables concurrent imaging of multiple radionuclides. Such radionuclides are easy to prepare and have longer half life than PET radionuclides. Further, the gamma cameras used in SPECT are cheaper. The advantage of PET and SPECT over other imaging modalities such as MRI and optical imaging is that these are quantitative techniques (Beer and Schwaiger 2008). However, low spatial resolution and poor anatomical details are some of the drawbacks of these techniques (Pimlott and Sutherland 2011).

6.4 Hybrid Imaging Modalities

Each imaging modality discussed above has its own advantages but also suffer some drawbacks. There is no single modality which is perfect in all respects. They have their own characteristic of sensitivity, resolution, and quantitative capabilities. The inability of single modality to assure the conformance of diagnosis is a major dilemma in determining the treatment. The synergistic combination of two imaging modalities can solve this problem, because each imaging modality offers its own unique benefits. The advantage of such hybrid modalities is that one imaging probe can overcome the intrinsic limitations of a specific modality and vice versa, or it is a combination of techniques with paired qualities. It is the combination of advantages of two modalities and simultaneous reduction of their limitations (Sosnovik et al. 2007; Nahrendorf et al. 2008). For example, PET is known for its high sensitivity biological and functional information about cancer. On the contrary, anatomical information can be collected by high resolution images from CT and MRI. Therefore, combination of these two modalities can provide complete information which includes high sensitivity and resolution simultaneously with more detailed anatomical or biological information about cancer. The detailed information of the target site by targeted delivery can also be achieved by these multimodal imaging probes. Multimodal imaging for cancer theranostics is a cutting-edge technology that maximizes the advantages of nanoparticles (Heidt and Nahrendorf 2012; Lee et al. 2012) They have lot of potential in the area of theragnosis, for instance they can be used in surgery to guide the scalpel and to track the delivery of drug inside the body (via fluorescence imaging), to ensure that all cancerous materials have been removed (MR imaging), and to track and identify tumor cells and physiological processes (PET or SPECT imaging). The nanoparticles are the best choice in the context of hybrid imaging modalities. Examples of the "dual modality" approach include: (i) the high sensitivity of the fluorescence phenomenon to the high spatial resolution of MRI which is obtained by combining nanoparticles having properties of fluorescence and magnetic resonance imaging, (ii) PET/MR is the combination of high soft tissue contrast and the functional information obtained by MRI and PET, respectively. MRI gives high resolution whereas PET gives high sensitivity—thus, overall giving anatomy and function. With regard to oncology, this leads to improved diagnostic accuracy and radiotherapy planning (Jennings and Long 2009), (iii) MRI/CT dual-modal agent is a combination of two anatomic modalities that share almost the same functional features (Hasebroock and Serkova 2009).

6.4.1 Optical Imaging/MRI

The combination of MRI and optical imaging is the well known and developed dual modality imaging technique in the area of research and clinical practices. The anatomical imaging can be successfully achieved by MRI, but it lacks in providing information at molecular level. This drawback of MRI can be overcome using NIRF dye-conjugated optical imaging contrast agent which provide information at molecular level (protease activity and gene expression) but provide poor anatomical information. Thus both the

techniques are complementary to each other and results in the improvement of imaging probe. The commonly used NIRF dye is cyanine (Cy5.5) in combination with SPION (Josephson et al. 2002; Park et al. 2008; Cha et al. 2011). SPION are regarded as the best choice for MRI contrast agents because they enhance the T_2-weighted MRI signal, and are also nontoxic in the biologically system, a good alternate to Gd-based contrast agents. In comparison to traditional paramagnetic contrast agents, SPION are required in very minute concentration (submolecular level), whereas the conventional contrast agents are detected at concentration of 10–100 μm by T_2-weighted MRI signal (Josephson et al. 2002; Acharya et al. 2015; Walia and Acharya 2015; Walia et al. 2016).

6.4.2 MR-PET/SPECT

The combination of magnetic resonance (MR) with nuclear imaging has synergistic applications in bioimaging. PET/SPECT are known for their high sensitivity but also have poor resolution, on the other hand MRI has excellent spatial resolution of soft tissue. The combination of these modalities decreases the risk of exposure of radiation to patients and one of the most suitable imaging modality for future generation (Key and Leary 2014). Choi et al. (2008) demonstrated the application of MR–PET using Mn-doped Fe_2O_4 providing MRI contrast effect, and the surface modified with serum albumin for high colloidal stability and then conjugated to PET radionuclide ^{124}I. The prepared nanoprobe was used as biomodal imaging probe for the visualization of sentinel lymph nodes. Similarly, de Rosales et al. (2011b) synthesized SPIONs coated with $^{64}Cu^{II}$–bis(dithiocarbamatebisphosphonate) conjugated with dextran, for the comparison of MR–PET imaging of lymph nodes with an image of PET–CT. The group also reported SPIONs-conjugated radiolabeled bisphosphonates (^{99m}Tc-dipicolylamine [DPA]-alendronate) agent for MR–SPECT imaging (de Rosales et al. 2011a). However, MRI–PET/SPECT is still not developed to that extent, as to the requirement of specialized equipments and skills, toxicity of contrasting agents is still unsolved. But advancement in research and technology will help in the establishment of these bioimaging modality in the near future as several clinical and preclinical PET–MRI and SPECT–MRI scanners have started to be installed worldwide (de Rosales 2014).

6.4.3 CT/MRI

The anatomical information with 3-D tomography and high resolution can be obtained by CT faster than MRI. But MRI is the best option for the high contrast imaging of soft tissues and to obtain physiological information of the treated tissue or organ. Combination of these two imaging modalities offer more advantages in imaging field. CT contrast can be improved by the use of targeted NPs with electron-dense core materials. For CT–MRI the gold NPs combined with SPIONs are widely used contrasting agents (Key and Leary 2014). For example, Kim et al. (2011) reported in vivo applications of amphiphilic dodecyl methacrylate (DMA), methacrylic acid, poly(ethylene glycol) methyl ether methacrylate (mPEGMA)-coated gold, and SPIONs hybrid NPs. The hepatoma regions of mouse models after 24 h treatment of these hybrid NPs showed time-dependent contrast. Liang et al. (2015) also demonstrated the applications of CT–MRI for the diagnosis of brain malignant gliomas using L-cysteine-coated FePt (FePt-Cys) NPs. They have done the in vitro studies to check CT–MRI characteristics of these nanoprobes using three different gliomas cell lines (C6, SGH44, U251). The results proved that these NPs can be used as CT–MRI imaging probe for the diagnosis of malignant gliomas. A dual-contrast agent with an IO core and a gold-layered shell with PEG coating was synthesized to provide synergistic effects of both CT and MRI. The intensity of the CT images for PEG coated IO–Au NPs was greater than iodine-based counterparts at the same concentration, but the T_2 signal efficiency decreased

compared to oleic acid/oleylamine coated SPION (Kim et al. 2009a). Thus, it is concluded that NPs with appropriate size and composition can enhance the imaging property of each of the modality and will pave great impact on healthcare (Key and Leary 2014).

6.4.4 PET/NIRF

NIRF imaging is a noninvasive technique to analyze disease at molecular level. It offers a variety of advantages viz., high spatial resolution, high sensitivity, and low risk of exposure to the living model by using nonionizing radiation. Increased depth penetration and quantification can be obtained by combining NIRF with PET. Ca et al. (2007) demonstrated the imaging of integrin $a_V ß_3$ expression in tumor-bearing mice using QD conjugated with arginine–glycine–aspartic acid (RGD) peptides and DOTA chelators through amide coupling. This QD–RGD–DOTA complex was then conjugated with radiolabeled copper-64 (^{64}Cu). The images of tumor obtained by this hybrid QD–RGD–DOTA–Cu were much better when compared with tumors exposed to QD–DOTA–Cu. Further, Chen et al. (2014a) synthesized the hybrid PET/NIRF imaging tool applying mesoporous silica NPs as a platform for the conjugation of ^{64}Cu, 800CW (NIRF dye), and TRC105 (a human/murine chimeric IgG1 monoclonal antibody). A detailed in vitro, in vivo, *and* ex vivo studies on 4T1 murine breast tumor-bearing mice were done to evaluate the efficacy and specificity of these hybrid NPs as suitable agents for PET/NIRF imaging of the tumor vasculature.

6.4.5 SPECT/NIRF

Another nuclear imaging system SPECT can also be conjugated with NIRF. The SPECT imaging uses signals received from gamma-emitting radioisotopes. Although SPECT imaging holds promising sensitivity, it also suffers by relatively poor spatial resolution. On the other hand, high spatial resolution and real-time imaging of tissues are the properties of optical imaging. Importantly, the ex vivo analysis of excised tissues can be done from fluorescent signal exerted by imaging probe. The combinations of these two techniques are considered to be of great value in biomedical system (Xing et al. 2014). Liang et al. (2010) reported the synthesis of DOTA chelator labeled with ^{111}In (as a SPECT agent) and a biotinylated Cy5.5 fluorophore to a streptavidin nanoparticle in conjugation with biotinylated anti-Her2 Herceptin antibody to provide tumor targeting. The detection of tumor in mouse model by combined optical and nuclear imaging was done by these streptavidin NPs-based complexes. It was concluded from the results that preferential tumor accumulation and strong tumor to normal tissue contrast can be observed by both SPECT/NIRF. Similarly Zhang et al. (2013) described the synthesis and use of heptamethine cyanine-based dual-mode SPECT/NIRF imaging probe ^{99m}Tc-PC-1007. The imaging of human breast cancer MCF-7 cells showed the higher accumulation of these complexes at tumor site. Also Zhang et al. (2011) proposed the dual-imaging probe for the noninvasive imaging of apoptosis by Annexin A5-conjugated polymeric micelles labeled with both NIR fluorophores and a radioisotope ^{111}In for SPECT. These NPs were injected in mice bearing EL4 lymphoma which were previously treated with anticancereous drug, cyclophosphamide and etoposide. Further, the mice bearing MDA-MB-468 breast tumors were treated with poly(L-glutamic acid)-paclitaxel and cetuximab (IMC-C225) anti-epidermal growth factor receptor antibody and the tumor apoptosis was clearly visualized by both SPECT and fluorescence molecular tomography.

6.5 Trimodal Imaging

Recent years have also seen tremendous development in the direction of multimodal imaging modalities, where more than two imaging modalities have been coupled in a single nanoprobe.

6.5.1 CT/MR/Optical

Earlier different imaging probes were applied for a complete diagnosis of a disease. This causes patients a great risk of exposure to radiations resulting in harmful and toxic effects due to the probe radiations. Xing et al. (2012) reported the synthesis of trimodal imaging probe of size 50 nm by combining PEGylated NaY/GdF_4: Yb, Er, Tm @SiO_2–Au@PEG_{5000}. This trimodal imaging probe showed the characteristics of strong emissions ranging from the visible to near-infrared for fluorescent imaging, T_1-weighted MRI by shorting T_1 relaxation time, and enhanced Hounsfield value as a CT contrast agent. The in vitro and in vivo studies demonstrated the potential of PEGylated NaY/GdF(4): Yb, Er, Tm @SiO(2)–Au@PEG(5000) NPs as trimodal imaging probe.

6.5.2 PET/MR/Optical

There is another example of trimodal imaging probe formed by the combination of PET, MR, and optical imaging agents. The integration of PET/MRI/optical imaging offers many applications in preclinic research and clinical studies (Park et al. 2010a). The biological and functional information of cancer can be obtained by PET with high sensitivity. On the contrary, CT and MRI provide anatomical information of targeted tissues with high resolution imaging characteristics (Thomas et al. 2013). Therefore, a combination of these imaging modalities can provide not only high sensitivity and resolution, but also more detailed anatomical or biological information about cancer. Xie et al. (2010a) synthesized DOTA-modified iron oxide nanoparticles (IONPs) encapsulated within the human serum albumin (HSA). Further, the NPs were labeled with ^{64}Cu-DOTA and Cy5.5. The potential of the hybrid imaging nanoprobe for trimodal imaging was tested in subcutaneous U87MG xenograft mouse model. The results suggested that there was a preferential accumulation of NPs at tumor site and lesions and HSA added to the prolonged circulation half life. Park et al. (2010a) also reported a facile methodology for the preparation of NIR/MR/optical imaging-based trimodal probe. They have used Cerenkov radiation (as optical imaging moiety) generated by PET radionuclide ^{124}I. Further, the optical and PET radionuclides were conjugated with PEG functionalized IONPs. The in vivo studies were carried out by injecting the NPs in 4T1 tumor-bearing BALB/c mouse. The results showed differentiation between tumor-metastasized sentinel lymph nodes (SLNs) and tumor-free SLNs using this trimodal imaging probe.

6.5.3 SPECT/MR/Optical

Hwang et al. (2010) reported the synthesis and application of multimodal cobalt–ferrite NPs conjugated with AS1411 aptamer for targeting nucleolin protein which is highly expressed on the membrane of cancer cells. The NPs were further labeled with silica-coated rhodamine and a chelating agent–2-(*p*-isothio-cyanatobenzyl)-1,4,7-triazacyclonane-1,4,7-triacetic acid (*p*-SCN-Bn-NOTA) which act as a source of Gallium-67 (^{67}Ga) labeling radionuclide. The nanomaterial was capable of simultaneous fluorescence imaging, radionuclide imaging, and MRI in vitro and in vivo (Hwang et al. 2010).

6.6 Nanoparticles as Theragnostic Probes

The effective treatment of any disease depends upon its early and curable stage. Nanotechnology displays a new paradigm in the arena of disease diagnosis and their treatment. Nanosystems provide platform for incorporating drugs that are efficient in cell-targeted delivery (Groneberg et al. 2006). NPs are engineered in such a manner that they are attracted by diseased cells and help in their treatment without harming normal cells. The properties of NPs were also utilized in the development of molecular imaging systems. The optical (fluorescent, surface-enhanced Raman spectroscopy (SERS), photoacoustic, etc.),

magnetic, radioactive (positron or γ-ray emitting), X-ray opaque (NPs with high electron density), and ultrasound-sensitive (nanobubbles) agents are some of the imaging agents based on nanomaterials. The polymer coating was used in NPs to make them efficient for medicinal applications (Fang and Zhang et al. 2010). The unique size of these NPs helps them to reach the target tissues thereby crossing the biological barriers (Nel et al. 2009). In the present scenario, the NPs with the properties of drug and NPs which were applied as diagnostic tool are integrated for the purpose of theragnosis (Kim et al. 2009b; Xie et al. 2010b).

6.6.1 Chemotherapy Via Theragnostic Nanotechnology

The chemotherapy, based on conventional small molecule drugs, carries many disadvantages including the lack of sufficient specificity to the tumor, severe and toxic side effects in healthy tissues, limited delivery of hydrophobic drugs to the tumor cells, and drug resistance (Khemtong et al. 2009; Shapira et al. 2011). The conventional chemotherapy can be made more efficient and patient friendly by nanomaterials (Gelperina et al. 2005; Park et al. 2010b; Shapira et al. 2011). Nanomaterials with anticancerous drugs viz., DOX or PTX were incorporated with imaging agents which provides dual applications for simultaneous imaging and targeted chemotherapy (Kelkar and Reineke 2011; Ahmed et al. 2012). Xiao et al. (2015) reported hyaluronic acid (HA)-functionalized camptothecin (CPT)/curcumin (CUR)-loaded polymeric NPs and investigated their synergistic effect in the targeted drug delivery and efficacy for colon cancer therapy (HA-CPT/CUR-NPs). The results suggested that these NPs hold high antitumor activity in combination with chemotherapy. Nanocarriers are helpful in preventing drug degradation by evading the reticuloendothelial system (RES), and thus a high blood circulation profile enables transport through biological barriers, increasing the availability of drug at the targeted intracellular compartments reducing the toxicity and other side effects associated with conventional drug delivery agents (Parhi et al. 2012). Kim et al. (2010) had developed a nanoprobe which is a conjugate of Cy5.5-labeled fluorescent probe for imaging and PTX as anticancerous drug coated by chitosan. This hybrid nanocomposite proved to be more effective than water soluble linear polymer or polystyrene beads in accumulation at tumor tissues. These therapeutic hybrid nanocomposites accumulated at the tumor tissues much more efficiently than water soluble linear polymer or polystyrene beads. The fast cellular uptake of the hybrid nanocomposite resulted in higher therapeutic efficacy. The NIRF label is allowed to noninvasively monitor the in vivo fate of the NPs in live animals. The controlled administration of PTX-loaded Cy5.5-labeled CNPs greatly minimized the tumor size, while minimizing the severe toxicity associated with free PTX administration. The real-time information of NPs on its location, release or efficacy of the contained drug, and detecting residual tumor cells with various optical imaging techniques are some of the advantages of theragnostic NPs (Ryu et al. 2012).

6.6.2 Photodyanamic Therapy

It is the commonly used minimally invasive technique in oncology (Chiaviello et al. 2011). This technique involves administration of a photo-triggered chemical drug as photosensitizer which produces singlet oxygen, and thus absorbs energy of particular wavelength and their emission generates fluorescence. The generated fluorescence can be used for imaging and singlet oxygen can damage major cellular organelles like mitochondria, resulting in cell death. So these can be applied for optical imaging and photodyanamic therapy (PDT) simultaneously (Celli et al. 2010). The nanoscale photosensitizer carriers have been used to improve therapeutic efficacy and to prevent the damage to normal tissues and cells (van Nostrum 2004; Chatterjee et al. 2008; Jeong et al. 2011; Lee et al. 2011b;

Park et al. 2011). Different PDT delivery carriers have been developed viz., PDT system with chlorin e6 (Ce6) and black hole quencher-3 (BHQ-3) as the photosensitizer and fluorescence resonance energy transfer (FRET) quencher (Fang and Zhang 2010). Lee et al. (2011a) reported the synthesis of tumor-targeted Ce6-conjugated glycol-chitosan NPs and suggested their efficient applications in PDT for the treatment of cancer.

6.6.3 Photothermal Therapy

The AuNPs play an important role in photothermal therapy. Their applications as simultaneous imaging and theragnostic agent have been demonstrated by many researchers. The AuNPs accomplished with different properties like optical absorption, scattering, quenching, and photothermal properties (Nikoobakht and El-Sayed 2003; Schultz 2003; Orendorff et al. 2006; Horimoto et al. 2008; Li et al. 2009). These properties are the results of their different shapes and sizes, which made them efficient for imaging and photothermal therapy. In this direction, Yi et al. (2010) have reported the synthesis and applications of Au nanorods (AuNRs) in cancer theragnosis. The AuNRs was modified with a matrix metalloprotease (MMP)-sensitive fluorescence probe. Further, the binding of fluorescent dye Cy5.5 to the AuNRs was done through MMP enzyme substrate peptide. The quenching effect of AuNRs decreases the fluorescence until the cleavage of MMP substrate lead to the detachment of Cy5.5. The imaging of cancer was possible when MMP-AuNRs was intratumorally injected in mouse models, because MMP enzymes are abundant in tumors. In addition, AuNRs can also be used in photothermal therapy as a heat source because these can convert light energy into heat upon laser irradiation. In the same study, the laser irradiation was used to increase the temperature of MMP-AuNRs. The absorption wavelength was adjusted to the NIR region by tuning their aspect ratio to enhance the laser absorption (671 nm), causing damage to the tumor tissue (Yi et al. 2010). The in vitro molecular imaging and photothermal therapy using AuNRs was also done by Huang et al. (2006). The selective accumulation of AuNRs on tumor was made possible by conjugating them with the anti-epidermal growth factor receptor (anti-EGFR) monoclonal antibodies. The NRs were incubated with nonmalignant and malignant cell lines viz., HOC 313 clone 8 and HSC 3, respectively. The confirmation of binding of AuNRs to malignant cell lines was done by dark-field microscopic images, and a strong signal was observed in malignant cell lines only. This result suggested the successful high affinity binding of anti-EGFR antibody-conjugated AuNRs to the malignant cells. Further malignant cells were destroyed through laser irradiation.

6.6.4 Hyperthermia Therapy

Hyperthermia is a well-known technique for the treatment of cancer at very high temperature (up to 113 °F). Magnetic hyperthermia in the presence of applied alternating magnetic field uses magnetic NPs for selectively heating of target tissues (Asín et al. 2013). The IONPs are used for noninvasive hyperthermia in preclinical and clinical trials (Maier-Hauff et al. 2007; Johannsen et al. 2010). The IONPs of size 1–100 nm are used for magnetically mediated hyperthermia. Jordon et al. (2006) applied small magnetities for hyperthermia but due to the drawbacks of unequal distribution of magnetites and heat at tumor site, their applications in clinics were hindered. High magnetic loading is the most important criteria for hyperthermia therapy. Following this Béalle et al. (2012) prepared ultra magnetic liposomes with up to 30 % IONPs volume fraction to take the maximum advantage of IONPs for hyperthermia. In a pioneer work done by Asín et al. (2013), magnetic NPs coated with dendrimers showed 100 % cell death. Fantechi et al. (2014) reported the application SPION conjugated with human ferritin protein cage (HFt) for cancer treatment by therapeutic drug delivery and magnetic fluid hyperthermia. Chiang et al. (2013) reported anticancer drug, DOX loaded with SPION encapsulated in a polymer, can be used for dual function. Such NPs showed increase in temperature triggered by

high-frequency magnetic field and pH reduction. The requirement of higher concentration of IONPs at solid tumor site for hyperthermia is a major challenge of this therapy.

6.7 Factors Affecting Disease Diagnosis and Therapy

The origin of nanotechnology brings new hope in the diagnosis and therapy of many diseases. The applications of NPs in diagnosis and therapy were due to their unique future of early detection of disease. Nanomaterials have wide range of applications in cancer diagnosis and therapy, molecular imaging, implant technology, tissue engineering, and nanodevices for drug, protein, gene and radionuclide delivery (Alharbi and Al-sheikh 2014). Nanotechnology also leads to the combination of these two different branches resulting in modified healthcare system. This was possible because of their unique characteristics of large surface to volume ratio (Yezhelyev et al. 2006). Though these NPs have many advantages, they are facing problems at clinical level. There are some important factors that have to be considered before using NPs at clinical level.

6.7.1 Biopersistence of NPs

The long-term tumor imaging can be done only by the prolonged circulation of NPs in the biological systems. The human body has a very strong defense system including physiological (blood, liver, spleen, kidneys, immune system) and cellular (lysosomes, nucleus, mitochondria) barrier which restricted the entry of foreign particles viz., bacteria, fungi, drugs, viruses, etc. Therefore to control the circulation of NPs, there is a need of designing or modifying NPs with biocompatible components so that the NPs can reach the target cells or tissues (Kievit and Zhang 2011). The surface modification of NPs with silica, polymers like PEG, zwitter ion, dextran, some protein coatings viz., bovine serum albumin (BSA) should be more explored (Xia et al. 2013). These stealth coatings will mimic the cell organelles and misguide the macrophages and help the NPs to escape immune attack in the body and avoid renal clearance. Sarparanta et al. (2012) also applied the same strategy to increase the circulation time of luminescent porous silicon NPs by coating them with self-assembled fungal hydrophobin protein shell via hydrophobic interaction which resulted in their increased accumulation in liver and spleen. Similarly, Xia et al. (2013) reported the encapsulation of silicon NPs with BSA by hydrophobic interaction and the results suggested reduced nonspecific cellular uptake in vitro and prolonged blood circulation in vivo of the BSA-coated silicon NPs. Hu et al. (2011) reported the top-down biomimetic approach for the encapsulation of PLGA biodegradable polymeric nanoparticles with natural erythrocyte membranes, (red blood corpuscles, RBCs). This approach has aimed at long-circulating cargo delivery of RBC-camouflaged polymeric NPs.

6.7.2 Efficacy of NPs

The physicochemical and physiological process occurring inside biological environment should be well explored before the extensive in vivo study of nanoparticles. The prediction of biodistribution of NPs is still difficult. The NPs get interacted with undesirable phagocyte systems. This might retard their circulation half life in the biological systems (Gref et al. 1994; Owens and Peppas 2006). The NPs even of very small size after reaching the target site cannot recognize biological targets, such as cells or organelles and thus failed to enter them. Therefore, there is a need of designing strategies by keeping in mind the intracellular uptake and proficient entry of the NPs into cell organelles like mitochondria, lysosomes, nucleus, etc., or in other words NPs should be very selective and specific toward their targets (Breunig et al. 2008). Tada et al. (2007) studied the processes and mechanism involved in the transport of drug carriers in vivo. The tumor-targeting monoclonal anti-HER2 (human epidermal growth factor) antibodies labeled with QDs were injected in

mice with HER2-overexpressing breast cancer. However, this approach is quite helpful only if the blood group of the patient matched to these conjugated RBCs on the NPs. The circulation barrier increases due to the conflict between strategies for prolonged circulation and strategies for targeting of NPs. Therefore, there is a need of approaches for the synthesis of NPs that maintain the balance between circulation and targeting of NPs (Rajeeva et al. 2014).

6.7.3 Target Specificity of Theragnostic NPs

The diagnosis of disease and administration of proper drug dosage depends on effective targeting of theragnostic NPs. The accumulation of NPs in tumor occurred through EPR effect which depends on the size and shape of NPs and also on surface modification with targeting ligands to target the cells (Mitragotri and Stayton 2014). Despite this, there are many barriers which inhibit their targeting efficiency. Intravascular administration of NPs leads their accumulation in liver and spleen. Moreover, protein adsorbed on to the surface of NPs hindered the specific interactions of NPs with target receptors (Rajeeva et al. 2014). It has been noticed that most of the targeted moieties are heterogeneous in terms of biology, the most common example is tumor. Therefore, this heterogeneity should be kept in mind during the targeting strategies. Multiple targeting might help in increasing the specificity of NPs toward the target organs (Mitragotri and Stayton 2014).

6.7.4 In Vivo Clearance of NPs

An ideal bioimaging probe should be least toxic or better to be biocompatible, with appropriate blood half life, high ability to bind specific, and selective binding target tissues or organs, and finally safer elimination from the body without any side effects and should have better fluorescence emission and stability (Choi and Frangioni 2010). The NPs for bioimaging should be tailored in such a manner that they can meet these parameters. Primarily, the physicochemical and pharmacokinetic properties of NPs depend on their size, shape, and chemical composition. These parameters can be optimized by adjusting their size, composition, shape, and surface characteristics. These properties are also responsible for in vitro and in vivo toxicity (Choi et al. 2007; Liu et al. 2007; Choi et al. 2009). The in vivo behavior of NPs played an important role in the future success of NPs-based theragnostic probes. Though few of the NPs are explored at in vivo level, still there are many unsolved mysteries. These include their biodistribution at disease site and their clearance from the body (Choi et al. 2007; Alexis et al. 2008). From the literature reports, it has been observed that the NPs of size ranging from 10 to 100 nm are widely studied for biomedical applications. The main drawback of these small sized NPs is their poor clearance, and thus absorption in the reticuloendothelial system (Zhang et al. 2008). It has been reported that QDs can retain in the body for almost 100 days and also retain their fluorescent properties as they are much photostable than fluorescent dyes (Ballou et al. 2007). The metallic NPs are much toxic and their prolonged retention time in body may cause adverse effects on the body. The synthesis of NPs with optimal clearance characteristics will minimize toxicity risks and decrease concerns of NP interference by reducing the duration of exposure to these agents. The NPs with improved optimal clearance properties will help in the production of agents with better clearance (Longmire et al. 2008). The inorganic NPs with optimal renal clearable characteristics are being synthesized in order to replace NPs that have prolonged clearance time and get accumulated in the reticuenothelium organs (liver, spleen) (Choi et al. 2007; Longmire et al. 2008; Liu et al. 2013). Choi et al. (2007) had devoted efforts to design renal clearable zwitterionic cysteine-coated QDs. The NPs due to very small hydrodyanamic diameter of $\sim$5.5 nm were rapidly excreted within 4 h through urinary system with <5 % accumulation in liver. The zwitter ion plays an important role in the rapid clearance of these QDs. The zwitter ion ligands acts as PEG ligands

to minimize serum protein adsorption which also increases the stability of these NPs by maintaining the hydrodyanamic diameter of the QDs below kidney filtration threshold (KFT: ~5.5 nm) (Choi et al. 2007). In a pioneer work done by Zhou et al. (2011), the fast renal clearance was observed for zwitter cysteine ion-coated AuNPs of ~3 nm hydrodyanamic diameter with very little amount of accumulation in liver. The Au NPs of same size without any coating were not renal clearable because of their low physiological stability. In an another report, Yang et al. (2015) had successfully designed glutathione (GSH)-coated copper NPs (CuNPs) and their dissociation products, Cu(II)-GSH disulfide complexes as models. The comparable in vitro and in vivo studies showed that GSH ligand can significantly enhance renal clearance of CuNPs. In a similar manner prolonged retention of many other NPs with specific coating can be decreased, and thus the adverse effects caused by these NPs can be minimized. Also these degradable NPs act as supplement to the conventional NPs and might help in solving the major issues of clearance and toxicity caused by the accumulation of these NPs for long period.

6.7.5 Nanotoxicity

The unique physicochemical properties that make NPs as novel biomedical agents are also responsible for their toxic effects on human health. Several studies have revealed that cytotoxicity of QDs is dependent on their size and concentration. The QDs with small size and high concentration are more toxic (Zhang et al. 2007). Lovric et al. (2005) found that the cellular accumulation and cytotoxicity of CdTe NPs were influenced by the physicochemical properties of NPs. The green emitting positively charged CdTe QDs with very small size ($2r = 2.2 \pm 0.1$ nm) exhibited marked cytotoxicity at concentrations as low as 10 µg/ml in PC12 (cell line derived from a pheochromocytoma of the rat adrenal medulla) and N9 (microglia cells derived from mouse) cells as compared to same concentration of large ($2r = 5.2 \pm 0.1$ nm), equally charged red-emitting QDs. However, NPs geometry also adds dimensions to the toxicity of NPs. For example, while comparing the in vitro cytotoxicity of carbon nanomaterials with different geometry, such as single-walled or multiwalled nanotubes and nano-60 fullerenes, it has been found that single-walled nanotubes were most toxic and nano-60 fullerenes were least toxic (Jia et al. 2005). Some NPs like QDs made up of Cd, Se, Te, Gd, As, Pb are also hazardous to human health (Nel et al. 2006; Choi and Frangioni 2010). Moreover surface coatings also enhance the toxicity of NPs. Conner et al. (2005) tested the cytoxicity on K562 leukemia cell line of Au NPs modified with different surface coatings. The results demonstrated that the NPs coated with citrate and biotin surface modifiers did not showed toxicity at concentration of 250 µm (gold atoms), whereas in case of gold salt precursor solution ($AuCl_4$) 90 % toxicity was observed at same concentration, while glucose or cysteine surface modifiers showed no toxicity up to 25 µm. Last but not least, the prominent chemical stability of NPs creates problems in their disposal which could led to their entry in the water cycle and also affects the environment. Nanotoxicology mainly aims at risk associated with exposure to the NPs and we should pay attention on short-term and long-term toxicities associated with NPs (Choi and Frangioni 2010; Singh 2013).

6.8 Current Scenario and Future Aspects

Theragnosis-based NPs act as multitasking agents by improving the diagnostic features and therapy by delivering the NPs to targeted disease site and also facilitate better efficacy and toxicity aspects (Lammers et al. 2010). The curing of diseases using more specific and efficient probes can be enhanced by the combination of therapeutic and diagnostic characteristics of different NPs on a single platform (Wang et al. 2012). There are number of NPs that have been synthesized including polymers, liposomes, micelles, QDs, and metallic NPs (Au, Ag, IO,

etc.) where these NPs have been used for theragnosis (Lammers et al. 2010; Wang et al. 2012). The biocompatible liposomes, micelles, and polymers which act as drug-targeting systems are functionalized with drugs and contrasting agents, whereas QDs and metallic NPs having intrinsic characteristics important for imaging purposes are extensively implemented for combining disease diagnosis and therapy (Lammers et al. 2010). One of the first theragnostic agent developed was Herceptin® and was approved for the treatment of HER2-positive metastatic breast cancer (Brenner and Adams 1999), but because of some limitations it was not that much commercialized. The development of NPs help to overcome drawbacks of conventional theragnostic agents, thereby providing sustained targeted delivery of therapeutics in combination with imaging probes, thus simultaneously real-time distribution of drugs to tissues can be followed (Lammers et al. 2011). The effective treatment without side effects is the main criteria which are considered while the development of these nanotheragnostic agents. There are many nanomedicines for theragnosis which are approved by US Food and Drug Administration (FDA) viz., Doxil® (Janssen Biotech) meant for the treatment of metastatic breast cancer, ovarian cancer, multiple myeloma, and AIDS-related Kaposi's sarcoma (KS) (Egusquiaguirre et al. 2012), Caelyx® (in Europe), Myocet® (Sopherion Therapeutics Inc., Princeton, NJ, USA), DaunoXome® (Galen US Inc, Souderton, PA, USA), DepoCyt® (Pacira Pharmaceuticals Inc, San Diego, CA, USA), Abraxane® (Celgene Corporation), Genexol-PM® (Samyang Biopharmaceuticals Corporation, Jongno-gu, Seoul, Korea), and Oncaspar® (Enzon Pharmaceuticals Inc, Bridgewater, NJ, USA) (BBC Research 2010). There are some magnetic NPs-based formulations which are approved for theragnosis and some are under clinical trials viz., Feridex®IV and Endorem® (Bayer Healthcare Pharmaceuticals) for liver and spleen imaging, Lumiren® (Guerbet SA, Villepinte, France) and Gastromark® (Advanced Magnetics Inc, Rochester, IN, USA) for bowel imaging (Mura et al. 2013). IONPs-based drug, NanoTherm® (Magforce AG, Berlin, Germany), is applicable for hyperthermia treatment of tumor, sparing adjacent healthy tissue (Etheridge et al. 2013) (Table 6.1). A recent report showed that there were approximately 200 patents on nanomedicine registered till 2012 for approval in the World Intellectual Property Organization (WIPO) (Hawkins et al. 2008).

Table 6.1 Commercially available nanotechnology-based drugs and contrast agents

Nanomedicine	Nanoparticles	Company	Application
Doxil® (Caelyx® in Europe)	Liposomes and doxorubicin	Jannsen Biotech	Treatment of metastatic breast cancer, ovarian cancer, multiple myolema, AIDS-related Kaposi's sarcoma
Myocet®	Liposomes and doxorubicin hydrochloride	Sopherion Therapeutics Inc, Princeton NJ, USA	Treatment of metastatic cancer
DaunoXome®	Daunorubicin citrate liposome	Galen US Inc, Soudern, PA, USA	Treatment of Kaposi' sarcoma, leukemia
Depocyt®	Cytarabine liposomal	Pacira Pharmaceuticals Inc, San Diego, CA, USA	Lyphoma treatment
Abraxane®	Paclitaxel	Celgene Corporation	Treatment of metastatic breast cancer
Feridex IV®, Endoderm®	Magnetic NPs	Bayer Healthcare pharmaceuticals	Liver, spleen imaging
Lumiren®	Magnetic NPs	Guerbet SA, France	Bowel imaging
Gastromark®	Magnetic NPs	Advanced Magnetics Inc, USA	Bowel imaging
Nanotherm®	Iron oxide NPs	Magforce AG, Germany	Hyperthermia treatment of tumor

Despite notable progress, there are still many challenges to meet clinical standards. Though it is well known that the majority of nanotheranostic probes posses advantages and unique properties but also suffers from limitations, viz, the cost of AuNPs, insufficient sensitivity of IONPs acting as MRI contrast agent, the large size of silica NPs, nonbiodegradable property of carbon materials, incomplete clearance QDs used for imaging, etc. (Wang et al. 2012). The versatile nanoparticles viz., Au, IONPs, QDs, and polymeric NPs are suitable probes for carrying therapeutic agents with simultaneous biosensing. The IONPs can be easily metabolized in blood serum (Ho et al. 2011). However the toxicity of QDs, Au NPs, and CNTs is a major challenge at present. The surface modification of these NPs with biocompatible coating can help in their renal clearance from animal body. These studies are not very well explored at in vivo level. Also scalability, reproducibility, in vivo administration and biodistribution, toxicity, clearance and safety issues should be considered for approval from FDA and European Medicines Agency (EMA) before their impact to be accessed at clinical level (Mura et al. 2013). So these reports suggested that there are many aspects that have to be addressed before the commercialization of the nanomedicines in the near future.

6.9 Conclusion

NPs provide tremendous opportunities in the field of theragnosis. The unique physicochemical properties influence the integration of multiple functionalities in a single domain, resulting in the development of theragnostic approach (Fang and Zhang 2010). Although there are many obstacles and hurdles that have to be solved, nanotheragnosis is an emerging field that is growing day by day. The most important advantage of theragnosis is that it provides the synergistic effect of diagnosis and therapy simultaneously by combining different NPs. It is clear that nanotheragnostic probes are much better than conventional treatments where the diagnosis and therapy are way apart from each other. There is the requirement of focused research and attention to provide answers of the queries regarding toxicity, efficacy scalability, etc. (Pedrosa et al. 2015). From the reports it has been observed that most of theragnostic NPs are studied only for in vitro level followed by very less little in vivo analysis (Muthu et al. 2014). Nanotheragnosis has extensive scope in near future and detailed study in this direction at in vitro and in vivo level can help in curing many severe diseases like cancer at its early stage.

Acknowledgments The authors are thankful to the Director, CSIR-IHBT for his constant support and encouragement. The authors are also thankful to Dr. Sudesh Kumar Yadav for his valuable comments and suggestions during the preparation of book chapter. AA acknowledges the financial support from CSIR, GOI in the form of BSC0213 and MLP0068. SW acknowledges CSIR for project fellowship in the form of BSC0213. The CSIR-IHBT Communication Number of this manuscript is 3969.

References

Acharya A (2013) Luminescent magnetic quantum dots for in *vitro/in vivo* imaging and applications in therapeutics. J Nanosci Nanotechnol 13:3753–3768

Acharya A, Rawat K, Bhat KA et al (2015) A multifunctional magneto-fluorescent nanocomposite for visual recognition of targeted cancer cells. Mater Res Express 2:115401

Ahmed N, Fessi H, Elaissari A (2012) Theranostic applications of nanoparticles in cancer. Drug Discov Today 17:928–934

Akerman ME, Chan WC, Laakkonen P et al (2002) Nanocrystal targeting *in vivo*. Proc Natl Acad Sci 99:12617–12621

Alexis F, Pridgen E, Molnar LK et al (2008) Factors affecting the clearance and biodistribution of polymeric nanoparticles. Mol Pharm 5:505–515

Alharbi KK, Al-sheikh YA (2014) Role and implications of nanodiagnostics in the changing trends of clinical diagnosis. Saudi J Biol Sci 21:109–117

Allen PM, Bawendi MG (2008) Ternary I-III-VI quantum dots luminescent in the red to near-infrared. J Am Chem Soc 130:9240–9241

Asín L, Goya GF, Tres A et al (2013) Induced cell toxicity originates dendritic cell death following magnetic hyperthermia treatment. Cell Death Dis 4: e596

Ballou B, Ernst LA, Andreko S et al (2007) Sentinel lymph node imaging using quantum dots in mouse tumor models. Bioconjug Chem 18:389–396

Barentsz J, Takahashi S, Oyen W et al (2006) Commonly used imaging techniques for diagnosis and staging. J Clin Oncol 24:3234–3244

Barnett SC, Riddell JS (2004) Olfactory ensheathing cells (OECs) and the treatment of CNS injury: advantages and possible caveats. J Anat 204:57–67

BBC Research. Nanotechnology in medical applications: the global market. Wellesley, MA, BBC Research, Jan 2010. http://www.bccresearch.com/market-research/healthcare/nanotechnology-medical-applications-hlc069a.html. Accessed 3 Jan 2015

Béalle G, Di Corato R, Kolosnjaj-Tabi J et al (2012) Ultra magnetic liposomes for MR imaging, targeting, and hyperthermia. Langmuir 28:11834–11842

Beer AJ, Schwaiger M (2008) Imaging of integrin alphavbeta3 expression. Cancer Metastasis Rev 27:631–644

Blomley MJ, Cooke JC, Unger EC et al (2001) Microbubble contrast agents: a new era in ultrasound. BMJ 322:1222–1225

Brenner TL, Adams VR (1999) First MAb approved for treatment of metastatic breast cancer. J Am Pharm Assoc 39:236–238

Breunig M, Bauer S, Goepferich A (2008) Polymers and nanoparticles: intelligent tools for intracellular targeting? Eur J Pharm Biopharm 68:112–128

Bruchez M Jr, Moronne M, Gin P et al (1998) Semiconductor nanocrystals as fluorescent biological labels. Science 281:2013–2016

Bulte JW, Douglas T, Witwer B et al (2002) Monitoring stem cell therapy *in vivo* using magnetodendrimers as a new class of cellular MR contrast agents. Acad Radiol 2:S332–S335

Bunge SD, Boyle TJ, Headley TJ (2003) Synthesis of coinage-metal nanoparticles from mesityl precursors. Nano Lett 3:901–905

Burns AA, Vider J, Ow H et al (2009) Fluorescent silica nanoparticles with efficient urinary excretion for nanomedicine. Nano Lett 9:442–448

Bwatanglang IB, Mohammad F, Yusof NA (2014) Role of multifunctional nanomaterials in disease diagnosis and therapy. J Chem Pharm Res 6:821–844

Cai W, Shin DW, Chen K et al (2006) Peptide-labeled near-infrared quantum dots for imaging tumor vasculature in living subjects. Nano Lett 6:669–676

Cai W, Chen K, Li ZB et al (2007) Dual-function probe for PET and near-infrared fluorescence imaging of tumor vasculature. J Nucl Med 48:1862–1870

Cassidy PJ, Radda GK (2005) Molecular imaging perspectives. J R Soc Interface R Soc 2:133–144

Celli JP, Spring BQ, Rizvi I et al (2010) Imaging and photodynamic therapy: mechanisms, monitoring, and optimization. Chem Rev 110:2795–2838

Cha EJ, Jang ES, Sun IC et al (2011) Development of MRI/NIRF 'activatable' multimodal imaging probe based on iron oxide nanoparticles. J Control Release 155:152–158

Chatterjee DK, Fong LS, Zhang Y (2008) Nanoparticles in photodynamic therapy: an emerging paradigm. Adv Drug Deliv Rev 60:1627–1637

Chen F, Nayak TR, Goel S et al (2014a) *In vivo* tumor vasculature targeted PET/NIRF imaging with TRC105 (Fab)-conjugated, dual-labeled mesoporous silica nanoparticles. Mol Pharm 11:4007–4014

Chen N, Shao C, Qu Y et al (2014b) Folic acid-conjugated MnO nanoparticles as a T_1 contrast agent for magnetic resonance imaging of tiny brain gliomas. ACS Appl Mater Interfaces 6:19850–19857

Cherry SR, Louie AY, Jacobs RE (2008) The integration of positron emission tomography with magnetic resonance imaging. Proc IEEE 96:416–438

Chiang WH, Ho VT, Chen HH et al (2013) Langmuir 29:6434–6443

Chiaviello A, Postiglione I, Palumbo G (2011) Targets and mechanisms of photodynamic therapy in lung cancer cells: a brief overview. Cancers 3:1014–1041

Choi HS, Frangioni JV (2010) Nanoparticles for biomedical imaging: fundamentals of clinical translation. Mol Imaging 9:291–310

Choi HS, Liu W, Misra P et al (2007) Renal clearance of quantum dots. Nat Biotechnol 25:1165–1170

Choi JS, Park JC, Nah H et al (2008) A hybrid nanoparticle probe for dual-modality positron emission tomography and magnetic resonance imaging. Angew Chem Int Ed Engl 47:6259–6262

Choi HS, Ipe BI, Misra P et al (2009) Tissue- and organ-selective biodistribution of NIR fluorescent quantum dots. Nano Lett 9:2354–2359

Choi KY, Liu G, Lee S et al (2012) Theranostic nanoplatforms for simultaneous cancer imaging and therapy: current approaches and future perspectives. Nanoscale 4:330–342

Connor EE, Mwamuka J, Gole A et al (2005) Gold nanoparticles are taken up by human cells but do not cause acute cytotoxicity. Small 1:325–327

Cormode DP, Skajaa T, Fayad ZA et al (2009) Nanotechnology in medical imaging: probe design and applications. Arterioscler Thromb Vasc Biol 29:992–1000

Cormode DP, Naha PC, Fayad ZA (2014) Nanoparticle contrast agents for computed tomography: a focus on micelles. Contrast Media Mol Imaging 9:37–52

Creighton JA, Blatchford CG, Albrecht MG (1979) Plasma resonance enhancement of Raman scattering by pyridine adsorbed on silver or gold sol particles of size comparable to the excitation wavelength. J Chem Soc Faraday Trans 2: Mol Chem Phys 75:790–798

Crooks RM, Zhao M, Sun L et al (2001) Dendrimer-encapsulated metal nanoparticles: synthesis, characterization, and applications to catalysis. Acc Chem Res 234:181–190

De Leo V, Catucci L, Falqui A et al (2014) Hybrid assemblies of fluorescent nanocrystals and membrane proteins in liposomes. Langmuir 30:1599–1608

de Rosales RTM (2014) Potential clinical applications of bimodal PET-MRI or SPECT-MRI agents. J Labelled Comp Radiopharm 57:298–303

de Rosales RTM, Tavaré R, Glaria A et al (2011a) ^{99m}Tc-bisphosphonate-iron oxide nanoparticle conjugates for dual-modality biomedical imaging. Bioconjugate Chem 22:455–465

de Rosales RTM, Tavaré R, Paul RL et al (2011b) Synthesis of $^{64}Cu^{II}$–Bis(dithiocarbamatebisphosphonate) and its conjugation with superparamagnetic iron oxide nanoparticles: *in vivo* evaluation as dual-modality PET–MRI Agent. Angew Chem Int Ed Engl 50:5509–5513

Dubertret B, Skourides P, Norris DJ et al (2002) *In vivo* imaging of quantum dots encapsulated in phospholipid micelles. Science 298:1759–1762

Egusquiaguirre SP, Igartua M, Hernandez RM et al (2012) Nanoparticle delivery systems for cancer therapy: advances in clinical and preclinical research. Clin Transl Oncol 14:83–93

Ell PJ (2006) The contribution of PET/CT to improved patient management. Br J Radiol 79:32–36

El-Sayed MA (2001) Some interesting properties of metals confined in time and nanometer space of different shapes. Acc Chem Res 34:257–264

Etheridge ML, Campbell SA, Erdman AG et al (2013) The big picture on nanomedicine: the state of investigational and approved nanomedicine products. Nanomedicine 9:1–14

Fang C, Zhang M (2010) Nanoparticle-based theragnostics: integrating diagnostic and therapeutic potentials in nanomedicine. J Control Release 146:2–5

Fantechi E, Innocenti C, Zanardelli M et al (2014) A smart platform for hyperthermia application in cancer treatment: cobalt-doped ferrite nanoparticles mineralized in human ferritin cages. ACS Nano 8:4705–4719

Figueiredo M, Esenaliev R (2012) PLGA nanoparticles for ultrasound-mediated gene delivery to solid tumors. J Drug Deliv 2012:1–20

Frangioni JV, Kim SW, Ohnishi S et al (2007) Sentinel lymph node mapping with type-II quantum dots methods. Mol Biol 374:147–159

Gao X, Cui Y, Levenson RM et al (2004) *In vivo* cancer targeting and imaging with semiconductor quantum dots. Nat Biotechnol 22:969–976

Gelperina S, Kisich K, Iseman MD et al (2005) The potential advantages of nanoparticle drug delivery systems in chemotherapy of tuberculosis. Am J Respir Crit Care Med 172:1487–1490

Giljohann DA, Seferos DS, Daniel WL et al (2010) Gold nanoparticles for biology and medicine. Angew Chem Int Ed Engl 49:3280–3294

Gonçalves MS (2009) Fluorescent labeling of biomolecules with organic probes. Chem Rev 109:190–212

Gref R, Minamitake Y, Peracchia MT et al (1994) Biodegradable long-circulating polymeric nanospheres. Science 263:1600–1603

Groneberg DA, Giersig M, Welte T et al (2006) Nanoparticle-based diagnosis and therapy. Curr Drug Targets 7:643–648

Han M, Gao X, Su JZ et al (2001) Quantum-dot-tagged microbeads for multiplexed optical coding of biomolecules. Nat Biotechnol 19:631–635

Hasebroock KM, Serkova NJ (2009) Toxicity of MRI and CT contrast agents. Expert Opinion Drug Metab Toxicol 5:403–416

Hawkins MJ, Soon-Shiong P, Desai N (2008) Protein nanoparticles as drug carriers in clinical medicine. Adv Drug Deliv Rev 60:876–885

Heidt T, Nahrendorf M (2012) Multimodal iron oxide nanoparticles for hybrid biomedical imaging. NMR Biomed 26:756–765

Herranz M, Ruibal A (2012) Optical imaging in breast cancer diagnosis: the next evolution J. Oncol 2012:8637–8647

Hirsch LR, Gobin AM, Lowery AR et al (2006) Metal nanoshells. Ann Biomed Eng 34:15–22

Ho D, Sun X, Sun S (2011) Monodisperse magnetic nanoparticles for theranostic applications. Acc Chem Res 44:875–882

Horimoto NN, Imura K, Okamoto H (2008) Dye fluorescence enhancement and quenching by gold nanoparticles: direct near-field microscopic observation of shape dependence. Chem Phys Lett 467:105–109

Hu CM, Zhang L, Aryal S et al (2011) Erythrocyte membrane-camouflaged polymeric nanoparticles as a biomimetic delivery platform. Proc Natl Acad Sci 108:10980–10985

Hu F, Li C, Zhang Y et al (2015) Real time *in vivo* visualization of tumor therapy by a near-infrared-II Ag_2S Quantum dot-based theranostic nanoplatform. Nano Res 8:1637–1647

Huang X, El-Sayed IH, Qian W et al (2006) Cancer cell imaging and photothermal therapy in the near-infrared region by using gold nanorods. J Am Chem Soc 128:2115–2120

Hwang do W, Ko HY, Lee JH et al (2010) A nucleolin-targeted multimodal nanoparticle imaging probe for tracking cancer cells using an aptamer. J Nucl Med 51:98–105

Jang WD, Selim KMK, Lee CH et al (2009) Bioinspired application of dendrimers: from bio-mimicry to biomedical applications. Prog Polym Sci 34:1–23

Janib SM, Moses AS, MacKay JA (2010) Imaging and drug delivery using theranostic nanoparticles. Adv Drug Deliv Rev 62:1052–1063

Jarrett BR, Gustafsson B, Kukis DL et al (2008) Synthesis of ^{64}Cu-labeled magnetic nanoparticles for multimodal imaging. Bioconjug Chem 19:1496–1504

Jennings LE, Long NJ (2009) 'Two is better than one'—probes for dual-modality molecular imaging. Chem Commun 28:3511–3524

Jeong H, Huh M, Lee SJ et al (2011) Photosensitizer-conjugated human serum albumin nanoparticles for effective photodynamic therapy. Theranostics 1:230–239

Jia G, Wang H, Yan L et al (2005) Cytotoxicity of carbon nanomaterials: single-wall nanotube, multi-wall nanotube, and fullerene. Environ Sci Technol 39:1378–1383

Johannsen M, Thiesen B, Wust P et al (2010) Magnetic nanoparticle hyperthermia for prostate cancer. Int J Hyperthermia 26:790–795

Jordan A, Maier-Hauff K, Wust P et al (2006) Nanoparticles for thermotherapy. In: Kumar C

(ed) Nanomaterials for cancer therapy. Wiley-VCH, Weinheim, pp 242–258
Josephson L, Kircher MF, Mahmood U et al (2002) Near-infrared fluorescent nanoparticles as combined MR/Optical imaging probes. Bioconj Chem 13:554–560
Kelkar SS, Reineke TM (2011) Theragnostics: combining imaging and therapy. Bioconjug Chem 22:1879–1903
Key J, Leary JF (2014) Nanoparticles for multimodal *in vivo* imaging in Nanomedicine. Int J Nanomedicine 9:711–726
Khemtong C, Kessinger CW, Gao J (2009) Polymeric nanomedicine for cancer MR imaging and drug delivery. Chem Commun 3497–3510
Kievit FM, Zhang M (2011) Cancer nanotheranostics: improving imaging and therapy by targeted delivery across biological barriers. Adv Mater 23:H217–H247
Kim S, Lim YT, Soltesz EG et al (2004) Near-infrared fluorescent type II quantum dots for sentinel lymph node mapping. Nat Biotechnol 22:93–97
Kim SW, Zimmer JP, Ohnishi S et al (2005) Engineering InAs(x)P(1-x)/InP/ZnSe III-V alloyed core/shell quantum dots for the near-infrared. J Am Chem Soc 127:10526–10532
Kim D, Kim JW, Jeong YY et al (2009a) Antibiofouling polymer coated gold@ iron oxide nanoparticle as a dual contrast agent for CT and MRI. Bull Korean Chem Soc 30:1855–1857
Kim J, Piao Y, Hyeon T (2009b) Multifunctional nanostructured materials for multimodal imaging, and simultaneous imaging and therapy. Chem Soc Rev 38:372–390
Kim K, Kim JH, Park H et al (2010) Tumor-homing multifunctional nanoparticles for cancer theragnosis: simultaneous diagnosis, drug delivery, and therapeutic monitoring. J Control Release 146:219–227
Kim D, Yu MK, Lee TS et al (2011) Amphiphilic polymer-coated hybrid nanoparticles as CT/MRI dual contrast agents. Nanotechnology 22:155101
Knapp DW, Adams LG, Degrand AM et al (2007) Sentinel lymph node mapping of invasive urinary bladder cancer in animal models using invisible light. Eur Urol 52:1700–1708
Kolosnjaj J, Szwarc H, Moussa F (2007) Toxicity studies of carbon nanotubes. Adv Exp Med Biol 620:181–204
Krishanan KM (2010) Biomedical nanomagnetics: a spin through possibilities in imaging, diagnostics, and therapy. IEEE Trans Magn 46:2523–2558
Lammers T, Kiessling F, Hennink WE et al (2010) Nanotheranostics and image-guided drug delivery: current concepts and future directions. Mol Pharm 7:1899–1912
Lammers T, Aime S, Hennink WE et al (2011) Theranostic nanomedicine. Acc Chem Res 44:1029–1038
Langer R (1998) Drug delivery and targeting. Nature 392:5–10
Larina IV, Evers BM, Ashitkov TV et al (2005) Enhancement of drug delivery in tumors by using interaction of nanoparticles with ultrasound radiation. Technol Cancer Res Treat 4:217–226
Lee IH, Bulte JW, Schweinhardt P et al (2004) *In vivo* magnetic resonance tracking of olfactory ensheathing glia grafted into the rat spinal cord. Exp Neurol 187:509–516
Lee SJ, Koo H, Jeong H et al (2011a) Comparative study of photosensitizer loaded and conjugated glycol chitosan nanoparticles for cancer therapy. J Control Release 152:21–29
Lee SJ, Koo H, Lee DE et al (2011b) Tumor-homing photosensitizer-conjugated glycol chitosan nanoparticles for synchronous photodynamic imaging and therapy based on cellular on/off system. Biomaterials 32:4021–4029
Lee DE, Koo H, Sun IC et al (2012) Multifunctional nanoparticles for multimodal imaging and theragnosis. Chem Soc Rev 41:2656–2672
Li X, Qian J, Jiang L et al (2009) Fluorescence quenching of quantum dots by gold nanorods and its application to DNA detection. Appl Phys Lett 94:063111–063113
Li L, Jiang W, Luo K et al (2013) Superparamagnetic iron oxide nanoparticles as MRI contrast agents for non-invasive stem cell labeling and tracking. Theranostics 3:595–615
Liang M, Liu X, Cheng D et al (2010) Multimodality nuclear and fluorescence tumor imaging in mice using a streptavidin nanoparticle. Bioconjug Chem 21:1385–1388
Liang S, Zhou Q, Wang M et al (2015) Water-soluble L-cysteine-coated Fe-Pt nanoparticles as dual MRI/CT imaging contrast agent for glioma. Int J Nanomedicine 10:2325–2333
Lin TY, Li YP, Zhang H et al (2013) Tumor-targeting multifunctional micelles for imaging and chemotherapy of advanced bladder cancer. Nanomedicine 8:1239–1251
Liu W, Choi HS, Zimmer JP et al (2007) Compact cysteine-coated CdSe(ZnCdS) quantum dots for *in vivo* applications. J Am Chem Soc 129:14530–14531
Liu J, Yu M, Zhou C et al (2013) Renal clearable inorganic nanoparticles: a new frontier of bionanotechnology. Mater Today 16:477–486
Longmire M, Choyke PL, Kobayashi H (2008) Clearance properties of nano-sized particles and molecules as imaging agents: considerations and caveats. Nanomedicine 3:703–717
Louie A (2010) Multimodality imaging probes: design and challenges. Chem Rev 110:146–3195
Lovrić J, Bazzi HS, Cuie Y et al (2005) Differences in subcellular distribution and toxicity of green and red emitting CdTe quantum dots. J Mol Med 83:377–385
Lusic H, Grinstaff MW (2013) X-ray-computed tomography contrast agents. Chem Rev 113:1641–1666
Mader H, Li X, Saleh S et al (2008) Fluorescent silica nanoparticles. Ann N Y Acad Sci 1130:218–223
Maier-Hauff K, Rothe R, Scholz R et al (2007) Intracranial thermotherapy using magnetic nanoparticles combined with external beam radiotherapy: results of a feasibility study on patients with glioblastoma multiforme. J Neurooncol 81:53–60

Makarov VV, Love AJ, Sinitsyna OV et al (2014) "Green" nanotechnologies: synthesis of metal nanoparticles using plants. Acta Naturae 6:35–44
Massoud TF, Gambhir SS (2003) Molecular imaging in living subjects: seeing fundamental biological processes in a new light. Genes Dev 17:545–580
Mazzola L (2003) Commercializing nanotechnology. Nat Biotechnol 21:1137–1143
Medina SH, El-Sayed ME (2009) Dendrimers as carriers for delivery of chemotherapeutic agents. Chem Rev 109:3141–3157
Medintz IL, Uyeda HT, Goldman ER et al (2005) Quantum dot bioconjugates for imaging, labelling and sensing. Nat Mater 4:435–446
Mitragotri S, Stayton P (2014) Organic nanoparticles for drug delivery and imaging. MRS Bull 39:219–223
Movassaghian S, Merkel OM, Torchilin VP (2015) Applications of polymer micelles for imaging and drug delivery. Wiley Interdiscip Rev Nanomed Nanobiotechnol 7:691–707
Mura S, Nicolas J, Couvreur P (2013) Stimuli-responsive nanocarriers for drug delivery. Nat Mater 12:991–1003
Murray CB, Kagan CR, Bawendi MG (2000) Synthesis and Characterization of monodispersenanocrystals and close packed nanocrystal assemblies. Annu Rev Mater Sci 30:545–610
Muthu MS, Leong DT, Mei L et al (2014) Nanotheranostics - Application and further development of nanomedicine strategies for advanced theranostics. Theranostics 4:660–677
Nahrendorf M, Zhang H, Hembrador S et al (2008) Nanoparticle PET-CT imaging of macrophages in inflammatory atherosclerosis. Circulation 117:379–387
Nel A, Xia T, Mädler L et al (2006) Toxic potential of materials at the nanolevel. Science 311:622–627
Nel A, Mädler L, Velegol D et al (2009) Understanding biophysicochemical interactions at the nano-bio interface. Nat Mater 8:543–557
Nie S, Xing Y, Kim GJ et al (2007) Nanotechnology applications in cancer. Annu Rev Biomed Eng 9:257–288
Nikalje AP (2015) Nanotechnology and its Applications in Medicine. Med Chem 5:81–89
Nikoobakht B, El-Sayed MA (2003) Surface-enhanced Raman scattering studies on aggregated gold nanorods. J Phys Chem A 107:3372–3378
Ohnishi S, Lomnes SJ, Laurence RG et al (2005) Organic alternatives to quantum dots for intraoperative near-infrared fluorescent sentinel lymph node mapping. Mol Imaging 4:172–181
Orendorff CJ, Gearheart L, Jana NR et al (2006) Aspect ratio dependence on surface enhanced Raman scattering using silver and gold nanorod substrates. Phys Chem Chem Phys 8:165–170
Owens DE, Peppas NA (2006) Opsonization, biodistribution, and pharmacokinetics of polymeric nanoparticles. Int J Pharm 307:93–102
Panigrahi S, Kundu S, Ghosh S et al (2004) General method of synthesis for metal nanoparticles. J Nanopart Res 6:411–414
Parhi P, Mohanty C, Sahoo SK (2012) Nanotechnology-based combinational drug delivery: an emerging approach for cancer therapy. Drug Discov Today 17:1044–1052
Park JH, von Maltzahn G, Ruoslahti E et al (2008) Micellar hybrid nanoparticles for simultaneous magnetofluorescent imaging and drug delivery. Angew Chem Int Ed Engl 47:7284–7288
Park JC, Yu MK, An GI et al (2010a) Facile preparation of a hybrid nanoprobe for triple-modality optical/PET/MR imaging. Small 6:2863–2868
Park JH, Saravanakumar G, Kim K et al (2010b) Targeted delivery of low molecular drugs using chitosan and its derivatives. Adv Drug Deliv Rev 62:28–41
Park SY, Baik HJ, Oh YT et al (2011) A smart polysaccharide/drug conjugate for photodynamic therapy. Angew Chem Int Ed Engl 50:1644–1647
Parungo CP, Ohnishi S, Kim SW et al (2005) Intraoperative identification of esophageal sentinel lymph nodes with near-infrared fluorescence imaging. J Thorac Cardiovasc Surg 129:844–850
Paull R, Wolfe J, Hébert P et al (2003) Investing in nanotechnology. Nat Biotechnol 21:1144–1147
Pedrosa P, Vinhas R, Fernandes A et al (2015) Gold Nanotheranostics: proof-of-concept or clinical tool? Nanomaterials 5:1853–1879
Pimlott SL, Sutherland A (2011) Molecular tracers for the PET and SPECT imaging of disease. Chem Soc Rev 40:149–162
Pison U, Welte T, Giersig M et al (2006) Nanomedicine for respiratory diseases. Eur J Pharmacol 533:341–350
Rajeeva BB, Menz R, Zheng Y (2014) Towards rational design of multifunctional theranostic nanoparticles: what barriers do we need to overcome? Nanomedicine 9:1767–1770
Ryu JH, Koo H, Sun IC et al (2012) Tumor-targeting multi-functional nanoparticles for theragnosis: new paradigm for cancer therapy. Adv Drug Deliv Rev 64:1447–1458
Salvador-Morales C, Gao W, Ghatalia P et al (2009) Multifunctional nanoparticles for prostate cancer therapy. Expert Rev Anticancer Ther 9:211–221
Samad A, Sultana Y, Aqil M (2007) Liposomal drug delivery systems: an update review. Curr Drug Deliv 4:297–305
Sanvicens N, Marco MP (2008) Multifunctional nanoparticles—properties and prospects for their use in human medicine. Trends Biotechnol 26:425–433
Sarparanta M, Bimbo LM, Rytkönen J et al (2012) Intravenous delivery of hydrophobin-functionalized porous silicon nanoparticles: stability, plasma protein adsorption and biodistribution. Mol Pharm 9:654–663
Scherzinger AL, Hendee WR (1986) Basic principles of magnetic resonance imaging- An update. Western J Med 143:782–792
Schultz DA (2003) Plasmon resonant particles for biological detection. Curr Opin Biotechnol 14:13–22
Shapira A, Livney YD, Broxterman HJ et al (2011) Nanomedicine for targeted cancer therapy: towards the

overcoming of drug resistance. Drug Resist Updat 14:150–163
Shen M, Shi X (2010) Dendrimer-based organic/inorganic hybrid nanoparticles in biomedical applications. Nanoscale 2:1596–1610
Shi X, Lee I, Baker JR (2008) Acetylation of dendrimer-entrapped gold and silver nanoparticles. J Mater Chem 18:586–593
Singh S (2013) Nanostructures: enhancing potential applications in biomedicals. J Biomater Nanobiotechnol 4:12–16
Slowing II, Vivero-Escoto JL, Wu CW et al (2008) Mesoporous silica nanoparticles as controlled release drug delivery and gene transfection carriers. Adv Drug Deliv Rev 60:1278–1288
Smith AM, Gao X, Nie S (2004) Quantum dot nanocrystals for *in vivo* molecular and cellular imaging. Photochem Photobiol 80:377–385
Sosnovik DE, Nahrendorf M, Weissleder R (2007) Molecular magnetic resonance imaging in cardiovascular medicine. Circulation 115:2076–2086
Tada H, Higuchi H, Wanatabe TM et al (2007) *In vivo* real-time tracking of single quantum dots conjugated with monoclonal anti-HER2 antibody in tumors of mice. Cancer Res 67:1138–1144
Tasis D, Tagmatarchis N, Georgakilas V et al (2003) Soluble carbon nanotubes. Chemistry 9:4000–4008
Taton TA (2002) Nanostructures as tailored biological probes. Trends Biotechnol 20:277–279
Thomas R, Park I-K, Jeong YY (2013) Magnetic iron oxide nanoparticles for multimodal imaging and therapy of cancer. Int J Mol Sci 14:15910–15930
Torchilin VP (2007) Micellar nanocarriers: pharmaceutical perspectives. Pharm Res 24:1–16
Tsien RY (1998) The green fluorescent protein. Annu Rev Biochem 67:509–544
Tunici P, Bulte JW, Bruzzone MG et al (2006) Brain engraftment and therapeutic potential of stem/progenitor cells derived from mouse skin. J Gene Med 8:506–513
Valden M, Lai X, Goodman DW (1998) Onset of catalytic activity of gold clusters on titania with the appearance of nonmetallic properties. Science 281:1647–1650
van Nostrum CF (2004) Polymeric micelles to deliver photosensitizers for photodynamic therapy. Adv Drug Deliv Rev 56:9–16
Walia S, Acharya A (2015) Silica micro/nanospheres for theranostics: from bimodal MRI and fluorescent imaging probes to cancer therapy Beilstein J Nanotechnol 6:546–558
Walia S, Sharma S, Kulurkar PM et al (2016) A bimodal molecular imaging probe based on chitosan encapsulated magneto-fluorescent nanocomposite offers biocompatibility, visualization of specific cancer cells *in vitro* and lung tissues *in vivo*. Int J Pharma 498:110–118
Wang L-S, Chuang M-C, Ho JA (2012) Nanotheranostics–a review of recent publications. Int J Nanomedicine 7:4679–4695
Weissleder R (2002) Scaling down imaging: molecular mapping of cancer in mice. Nat Rev Cancer 2:11–18
Weissleder R, Pittet MJ (2008) Imaging in the era of molecular oncology. Nature 452:580–589
Willmann JK, van Bruggen N, Dinkelborg LM et al (2008) Molecular imaging in drug development. Nat Rev Drug Discov 7:591–607
Wu H-C, Chang X, Liu L et al (2010) Chemistry of carbon nanotubes in biomedical applications. J Mater Chem 20:1036–1052
Xia B, Zhang W, Shi J et al (2013) Engineered stealth porous silicon nanoparticles *via* surface encapsulation of bovine serum albumin for prolonging blood circulation *in vivo*. ACS Appl Mater Interfaces 5:11718–11724
Xiao B, Han MK, Viennois E et al (2015) Hyaluronic acid-functionalized polymeric nanoparticles for colon cancer-targeted combination chemotherapy. Nanoscale 7:17745–17755
Xie J, Chen K, Huang J et al (2010a) PET/NIRF/MRI triple functional iron oxide nanoparticles. Biomaterials 31:3016–3022
Xie J, Lee S, Chen X (2010b) Nanoparticle-based theranostic agents. Adv Drug Deliv Rev 62:1064–1079
Xing H, Bu W, Zhang S et al (2012) Multifunctional nanoprobes for upconversion fluorescence, MR and CT trimodal imaging. Biomaterials 33:1079–1089
Xing Y, Zhao J, Conti PS et al (2014) Radiolabeled nanoparticles for multimodality tumor imaging. Theranostics 4:290–306
Yang X, Hong H, Grailer JJ et al (2011) cRGD-functionalized, DOX-conjugated, and ^{64}Cu-labeled superparamagnetic iron oxide nanoparticles for targeted anticancer drug delivery and PET/MR imaging. Biomaterials 32:4151–4160
Yang S, Sun S, Zhou C et al (2015) Renal clearance and degradation of glutathione-coated copper nanoparticles. Bioconjugate Chem 26:511–519
Yezhelyev MV, Gao X, Xing Y et al (2006) Emerging use of nanoparticles in diagnosis and treatment of breast cancer. Lancet Oncol 7:657–667
Yi DK, Sun IC, Ryu JH et al (2010) Matrix metalloproteinase sensitive gold nanorod for simultaneous bioimaging and photothermal therapy of cancer. Bioconjug Chem 21:2173–2177
Zhang Y, Chen W, Zhang J et al (2007) *In vitro* and *in vivo* toxicity of CdTe nanoparticles. J Nanosci Nanotechnol 7:497–503
Zhang L, Gu FX, Chan JM et al (2008) Nanoparticles in medicine: therapeutic applications and developments. Clin Pharmacol Ther 83:761–769
Zhang R, Lu W, Wen X et al (2011) Annexin A5-conjugated polymeric micelles for dual SPECT and optical detection of apoptosis. J Nucl Med 52:958–964
Zhang Y, Xiao L, Popovic K et al (2013) Novel cancer-targeting SPECT/NIRF dual-modality imaging probe ^{99m}Tc-PC-1007: synthesis and biological evaluation. Bioorg Med Chem Lett 23:6350–6354

Zheng J, Liu J, Dunne M et al (2007) *In vivo* performance of a liposomal vascular contrast agent for CT and MR-based image guidance applications. Pharmaceut Res 24:1193–1201

Zhou C, Long M, Qin Y et al (2011) Luminescent gold nanoparticles with efficient renal clearance. Angew Chem Int Ed 50:3168–3172

Zhou J, Yang Y, Zhang CY (2015a) Toward biocompatible semiconductor quantum dots: from biosynthesis and bioconjugation to biomedical application. Chem Rev 115:11669–11717

Zhou Q, Mu K, Jiang L et al (2015b) Glioma-targeting micelles for optical/magnetic resonance dual-mode imaging. Int J Nanomedicine 10:1805–1818

Zhu HW, Xu CL, Wu DH et al (2002) Direct synthesis of long single-walled carbon nanotube strands. Science 296:884–886

Zimmer JP, Kim SW, Ohnishi S (2006) Size series of small indium arsenide-zinc selenide core-shell nanocrystals and their application to *in vivo* imaging. J Am Chem Soc 128:2526–2527

Cellular Response of Therapeutic Nanoparticles

7

Avnesh Kumari, Rubbel Singla, Anika Guliani, Amitabha Acharya and Sudesh Kumar Yadav

Abstract

Nanoparticles (NPs) are being extensively used in the field of nanomedicines. Different types of NPs are administered into the body by various routes. NPs come in contact with cells inside the body. Cellular response of NPs is affected by size, shape, surface chemistry, and cellular uptake pathways of NPs. In addition to this, type of cells, various cell lines, and growth media are also found to affect the cellular response of NPs. NPs induce diverse cellular responses like apoptosis, necrosis, and reactive oxygen species (ROS) production. NPs also form a protein corona inside the biological media which may alter their identity and behaviour as compared to bare NPs. In this chapter, we have made an attempt to throw light on cellular uptake pathways of NPs, monitoring of endocytic pathways followed by NPs, factors affecting cellular responses of therapeutic NPs, and protein corona formation, characterisation and its implications on fate of NPs.

Keywords

Cellular uptake · Endocytic pathways · Protein corona · Hard corona · Soft corona

A. Kumari · R. Singla · A. Guliani · A. Acharya (✉) · S.K. Yadav
Department of Biotechnology, Council of Scientific and Industrial Research-Institute of Himalayan Bioresource Technology, Palampur 176061, Himachal Pradesh, India
e-mail: amitabhachem@gmail.com
amitabha@ihbt.res.in

A. Kumari · R. Singla · A. Guliani · A. Acharya · S.K. Yadav
Academy of Scientific and Innovative Research, New Delhi, India

S.K. Yadav (✉)
Department of Biotechnology, Center of Innovative and Applied Bioprocessing (CIAB), Mohali 160071, Punjab, India
e-mail: skyt@rediffmail.com; sudesh@ciab.res.in

© Springer Science+Business Media Singapore 2016
S.K. Yadav (ed.), *Nanoscale Materials in Targeted Drug Delivery, Theragnosis and Tissue Regeneration*, DOI 10.1007/978-981-10-0818-4_7

Contents

7.1 Introduction

Recent developments in the biomedical sciences such as hyperthermia cancer therapy (Hainfeld et al. 2004; El-Sayed et al. 2005; El-sayed et al. 2006), targeted gene, and drug delivery (Sandhu et al. 2002; Koo et al. 2005) involve the interaction of nanoparticles (NPs) with living organisms, at the cellular level (Alivisatos et al. 2005; Parak et al. 2005; Luccardini et al. 2007). All these applications of NPs involve administration of NPs by different routes. After administration by various routes, NPs come in contact with cells. NPs may not only enhance the pharmacological effects of drugs, but also cause unwanted effects in the target cells (Nishikawa et al. 2009). Many factors affect the biological response of NPs with cells.

Cellular response of NPs can be varied by changing the type of NPs. Changing of even one variable can induce a very different outcome for NPs exposed to cells (Oh et al. 2011). The biological responses of NPs are dependent on size, charge, chemical composition, shape and surface chemistry (Verma and Stellacci 2010). In addition, targeting moieties such as tripeptide glutathione, cell penetrating peptides, nuclear localisation signal peptides, and proteins can also affect the cellular response (Oh et al. 2011). These parameters can also affect the cellular uptake, and the biological response of NPs (Oberdorster et al. 2005; Xia et al. 2008a, b). NPs in the blood stream are known to encounter with plasma proteins and immune cells. Processes such as adsorption of proteins create unfavourable condition for cellular uptake. Uptake of NPs by immune cells may occur by various pathways and can be enhanced by adsorption of plasma proteins. NPs coated with targeting moieties activate their receptor-mediated internalisation. The activation of membrane receptors strongly depends on the size of nanomaterials. NPs coated with targeting moieties are also found to be activating cell signalling processes essential for basic cell functions including cell death (Jiang et al. 2008).

Cellular uptake of NPs also has an influence on response of NPs towards cells. They are involved in manipulation of signal transductions leading to the expression of cell functions (Nishikawa et al. 2009).

Owing to currently arising opportunities and concerns associated with NPs in living systems, it is of immense importance to develop an understanding of the complex processes that govern their cellular response and intracellular

fate of nanomaterials (NMs). Interestingly, the interaction between NPs and molecules of the biological milieu results in the formation of a biological coating on the surface of NPs (Lynch and Dawson 2008). Therefore, biological entity which interacts with cells, tissues and organs, is completely different from the original surface of the NPs. Formation of biomolecule corona is a dynamic process and biomolecules like proteins and lipids present in the biological fluids compete for NPs surface to form biomolecule corona (Mahmoudi et al. 2011a, b). The biomolecule corona is usually enriched with about 10–50 proteins, that have the maximum affinity for the NPs surface, out of several thousand proteins of the biological milieu. New and advanced techniques are required for deep understanding of both the thermodynamics and kinetics of the biomolecule corona evolution and its subsequent biological impacts (Mahmoudi et al. 2011a, b).

The biological responses to NPs are greatly affected by the key forces at the bio-nano interface and also by the inherent characteristics of the NPs like size, shape, charge, coatings, surface modifications with targeting ligands, crystallinity, electronic states, surface wrapping in the biological medium, hydrophobicity, and wettability. Therefore, a thoughtful investigation of the NP biomolecule complex is essential for the development of therapeutically safe NPs (Nel et al. 2009). In this chapter, we have covered pathways for cellular uptake of NPs, monitoring of endocytic pathways, cellular response of therapeutic NPs, and formation, characterisation, and factors affecting biomolecule corona of NPs.

7.2 Pathways for Cellular Uptake of Nanoparticles

The invasion of NPs in human body occurs via inhalation, ingestion or through the skin. Once these tiny particles enter a biological milieu, they will inevitably come into contact with a huge variety of biomolecules including proteins, sugars and lipids which are dissolved in body fluids. Thus, the NPs have to be viewed as evolving systems which adapt to varying concentrations of the biomolecules present in the fluid. NPs enter the cells mainly through the passive diffusion or active transport, while nanomedicines got entry into cells via endocytosis which helps the drug to penetrate the specific cells and get accumulated (Fig. 7.1). The endocytosis pathway has been classified according to the proteins which play a major role in the process. Correspondingly, the mechanism of interaction of NPs with cytomembrane which governs the entrance and travel of NPs inside cells has also been extensively studied.

Various aspects such as pathways of entrance, factors affecting the pathways, functions of some proteins involved in endocytosis are still uncertain and are not absolutely proven. Such study is necessary for better understanding of the novel field of multifunction nanomedicines. NPs uptake into cells occurs through endocytosis (Jones et al. 2003), a process by which cells absorb NPs from outside by engulfing them within their cell membrane (Conner and Schmid 2003). This process of cellular uptake is further categorised into two phenomena, namely phagocytosis and pinocytosis (Fig. 7.1). Phagocytosis was originally discovered in macrophages. Phagocytes such as macrophages, neutrophils and monocytes destroy foreign particles such as NPs in blood through the phagocytosis process (Watson et al. 2005). Relatively, large NPs prefer this mechanism which initially involves recognition by opsonin viz., immunoglobulin (IgG and IgM), complement component (C3, C4, and C5) and blood serum proteins. Thereafter, the NPs bind to the cell surface receptors inducing the cup-shaped membrane extension formation. Such membrane extensions encircle the NPs and then internalise them, forming the phagosomes of diameter 0.5–10 μm which finally move to fuse with lysosomes (Aderem and Underhill 1999). Pinocytosis has been reported to occur by four different mechanisms: macropinocytosis, caveolin-dependent endocytosis, clathrin-dependent endocytosis and clathrin/caveolin-independent endocytosis (Fig. 7.1) (Swanson and Watts 1995; Patel et al. 2007; Xu et al. 2009). Macropinocytosis is a growth factor-induced, actin-driven endocytosis and a non-selective process for uptake of solute molecules or cargo. Macropinocytosis involves the formation

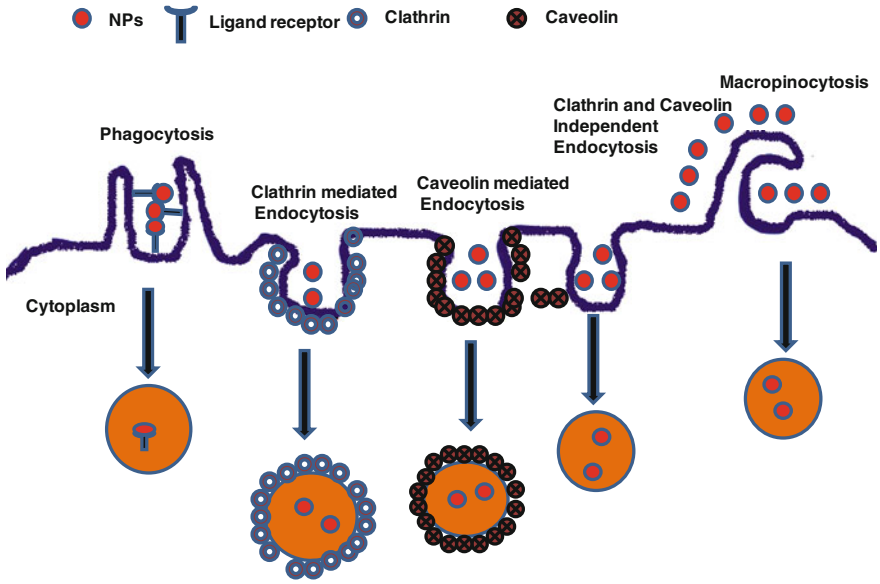

Fig. 7.1 Different uptake pathways followed by NPs for internalisation inside the cells. NPs follow phagocytosis, clathrin mediated endocytosis, caveolin mediated endocytosis, clathrin and caveolin-independent endocytosis and macropinocytosis pathways

of lamellipodia-like plasma membrane extensions. Interestingly, macropinosomes can uptake NPs of >200 nm in size (Walsh et al. 2006). Cellular uptake by macropinocytosis has been reported for PEGylated-poly-L-lysine NPs (Walsh et al. 2006). Receptor-mediated endocytosis process is assisted by specific proteins, either clathrin or caveolae (Bao and Bao 2005). Caveolin, a protein exists in most cells plays a dominant role in caveolae-dependent endocytosis process. This pathway bypasses lysosomes (Benmerah and Lamaze 2007), thus many pathogens including viruses and bacteria select this pathway to avoid lysosomal degradation (Medina-Kauwe 2007). Transferrin-coated PLGA NPs are highly absorbed by brain endothelial cells via caveolae pathway (Chang et al. 2009). Similarly, clathrin-coated pits have the ability to accumulate NPs only up to 100 nm (Pelkmans and Helenius 2002) and targeted (receptor) NPs are internalised by clathrin-mediated endocytosis (Walsh et al. 2006). The internalisation is more efficient for NPs smaller than the caveolae. Clathrin/caveolae-independent endocytosis is a distinct pathway which relies on cholesterol and requires specific lipid compositions. NPs endocytosis by cells not only depends on the size, but also on surface properties of the NPs. Carboxy dextran-coated superparamagnetic iron oxide NPs (SPION) have been internalised by human mesenchymal stem cells and the efficiency of internalisation was correlated with the amount of carboxyl groups on the NPs surface (Mailänder et al. 2008). Cationic NPs enter HeLa cells in greater amounts than anionic NPs (Harush-Frenkel et al. 2007; Dausend et al. 2008). NPs uptake may also depends on the length of the molecules on the surface coating (Chang et al. 2009), or the type of cells (Xia et al. 2008a, b).

7.3 Monitoring Endocytic Pathways

Researchers have been interested in identifying the different pathways that NPs use during their internalisation to cells. Either endocytic markers or inhibitors have been used for long time to locate NPs and confirm whether the corresponding pathway plays an important role in the

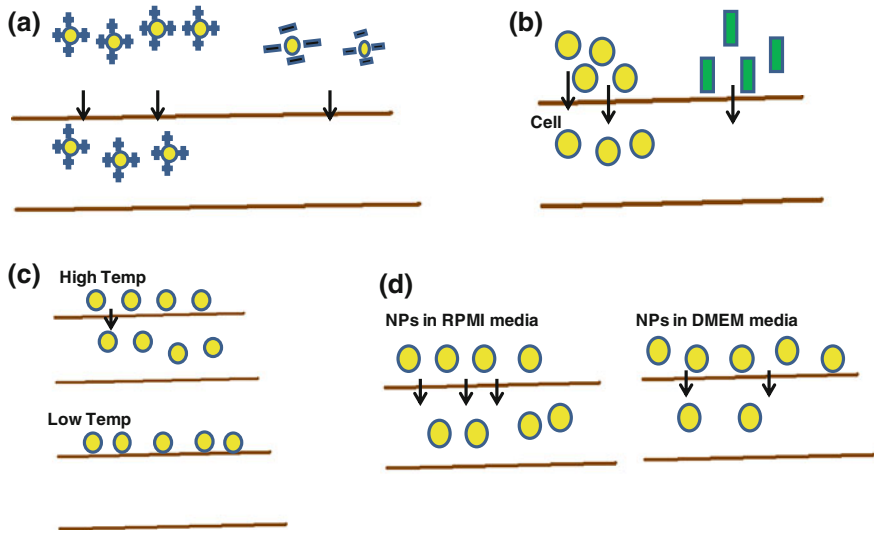

Fig. 7.2 Factors affecting cellular response of NPs **a** *Size* Positively charged NPs are well taken up by cells. **b** *Shape* Spherical NPs are efficiently taken up by cells **c** *Temperature* High temperature allows both cellular uptake and interaction, whereas at low temperature only interaction of NPs takes place. **d** *Cell culture media* NPs incubated in RPMI media showed more cell uptake than NPs incubated in DMEM media

uptake of the NPs. More recently, a combined approach has been postulated for better understanding of such mechanisms. Low-density lipoprotein (Duit et al. 2010) and transferrin (Liu et al. 2010a) enter into cells through clathrin-dependent endocytosis, and hence these are commonly used markers for clathrin-dependent endocytosis process. Similarly, caveolin-1 is mostly used as a marker of caveolae-dependent endocytosis, and dextran is the marker of macropinocytosis (Petrescu et al. 2009). Inhibitors can be used to block certain endocytic pathways to verify whether this route has been used by NPs to enter cells. It has been reported that amiloride, cytochalasin D and rottlerin can block macropinocytosis (Diken et al. 2011), whereas chlorpromazine (50–100 μm), hypertonic sucrose (0.4–0.5 m) and potassium depletion can be used to inhibit the clathrin-dependent endocytosis (Ivanov 2008). Similarly, methyl-β-cyclodextrin, filipin, nystatin and cholesterol oxidase can be used as the inhibitors for caveolae-dependent endocytosis (Diken et al. 2011).

7.4 Factors Affecting Cellular Response of Nanoparticles

NPs possess intricate structures and surface chemistry. In biological systems, they may play an undecided role (Xie et al. 2009). Response of NPs with cells depends on the type of cells, cell culture media, size, shape, surface charge, surface moieties, temperature and route of administration of NPs (Fig. 7.2). These are the key parameters for particle binding and wrapping by the surface membrane as well as defining the path of cellular uptake (Xia et al. 2008a, b). Type of cells and cell lines also affect the cellular response. Cell lines grown in different culture media showed different cellular response to NPs (Maiorano et al. 2010). In addition to this, type of NPs also has an effect on its fate inside the cells. NPs are synthesised from materials of different compositions. Biodegradable NPs are rapidly cleared from the cells (Chellat et al. 2005), while non-biodegradable particles are retained inside the body for longer duration (Niidome et al.

2006). NPs uptake by cells is also affected by their shape. Shape of NPs has not only affected the cellular uptake but also the internalisation. Spherical particles are internalised at a higher rate in endothelial cells (Jun et al. 2005).

Surface chemistry of NPs has immense role to play in the cellular response of NPs (Bartneck et al. 2010) Polyethylene oxide (PEO)-coated gold nanorods with amine end groups have exhibited anti-inflammatory properties, whereas carboxy terminated led to proinflammatory effects. NMs surface chemistry has influence on the expression of inflammatory genes and phenotype of macrophages (Bartneck et al. 2010). Surface charge of NPs is also reported to affect the response of NPs with cells. NPs with cationicsurface charge show positive response with negatively charged cell membrane. The internalisation of negatively charged NPs is believed to occur through non-specific binding and clustering of NPs on cationic sites of the plasma membrane and their subsequent endocytosis. Negatively charged NPs have displayed a less efficient rate of endocytosis. NPs with positive surface charge depolarize the plasma membrane leading to increased Ca^{2+} influx (Yue et al. 2011). Positively charged NPs normally escape from lysosome and reside in perinuclear region, whereas the negatively charged NPs prefer to co-localise with lysosome (Yue et al. 2011).

Cellular uptake of positively charged particles into lysosomal compartments could lead to cytotoxicity by acidifying proton pump (Boussif et al. 1995). In addition, the positively charged NPs (Fig. 7.2) have been shown to target cell membranes through strong binding to phospholipid components, which can lead to membrane disruption (Asokan and Cho 2002).

Charged NPs can also activate complement system, hemolysis and thrombogenicity. Charged NPs are more aggressively invoked complement system than neutral ones (Bartlett and Davis 2007; Nagayama et al. 2007). Gold NPs activate the immune system (Bastus et al. 2009). Bare lipid NMs show high cellular uptake due to non-specific internalisation through charge interaction of the positively charged NPs with the negatively charged cell surface. The PEGylation of the NPs limited the non-specific charge interaction and resulted in reduced cellular uptake of NPs (Wang et al. 2009).

Targeting moieties attached to the surface of NPs decide their fate inside the cells. NPs with specific recognition moieties bound to the surface have a good potential for site-selective uptake as well as improved specificity for drug targeting (Dinauer et al. 2005). This strategy is used to direct NPs to cell surface carbohydrates, receptors and antigens (Sinha et al. 2006). Moieties attached to the surface can include any molecule that selectively recognises and binds molecules on target cells (Sapra and Allen 2003). Antibodies, oligopeptides, carbohydrates, glycolipids and folic acid are the most widely used moieties for targeting different cells and tissues. Targeted NPs can bind more specifically to cancer cells than normal cells. NPs without specific moieties can attack normal cells as well. Peptide-conjugated gold NPs activate the macrophage system. Macrophage activation by gold NPs depend on the peptide pattern at the NPs surface (Bastus et al. 2009). Targeted NPs are internalised by cancer cells through receptor-mediated endocytosis enhancing cancer cell killing (Hu et al. 2010). NPs are internalised by different uptake pathways which also affect the cellular response (Xia et al. 2008a, b; Kumari and Yadav 2011). Multiwalled carbon nanotubes (MWCNTs) and quantum dots delivered by nano-channel electroporation undergo nonendocytic uptake in BEAS-2B cells and result in higher cell death (Zhao et al. 2015). Cellular uptake of NPs is also affected by the type of cells. Different types of cells internalise NPs to a different extent. Gold NPs with positive surface charge have shown more cell internalisation ability than those with negative surface charge in non-phagocytic cells. However, the internalised amount of negatively charged gold NPs was similar with that of the positively charged gold NPs in phagocytic cells (Liu et al. 2013).

Polystyrene NPs have been efficiently internalised by human ATI cell line (TT1) cells, while uptake of NPs by primary human ATII cells was negligible (Thorley et al. 2014). It has been

shown that extent of NPs uptake, kinetics of NPs uptake and NPs internalisation mechanisms differ between primary cells and phenotypically linked cells (Lunov et al. 2011). Pericellular matrix (PCM) of cell has been documented for a role in accumulation and enhancing uptake of NPs (Zhou et al. 2012). Cellular uptake of NPs is also modulated by cell surface area and membrane tension. It has been reported that cellular internalisation is enhanced linearly with cell surface area and decreased exponentially with increasing membrane tension (Huang et al. 2013). Cell culture media also has an influence on NPs uptake and internalisation. TiO_2 NPs incubated in three different media showed different extent of uptake and internalisation. Uptake of TiO_2 NPs was maximum in media with highest amount of protein (Strickland et al. 2013). Gold NPs incubated in RPMI media showed more cellular uptake than NPs incubated in DMEM media (Maiorano et al. 2010).

7.5 Cellular Response of Therapeutic Nanoparticles

NPs are increasingly used in the field of drug delivery. NPs show various responses with cells. These include interactions with cellular membrane and cellular uptake, signalling pathways, ROS production, cell cycle dysregulation and necrosis or apoptosis (Jones and Grainger 2009). Many in vitro models are used to study the response of NPs with cells (Kumar et al. 2012). Metallic and polymeric NPs are extensively used in the field of nanomedicine due to their ease of preparation and surface modification. Understanding the cellular response of metallic, polymeric and silica NPs has recently fascinated the attention of scientific community.

7.5.1 Metallic Nanoparticles

Toxicity of silver nanoparticles (Ag NPs) to human hepatoma cells is the result of oxidative stress and is independent of the toxicity of Ag^+ ions (Jun et al. 2005). Polysaccharide-coated and uncoated Ag NPs are distributed differently and cause different levels of DNA damage in mouse embryonic stem cells (MES) and mouse embryonic fibroblast cells (MEF). Both types of Ag NPs induce p53 protein expression, DNA double-strand breakage and apoptosis responses in MES and MEF cells (Ahamed et al. 2008). Upon exposure to 6.25 μg/mL Ag NPs, morphology of both HT-1080 and A431 types of cells remain unaltered. However, at higher concentrations (6.25–50 μg/mL) of Ag NPs, cells became less polyhedra, more fusiform and shrunken. Changes in the levels of catalase and glutathione peroxidase in A431 and A431 types of cells are statistically insignificant. Ag NP exposure caused the DNA fragmentation in cells (Arora et al. 2008). Citrate-stabilised NPs show significant cellular response, while cellular treatment with nucleic acid or BSA functionalised NPs caused no detectable changes in gene expression, cell cycle progression or apoptosis induction (Massich et al. 2010). Nucleic acid-modified gold NPs have been reported for less immune response (Massich et al. 2009). The L929 cells become round and even shrunken on exposure to TiO_2 NPs (Jin et al. 2008). Moreover, TiO_2 NPs-treated cells either show condensation of fragmented chromatin or directly necrosed. Cells cultured in a medium containing 300 μg/mL TiO_2 have increased the number of lysosomes and damaged some of the cytoplasmic organelles. Gold NPs with weakly bound ligands have shown significant cellular responses, while gold NPs with strongly bound ligands have shown weak cellular responses (Massich et al. 2010). Gold NPs have also been observed to induce cell death in human carcinoma lung cell line A549. In contrast, BHK21 (baby hamster kidney) and HepG2 (human hepatocellular liver carcinoma) cell lines remain unaltered by gold NPs treatment (Patra et al. 2007). ZnO NPs showed dose-dependent toxicity in RAW 264.7 cells, higher cellular uptake and elevated intracellular ROS level (Hong et al. 2013).

7.5.2 Silica Nanoparticles

SiO_2 NPs are extensively used in the field of cancer therapy (Hirsch et al. 2003), DNA delivery (Bharali et al. 2005), drug delivery (Venkatesan et al. 2005) and enzyme immobilisation (Qhobosheane et al. 2001; Chen and von Mikecz 2005). SiO_2 NMs have caused decrease in number of molecules released per mast cell granule (Maurer-Jones et al. 2010). Exposure to 25–500 μg/mL of mesoporus SiO_2 NPs have been reported to inhibit cellular respiration in a concentration and time-dependent manner (Jin et al. 2007). Dye-doped silica NPs have shown low level of genotoxicity and cytotoxicity against the tested A549 cells (Jin et al. 2007). Silica nanotubes have exhibited growth inhibition in epithelial breast cancer cell line (MDA-MB-231) and primary umbilical vein endothelial cell line (HUVEC) (Nan et al. 2008) in a concentration-dependent manner.

7.5.3 Polymeric Nanoparticles

PLA NPs have elicited a strong cytotoxic T lymphocyte (CTL) response and a strong T helper cells-biased cytokine release in mice (Ataman-Önal et al. 2006). HIV envelope glycoproteins 140 carrying carnuba wax NPs have been reported to induce strong cellular/humoral response without inflammation (Arias et al. 2011). Polysiloxane NPs were endocytosed via caveolae in human aortic endothelial cells and enhanced nitric oxide release (Nishikawa et al. 2009). The incorporation of a bombesin peptide or RGD peptide via a PEG spacer in polymeric NMs was resulted in receptor-mediated cellular uptake and high gene silencing efficiency in U87 cells (Wang et al. 2009). Ligand-receptor recognition between cRGD and $\alpha_v\beta_3$ integrin has mediated the surface binding of RGD-targeted NMs to HUVECs and probably induced cRGD- targeted NPs to enter cells through caveolae and localised in the perinuclear regions (Liu et al. 2010b). cRGD functionalization of PLGA NPs has appreciably improved NP accumulation in tumour cells in vitro and resulted in improved tumour accumulation of NPs in a mouse model (Toti et al. 2010). Cationic polystyrene NPs have caused necrotic and apoptotic cell deaths in BEAS-2B and RAW264.7 cells, respectively (Xia et al. 2008a, b).

7.5.4 Quantum Dots

Quantum dots (QDs) with unique photochemical properties such as high photoluminescence and photo stability have shown great potential as a bimodal imaging agent, cancer diagnostics and drug delivery (Lee et al. 2010). Cetuximab-coated quantum dots have shown enhanced uptake in EGFR overexpressing A549 cells (Lee et al. 2010). Quantum dots have also undergone transformation in biological systems (Mahendra et al. 2008; Pettibone et al. 2013). Speciation of four types of CdSe/ZnS QDs in HepG2 cells has been studied in a recent report and it was observed that two chemical forms, named as QD-1 and QD-2, have been detected in HepG2 cells. QD-1 and QD-2 has been confirmed as QD-like NPs and a kind of cadmium metallothioneins complex, respectively (Peng et al. 2015). Matrix metalloproteases (MMP-2 and MMP-7) decorated quantum dots also have shown enhanced uptake in HT-1080 cells (Zhang et al. 2006). Ligand-conjugated QDs were not accumulated in vesicles of the early sorting pathways and were also able to reach the lysosomes of dendritic cells (Cambi et al. 2007). Tat peptide-conjugated quantum dots (Tat-QDs) has been internalised by macropinocytosis. The internalised Tat-QDs have sticked to the inner vesicle surfaces and trapped in cytoplasmic organelles and actively transported by molecular machines such as dyneins along microtubule tracks (Ruan et al. 2007).

7.5.5 Liposomes

Liposomes have long been considered good candidates for drug delivery. Effect of surface charge on the binding and endocytosis of

liposomes has been investigated on human ovarian carcinoma cell line (HeLa) and a murine-derived mononuclear macrophage cell line J774. HeLa cells have been found to endocytose positively charged liposomes to a greater extent than either neutral or negatively charged liposomes (Miller et al. 1998). In contrast, the extent of liposome interaction with J774 cells was greater for both cationic and anionic liposomes than for neutral liposomes (Miller et al. 1998). Tumour penetrating peptides (TPP) targeting liposomes have exhibited remarkably increased cellular accumulation by PC-3 tumour cells than bare liposomes (Yan et al. 2014). Liposomes modified with octaarginine have enhanced the efficiency of cross-presentation of ovalbumin in mouse bone marrow-derived dendritic cells (Nakamura et al. 2014). Hyaluronan (HA) coated liposomes have shown cellular uptake via lipid raft-mediated endocytosis in A549 cells. Once within cells, HA-liposomes have localised primarily to endosomes and lysosomes (Qhattal and Liu, 2011). Aptamer targeted liposomes have shown enhanced binding specificity and selectivity to CD44 expressing A549 and MDA-MB-231 cells (Alshaer et al. 2015). Annexin A5 functionalised liposomes bind to phosphatidylserine exposing apoptotic K562 cells with high specificity (Garnier et al. 2009).

7.6 Protein Corona Formation on Therapeutic Nanoparticles

Upon entering in biofluids, NPs surfaces were rapidly covered by selective sets of blood plasma proteins forming the protein corona (Cedervall et al. 2007a, b; Lindman et al. 2007; Mahmoudi et al. 2009; Mahmoudi et al. 2010; Walczyk et al. 2010). Upon entry of NPs into biological millieu, they were initially surrounded by high concentrations of free protein. Proteins moved towards the NP surface either by diffusion, or by travelling down a potential energy gradient. Protein adsorption in the neighbourhood of the NPs surface has occurred spontaneously only if it is thermodynamically favourable (Walkey and Chan 2012). In other words, if:

$$\Delta G_{ads} = \Delta H_{ads} - T\Delta S_{ads} < 0$$

where ΔG_{ads}, ΔH_{ads} and ΔS_{ads} are the changes in Gibbs free energy, enthalpy and entropy, respectively, during adsorption, and T is the temperature.

The formation of covalent and non-covalent bonds between NPs and protein, rearrangement of interfacial water molecules or conformational changes in either the protein or the NPs surface contribute to favourable changes in enthalpy ($\Delta H_{ads} < 0$), or entropy ($\Delta S_{ads} > 0$) (Walkey and Chan 2012). Type of protein (Lindman et al. 2007) and physiochemical properties of NPs determine the mechanism involved during adsorption and protein corona formation (De et al. 2007). Proteins interact with NPs surface through a portion known as domain during adsorption and protein corona formation. Adsorption of high-molecular weight protein kininogen to iron oxide NPs has occurred through its domain 5 (Simberg et al. 2009). Adsorption of proteins to NPs surface may involve interactions through many domains of the proteins (Walkey and Chan 2012). ΔG_{ads} determines the stability of the protein NPs corona. Proteins with large ΔG_{ads} stay with NPs surface, while proteins with small ΔG_{ads} desorb and return to solution (Norde 1994). Hydrophobic NPs interact strongly with proteins than those of hydrophilic (Walkey and Chan 2012). Hydrophobic or charged NPs cause more conformational changes in protein than their hydrophilic counterparts. Conformational changes of proteins are either reversible or irreversible and depend on the structure and chemistry of protein and NPs (Walkey and Chan 2012).

Protein corona is further divided into two types, viz. hard corona and soft corona (Fig. 7.3). Hard corona consists of an inner layer of selected proteins with a lifetime of several hours in slow exchange with the environment (Fig. 7.3). Soft corona

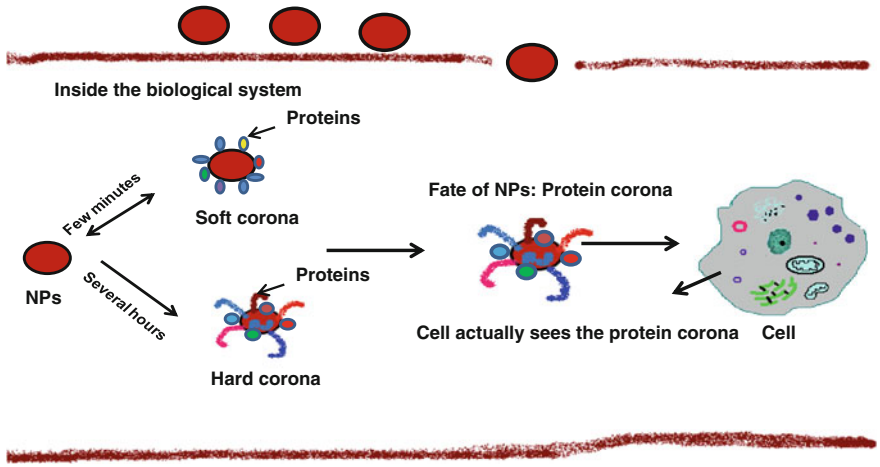

Fig. 7.3 Nanoparticles inside the biological systems. NPs form soft and hard corona after interaction with plasma proteins. Fate of NPs is decided by the protein corona of NPs

comprises of an outer layer of weakly bound proteins, which are characterised by a faster exchange rate with the free proteins (Mahmoudi et al. 2010). It is now believed that the hard corona interacts with cellular receptors and defines the fate of NPs in a biofluid due to the long lifetime of the hard protein corona (Mahmoudi et al. 2011a). It has been documented in a study that negatively charged NPs did not show the formation of hard protein corona while positively charged NPs show the formation of hard protein corona (Casals et al. 2010). First monolayer (hard corona) of transferrin binds irreversibly to polystyrene NPs and second monolayer (soft corona) is capable of exchanging proteins with solution (Milani et al. 2012).

7.7 Characterisation of Protein Corona on Nanoparticles

Upon contact with biological fluids, NPs interact strongly with proteins and other biomolecules, which drastically alter their surface characteristics. NPs with improved and changed biological activity will have the influence on NPs bio-distribution and their in vivo fate. Therefore, it is essential to apply and develop analytical tools and techniques to investigate the interactions of NPs with proteins in order to understand the protein corona composition and their possible biological activity. When NPs are meant for biological applications, it is necessary to investigate their physicochemical characteristics in the biological milieu (Mahmoudi et al. 2011a, b). As reported, many studies have been performed to shed light on the protein NPs association/dissociation processes in serum and plasma. As more than 3700 proteins coexist and compete for binding to the NPs surface, the determination of binding rates, affinities, and stoichiometries of protein association, and dissociation with NPs in biological fluids is particularly tedious and complicated process (Mahmoudi et al. 2011a, b). Protein corona is characterised by five parameters like thickness and density, identity and quantity, arrangement and orientation, conformation, and affinity of proteins on NPs. Together, these parameters describe the interaction of NPs with a biological environment (Walkey and Chan 2012). The composition and structure of the protein corona has been studied using either in situ or ex situ techniques. In situ techniques measure the protein corona, while the NPs is dispersed in a biological milieu. These techniques are limited in number and typically provide the least amount of information. Ex situ measurements require isolation of the NPs with its bound protein from the biological environment (Walkey and Chan 2012). Methods used for the characterisation of protein corona are Fourier transform infrared spectroscopy (FTIR), Raman spectroscopy, fluorescence correlation

spectroscopy, differential centrifugal sedimentation (DCS), isothermal titration calorimeter (ITC), LC-MS, electrophoresis, size exclusion chromatography, and dynamic light scattering.

7.7.1 Fourier Transform Infrared Spectroscopy (FTIR)

FTIR spectroscopy is known as an important technique for the examination of protein conformation in H_2O-based solution, resulting in a greatly expanded use in studies of protein secondary structure and protein dynamics in the past decade (Kong and Yu 2007). FTIR spectroscopy has been used for characterising the interactions of NPs with proteins (Wang et al. 2012).

7.7.2 Raman Spectroscopy

Raman scattering technique is a vibrational molecular spectroscopy in which a laser photon is scattered by a sample molecule and during the process energy is either lost or gained (Kengne-Momo et al. 2012). The amount of energy lost is seen as a change in energy (wavelength) of the irradiating photon which is characteristic for a particular bond in the molecule. The Raman signal produces a precise spectral sample fingerprint, unique to each atom, group of atoms or individual molecule (Kengne-Momo et al. 2012). A recent study has used surface enhanced Raman scattering spectroscopy to study changes in the proteins secondary structure as well as the effect on integrity and conformations of disulfide bonds immediately on the NP surface (Grass and Treuel 2014).

7.7.3 Fluorescence Correlation Spectroscopy

Fluorescence correlation spectroscopy (FCS) is a technique used to study the molecular movements and interactions. This technique monitors the fluctuation in the fluorescence signal from fluorescently labelled molecules inside the small confocal volume (Röcker et al. 2009; Maffre et al. 2011). In FCS, one usually considers the dynamics of number fluctuations in an open sampling volume of a macroscopic system that fluctuates about average equilibrium concentrations which are determined by the surrounding medium and its thermodynamics (Röcker et al. 2009; Maffre et al. 2011). The concentration fluctuations of each species can occur by in situ chemical reactions and by diffusion of each species in and out of the sampling volume. FCS is a highly accurate method to simultaneously determine binding affinities and the thickness of the protein corona on NPs (Röcker et al. 2009; Maffre et al. 2011). This method permits the quantitative observation of protein adsorption in situ on NPs (Treuel et al. 2014). Recent study has used FCS to quantitatively monitor HSA adsorption onto dihydrolipoic acid quantum dots (Treuel et al. 2014).

7.7.4 Differential Centrifugal Sedimentation

Differential centrifugal sedimentation (DCS) is based on the ability to separate NPs of the same density by mass, i.e. size (Cölfen 2004). DCS is a fast, accurate and relatively inexpensive, resolves multimodal size distributions, and uses relatively small sample volumes (Krpetic et al. 2012). DCS have been extensively used to measure size distribution, and hydrodynamic radii of NPs (Machtle 1999; Müller 2004, 2006). In addition to particle size, DCS has been used to determine changes in surface structure, study of binding isotherms of NPs and showed the attachment of DNA binding protein to NPs (Salvati et al. 2013). DCS can also be used for measuring thickness of protein corona.

7.7.5 Isothermal Titration Calorimetry

Isothermal titration calorimetry (ITC) is the only technique that can simultaneously determine all binding parameters in a single experiment. ITC measures heat transfer during binding which

enables accurate determination of binding constants (K_D), reaction stoichiometry (n), enthalpy (ΔH) and entropy (ΔS). This provides a complete thermodynamic profile of the molecular interaction. ITC also helps in elucidating the mechanisms underlying molecular interactions. The strength of protein interactions can be assessed using ITC and it also provides additional information on the thermodynamics of protein adsorption (Lindman et al. 2007).

7.7.6 Liquid Chromatography-Mass Spectrometry

Liquid chromatography-mass spectrometry (LC-MS) is a technique applied to a wide range of biological molecules. Mass spectrometers operate by converting the analyte molecules to a charged state, with subsequent analysis of fragment ions that are produced during the ionisation process, on the basis of their mass to charge ratio (*m*/*z*) (Pitt 2009). LC-MS plays an important role in several areas of clinical biochemistry and competes with conventional liquid chromatography and other techniques such as immunoassay. LC-MS has been used recently in a study to quantify the proteins in protein corona formed on SiO_2 and polystyrene NPs. The composition of protein corona has been investigated by LC-MS on polystyrene NPs with average diameters slightly above 100 nm and resulted in identification of approximately 170 different adsorbed proteins (Ritz et al. 2015).

7.7.7 Matrix-Assisted Laser Desorption/Ionisation Time of Flight Mass Spectrometer (MALDI-TOF MS)

The sample for matrix-assisted laser desorption/ionisation (MALDI) is uniformly mixed in a large quantity of UV-absorbing matrix and then followed by time of flight mass spectrometry (Marvina et al. 2003).The matrix absorbs the UV light and converts it into heat energy. A small part of the matrix is heated and rapidly vaporised, together with the sample. Different matrices are used for different kind of samples. Derivatives of benzoic acid, cinnamic acid and other related aromatic compounds are usually approved as good quality MALDI matrices for protein analysis (Hillenkamp et al. 1991). Charged ions of various sizes are generated on the sample slide, a potential difference between the sample slide and ground attracts the ions in a direction. As the potential difference is constant with respect to all ions, ions with smaller m/z value and more highly charged ions move faster through the drift space until they reach the detector. Consequently, the time of ion flight differs according to m/z value of the ion (Marvina et al. 2003). MALDI-TOF-MS has recently been used in a study to identify the proteins of NPs protein corona of nanosized welding particles formed in vitro (Ali et al. 2015).

7.7.8 Electrophoresis

Electrophoresis is used for the identification of proteins after separation of the NPs protein complex that has been separated from excess plasma proteins. Most commonly used method for this purpose is two-dimensional polyacrylamide gel electrophoresis (2D-PAGE) (Blunk et al. 1993; Gessner et al. 2002; Seehof et al. 2000). To identify individual proteins, it is common practice to compare the 2-D protein gels to a 2-D master map of human plasma proteins. However, differences in donor plasma and anticoagulants used during the blood collection process (EDTA, sodium citrate, lithium heparin), can result in variations in plasma protein maps, and hence may contribute to a misinterpretation of the 2D data when compared to a specific protein master map. The sodium dodecyl sulphate polyacrylamide gel electrophoresis (SDS-PAGE) is used for identifying proteins in hard protein corona (Winzen et al. 2015).

7.7.9 Size Exclusion Chromatography

Size exclusion chromatography (SEC) separates the NPs according to their size in dilute solutions (Sun et al. 2004). SEC is the second method investigated for its potential to reveal quantitative information on protein–NPs interactions. NPs and protein solution was passed through the chromatographic resin which allows protein and NPs to be resolved, but not different proteins. There has been a clear difference in the elution profile of HSA mixed with NPs, compared with free albumin, which implies an interaction between the protein and the NPs. Different proteins show different elution profiles when in protein NPs mixture than in free form. The rates of association/dissociation are very different from protein to protein, depending on the overall protein NP composition (Cedervall et al. 2007a, b). The strength of interactions of proteins with NPs can also be studied using SEC (Cedervall et al. 2007a, b).

7.7.10 Dynamic Light Scattering

Dynamic light scattering (DLS) measures the hydrodynamic diameter of NPs. DLS measures the size of NPs typically in the sub-micron region, also referred to as photon correlation spectroscopy or quasi-elastic light scattering. NPs suspended within a liquid undergo Brownian motion. DLS monitors the Brownian motion with light scattering. DLS measurements have been used to determine changes in the NP diameter before and after incubation with proteins. Proteins bind strongly to the NPs surface when the incubation time is increased, and they are stable against desorption in the serum free media. NPs hydrodynamic diameter is also increased as a result of the interactions of proteins with NPs. Adsorption of proteins onto the NPs surface has increased the overall size of NPs and not due to NPs aggregation (Casals et al. 2010). The thickness of the protein corona can be measured in situ using DLS (Walczyk et al. 2010).

7.7.11 Bioinformatic Tools

In silico simulation studies of protein NPs interactions is attracting attention as an alternative to experimental techniques (Walkey and Chan 2012). Simulation has been successfully adapted to study the adsorption of proteins on NPs. Simulation results have been used to study the interaction of a nanomaterial with individual amino acids to be observed over femto second timescales (Walkey and Chan 2012). Three strategies commonly used to simulate protein adsorption are quantum mechanical (QM), all atom empirical force field (AA) and coarse grained (CG) (Makarucha et al. 2011). Experimentally measured reference values are required to ensure the validity of simulation results. In silico simulations have been used to study the protein adsorption onto NPs as a function of surface ligand structure (Makarucha et al. 2011), surface curvature (Hung et al. 2011), and protein identity (Ge et al. 2011). However, computational power is presently unable to handle the complexity of competitive protein adsorption in a biological milieu, and there is a scarcity of availability of relevant force fields and descriptions of salvation (Walkey and Chan 2012).

7.8 Properties of NPs Affecting Protein Corona Formation

Interaction of NPs with biomolecules and composition of the resulting protein corona is affected by many factors (Foroozandeh and Aziz 2015). The physicochemical properties of NPs and the biological environment are vital parameters governing protein corona formation. Therefore, studying and understanding each of these parameters are essential for safe and smart designing of NPs for targeted drug delivery. The affinities and identities of proteins that bind to NPs are affected by the composition and surface chemistry of NPs. It has been reported that different proteins bind to different NPs with the same surface charge (Deng et al. 2009). Similar proteins can be adsorbed onto the TiO_2 and SiO_2

NPs, whereas significantly different proteins can compose the hard corona of ZnO NPs. The corona of TiO_2 and SiO_2 NPs were comprised of clusterin, apolipoprotein D and alpha-2-acid glycoprotein, while these were not observed in the corona of ZnO. Fascinatingly, transferrin, Ig heavy chain alpha and haptoglobin have been reported in the corona of ZnO NPs.

The size of NPs plays a vital role in the adsorption of proteins, conformational changes and composition of protein corona (Lundqvist et al. 2008; Lynch and Dawson 2008). It has been reported that the thickness of protein corona progressively increases as the size of NP increases. In addition, conformational change upon adsorption on the NPs surface showed enhancement with the size of NPs. Moreover, more proteins adsorbed on smaller sized NPs than on larger sized NPs (Dobrovolskaia et al. 2009). Interestingly, even 10 nm variations in NPs size have remarkably affected the protein corona composition (Tenzer et al. 2011). Shape of NPs has also affected the formation of protein corona on NPs surface (Deng et al. 2009). Surface charge of NPs also play vital role in the composition and formation of protein corona on NPs. Negatively charged NPs have been shown for enhancement in plasma protein absorption with an increase in the surface charge density of NPs (Gessner et al. 2002). In addition, proteins with isoelectric points (PI) of less than 5.5 adsorbed on positively charged NPs whereas proteins with isoelectric points of higher than 5.5 bound to negatively charged NPs (Foroozandeh and Aziz 2015). More proteins can adsorb onto the surface of hydrophobic NPs than their hydrophilic counterparts and lose their native structure (Roach et al. 2005). It has been observed that protein corona can drastically affect the cellular uptake and internalisations of NPs. Distinct corona signatures are indeed able to predict the cellular uptake of NPs. Hence, covering NPs surface with physiological proteins can indeed enhance or inhibit their cellular uptake, whereas the surface charge of the uncoated NPs appear to be less important (Monopoli et al. 2012; Lesniak et al. 2012; Zhang et al. 2014). Protein corona fingerprints can be modulated for increasing the cellular uptake of NPs across many biological barriers. It has been shown that apolipoproteins promote the transport of NPs across the blood brain barrier (Zhu et al. 2013) and different immunoglobulins and opsonins enable their uptake into monocytes (Riehemann et al. 2009), while dysopsonins inhibit the uptake of NPs (Cedervall et al. 2007a, b). NPs targeted with transferrin have been studied in foetal bovine serum albumin for their targeting efficiency (Salvati et al. 2013). It has been observed that serum decreased the overall uptake of NPs through transferrin receptors. These results have demonstrated that targeted NPs may lose their targeting abilities in biological media. This behaviour is attributed to the proteins in the serum forming a protein corona around the NPs, which masks the transferrin and stops it from binding to the targeted receptors on the cells. Hence, experiments carried out in vitro cannot be used to provide a conclusive analysis of targeting efficiency. Therefore, targeted NPs formulations should be smartly designed by taking into account the protein corona effect, and the problems faced due to the route of administration, organs, tissues and cellular uptake. This will help in developing targeted NPs with clinical applications and achieving the concept of personalised medicine (Gaspar 2013).

In addition to the properties of NPs, the composition of protein corona is also affected by the biological media in which NPs are incubated. It has been reported that formation of protein corona by utilising Dulbecco's Modified Eagle's Medium (DMEM) media is significantly time dependent, while using Roswell Park Memorial Institute (RPMI) media leads to different dynamics and reduction of protein corona (Maiorano et al. 2010). Besides NPs properties and biological milieu, other factors which affect protein corona at bio-nano interfaces are gradient plasma, plasma concentration, cell observer, temperature and cell membrane composition. Detailed investigations must be carried out to understand these ignored factors as to enable the development of better and effective nanomedicine (Foroozandeh and Aziz 2015).

Protein corona has been recently exploited for evading mononuclear phagocytic system. Albumins form tight binding to SiO_2 NPs and may undergo

rapid unfolding to form hard corona. Albumin has been documented to promote NPs uptake into cells that are expressing class A scavenger receptors and resulted in internalisation of the protein NP complex via receptor-mediated endocytosis (Mortimer et al. 2014).

7.9 Conclusions

NPs may not only promote the pharmacological effects of delivered therapeutic molecules, but also cause undesirable effects in the target cells. Factors like size, shape and surface chemistry of NPs can influence their cellular responses. NPs have been observed to induce cellular responses like ROS production, apoptosis, necrosis and expression of genes. Most of the studies involving the cellular responses of NPs have been carried out on in vitro cell lines, and therefore final validation is required with primary cells. Effect of various surface ligands and the use of targeting moieties should be investigated to better understand the cellular responses of NPs. NPs should no longer be viewed as simple carriers for biomedical applications, but can also play dynamic role in mediating biological responses. NPs-biomolecule corona should be more carefully characterised and quantified for safe and effective use of NPs in nanomedicine. The molecular design of basic molecules for NPs and the response between NPs and cells should be considered more carefully in terms of the activation of cell functions.

Acknowledgments We are grateful to Director, IHBT for critical and valuable suggestions. Financial assistance from Council of Scientific and Industrial Research, Government of India is genuinely acknowledged.

References

Aderem A, Underhill DM (1999) Mechanisms of phagocytosis in macrophages. Annu Rev Immunol 17:593–623

Ahamed M, Karns M, Goodson M et al (2008) DNA damage response to different surface chemistry of silver nanoparticles in mammalian cells. Toxicol Appl Pharmacol 233:404–410

Ali N, Mattsson K, Rissler J et al (2015) Analysis of nanoparticle—protein coronas formed in vitro between nanosized welding particles and nasal lavage proteins. Nanotoxicology 1–9

Alivisatos AP, Gu W, Larabell C (2005) Quantum dots as cellular probes. Annu Rev Biomed Eng 7:55–76

Alshaer W, Hillaireau H, Vergnaud J et al (2015) Functionalizing liposomes with anti-CD44 aptamer for selective targeting of cancer cells. Bioconjugate Chem 26:1307–1313

Arias MA, Loxley A, Eatmon C et al (2011) Carnauba wax nanoparticles enhance strong systemic and mucosal cellular and humoral immune responses to HIV-gp140 antigen. Vaccine 29:1258–1269

Arora S, Jain J, Rajwade JM et al (2008) Cellular responses induced by silver nanoparticles: In vitro studies. Toxicol Lett 179:93–100

Asokan A, Cho MJ (2002) Exploitation of intracellular pH gradients in the cellular delivery of macromolecules. J Pharm Sci 91:903–913

Ataman-Önal Y, Munier S, Ganée A et al (2006) Surfactant-free anionic PLA nanoparticles coated with HIV-1 p24 protein induced enhanced cellular and humoral immune responses in various animal models. J Control Rel 112:175–185

Bao G, Bao XR (2005) Shedding light on the dynamics of endocytosis and viral budding. Proc Natl Acad Sci USA 102:9997–9998

Bartlett DW, Davis ME (2007) Physicochemical and biological characterization of targeted nucleic acid-containing nanoparticles. Bioconjugate Chem 18:456–468

Bartneck M, Keul HA, Singh S et al (2010) Rapid uptake of gold nanorods by primary human blood phagocytes and immunomodulatory effects of surface chemistry. ACS Nano 4:3073–3086

Bastus NG, Sanchez-Tillo E, Pujals S et al (2009) Homogeneous conjugation of peptides onto gold nanoparticles enhances macrophage response. ACS Nano 3:1335–1344

Benmerah A, Lamaze C (2007) Clathrin-coated Pits: Vive la Difference? Traffic 8:970–982

Bharali DJ, Klejbor I, Stachowiak EK et al (2005) Organically modified silica nanoparticles: a nonviral vector for in vivo gene delivery and expression in the brain. Proc Natl Acad Sci USA 102:11539–11544

Blunk T, Hochstrasser DF, Sanchez JC et al (1993) Colloidal carriers for intravenous drug targeting: plasma protein adsorption patterns on surface-modified latex particles evaluated by two-dimensional polyacrylamide gel electrophoresis. Electrophoresis 14:1382–1387

Boussif O, Lezoualc'h F, Zanta MA et al (1995) A versatile vector for gene and oligonucleotide transfer into cells in culture and in vivo: polyethylenimine. Proc Natl Acad Sci 92:7297–7301

Cambi A, Lidke DS, Arndt-Jovin DJ et al (2007) Ligand-conjugated quantum dots monitor antigen uptake and processing by dendritic cells. Nanolett 7:970–977

Casals E, Pfaller T, Duschl A et al (2010) Time evolution of the nanoparticle protein corona. ACS Nano 4:3623–3632

Cedervall T, Lynch I, Foy M et al (2007a) Detailed identification of plasma proteins adsorbed on copolymer nanoparticles. Angew Chem Int Ed 46:5754–5756

Cedervall T, Lynch I, Lindman S et al (2007b) Understanding the nanoparticle-protein corona using methods to quantify exchange rates and affinities of proteins for nanoparticles. Proc Natl Acad Sci USA 104:2050–2055

Chang J, Jallouli Y, Kroubi M et al (2009) Characterization of endocytosis of transferrin-coated PLGA nanoparticles by the blood-brain barrier. Int J Pharm 379:285–292

Chellat F, Grandjean-Laquerriere A, Le Naour R et al (2005) Metalloproteinase and cytokine production by THP-1 macrophages following exposure to chitosan-DNA nanoparticles. Biomaterials 26:961–970

Chen M, von Mikecz A (2005) Formation of nucleoplasmic protein aggregates impairs nuclear function in response to SiO2 nanoparticles. Exp Cell Res 305:51–62

Cölfen H (2004) Analytical ultracentrifugation of nanoparticles. In: Nalwa HS (ed) Encyclopedia of nanoscience and nanotechnology, vol. 1. American Scientific Publishers, Stevenson Ranch, pp 67–88

Conner SD, Schmid SL (2003) Regulated portals of entry into the cell. Nature 422:37–44

Dausend J, Musyanovych A, Dass M et al (2008) Uptake mechanism of oppositely charged fluorescent nanoparticles in HeLa cells. Macromol Biosci 8:1135–1143

De M, You CC, Srivastava S et al (2007) Biomimetic interactions of proteins with functionalized nanoparticles: A thermodynamic study. J Am Chem Soc 129:10747–10753

Deng ZJ, Mortimer G, Schiller T et al (2009) Differential plasma protein binding to metal oxide nanoparticles. Nanotechnology 20:455101

Diken M, Kreiter S, Selmi A et al (2011) Selective uptake of naked vaccine RNA by dendritic cells is driven by macropinocytosis and abrogated upon DC maturation. Gene Ther 18:702–708

Dinauer N, Balthasar S, Weber C et al (2005) Selective targeting of antibody-conjugated nanoparticles to leukemic cells and primary T-lymphocytes. Biomaterials 26:5898–5906

Dobrovolskaia MA, Patri AK, Zheng J et al (2009) Interaction of colloidal gold nanoparticles with human blood: effects on particle size and analysis of plasma protein binding profiles. Nanomed Nanotechnol Biol Med 5:106–117

Duit S, Mayer H, Blake SM et al (2010) Differential functions of ApoER2 and very low density lipoprotein receptor in Reelin signaling depend on differential sorting of the receptors. J Biol Chem 285:4896–4908

El-Sayed IH, Huang X, El-Sayed MA (2005) Surface plasmon resonance scattering and absorption of anti-EGFR antibody conjugated gold nanoparticles in cancer Diagnostics: applications in oral cancer. Nano Lett 5:829–834

El-Sayed IH, Huang XH, El-Sayed MA (2006) Photo-Thermal therapy of epithelial carcinoma using anti-EGFR antibody conjugated gold nanoparticles. Cancer Lett 239:129–135

Foroozandeh P, Aziz AA (2015) Merging worlds of nanomaterials and biological environment: factors governing protein corona formation on nanoparticles and its biological consequences. Nanoscale Res Lett 10:221

Garnier B, Bouter A, Gounou C et al (2009) Annexin A5-Functionalized liposomes for targeting phosphatidylserine-exposing membranes. Bioconjugate Chem 20:2114–2122

Gaspar R (2013) Nanoparticles pushed off target with proteins. Nature Nanotech 8:79–80

Ge C, Du J, Zhao L et al (2011) Binding of blood proteins to carbon nanotubes reduces cytotoxicity. Proc Natl Acad Sci 108:16968–16973

Gessner A, Lieske A, Paulke B et al (2002) Influence of surface charge density on protein adsorption on polymeric nanoparticles: analysis by two-dimensional electrophoresis. Eur J Pharm Biopharm 54:165–170

Grass S, Treuel L (2014) Mechanistic aspects of protein corona formation: insulin adsorption onto gold nanoparticle surfaces. J Nanopart Res 16:2254–2265

Hainfeld JF, Slatkin DN, Smilowitz HM (2004) The use of gold nanoparticles to enhance radiotherapy in mice. Phys Med Biol 49:N309–N315

Harush-Frenkel O, Debotton N, Benita S et al (2007) Targeting of nanoparticles to the clathrin-mediated endocytic pathway. Biochem Biophys Res Commun 353:26–32

Hillenkamp F, Karas M, Beavis RC et al (1991) Matrix-assisted laser desorption/ionization MS of biopolymers. Anal Chem 63:1193–1202

Hirsch LR, Stafford RJ, Bankson JA et al (2003) Nanoshell-mediated near-infrared thermal therapy of tumors under magnetic resonance guidance. Proc Natl Acad Sci 100:13549–13554

Hong T, Tripathy N, Son H et al (2013) A comprehensive in vitro and in vivo study of ZnO nanoparticles toxicity. J Mater Chem B 1:2985–2992

Hu CM, Kaushal S, Tran Cao HS et al (2010) Half-antibody functionalized lipid-polymer hybrid nanoparticles for targeted drug delivery to carcinoembryonic antigen presenting pancreatic cancer cells. Mol Pharm 7:914–920

Huang C, Butler PJ, Tong S et al (2013) Substrate stiffness regulates cellular uptake of nanoparticles. Nano Lett 13:1611–1615

Hung A, Mwenifumbo S, Mager M et al (2011) Ordering surfaces on the nanoscale: implications for protein adsorption. J Am Chem Soc 133:1438–1450

Ivanov AI (2008) Pharmacological inhibition of endocytic pathways: is it specific enough to be useful? Methods Mol Biol 440:15–33

Jiang W, Kim BY, Rutka JT et al (2008) Nanoparticle-mediated cellular response is size-dependent. Nat Nanotechnol 3:145–150

Jin Y, Kannan S, Wu M et al (2007) Toxicity of luminescent silica nanoparticles to living cells. Chem Res Toxicol 20:1126–1133

Jin CY, Zhu BS, Wang XF et al (2008) Cytotoxicity of titanium dioxide nanoparticles in mouse fibroblast cells. Chem Res Toxicol 21:1871–1877

Jones CF, Grainger DW (2009) In vitro assessments of nanomaterial toxicity. Adv Drug Deliv Rev 61:438–456

Jones AT, Gumbleton M, Duncan R (2003) Understanding endocytic pathways and intracellular trafficking. A prerequisite for effective design of advanced drug delivery systems. Adv Drug Deliv Rev 55:1353–1357

Jun YW, Huh YM, Choi JS et al (2005) Nanoscale size effect of magnetic nanocrystals and their utilization for cancer diagnosis via magnetic resonance imaging. J Am Chem Soc 127:5732–5733

Kengne-Momo RP, Daniel P, Lagarde F et al (2012) Protein interactions investigated by the raman spectroscopy for biosensor applications. Int J Spectroscopy 2012: Article ID 462901, 7 pages. doi:10.1155/2012/462901

Kong J, Yu S (2007) Fourier transform infrared spectroscopic analysis of protein secondary structures. Acta Biochim Biophys Sin 39:549–559

Koo OM, Rubinstein I, Onyuksel H (2005) Role of nanotechnology in targeted drug delivery and imaging: A concise review. Nanomed Nanotechnol Biol Med 1:193–212

Krpetic Z, Singh I, Su W et al (2012) Directed assembly of DNA-functionalized gold nanoparticles using pyrrole-imidazole polyamides. J Am Chem Soc 134:8356–8359

Kumar V, Kumari A, Guleria P et al (2012) Evaluating the toxicity of selected types of nanochemicals. Rev Environ Contamin Toxicol 215:40–112

Kumari A, Yadav SK (2011) Cellular interactions of therapeutically delivered nanoparticles. Expert Opin Drug Deliv 8:141–151

Lee J, Choi Y, Kim K et al (2010) Characterization and cancer cell specific binding properties of anti-EGFR antibody conjugated quantum dots. Bioconj Chem 21:940–946

Lesniak A, Fenaroli F, Monopoli MP et al (2012) Effects of the presence or absence of a protein corona on silica nanoparticle uptake and impact on cells. ACS Nano 6:5845–5857

Lindman S, Lynch I, Thulin E et al (2007) Systematic investigation of the thermodynamics of HSA adsorption to N-iso-propylacrylamide/N-tert-butylacrylamide copolymer nanoparticles. Effects of particle size and hydrophobicity. Nano Lett 7:914–920

Liu AP, Aguet F, Danuser G et al (2010a) Local clustering of transferrin receptors promotes clathrin-coated pit initiation. J Cell Biol 191:1381–1393

Liu XQ, Song WJ, Sun TM et al (2010b) Targeted delivery of antisense inhibitor of miRNA for antiangiogenesis therapy using cRGD-functionalized nanoparticles. Mol Pharm 8:250–259

Liu X, Huang N, Li H et al (2013) Surface and size effects on cell interaction of gold nanoparticles with both phagocytic and nonphagocytic cells. Langmuir 29:9138–9148

Luccardini C, Yakovlev A, Gaillard S et al (2007) Intracellular uses of colloidal semiconductor nanocrystals. J Biomed Biotechnol 2007:1–9

Lundqvist M, Stigler J, Elia G et al (2008) Nanoparticle size and surface properties determine the protein corona with possible implications for biological impacts. Proc Natl Acad Sci 105:14265–14270

Lunov O, Syrovets T, Loos C et al (2011) Differential uptake of functionalized polystyrene nanoparticles by human macrophages and a monocytic cell line. ACS Nano 5:1657–1669

Lynch I, Dawson KA (2008) Protein-nanoparticle interactions. Nano Today 3:40–47

Machtle W (1999) High-Resolution submicron particle size distribution analysis using gravitational-sweep sedimentation. Biophys J 76:1080–1091

Maffre P, Nienhaus K, Amin F et al (2011) Characterization of protein adsorption onto Fept nanoparticles using dual-focus fluorescence correlation spectroscopy. Beilstein J Nanotechnol 2:374–383

Mahendra S, Zhu HG, Colvin VL et al (2008) Quantum dot weathering results in microbial toxicity. Environ Sci Technol 42:9424–9430

Mahmoudi M, Simchi A, Imani M (2009) Cytotoxicity of uncoated and polyvinyl alcohol coated superparamagnetic iron oxide nanoparticles. J Phys Chem C 113:9573–9580

Mahmoudi M, Simchi A, Imani M et al (2010) A new approach for the in vitro identification of the cytotoxicity of superparamagnetic iron oxide nanoparticles. Colloid Surf B 75:300–309

Mahmoudi M, Lynch I, Ejtehadi MR et al (2011a) Protein nanoparticle interactions: opportunities and challenges. Chem Rev 111:5610–5637

Mahmoudi M, Sant S, Wang B et al (2011b) Superparamagnetic iron oxide nanoparticles (SPIONs): development, surface modification and applications in chemotherapy. Adv Drug Delivery Rev 63:24–46

Mailänder V, Lorenz MR, Holzapfel V et al (2008) Carboxylated superparamagnetic iron oxide particles label cells intracellularly without transfection agents. Mol Imaging Biol 10:138–146

Maiorano G, Sabella S, Sorce B et al (2010) Effects of cell culture media on the dynamic formation of protein-nanoparticle complexes and influence on the cellular response. ACS Nano 4:7481–7491

Makarucha J, Todorova N, Yarovsky I (2011) Nanomaterials in biological environment: a review of computer modelling studies. Eur Biophys J 40:103–115

Marvina LF, Robertsb MA, Faya LB (2003) Matrix-assisted laser desorption/ionization time-of-flight mass spectrometry in clinical chemistry. Clin Chim Acta 337:11–21

Massich MD, Giljohann DA, Seferos DS et al (2009) Regulating immune response using polyvalent nucleic

acid-gold nanoparticle conjugates. Mol Pharm 6:1934–1940
Massich MD, Giljohann DA, Schmucker AL et al (2010) Cellular response of polyvalent oligonucleotide-gold nanoparticle conjugates. ACS Nano 4:5641–5646
Maurer-Jones MA, Lin YS, Haynes CL (2010) Functional assessment of metal oxide nanoparticle toxicity in immune cells. ACS Nano 4:3363–3373
Medina-Kauwe LK (2007) "Alternative" endocytic mechanisms exploited by pathogens: new avenues for therapeutic delivery? Adv Drug Del Rev 59:798–809
Milani S, Bombelli FB, Pitek AS et al (2012) Reversible versus irreversible binding of transferrin to polystyrene nanoparticles: Soft and hard corona. ACS Nano 6:2532–2541
Miller CR, Bondurant B, McLean SD et al (1998) Liposome-cell interactions in vitro: effect of liposome surface charge on the binding and endocytosis of conventional and sterically stabilized liposomes. Biochemistry 37:12875–12883
Monopoli MP, Aberg C, Salvati A et al (2012) Biomolecular coronas provide the biological identity of nanosized materials. Nat Nanotechnol 7:779–786
Mortimer GM, Butcher NJ, Musumeci AW et al (2014) Cryptic epitopes of albumin determine mononuclear phagocyte system clearance of nanomaterials. ACS Nano 8:3357–3366
Müller HG (2004) Determination of very broad particle size distributions via interferences optics in the analytical ultracentrifuge. Prog Colloid Polym Sci 127:9–13
Müller HG (2006) Determination of particle size distributions of swollen (Hydrated) particles by analytical ultracentrifugation. Prog Colloid Polym Sci 131:121–125
Nagayama S, Ogawara K, Fukuoka Y et al (2007) Time-dependent changes in opsonin amount associated on nanoparticles alter their hepatic uptake characteristics. Int J Pharm 342:215–221
Nakamura T, Ono K, Suzuki Y et al (2014) Octaarginine-modified liposomes enhance cross-presentation by promoting the C-terminal trimming of antigen peptide. Mol Pharm 11:2787–2795
Nan A, Bai X, Son SJ et al (2008) Cellular uptake and cytotoxicity of silica nanotubes. Nano Lett 8:2150–2154
Nel AE, Madler L, Velegol D et al (2009) Understanding biophysicochemical interactions at the nano-bio interface. Nat Mater 8:543–547
Niidome T, Yamagata M, Okamoto Y et al (2006) PEG-modified gold nanorods with a stealth character for in vivo applications. J Control Rel 114:343–347
Nishikawa T, Iwakiri N, Kaneko Y et al (2009) Nitric oxide release in human aortic endothelial cells mediated by delivery of amphiphilic polysiloxane nanoparticles to caveolae. Biomacromolecules 10:2074–2085
Norde W (1994) Protein adsorption at solid surfaces: A thermodynamic approach. Pure Appl Chem 66:491–496
Oberdorster G, Oberdorster E, Oberdorster J (2005) Nanotoxicology: an emerging discipline evolving from studies of ultrafine particles. Environ Health Perspect 113:823–839
Oh E, Delehanty JB, Sapsford KE et al (2011) Cellular uptake and fate of pegylated gold nanoparticles is dependent on both cell-penetration peptides and particle size. ACS Nano 5:6434–6448
Parak WJ, Pellegrino T, Plank C (2005) Labelling of Cells with Quantum Dots. Nanotechnol 16:R9–R25
Patel LN, Zaro JL, Shen WC (2007) Cell penetrating peptides: intracellular pathways and pharmaceutical perspectives. Pharm Res 24:1977–1992
Patra HK, Banerjee S, Chaudhuri U et al (2007) Cell selective response to gold nanoparticles. Medicine 3:111–119
Pelkmans L, Helenius A (2002) Endocytosis via caveolae. Traffic 3:311–320
Peng L, He M, Chen B et al (2015) Metallomics study of CdSe/ZnS quantum dots in HepG2 Cells. ACS Nano 9:10324–10334
Petrescu AD, Vespa A, Huang H et al (2009) Fluorescent sterols monitor cell penetrating peptide Pep-1 mediated uptake and intracellular targeting of cargo protein in living cells. Biochim Biophys Acta Biomembr 1788:425–441
Pettibone JM, Gigault J, Hackley VA (2013) Discriminating the states of matter in metallic nanoparticle transformations: what are we missing? ACS Nano 7:2491–2499
Pitt JJ (2009) Principles and applications of liquid chromatography mass spectrometry in clinical biochemistry. Clin Biochem Rev 30:19–34
Qhattal HSS, Liu X (2011) Characterization of CD44-mediated cancer cell uptake and intracellular distribution of hyaluronan-grafted liposomes. Mol Pharmaceutics 8:1233–1246
Qhobosheane M, Santra S, Zhang P et al (2001) Biochemically functionalized silica nanoparticles. Analyst 126:1274–1278
Riehemann K, Schneider SW, Luger TA et al (2009) Nanomedicine challenge and perspectives. Angew Chem Int Ed 48:872–897
Ritz S, Schottler S, Kotman N, Baier G et al (2015) Protein corona of nanoparticles: distinct proteins regulate the cellular uptake. Biomacromolecules 16:1311–1321
Roach P, Farrar D, Perry CC (2005) Interpretation of protein adsorption: Surface induced conformational changes. J Am Chem Soc 127:8168–8173
Röcker C, Pötzl M, Zhang F et al (2009) A quantitative fluorescence study of protein monolayer formation on colloidal nanoparticles. Nat Nanotechnol 4:577–580

Ruan G, Agrawal A, Marcus AI et al (2007) Imaging and tracking of tat peptide-conjugated quantum dots in living cells: new insights into nanoparticle uptake, intracellular transport, and vesicle shedding. J Am Chem Soc 129:14759–14766

Salvati A, Pitek AS, Monopoli MP et al (2013) Transferrin-functionalized nanoparticles lose their targeting capabilities when a biomolecule corona adsorbs on the surface. Nat Nanotech 8:137–143

Sandhu KK, McIntosh CM, Simard JM et al (2002) Gold nanoparticle-mediated transfection of mammalian cells. Bioconjugate Chem 13:3–6

Sapra P, Allen TM (2003) Ligand-targeted liposomal anticancer drugs. Prog Lipid Res 42:439–462

Seehof K, Kresse M, Mader K et al (2000) Interactions of nanoparticles with body proteins-improvement of 2D-PAGE-analysis by internal standard. Int J Pharm 196:231–234

Simberg D, Park JH, Karmali PP et al (2009) Differential proteomics analysis of the surface heterogeneity of dextran iron oxide nanoparticles and the implications for their in vivo clearance. Biomaterials 30:3926–3933

Sinha R, Kim GJ, Nie S et al (2006) Nanotechnology in cancer therapeutics: Bioconjugated nanoparticles for drug delivery. Mol Cancer Ther 5:1909–1917

Strickland J, Dreher K, Kligerman AD et al (2013) Effect of treatment media on the agglomeration of titanium dioxide nanoparticles: impact on genotoxicity, cellular interaction, and cell cycle. ACS Nano 7:1929–1942

Sun T, Chance RR, Graessley WW et al (2004) A study of the separation principle in size exclusion chromatography. Macromolecules 37:4304–4312

Swanson JA, Watts C (1995) Macropinocytosis. Trends Cell Biol 5:424–428

Tenzer S, Docter D, Rosfa S et al (2011) Nanoparticle size is a critical physicochemical determinant of the human blood plasma corona: a comprehensive quantitative proteomic analysis. ACS Nano 5:7155–7167

Thorley AJ, Ruenraroengsak P, Potter TE et al (2014) Critical determinants of uptake and translocation of nanoparticles by the human pulmonary alveolar epithelium. ACS Nano 8:11778–11789

Toti US, Guru BR, Grill AE et al (2010) Interfacial activity assisted surface functionalization: a novel approach to incorporate maleimide functional groups and cRGD peptide on polymeric nanoparticles for targeted drug delivery. Mol Pharm 7:1108–1117

Treuel L, Brandholt S, Maffre P et al (2014) Impact of protein modification on the protein corona on nanoparticles and nanoparticles cell interactions. ACS Nano 8:503–513

Venkatesan N, Yoshimitsu J, Ito Y et al (2005) Liquid filled nanoparticles as a drug delivery tool for protein therapeutics. Biomaterials 26:7154–7163

Verma A, Stellacci F (2010) Effect of surface properties on nanoparticle-cell interactions. Small 6:12–21

Walczyk D, Bombelli FB, Monopoli MP et al (2010) What the cell "sees" in bionanoscience. J Am Chem Soc 132:5761–5768

Walkey CD, Chan WCW (2012) Understanding and controlling the interaction of nanomaterials with proteins in a physiological environment. Chem Soc Rev 41:2780–2799

Walsh M, Tangney M, O'Neill MJ et al (2006) Evaluation of cellular uptake and gene transfer efficiency of pegylated poly-L-lysine compacted DNA: implications for cancer gene therapy. Mol Pharm 3:644–653

Wang XL, Xu R, Wu X et al (2009) Targeted systemic delivery of a therapeutic siRNA with a multifunctional carrier controls tumor proliferation in mice. Mol Pharm 6:738–746

Wang T, Bai J, Jiang X et al (2012) Cellular uptake of nanoparticles by membrane penetration: a study combining confocal microscopy with FTIR spectroelectrochemistry. ACS Nano 6:1251–1259

Watson P, Jones AT, Stephens DJ (2005) Intracellular trafficking pathways and drug delivery: fluorescence imaging of living and fixed cells. Adv Drug Deliv Rev 57:43–61

Winzen S, Schoettler S, Baier G et al (2015) Complementary analysis of the hard and soft protein corona: sample preparation critically effects corona composition. Nanoscale 7:2992–3001

Xia T, Kovochich M, Liong M et al (2008a) Cationic polystyrene nanosphere toxicity depends on cell-specific endocytic and mitochondrial injury pathways. ACS Nano 2:85–96

Xia T, Kovochich M, Liong M et al (2008b) Comparison of the mechanism of toxicity of zinc oxide and cerium oxide nanoparticles based on dissolution and oxidative stress properties. ACS Nano 2:2121–2134

Xie J, Huang J, Li X et al (2009) Iron oxide nanoparticle platform for biomedical applications. Curr Med Chem 16:1278–1294

Xu P, Gullotti E, Tong L et al (2009) Intracellular drug delivery by poly (lactic-co-glycolic acid) nanoparticles, revisited. Mol Pharm 6:190–201

Yan Z, Yang Y, Wei X et al (2014) Tumor-penetrating peptide mediation: An effective strategy for improving the transport of liposomes in tumor tissue. Mol Pharm 11:218–225

Yue ZG, Wei W, Lv PP et al (2011) Surface charge affects cellular uptake and intracellular trafficking of chitosan-based nanoparticles. Biomacromolecules 12:2440–2446

Zhang Y, So MK, Rao J (2006) Protease-modulated cellular uptake of quantum dots. Nanolett 6:1988–1992

Zhang Y, Bai Y, Jia J et al (2014) Perturbation of physiological systems by nanoparticles. Chem Soc Rev 43:3762–3809

Zhao X, Wu Y, Gallego-Perez D et al (2015) Effect of nonendocytic uptake of nanoparticles on human bronchial epithelial cells. Anal Chem 87:3208–3215

Zhou R, Zhou H, Xiong B et al (2012) Pericellular matrix enhances retention and cellular uptake of nanoparticles. J Am Chem Soc 134:13404–13409

Zhu M, Nie G, Meng H et al (2013) Physicochemical properties determine nanomaterial cellular uptake, transport, and fate. Acc Chem Res 46:622–631